U.S. DEPARTMENT OF COMMERCE
National Technical Information Service

PB-256 252

Study of Factors Affecting Reactions in Environmental Chambers

Lockheed Missiles and Space Co., Inc.

Prepared For
Environmental Protection Agency

June 30, 1975

PB 256 252

REPRODUCED BY
NATIONAL TECHNICAL
INFORMATION SERVICE
U. S. DEPARTMENT OF COMMERCE
SPRINGFIELD, VA. 22161

BIBLIOGRAPHIC DATA SHEET

1. Report No.
CRC-APRAC-CAPA-1-69-3

2.

3. Recipient's Accession No.

4. Title and Subtitle
Study of Factors Affecting Reactions in Environmental Chambers -- Final Report -- Phase III

5. Report Date
June 30, 1975

6.

7. Author(s)
Raphael J. Jaffe

8. Performing Organization Rept. No.
LMSC-D406484

9. Performing Organization Name and Address
Lockheed Missiles & Space Company, Inc.
P. O. Box 504
Sunnyvale, California 94088

10. Project/Task/Work Unit No.

11. Contract/Grant No.

12. Sponsoring Organization Name and Address
Environmental Protection Agency, Research Triangle Park, North Carolina 27711 and Coordinating Research Council, Inc., 30 Rockefeller Plaza, New York, New York 10020

13. Type of Report & Period Covered
Phase III Final Report

14.

15. Supplementary Notes
Not releasable to the general public until August 1, 1976

16. Abstracts

An experimental study has been conducted of effects of materials, spectrum, surface/volume ratio (S/V) and cleaning technique on the photochemical reactions observed in a smog chamber. A unique chamber and lighting system was used, which permitted independent variation in chamber materials and in light conditions. A xenon arc lamp-parabolic relector combination provided a collimated light beam. By orienting plates of materials parallel to the beam, it was possible to independently vary light conditions and materials.

17. Key Words and Document Analysis. 17a. Descriptors

Irradiation Chamber
Illuminator
NO_2-NO_x
Ozone
Hydrocarbons
Propylene
Acetaldehyde
Peroxyacetly Nitrate (PAN

Aluminum
Stainless Steet
Air Pollution

17b. Identifiers/Open-Ended Terms

17c. COSATI Field/Group 07C; 07E; 07B; 20F; 04B; 13B

PRICES SUBJECT TO CHANGE

18. Availability Statement
Releasable to the general public

19. Security Class (This Report)
UNCLASSIFIED

20. Security Class (This Page)
UNCLASSIFIED

21. No. of Pages
234

22. Price
$8.00

FORM NTIS-35 (REV. 3-72)

THIS FORM MAY BE REPRODUCED

USCOMM-DC 14952-P72

LMSC-D406484
June 30, 1975

STUDY OF FACTORS AFFECTING REACTIONS IN ENVIRONMENTAL CHAMBERS

Final Report
by Raphael J. Jaffe

Prepared for
COORDINATING RESEARCH COUNCIL
New York, N.Y.
Under Contracts CAPA 1-69(1-72) and (1-73)
and
ENVIRONMENTAL PROTECTION AGENCY
Research Triangle Park, North Carolina
Under Contract 68-02-0287 and 68-02-1270

Biotechnology
Lockheed Missiles & Space Company, Inc.
Sunnyvale, California

i (a)

PROJECT PERSONNEL

Name	Area of Contribution
Raphael J. Jaffe	Project Direction
Frank C. Smith, Jr.	Analytical Chemistry/Chamber Operation
Ken W. Last	Statistical Analysis
Michael W. Reeder	Statistical Analysis
E. H. Kawasaki	Analytical Chemistry
R. C. Tuttle	Analytical Chemistry
Dr. H. S. Johnston, Consultant	Photochemistry

PROJECT MONITORSHIP
COORDINATING RESEARCH COUNCIL
PROJECT CAPA 1-69

Member	Affiliation
Mr. D. B. Wimmer, Chairman	Phillips Petroleum Company
Mr. Frank Bonamassa	California Air Resources Board
Mr. Basil Dimitriades	Environmental Protection Agency
Dr. J. M. Heuss	General Motors Corporation
Mr. Stanley Kopezynski*	Environmental Protection Agency
Dr. Hiromi Niki	Ford Motor Company
Dr. E. E. Wigg	Esso Research & Engineering Company

---

*Until January 1973

SUMMARY

An experimental study has been conducted of effects of materials, spectrum, surface/volume ratio (S/V) and cleaning technique on the photochemical reactions observed in a smog chamber. A unique chamber and lighting system was used, which permitted independent variation in chamber materials and in light conditions. A xenon arc lamp-parabolic reflector combination provided a collimated light beam. By orienting plates of materials parallel to the beam, it has been possible to independently vary light conditions and materials.

The propylene (3 ppm)/NO_x (1.5 ppm) reaction system was used, at 95° F and 25% relative humidity. Initial NO_2 content was nominally 10% of NO_x. Chamber background was <0.1 ppm C. All photochemical runs were at k_d of 0.3 min^{-1} as determined by frequent NO_2 in N_2 photolysis tests.

The study included four materials – Teflon, Pyrex, aluminum and stainless steel, and two conditions each of spectrum, S/V, and cleaning. A complete factorial testing sequence was performed, with many replicates. Effects of the four materials and the two levels of each parameter have been determined. The base chamber was mainly Pyrex at an S/V of 1.4 ft^{-1}. The four materials were added to the chamber at S/V of 1.3 and 2.7 ft^{-1}. The full spectrum extends from 300 nm to higher wavelengths, simulating sunlight at the earth's surface. The cut spectrum starts at 340 nm. Two cleaning methods – vacuum offgassing or purging at 110° F – were used.

The table below summarizes the results by giving the data averaged in several ways for each material. For each material, eight conditions (2 spectrum × 2 S/V × 2 cleaning) were used and the "all runs" average gives the average result. "Full Spectrum" average gives the average of the four (2 S/V × 2 Cleaning) conditions at full spectrum; and "Cut Spectrum" gives the average of the four conditions at cut spectrum. High S/V-Low S/V and Vacuum Clean-Purge Clean averages have similar meanings. The last entry-Full, Low S/V, Purge gives the results for that specific condition.

Of the three factors studied, spectrum is the factor that has the largest effect. The presence of this large spectral effect at constant light intensity – as measured by constant k_d – was not anticipated. However, it has been explained by consideration of the spectrally sensitive photochemical reactions, and in fact appears upon reinterpreting old literature data. The cut-off spectrum lowers the photochemical reaction rate by about 50%, as compared to the full spectrum. Chamber size (S/V) is the next most important factor, and the larger chamber usually shows a higher oxident maximum and a slower reaction. Cleaning technique is important for maximum oxidant (vacuum cleaning gives higher values) and in the behavior of stainless steel.

The comparison between materials shows that stainless steel behaves in a manner unlike the other three materials. The photochemical reaction is slowest in the presence of Teflon, with increasing reaction rates for Pyrex, aluminum, and stainless steel.

Tests were also conducted at lower relative humidity. For stainless steel and aluminum, lowering the relative humidity lowered the reaction rate. For Teflon, the opposite effect occurred.

Several runs were conducted for the n-butane (3 ppm)/NO_x (0.6 ppm) system. Results for the full spectrum conditions were similar to those previously reported in the literature.

The ultimate goal of this project was to determine how various design and operational factors affect reactions in smog chambers, in an attempt to reconcile the observations reported from some ten smog chambers previously involved in a round-robin test program. Regression equations have been determined that account for 75 to 90% of the observed variability. These models use the following independent variables: chamber material S/V, chamber light intensity (k_d), spectral distribution correction factor, chamber volume, and initial conditions.

RESULTS SUMMARY

	Material			
	Teflon	Pyrex	Aluminum	Stainless Steel
NO_2 FORMATION RATE (ppb/min)				
Averages				
All runs	8.63	10.0	13.1	25.4
Full Spectrum	10.2	12.6	15.3	30.2
Cut Spectrum	7.4	7.4	10.9	20.6
High S/V	8.50	9.7	13.3	32.2
Low S/V	8.76	10.4	12.9	18.6
Vacuum Clean	7.77	10.2	12.4	20.2
Purge Clean	9.58	9.7	13.8	30.5
Full, Low S/V, Purge	11.1	10.1	18.1	25.6
TIME TO NO_2 MAXIMUM				
All runs	154	131	106	70
Full Spectrum	116	94	86	56
Cut Spectrum	192	168	126	84
High S/V	144	150	106	59
Low S/V	164	112	106	81
Vacuum Clean	178	129	118	80
Purge Clean	162	132	110	60
Full, Low S/V, Purge	115	102	76	61
TIME TO 50% PROPYLENE CONSUMPTION (min)				
All runs	180	157	133	97
Full Spectrum	145	179	111	80
Cut Spectrum	215	135	154	114
High S/V	172	119	135	86
Low S/V	187	195	131	108
Vacuum Clean	183	153	139	87
Purge Clean	177	161	127	107
Full, Low S/V, Purge	144	120	92	81

	Teflon	Pyrex	Aluminum	Stainless Steel
MAXIMUM OXIDANT CONCENTRATION (ppm)				
All runs	1.03	.93	1.00	.90
Full Spectrum	1.13	.98	1.02	1.10
Cut Spectrum	.93	.89	.98	.70
High S/V	1.00	.87	.93	.97
Low S/V	1.06	.99	1.07	1.03
Vacuum Clean	1.11	1.00	1.04	.92
Purge Clean	.96	.87	.96	.88
Full, Low S/V, Purge	1.11	.98	1.04	1.14

CONTENTS

Section		Page
	PROJECT PERSONNEL	ii
	SUMMARY	iii
	ILLUSTRATIONS	xi
	TABLES	xiii
1	INTRODUCTION	1-1
2	EXPERIMENTAL METHOD	2-1
	2.1 Test Conditions	2-1
	2.2 Apparatus	2-2
	2.2.1 Irradiation Chamber	2-2
	2.2.2 Illuminator	2-8
	2.2.3 Thermal Enclosure	2-9
	2.2.4 Material and S/V Changes	2-11
	2.2.5 Spectral Distribution and Spectral Changes	2-13
	2.2.6 Cleaning Technique	2-15
	2.2.7 Chamber Charging Technique	2-16
	2.3 Chemical Analysis Methodology	2-16
	2.3.1 NO_2-NO_x	2-16
	2.3.2 Ozone	2-19
	2.3.3 Total Hydrocarbons	2-21
	2.3.4 Propylene	2-22
	2.3.5 Acetaldehyde	2-22
	2.3.6 Peroxyacetyl Nitrate (PAN)	2-22
	2.3.7 Moisture (Water)	2-23
3	RESULTS	3-1
	3.1 Detailed Statistical Analysis	3-10
	3.1.1 Covariate Analysis	3-10
	3.1.2 Principal Components	3-10

Section | Page

3.1.3 Effects by Materials 3-11
3.2 Material Differences 3-16
3.3 Effects of Factors 3-16
3.4 Ozone Decay Results 3-18
3.5 Relative Humidity Effects 3-19
3.6 Butane Runs 3-22
3.7 Background Reactivity Runs 3-24
3.8 "Virgin Surface" Effect 3-24
3.9 Nitrogen Balance 3-25
4 DISCUSSION 4-1
4.1 General Observations 4-1
4.2 NO_2 Photolysis Distribution 4-3
4.3 Possible Mechanisms 4-4
4.4 Background Reactivity Runs 4-6
4.5 Ozone Decay Results 4-7
5 RECONCILIATION OF CAPI-6 DATA 5-1
5.1 CAPI-6 Data Handling 5-4
5.2 Factorial Experiment Data Handling 5-4
5.3 Multiple Regression Results 5-5
5.4 Normalization for k_d Effects 5-13
5.5 Computations Using Normalized CAPI Data 5-16
5.6 Correlation Coefficients 5-16
6 RECOMMENDATIONS 6-1
REFERENCES R-1

Appendix

A PHOTOCHEMICAL RUN DATA A-1
A.1 Propylene Graphs A-1
A.2 Propylene Data Tabulation A-1
B STATISTICAL ANALYSIS B-1
1.0 Introduction and Overview B-1
2.0 Background B-3
2.1 The Experimental Design B-4

Section Page

2.2 The Data B-4
2.3 Covariates B-4
2.4 The Unbalanced Design and Its Consequences B-7
2.5 Principal Comments B-8
2.6 Outliers B-8
2.7 Time Trends B-10
  2.7.1 Drifts within Material B-15
  2.7.2 Material to Material Time Drift Analysis B-20
2.8 Computer Program B-23
3.0 Covariance Analysis B-24
3.1 Univariate Covariance Results B-24
3.2 Multivariate Covariance Results B-26
3.3 Comparison of Covariate Corrected Data to Adjusted Data B-29
4.0 Analysis of Variance B-29
4.1 Results of Univariate Analysis B-32
4.2 Results of Multivariate Analysis B-39
5.0 Principal Components B-46
5.1 Selection B-46
5.2 Calculation B-51
  5.2.1 Time B-53
  5.2.2 Dose B-53
  5.2.3 MISC I and MISC II B-54
5.3 Results and Interpretation B-55
  5.3.1 Stainless Steel B-55
  5.3.2 Teflon B-73
  5.3.3 Pyrex B-81
  5.3.4 Aluminum Reruns B-88
5.4 Univariate Analysis B-96
5.5 Results of Multivariate Analysis B-102
5.6 Recommended Model B-102

ILLUSTRATIONS

Figure		Page
2-1	Smog Chamber Assembly	2-4
2-2	Stand Assembly	2-6
2-3	Environmental Chamber Showing Side Stream Mixer, Charge Ports, and Clean-Out Port	2-7
2-4	Chamber Inside Thermal Enclosure	2-10
2-5	Arrangement of Surface Plates	2-12
2-6	Measured Spectral Irradiance Inside LMSC Smog Chamber – Full and Cut Spectra	2-14
2-7	Typical Raw Data for Determining k_d	2-15
2-8	Smog Chamber During Vacuum Off-Gassing Cleaning	2-17
2-9	Typical Linearity Check of NO Instrument	2-20
3-1	Composite Photochemical Test Results for Teflon Film Surfaces	3-5
3-2	Composite Photochemical Test Results for Pyrex Surfaces	3-5
3-3	Composite Photochemical Test Results for Aluminum Surfaces	3-5
3-4	Composite Photochemical Test Results for Stainless Steel Surfaces	3-5
4-1	Distribution of NO_2 Photodisintegrations for Various Spectra	4-3
B5-1	Time to NO_2 Maximum vs NO_2 Formation Rate	B-50
B5-2	Dose vs. Run Sequence	B-63
B5-3	Time vs Run Sequence	B-63
B5-4	Misc I vs Run Sequence	B-65
B5-5	Misc II vs Run Sequence	B-65
B5-6	Stainless Steel Dose vs Time	B-67
B5-7	Stainless Steel Misc I vs Time	B-68
B5-8	Stainless Steel Misc II vs Time	B-69
B5-9	Stainless Steel Dose vs Misc I	B-70
B5-10	Stainless Steel Dose vs Misc II	B-71
B5-11	Stainless Steel Misc I vs Misc II	B-72

Figure		Page
B5-12	Teflon Dose vs Time	B-75
B5-13	Teflon Misc I vs Time	B-76
B5-14	Teflon Misc II vs Time	B-77
B5-15	Teflon Dose vs Misc I	B-78
B5-16	Teflon Dose vs Misc II	B-79
B5-17	Teflon Misc I vs Misc II	B-80
B5-18	Pyrex Dose vs Time	B-82
B5-19	Pyrex Misc I vs Time	B-83
B5-20	Pyrex Misc II vs Time	B-84
B5-21	Pyrex Dose vs Misc I	B-85
B5-22	Pyrex Dose vs Misc II	B-86
B5-23	Pyrex Misc I vs Misc II	B-87
B5-24	Aluminum Dose vs Time	B-89
B5-25	Aluminum Misc I vs Time	B-90
B5-26	Aluminum Misc II vs Time	B-91
B5-27	Aluminum Dose vs Misc I	B-92
B5-28	Aluminum Dose vs Misc II	B-93
B5-29	Aluminum Misc I vs Misc II	B-94
B5-30	Mean Values by Materials	B-95

TABLES

Table		Page
1-1	Characteristics of Chambers Used for Previous Intercomparison Investigations	1-2
2-1	Chamber Description	2-8
3-1	Photochemical Test Calculated Parameter Definitions	3-2
3-2	Effects by Material	3-6
3-3	Effects by Material	3-12
3-4	Significant Effects by Materials	3-17
3-5	Maximum Ozone Concentrations (ppm)	3-17
3-6	Cut/Full Spectrum Ratio	3-16
3-7	Ozone Half-Life Study	3-18
3-8	Correlation of Ozone Half-Life with Run Parameters Averaged Over Cleaning	3-20
3-9	Relative Humidity Variation Effects	3-21
3-10	Butane Effects by Materials	3-23
3-11	NO_2 at Maximum/NO_x Initially	3-26
3-12	NO_2 Rate Divided by NO Rate	3-27
4-1	"Mylar/Teflon" Spectral Effect	4-2
4-2	Spectral Effect on Time to NO_2 Maximum Caused by Each Species	4-6
4-3	Background Reactivity Results	4-7
5-1	Chamber Characteristics	5-2
5-2	CRC-APRAC Irradiation Chamber Comparison	5-3
5-3	Results of Multiple Regression with Full Model	5-7
5-4	Run Parameters Predicted From Multiple Regression	5-8
5-5	Run Parameters Residuals from Multiple Regression	5-9
5-6	Normalized Residuals from Multiple Regression	5-10
5-7	Comparison of R^2 from Dual and Single k_d Models	5-11
5-8	Reduced Multiple Regression Models	5-12

Table		Page
5-9	Effect of k_d Variation	5-14
5-10	CAPI Chambers Adjusted to k_d of 0.4	5-15
5-11	Correlation Coefficients of Run Parameters	5-17
5-12	Correlation Coefficients of Run Parameters and Ozone Half-Lives	5-19
B2-1	Standard Deviation of Parameters	B-6
B2-2	Rank Sum and Sign Test Results for Adjusted Data	B-16
B2-3	Sign Test Results for Covariate Corrected Data	B-17
B2-4	Covariate Corrected Data (Original Alum Omitted)	B-18
B2-5	Means by Material	B-21
B3-1	Univariate Covariate Adjustment Coefficient	B-25
B3-2	Multivariate Covariate Adjustment Coefficients	B-27
B3-3	Results of Covariate Multrivariate Forward Approach	B-28
B3-4	Comparison of Covariate Corrected Data to Adjusted Data	B-30
B4-1	Contrasts Used in the Analyses of Variance	B-31
B4-2	Significance of Effects & Interactions on Univariate Data Given HC Init and % NO_2	B-33
B4-3	Univariate Prediction Coefficients for Covariate Adjusted Data	B-34
B4-4	Significance of Univariate Material Contrasts Given HC Init and % NO_2	B-38
B4-5	Univariate Original Aluminum Analysis, After HC Init and % NO_2	B-40
B4-6	Univariate Pyrex Analysis After HC Init and % NO_2	B-41
B4-7	Univariate Teflon Analysis, After HC Init and % NO_2	B-42
B4-8	Univariate Stainless Steel Analysis, After HC Init and % NO_2	B-43
B4-9	Univariate Rerun Aluminum Analysis, After HC Init and % NO_2	B-44
B4-10	Abbreviated MANOVA, Given HC Init, TADJ, and NO_x	B-45
B5-1	Correlation Coefficients for Unadjusted Data	B-46
B5-2	Correlation Coefficient for Adjusted Data	B-48
B5-3	Correction Coefficients for Covariate Adjusted Data	B-49
B5-4	Ratio of Mean Variation to Error Variation	B-52
B5-5	Transformations Used in Obtaining Principal Components	B-56

Table		Page
B5-6	Principal Components Values	B-57
B5-7	Material Effects for Principal Components	B-74
B5-8	Univariate Tests of Effects	B-97
B5-9	Univariate Tests of Reduced Models	B-98
B5-10	Optimum Univariate Models on Principal Components	B-99
B5-11	Coefficients for Univariate Models After Prin Components	B-100
B5-12	Material Contrasts in Optimum Models	B-101
B5-13	By Materials	B-103
B5-14	Tests of Reduced "By Materials" Models	B-104
B5-15	"By Material" Prediction Coefficients for Univariate Principal Components Data	B-105
B5-16	Multivariate Test of Effects	B-106
B5-17	Coefficients for Multivariate Model After Principal Components	B-107

Section 1

INTRODUCTION

Chambers in which systematic studies can be made of the reactions between hydrocarbons and nitrogen oxide in the presence of simulated sunlight have been in use for some twenty years. Such chambers have generally been successful in simulating the gross features of photochemical smog, such as production of oxidants and eye irritants, and haze. Intercomparison of the results obtained in these smog chambers has not been extensively attempted until relatively recently (Ref. 1), at which time the interest in individual hydrocarbon reactivity measurements led to an understanding of the need to compare the various facilities. Intensive comparisons of results obtained in ten smog chambers have been performed by the Coordinating Research Council project CAPI-6, Techniques for Irradiation Chamber Studies, and CAPA 1-69 (Factors Affecting Reactions in Environmental Chambers). The range of physical characteristics of these chambers is shown in Table 1-1. A group of round-robin tests was conducted using these chambers as follows: (1) irradiation of seven different hydrocarbons with nitrogen oxide; (2) replicate runs to establish reproducibility using the propylene-nitrogen oxide system; (3) a reactant concentration study in which 3.0 ppm propylene was reacted with 3.0, 1.5, and 0.5 ppm nitrogen oxides (Ref. 2).

The differences observed among the chambers could not be accounted for analytically, and an experimental study of how various design and operational variables affect the photochemical reactions observed in smog chambers was instituted. This is a report of the results of this study, which are also the first reported results for a smog chamber illuminated by a xenon arc lamp. The facility was developed and initial tests performed under Phase I of the project, which has been previously reported (Ref. 3). This report covers Phase II and III of the project, and includes all information contained in the Phase II report (Ref. 4).

Table 1-1

CHARACTERISTICS OF CHAMBERS USED FOR PREVIOUS INTERCOMPARISON INVESTIGATIONS

Volume (ft^3)	2.9 to 1140
Surface/Volume Ratio (ft^{-1})	0.78 to 4.91
Surface Type as S/V	
Stainless Steel	0 to 2.44
Aluminum	0 to 0.92
Glass	0 to 2.81
Plastic Film	0 to 0.83
Light Intensity (k_d, min^{-1})	0.16 to 0.6
Type of Lighting	Fluorescent lamp combinations, of sunlamps, black lamps, and blue lamps (both internal and external)

Section 2
EXPERIMENTAL METHOD

2.1 TEST CONDITIONS

The following combinations of factors have been studied in a full factorial test plan:

Materials	S/V	Spectrum	Cleaning
Aluminum	2.7 ft^{-1}	Full	Vacuum Off-gas
Pyrex	1.3 ft^{-1}	Cutoff	Purge at 110°F
Teflon			
Stainless Steel			

The testing sequence consisted of performing the photochemical tests for the aluminum surfaces, followed by Pyrex, Teflon, stainless steel, and a retest of the aluminum. This has allowed an analysis for time trend, to see if a systematic drift was present in the experiment. A number of replicate tests were performed. These were distributed among immediate replicates, replicates with 1 to 15 intervening runs, and the aluminum re-test replicates, which had greater than 50 intervening runs.

The propylene/NO_x system was used for most tests, at 3.0 ppm propylene and 1.5 ppm NO_x. The initial NO_2 content was nominally held at 10 percent. The chamber was held at 95 ± 3°F throughout all tests. Relative humidity was 25 ± 5 percent (49 to 59°F dew point). Chamber pressure was slightly above atmospheric (0.1 in. H_2O). Zero air was used to maintain chamber pressure, to make up for sampling and leakage, at about 3 percent/hour make-up rate. A series of tests were performed at lower relative humidity. Another set of tests were performed for the n-butane 3.0 ppm)/NO_x (0.6 ppm) system.

2.2 APPARATUS

The apparatus used was specifically designed to meet the objectives of the study by allowing independent variation in materials configuration, lighting conditions, and cleaning technique. The illuminator produces a collimated light beam. Plates of materials can be placed parallel to the beam axis without affecting the light conditions. This decoupling of light and materials allows independent variation of the two factors. Major apparatus items are the smog chamber, the xenon arc lamp illuminator, the thermal enclosure for the chamber, and the gas analysis instrumentation.

2.2.1 Irradiation Chamber

The irradiation chamber is hexagonal in cross section, measuring 54 in. across the diagonal of the cross section. The chamber configuration is shown in Fig. 2-1 and the chamber support stand is shown in Fig. 2-2. Figure 2-3 represents a pictorial view of the chamber. The chamber is constructed of six flat side panels that fit into an extruded aluminum framework. The aluminum framework is coated with 5 to 8 mils of FEP Teflon. The resultant panels are bolted together and are supported from circular rings on the stand.

The faces of the chamber are of tempered 1/4 in. Pyrex glass to admit the light and pass the beam through the chamber with minimal reflection or absorption. The flat sides of the chamber are also fabricated from 1/4 in. tempered Pyrex glass. The working stress of the tempered Pyrex is 3600 psi, which results in an allowable pressure differential of 7.1 in. of water. This is based on the hexagonal faces, which are the weakest members. Sealing of the 1/4 in. Pyrex to the aluminum extrusion is accomplished with silicon rubber gaskets that have been off-gassed at about 10^{-5} torr for over 24 hours. The gasket is fitted between the aluminum channel and the Pyrex, and the Pyrex is pressed into a channel section in the extrusion. A silicon rubber O-ring is used to seal adjacent aluminum extrusions which are bolted together. Additional sealing is accomplished with a coat of Dow Corning 30-121 RTV silicon rubber on all external joints.

Three 1-in. diameter ports are located in one of the lower side panels. The ports are fabricated from brass and are coated with FEP Teflon. Sealing of these ports to the Pyrex chamber walls is accomplished with silicon rubber gaskets. Sealing of tubes inserted into the ports is accomplished with Teflon seals. Tubes can be fitted into these ports and adjusted to various distances into the hexagon. The rear port is used for a gas thermocouple, which is Teflon coated and shielded from direct illuminator radiation. The front port has a 1-in. diameter Pyrex tube installed that is used for venting the chamber.

The center port is used for gas sampling. A 1-in. diameter Pyrex tube containing a concentric 7-mm tube is used. The sample enters at about the geometric center of the chamber, and is drawn to a sample manifold through a 1/4-in. Teflon tube, and thence to the analysis instrumentation. The sample contacts only Pyrex or Teflon before entering the instruments. Delay time from sample withdrawal to instrument inlet is about 30 seconds. The effect of this delay is discussed in Section 3.9.

A cleanout port is located in this same Pyrex panel. This port is 3-in. diameter and is used for chamber outgassing during vacuum off-gas cleaning. A Pyrex disc with a silicon rubber gasket is used to seal this port during normal operation. Metallic parts are all coated with FEP Teflon. A Pyrex relief valve is also mounted on this panel. This relief valve has a 2-in. diameter opening leading to the chamber. The valve utilizes a water seal principle and the relief setting is adjusted by the addition or withdrawal of water. Both negative and positive differential pressure protection are provided. An overflow trap is included to prevent water from entering the chamber.

A side stream mixer is also located on this panel. This mixer consists of a 6-in. diameter duct connected to the panel at a point 1/3 of the way from the front and 1/3 of the way from the rear of the chamber. Gas is circulated through the duct by means of a Teflon-coated fan blade installed in the duct. The blade is connected to a shaft that penetrates the duct through a rotary Teflon seal. The shaft is connected to a motor via a pulley and belt which are located outside the chamber. The fan is rotated

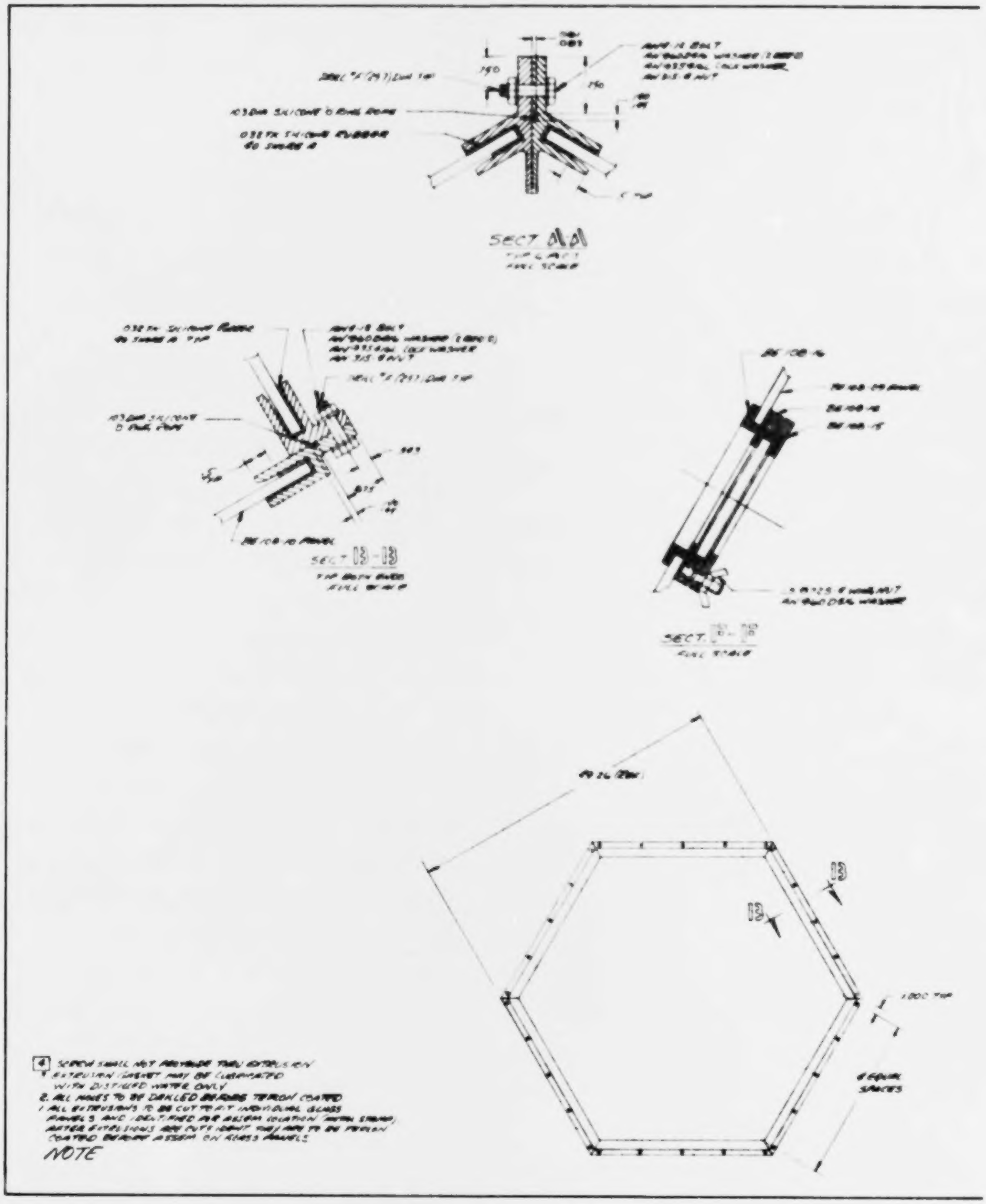
.150
.150
SECT AA
FULL SCALE
AN4-18 BOLT
SECT B-B
FULL SCALE
SECT
FULL SCALE
B
B
1.000 TYP
6 EQUAL SPACES
4
2. ALL HOLES TO BE DRILLED
NOTE

Fig. 2-1 Smog Chamber Assembly

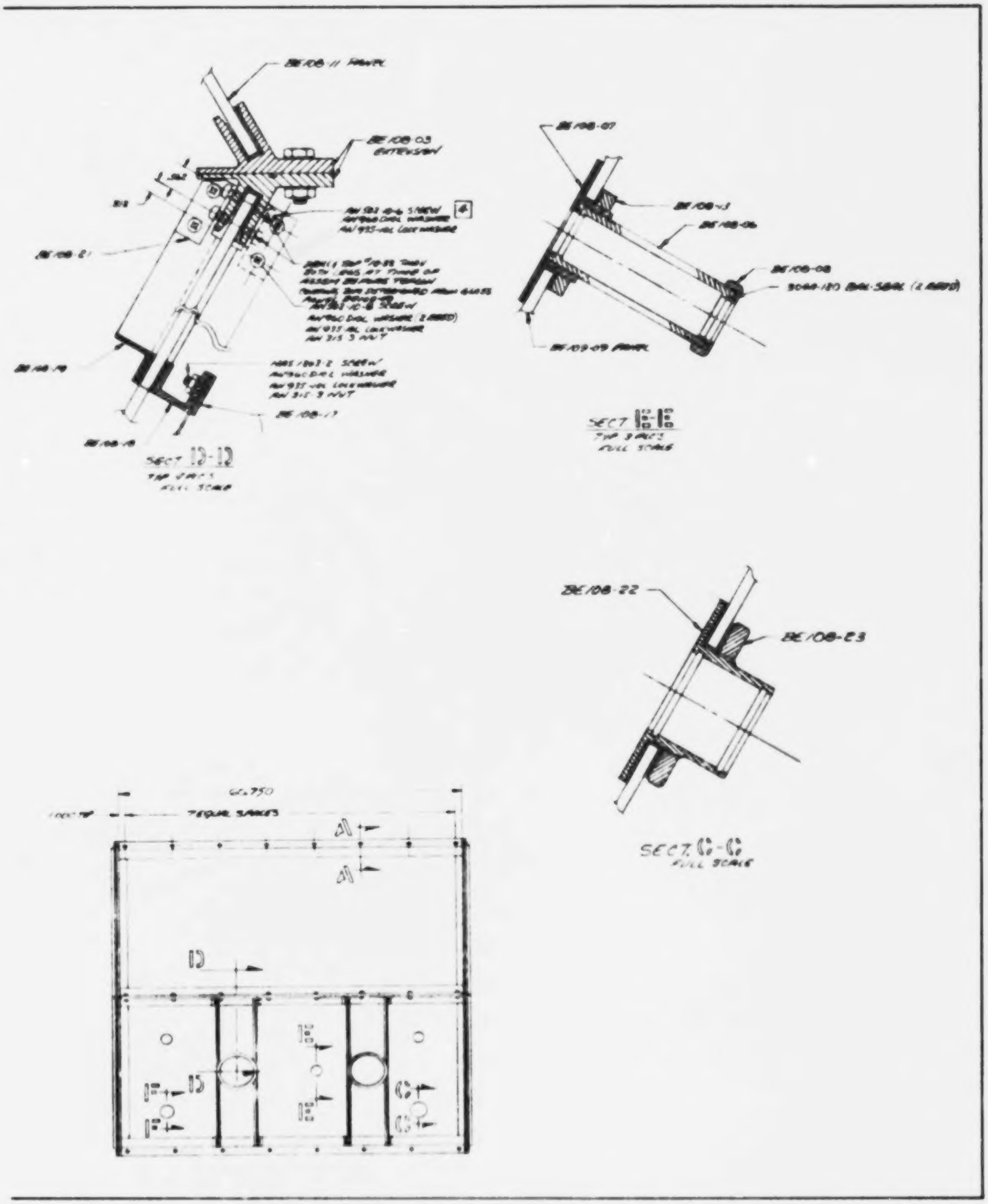
BE108-11 PANEL
BE108-03 EXTENSION
BE108-21
BE108-19
BE108-17
BE108-18
SECT D-D
TYP 2 PLCS
FULL SCALE
BE108-07
BE108-13
BE108-06
BE108-08
BE109-09 PANEL
SECT E-E
TYP 3 PLCS
FULL SCALE
BE108-22
BE108-23
SECT C-C
FULL SCALE
7 EQUAL SPACES
A
D
E
F
C

Fig. 2-1 Smog Chamber Assembly (Cont.)

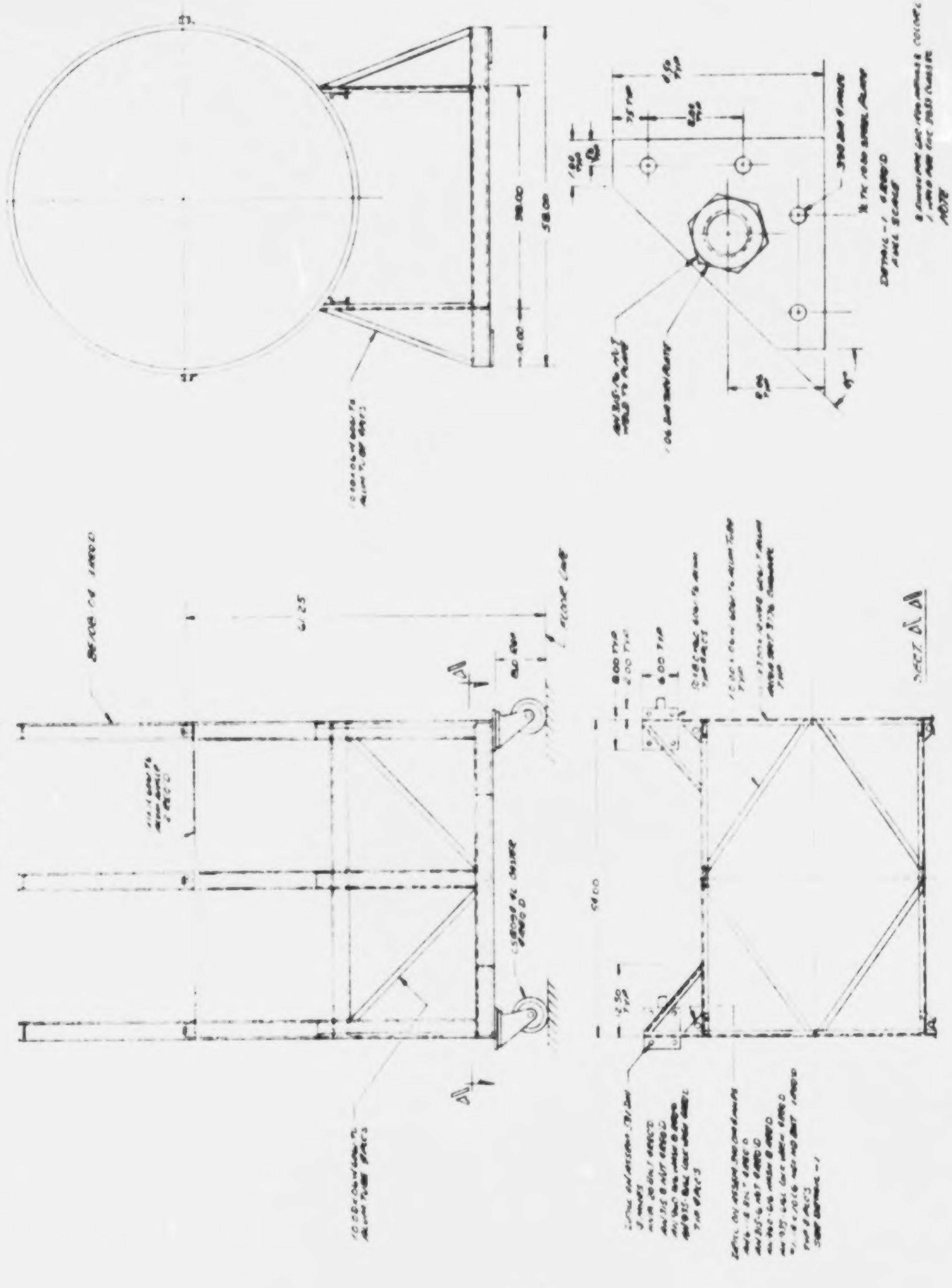

Fig. 2-2 Stand Assembly

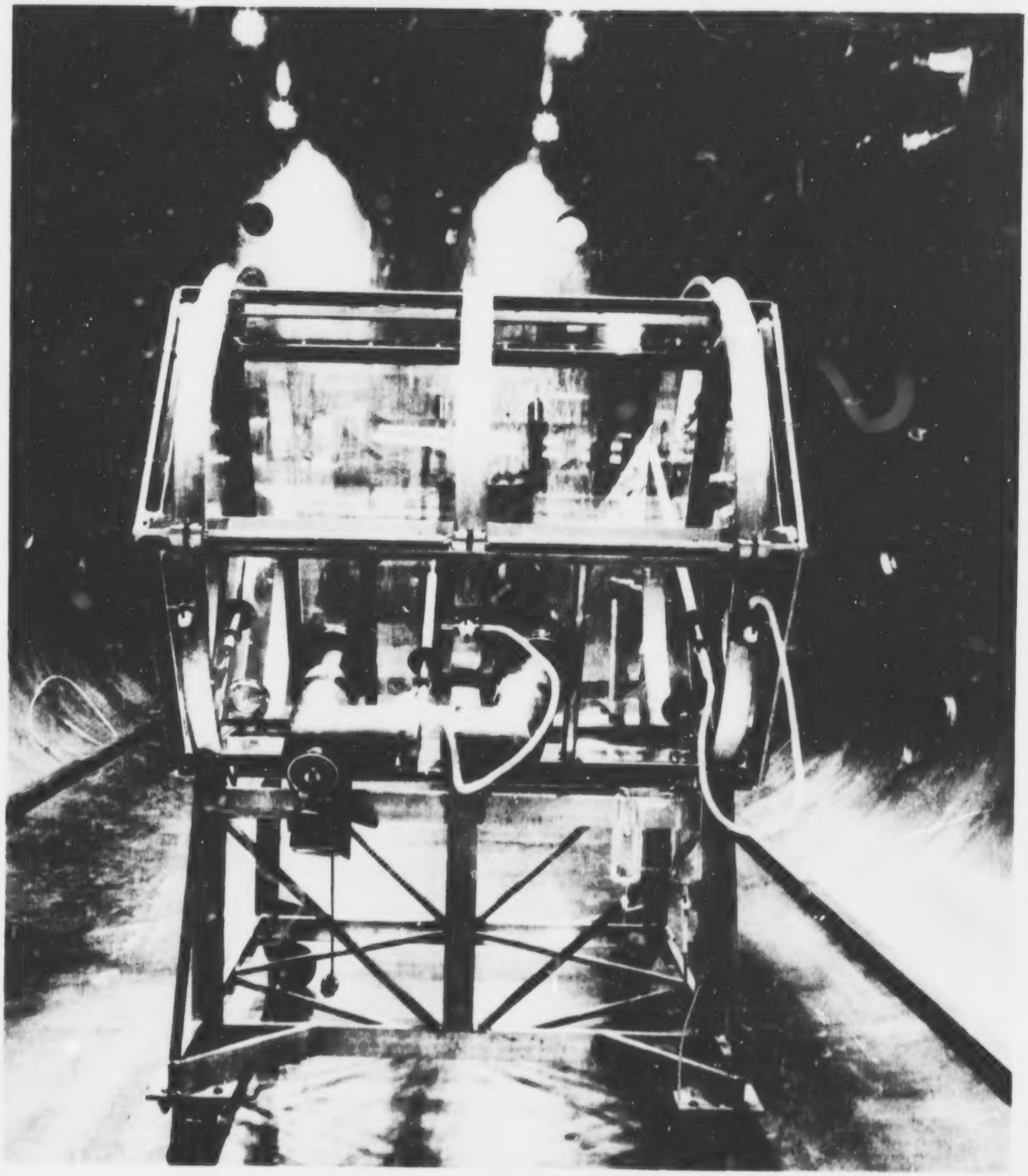

Fig. 2-3 Environmental Chamber Showing Side Stream Mixer, Charge Ports, and Clean-Out Port

at 250 rpm, producing a circulation rate of approximately 75 cfm. The inlet end of the duct enters the chamber at a 45-deg angle to minimize short circuiting of the gas circulation. All parts of the side stream recirculator are coated with Teflon. The mixer is operated during charging of the chamber only. It is shut off during photochemical tests.

The chamber is mounted at each hexagonal apex to a circular structural framework, which in turn mounts to a dolly with casters for easy transport of the chamber. The structural frame is configured to allow chamber assembly within the framework. A locating jack system is used to adjust the height of the chamber to exactly match the height of the light source.

Geometric characteristics of the chamber are summarized in Table 2-1.

Table 2-1

CHAMBER DESCRIPTION

Configuration	Hexagonal Prism
Length	60 in.
Diagonal	54 in.
Volume	65.9 ft^3
Surface Area	
End Plates	26.4 ft^2
Side Plates	67.5 ft^2
Total	93.9 ft^2
S/V	1.43 ft^{-1}

2.2.2 Illuminator

The irradiation source for the chamber is external to the chamber. This external source consists of an arc lamp situated in front of a large parabolic reflector.

Collimated energy from the reflector is directed toward the chamber. The collimated beam used as the light source for the irradiation chamber is 5 ft in diameter. The light source for the illumination system is an air cooled Osram compact xenon arc lamp (6,500 watt nominal rating). The fireball for the lamp is 2.4 by 9 mm. The optical system consists of a 5-ft diameter parabolic primary mirror and a spherical back-collector mirror. The primary mirror is made of copper with a rhodium plating with vacuum deposited aluminum over the rhodium. An SiO coating is used to protect the aluminum. Reflectance is approximately 0.9 at a wavelength of 300 nm. The spherical back reflector is similarly coated. The back reflector is utilized to capture energy from the lamp that would normally not strike the parabola, and focus it back on the parabolic reflector. The optical system collects about 35 percent of the lamp radiated light and directs it as a collimated beam into the chamber front face. The lampholder casts a shadow about 1.5 ft^2 in area, which obscures about 8 percent of the beam. As the chamber gases are well mixed, and all samples are taken from one representative lighted area of the chamber, the shadowed area of the chamber has no appreciable effect on the data.

For the cut spectrum configuration, a plane reflector is mounted behind the chamber rear face. This reflector provides a second pass of the light through the chamber. It is a front-surfaced, aluminized SiO_x-coated reflector, to maintain reflection down to 300 nm wavelength.

The illuminator is integrated into a searchlight housing. The housing is on casters, which allows the illuminator to be moved readily.

2.2.3 Thermal Enclosure

A thermal enclosure is used to control the chamber temperature during a photochemical run. Design requirements for the thermal enclosure are maintenance of chamber gas temperature at 95 ± 3° F. The enclosure, depicted pictorally in Fig. 2-4 with the chamber installed, consists of a plywood housing insulated with fiberglass, with heated air circulating throughout the enclosure. The enclosure has a hexagonal-shaped hole in the rear to allow the chamber to protrude. The front end of the thermal enclosure

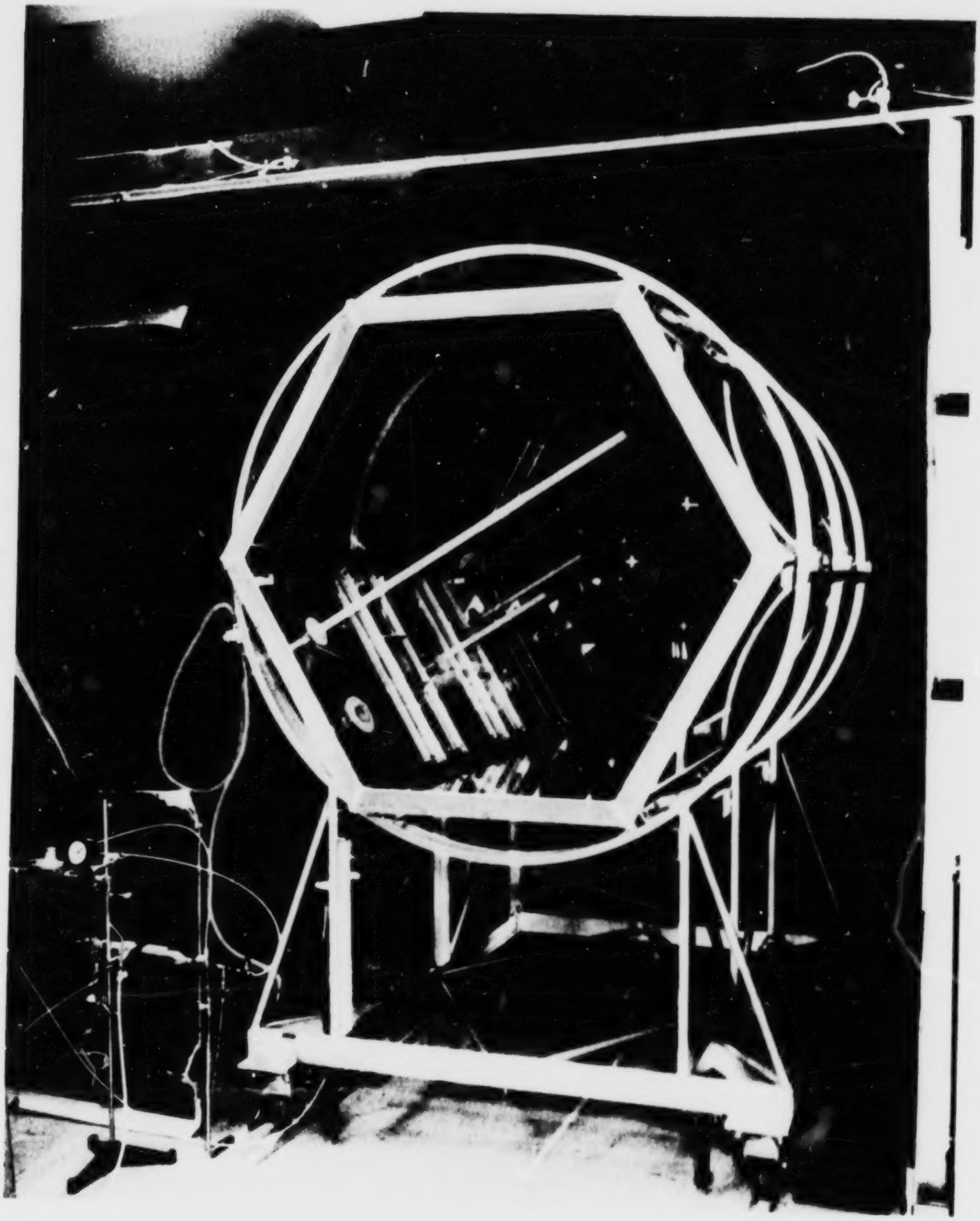

Fig. 2-4 Chamber Inside Thermal Enclosure

has sliding doors that allow easy removal and installation of the chamber. These doors also have a hexagonal-shaped hole that will allow the forward end of the irradiation chamber to protrude. This allows the illuminator energy to enter the chamber. Both the rear and forward hexagonal openings in the enclosure fit tightly to the chamber to minimize gas leakage from the enclosure. The interior surfaces of the enclosure are insulated with 3 in. of fiberglass.

A centrifugal blower is utilized to circulate approximately 1500 cfm of air over four 1.3-kw heaters that are used for thermal control. Three of the heaters are manually switched on or off and the fourth heater is thermostatically controlled to maintain the enclosure air temperature at a fixed level. This system allows use of the fixed heaters for purge cleaning, or warm-up, and coarse temperature control, with fine temperature control being accomplished with the thermostatically controlled heater. The thermal sensor is a West resistance bulb controller. This controls the air temperature in the thermal enclosure. Air circulation is accomplished with a centrifugal blower that passes air through plenums located at the bottom of the thermal enclosure. The heaters are located in these plenums. Air passes out of the plenums, over the chamber and is withdrawn out of the top of the thermal enclosure, where it is recirculated to the heater plenum. The thermal enclosure is approximately 8 ft high by 8 ft wide by 6 ft long.

2.2.4 Material and S/V Changes

Plates of the material under study are inserted into the chamber, oriented parallel to the light-beam axis of collimation, and vertically. These plates vary from 5-3/8 to 22-3/8 in. in width and are the height of the chamber. Plates are arranged in six sets, with each set running the length of the chamber. Frequent open spaces interrupt each set of plates, and form openings that are the height of the chamber and 2 to 4-1/2 in. wide, to allow the sampling and vent tubes to penetrate into the chamber, and to promote mixing of the entire chamber contents. Figure 2-5 gives the plate layout. Either six or three sets of plates are used, which gives either 2.7 or 1.3 ft^{-1}

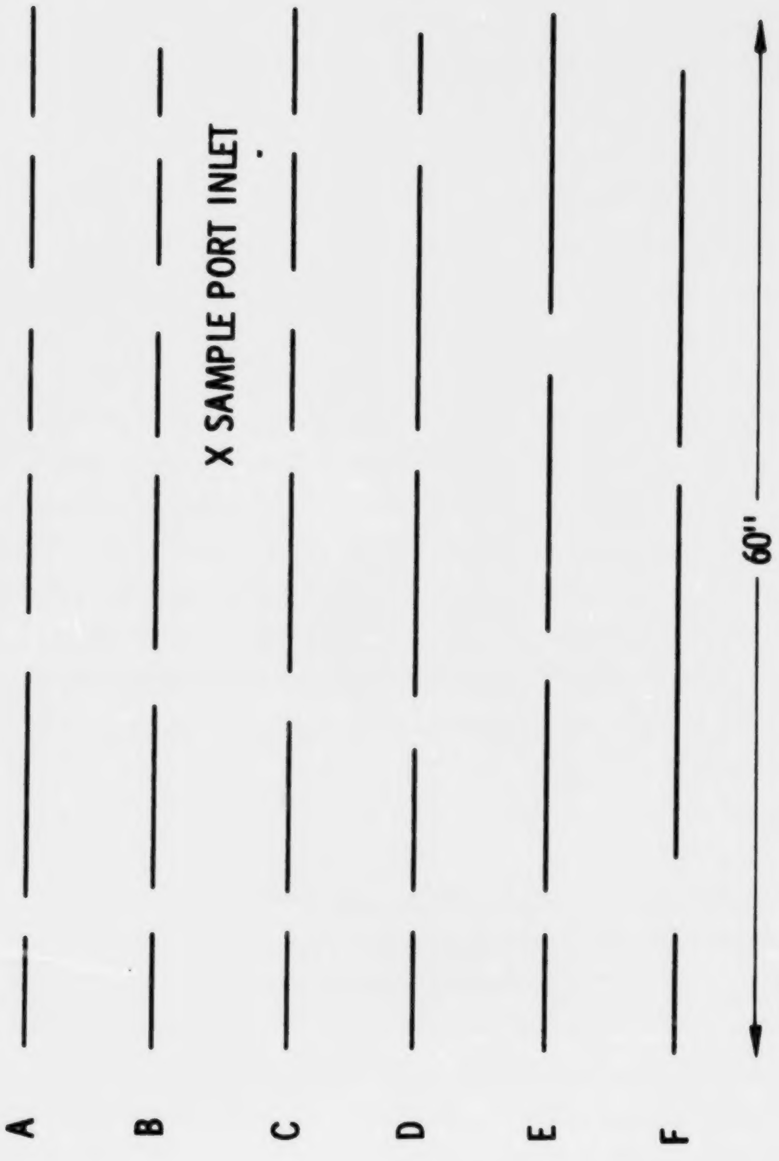
A
B
C
D
E
F
X SAMPLE PORT INLET
60"

NOTE: Plate sets B, C, E removed for low S/V configuration

Fig. 2-5 Arrangement of Surface Plates

of the material under study. The metallic materials are polished to a mirror finish. The materials details are aluminum – 1100 H 14 alloy, stainless steel – type 304, Pyrex-Corning 7740 plates, and Teflon – 5 mil FEP film.

2.2.5 Spectral Distribution and Spectral Changes

The spectral interval of interest in atmospheric photochemical simulation is 300 to about 400 nm. The lower wavelength is the natural cutoff provided by the earth's ozone layer, and the upper wavelength is set by the energy required to dissociate NO_2. It is generally recognized that compact xenon arc lamps provide the best available match for this UV region.

Two spectral distributions were used in these experiments. The full spectrum configuration is shown in Fig. 2-6. The second distribution is the cutoff spectrum, and is also shown in the figure. This is obtained by placing a sheet of 3/16 in. thick Plexiglas between the light source and the smog chamber. To avoid aging effects, a fresh sheet of Plexiglas is used after about each fifth test. Total light intensity is restored to the same value as used for the full spectrum runs by providing a second pass of the light through the chamber. The front surfaced aluminized reflector is used for this purpose.

Spectral data were taken with an Optronics Laboratory spectroradiometer. The radiometer consists of a calibrated photovoltaic cell, a grating prism spectrometer, and blocking filters. Digital readout is provided over a range of 10^{-9} to 10^{-2} watt/cm^2-nm. Bandpass is 5 nm. The unit is calibrated against an NBS standard quartz iodide lamp, over the wavelength interval of 250 to 1100 nm. Note that the characteristic xenon arc lamp peak at 467 nm is easily seen by the radiometer. These data are in agreement with earlier data taken using a photomultiplier tube spectroradiometer unit.

Measurements of the light beam were made at the plane corresponding to the front window of the chamber, and of the beam at the exit of the chamber, after passing through the front and rear 1/4-in. Pyrex window. To measure spectral irradiance inside the chamber, the rear window is removed, and the spectroradiometer entrance

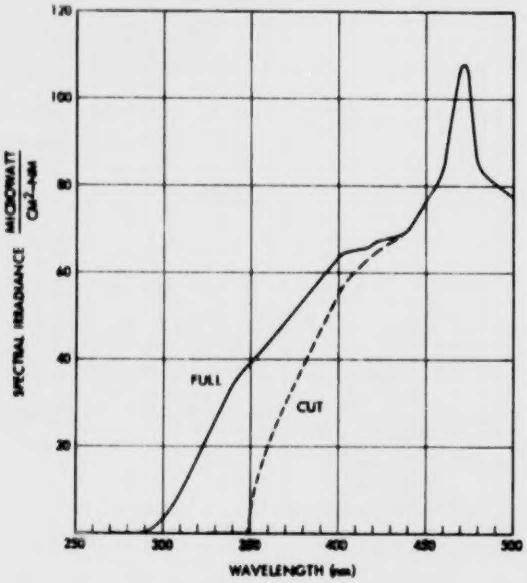

Fig. 2-6 Measured Spectral Irradiance Inside LMSC Smog Chamber – Full and Cut Spectra

slit positioned two inches inside the chamber from the plane of the rear window. These are the values shown in Fig. 2-6. Uniformity of radiation intensity was determined by measurements at six points across the face of the chamber. These are located 10 inches in from the apex points of the hexagonal, and give relative light intensities of 88, 96, 117, 89, 89, and 113% of the average (starting in the upper right corner of the hexagonal and going counter-clockwise). Such a distribution, with an increased intensity in the midplane of the beam, is normally expected for the optical system used. The spectral distribution at these six points was studied and did not vary with location.

Total light intensity has been maintained at k_d of 0.3 min^{-1} throughout the test series. To measure k_d the smog chamber is filled with pure N_2 (< 20 ppm O_2, < 0.1 ppm HC) and about 1.5 ppm NO_2 added. The lamp is turned on, allowed to stabilize, and the chamber illuminated for three or four successive one-minute intervals. The data are plotted on semi-log paper and usually show the expected upward deviation from linearity after the third one-minute interval. Two or three NO_2 instruments are used for each k_d determination, and usually agree within 10 percent. Figure 2-7 shows a typical plot.

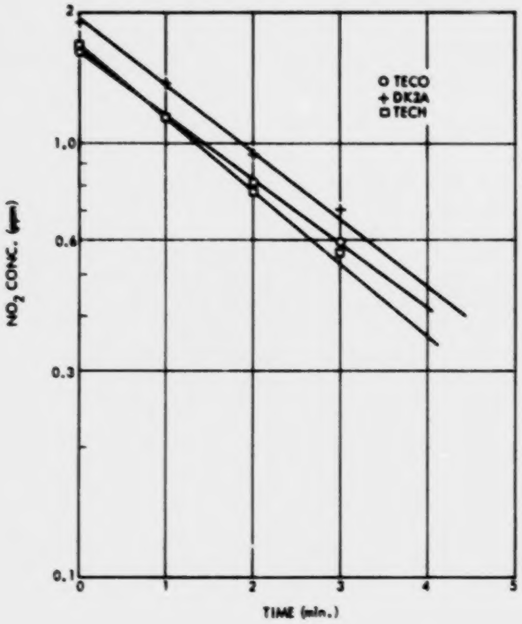

Fig. 2-7 Typical Raw Data for Determining k_d

To maintain the k_d constant throughout the study, lamp power was adjusted. Intensity was determined each time a new material was placed in the chamber and each time S/V was changed. Measurement of k_d was performed for both the full spectrum and the cut spectrum. On the average k_d was determined each four runs (including replicates). To guard against any unanticipated unusual drift in the lamp light output, an intensity meter was used to monitor the light. No unexplained readings were observed. It was thus concluded that the entire set of runs submitted for statistical analysis was performed at 0.3 min^{-1}, within perhaps a 10% variation.

2.2.6 Cleaning Technique

The two cleaning techniques used are: purging at 110° F, or vacuum off-gassing. Purge cleaning consists of holding the chamber overnight at a temperature of 110 ± 3° F while 4 to 6 chamber volumes of pure air are purged through the chamber. For vacuum off-gassing, the smog chamber is moved to an adjoining 18 by 18 by 36-ft vacuum chamber.

The vacuum chamber is pumped by Roots Blowers and mechanical pumps which prevents any back migration of pump oil. The chamber walls are 304 stainless steel, polished to a No. 4 mill finish. The smog chamber is held at about 2 microns pressure (or less) for at least 16 hours. During this time, the chamber is maintained at about 100° F. After the off-gassing, the smog chamber is repressurized by bleeding charge gas into the smog chamber while repressurizing the vacuum chamber. Figure 2-8 shows the smog chamber inside the vacuum chamber.

2.2.7 Chamber Charging Technique

The chamber is charged with synthetic compressed air. The air is purchased from a single vendor to a specification of <0.1 ppm total hydrocarbons (as methane), and <10 ppm hydrogen. The air is produced by combining nitrogen gasified from liquid nitrogen and electrolytic oxygen. The oxygen is made by electrolysis of distilled water. It then is further purified by catalytic combustion of the trace hydrogen, followed by molecular-sieve drying of the oxygen. A pre-charge determination of total hydrocarbons verifies the air purity. The chamber is charged through a stainless steel humidifier, packed with Rashig rings and filled with triple distilled water. Starting dew point is adjusted to 54 ±5° F by dilution with the dry pure air.

Reactants are added to the chamber from stock cylinders of about 350 ppm in nitrogen. The reactant blends are transferred using separate 1/2 liter sampling cylinders. The transfer cylinder is pressurized at about 200 psi, placed in the charge manifold, and slowly bled to the smog chamber. In this technique, the transfer cylinder pressure (which is read to 0.5 psi) becomes the reproducibility limit for the initial reactant charge.

2.3 CHEMICAL ANALYSIS METHODOLOGY

2.3.1 NO_2-NO_x

Nitrogen dioxide is monitored by the modified Saltzman-Lyskow wet chemical technique, utilizing a continuous sampling Technicon Autoanalyzer unit. The NO_2 absorbing solution is made from 2.0-gm N-1-naphthylethylenediamine dihydrochloride, 100-gm sulfanilic acid, 5-cc Kodak Photoflo, and 1 liter glacial acetic acid in 5 gallons of water. The lifetime of the solution is greater than 1 month when stored in an aluminum foil covered bottle and shielded from air exposure. The gas sampling system consists of

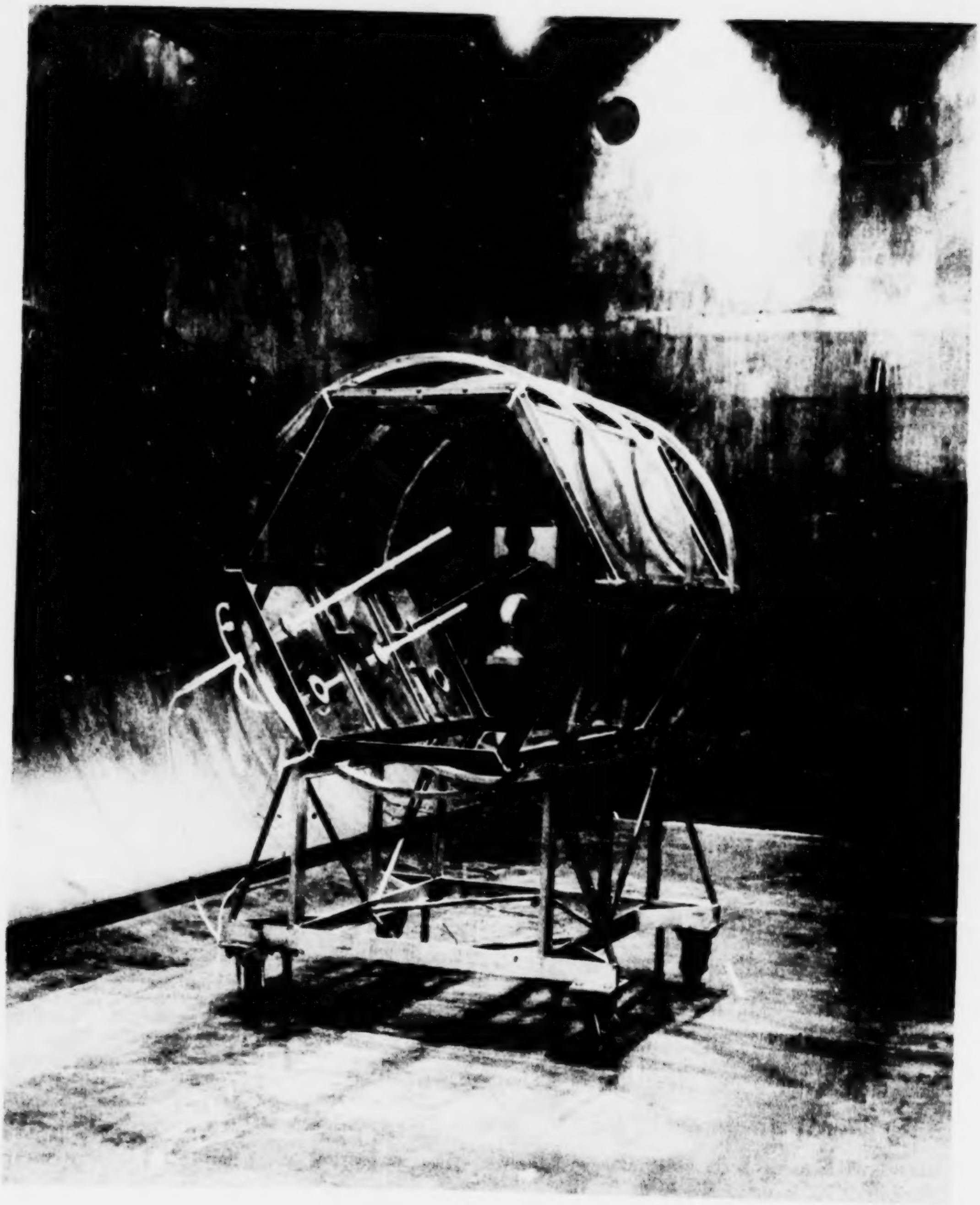

Fig. 2-8 Smog Chamber During Vacuum Off-Gassing Cleaning

two 15-cm by 2.4-mm I.D. (28 turn) glass mixing coils in series where the gas sample stream contacts the absorbing solution, an accumulator/liquid-gas separator, a flowmeter to measure sampling rate, a chain driven peristaltic pump using variable flow fluoroelastomer tubes, a colorimeter with a 50-mm flow cell, and an extended range recorder. Gas sampling rate is 150 cc/min and liquid sampling rate is 1.5 cc/min.

When new absorbing solution is prepared, a static calibration using $NaNO_2$ solutions ranging from 1.5×10^{-3} to 1.5×10^{-1} μl NO_2/ml is performed. NO_2 gas concentrations are determined from the formula

$$\text{pphm } NO_2 = \frac{(A)\ (B)}{(C)\ (D)}\ 100$$

where:

A = microliters NO_2 gas per milliliter of liquid standards

$$= \frac{(\text{mg/liter } NaNO_2)}{(\text{Mol wt. } NaNO_2)} \quad \frac{(24.5 \text{ liters/mole})}{0.72 \text{ moles } NaNO_2/\text{mole } NO_2}$$

where 24.5 is the molar volume at 25° C and 760 torr and 0.72 is the Saltzman factor

B = flow rate of absorbing solution reagent (ml/min)

C = gas stream flow rate (liters/min)

D = column efficiency (expressed decimally)

Daily dynamic calibrations are performed using standard Metronics 4-cm constant rate NO_2 permeation tube. The permeation tube is placed inside a constant-temperature condenser. Low NO_2 concentrations are obtained by passing compressed air through a calibrated flow meter and then sweeping the NO_2 from the permeation tube into a 12.5 liter dilution flask. The NO_2 stream enters the bottom of the flask and sampling is done at the top using a single 4-way path to the gas stream. The dilution flask pressure is measured with a -0.5 to +0.5 in. water Magnihelic gage and is adjusted with a vent line constriction to get pressure resembling chamber run conditions (+0.02 in. H_2O). The dilution system is all Teflon and glass except for small Tygon connections. The permeation tubes are calibrated gravimetrically and are within ±5% of the stated rates.

Permeation tube NO_2 concentrations are determined from the formula

$$C = \frac{(L)\,(K)\,(P_t)}{F} \times 100$$

where:

C = gas concentration (pphm)
L = length of permeation tube (cm)
K = molar volume/molecular weight = 0.532 for NO_2 at 25° C and 760 torr (liter/gm)
P_t = permeation rate of NO_2 at temperature t (ng/min per cm of tube length)
F = carrier gas flow rate past tube (cm^3/min)

Nitric oxide is continuously measured with a Thermo Electron Corporation Model 12A chemiluminescent gas monitor and Honeywell 18 recorder. This instrument measures the chemiluminescent reaction of NO and O_3. Gas flow to the instrument is 150 cc/min. The NO_x mode of the instrument uses a stainless steel converter run at 800° C to reduce NO_2 to measurable NO. Converter efficiency has been established at 99+ percent. Instrument zero, full scale and photomultiplier tube dark current are checked prior to turning on the O_3 generator. The instrument is calibrated daily by the dynamic NO_2 dilution gases and by a stock 88 ppm NO in N_2 standard gas. This stock gas was checked at 88 ppm by the supplier using long-path IR and a chemiluminescent monitor; and by an independent chemiluminescent monitor in an informal exchange. Linearity of the instrument is periodically confirmed by the exponential dilution technique. Precision is within 5 percent. Figure 2-9 shows an exponential dilution linearity check.

2.3.2 Ozone

Ozone is measured directly and continuously by a McMillan Model 1100 Ozone Meter. This instrument measures the chemiluminescent reaction of ozone and ethylene. The meter has four scales, with 0 to 2 ppm scale most commonly used. Daily meter calibration is done at 1 ppm before and after a photochemical run by using a McMillan 1000 ozone generator. The output of the generator is regulated by sliding cover for the UV lamp and output at 1.00 ppm (999 dial setting) is checked with a null meter. Periodic

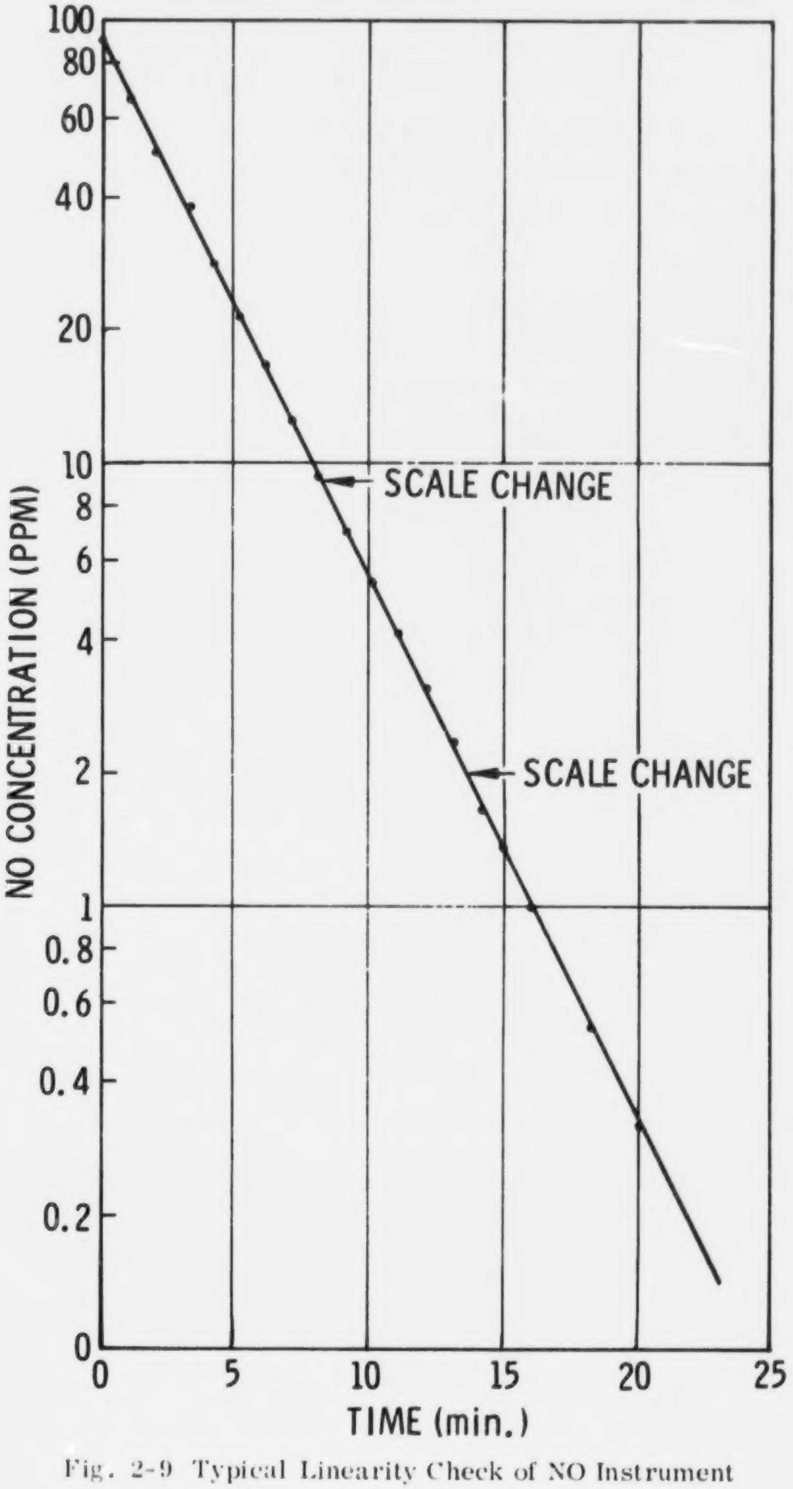

Fig. 2-9 Typical Linearity Check of NO Instrument

calibrations of the generator and meter are done with the neutral buffered KI technique. The 2-percent KI absorbing solution is calibrated with a stock I_2 solution titrated against standard $Na_2S_2O_3$. The absorbance of the resulting KI/I_2 solution is measured on a Perkin-Elmer 202 spectrometer at 350 nm. Precision is about 4 percent. In the first 20 months of usage of the ozone generator, the calibrations against neutral KI showed no significant drift (< 5%). The null meter-front panel adjustment potentiometer technique, which is used to maintain the ozone generating lamp light output, was evidently effective. At that time the generator malfunctioned and was returned for repair and recalibration. The good stability observed may also reflect the constant air flow system and the air pre-treatment. Room air is filtered through an MSA Type N canister and a pre-ozonation UV lamp. This lamp produces ozone which converts trace NO to NO_2. The air then goes through a molecular sieve 13X filter which destroys the ozone. This scheme avoids loss of part of the calibrated ozone output by the NO-O_3 reaction.

Ozone concentration is corrected by checking 1.00 ppm before and after a run. If a discrepancy is noted, the initial and final readings at 1 ppm from the generator are plotted linearly against time. Corrections are read from the line and applied to the readings. Corrections are applied if the meter is more than 5 percent different from the generator. The largest drift noted was about 18 percent.

2.3.3 Total Hydrocarbons

Chamber total hydrocarbons as CH_4 are monitored with a F&M Model 700 gas chromatograph with a Model 810 electrometer using an O_2-H_2 flame ionization detector and an unpacked 1/8 in. O.D. stainless steel column. Calibration is done from a zero air cylinder with a THC concentration of 0.07 ± 0.03 CH_4. The cylinder concentration was determined at the supplier and checked upon delivery. Chamber samples from the glass manifold are drawn through a 1/8 in. O.D. Teflon line and then through a sliding sampling valve by a small vacuum pump.

2.3.4 Propylene

Propylene is measured using the same detector and valve used for total hydrocarbons. A Carle Microvolume Switching Valve is used for analysis selection. The column for propylene is .6 ft × 1/8 in. 100/120 mesh Porapak S stainless steel. The oven temperature is 105° C; the detector is set at 150°; and the injection port is set at 125°. The sampling loop has a 5.0 cc volume, which gives an LLD of 0.03 ppm.

Calibration was done using a stock cylinder. The concentration and linearity from 0.05 to 3.00 ppm of the analysis were confirmed. Precision at 3.00 ppm is less than 5 percent.

2.3.5 Acetaldehyde

Acetaldehyde uses the other detector of Model 700 gas chromatograph and a separate Model 810 electrometer. The column is a 20-percent FFAP Chromosorb W (DMSC treated), 60/80 mesh, 20 ft × 1/8 in. stainless steel column. The 10.0 cc sampling loop and valve use the same Teflon line from the manifold and vacuum pump as do the propylene and total hydrocarbon analyses. Oven, detector, and injection port temperatures are the same as for propylene. Calibration is done with a stock cylinder and linearity has been established from 0.08 to 1.50 ppm, with an LLD of 0.03 ppm and precision less than 10 percent at 1.50 ppm. When the column is too noisy to give useful data, the Porapak S column used for propylene can be used for acetaldehyde analysis, although the acetaldehyde peak is broad and LLD is 0.07 ppm. A comparison of acetaldehyde concentration indicated by both columns shows quite good agreement.

2.3.6 Peroxyacetyl Nitrate (PAN)

Peroxyacetyl nitrate is measured on a Varian Model 600C gas chromatograph using a tritium electron capture detector with an N_2 carrier and a 5-percent Carbowax 600 on 60/100 mesh Chromosorb W (DMSC treated) 22 in. × 1/8 in. Teflon column run at ambient temperature (25° C). The 0.5 cc sampling loop is made of Teflon and gives an LLD of about 0.003 ppm PAN. Standards are prepared by irradiation of an ethyl nitrate-oxygen mixture with a UV lamp. Concentration of PAN in this standard is determined by infrared analysis, and the 10 cm cell containing the mixture is purged into a Tedlar bag with air measured by a wet test meter. Extensive calibration has shown good linearity from 0.05 to 1.0 ppm with precision estimated at 25 percent.

2.3.7 Moisture (Water)

Moisture content was monitored with a Cambridge System Model 992 Hygrometer. Samples were drawn periodically from the chamber manifold through a two-way sampling valve. Otherwise, room air was purged through the instrument allowing continuous instrument readout. Stable instrument response at 250 cc/min sample flow was less than 3 minutes for dew points ranging from 48° F to 56° F. Precision was less than 0.1 percent, based on saturation pressure.

Section 3

RESULTS

Behavior of photochemical reaction systems is usually characterized by a few chosen calculated parameters. In this work, the parameters used are those defined by the CAPI-6-69 Project, with the addition of several measures that appear interesting, for a total of 23, as defined in Table 3-1.

Parameter 17 was added to describe the NO disappearance as good NO data are available from the chemiluminescent instrument.

Parameters 18 and 19 are calculated to give additional insight into the NO_2 and oxidant dosage values, by normalizing them to a potential maximum dosage represented by the denominator.

Parameter 20 describes the NO_2 curve to some extent, by giving the full width at half maximum of the curve. It has been included to facilitate comparisons of the NO_2 curve shape on a numerical basis.

Parameters 21 to 23 give various defined intervals in the photochemical run. The crossover time is used because it is well demarked on the run graphs. Measuring time from the crossover time yields system behavior characteristics that are less dependent on initial conditions.

Table 3-1

PHOTOCHEMICAL TEST CALCULATED PARAMETER DEFINITIONS

NO_2 Formation

① Rate $= \frac{NO_i}{2T_{1/2}}$ where $T_{1/2}$ is the time to form an amount of NO_2 equal to 1/2 the initial NO in addition to the NO_2 present initially; and NO_i is the initial NO concentration in ppb (ppb/min)

② T_{max} = time, in minutes, to the maximum NO_2 concentration (min)

③ Dose $= \int_0^{300} NO_2\,dt$ where NO_2 is NO_2 ppm and t = minutes (ppm-min)

Oxidant Formation

④ Max. Rate $= \frac{\text{Max. Oxidant}}{2(T_{3/4} - T_{1/4})}$ where $T_{3/4}$ and $T_{1/4}$ are the times to form 3/4 and 1/4 the maximum oxidant; and max. oxidant is the maximum oxidant concentration (ppb/min)

⑤ Avg. Rate $= \frac{\text{Max. Oxidant}}{2T_{1/2}}$ where $T_{1/2}$ is the time to form 1/2 the maximum oxidant, and Max. Oxidant is the maximum oxidant concentration (ppb/min)

⑥ Max. Conc. = maximum oxidant concentration (ppm)

⑦ T_{max} = time to the maximum oxidant concentration (min)

⑧ Dose $= \int_0^{300}$ Oxid. dt where Oxid. is oxidant and t = minutes (ppm-min)

Hydrocarbon Disappearance

⑨ Final Conc. = ppm hydrocarbon after 300 minutes irradiation (ppm)

⑩ $T_{0.75}$, $T_{0.5}$ and $T_{0.25}$ = the times required to reduce the hydrocarbon concentration to 3/4, 1/2, and 1/4 of the original (min)

⑪

⑫

⑬ Max. Rate $= \frac{HC_i - HC_f}{2(T_{3/4} - T_{1/4})}$ where $T_{3/4}$ and $T_{1/4}$ are times for the disappearance of 3/4 and 1/4, respectively, of the hydrocarbon disappearing in 300 minutes; HC_i is the initial hydrocarbon concentration; and HC_f is the final hydrocarbon concentration (ppb/min)

Table 3-1 (Cont.)

⑭ Avg. Rate = $\frac{HC_i - HC_f}{2T_{1/2}}$ where $T_{1/2}$ is time for the disappearance of 1/2 the hydrocarbon disappearing in 300 minutes; HC_i is the initial hydrocarbon concentration; and HC_f is the final hydrocarbon concentration (ppb/min)

⑮ Max. Ald. = Maximum total aldehyde concentration (acetaldehyde for these runs) (ppm)

⑯ Max. PAN = Maximum peroxyacetylnitrate concentration (ppm)

⑰ NO Rate = $\frac{NO_i}{2T_{1/2}}$ where NO_i = initial NO and $T_{1/2}$ = time to reduce NO to half of original concentration (ppb/min)

⑱ NO_2 Dose Factor = $\frac{NO_2 \text{ Dose}}{300\ NO_{x_i}} \times 100$ where NO_{x_i} = initial NO_x (%)

⑲ Ozone Dose Factor = $\frac{\text{Ozone Dose}}{300\ NO_{x_i}} \times 100$ (%)

⑳ NO_2 FWHM = Full width at half-maximum of NO_2 curve (min)

㉑ Crossover Time = Time at which NO and NO_2 curves cross (min)

㉒ 2-21 = NO_2 T_{max} - Crossover time (min)

㉓ 7-21 = Ozone T_{max} - Crossover time (min)

The four materials affect the behavior of the propylene/NO_x reaction system differently. As a summary, Figs. 3-1 to 3-4 show the photochemical results for Teflon, Pyrex, aluminum, and stainless steel, respectively. Each figure gives the average for the two S/V ratios and the two cleaning techniques for each spectral distribution. Run parameter data are given in Appendix A for each run. To account for differences in initial NO_2 percentage in the NO_x, a linear adjustment was made to the Table 3-2 input data, as discussed in Appendix A.

Table 3-2 gives the effects of the three independent variables, for the four materials separately. Notations for that table are:

m = mean value of the parameter

A = effect of changing from low S/V value (1.3 ft^{-1}) (represented by -1) to high S/V value (represented by +1) (2.7 ft^{-1})

B = effect of changing from cutoff spectrum (-) to full spectrum (+)

C = effect of changing from purge cleaning technique (-) to vacuum offgassing (+) cleaning technique

AB, AC, BC, ABC = interaction effects

s = estimate of the standard deviation of replicates

10% = value of parameter that would be exceeded by chance 1 time in 10 if true value of effect were zero, i.e., significant at 10% level

1% = value of parameter that would be exceeded by chance 1 time in 100 if true value of effect were zero, i.e., significant at 1% level

The table is calculated using standard methods for factorial tests (Ref. 4). For each material, 2 levels of A × 2 levels of B × 2 levels of C = 8 runs are available. From these we form 4 pairs that differ only with respect to one of the independent variables (A, B, or C). The average of the four differences is then the estimated effect of the independent variable. This procedure is repeated three times. For this balanced experimental plan the estimated effects are uncorrelated with each other, a decided advantage in interpretation. Interactions are determined from the intereffects of the variables.

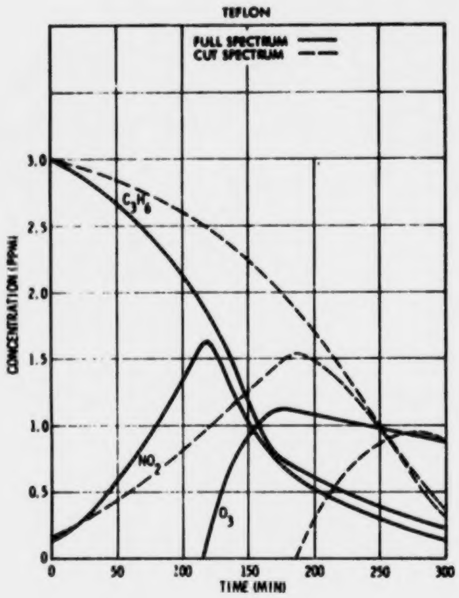

Fig. 3-1 Composite Photochemical Test Results for Teflon Film Surfaces

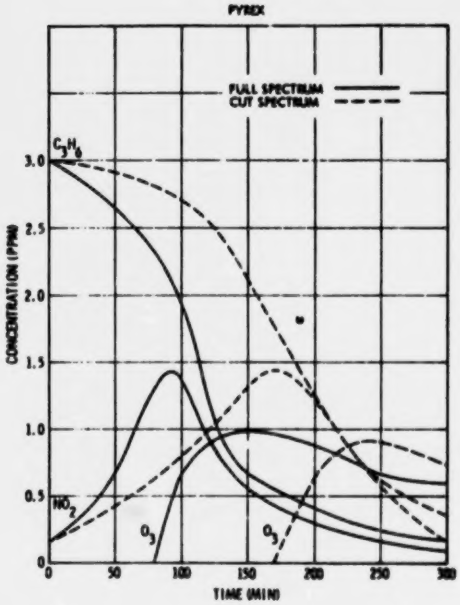

Fig. 3-2 Composite Photochemical Test Results for Pyrex Surfaces

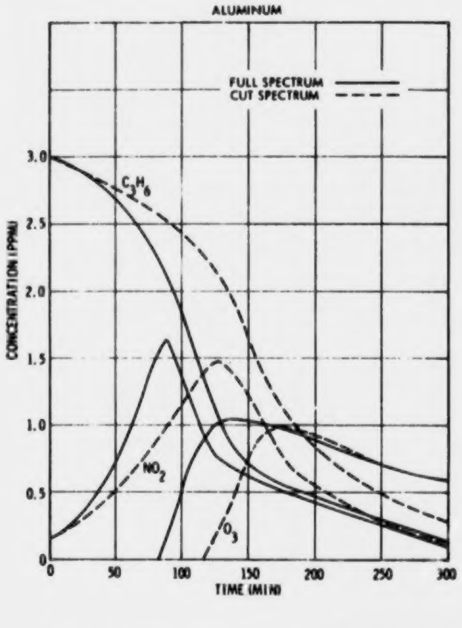

Fig. 3-3 Composite Photochemical Test Results for Aluminum Surfaces

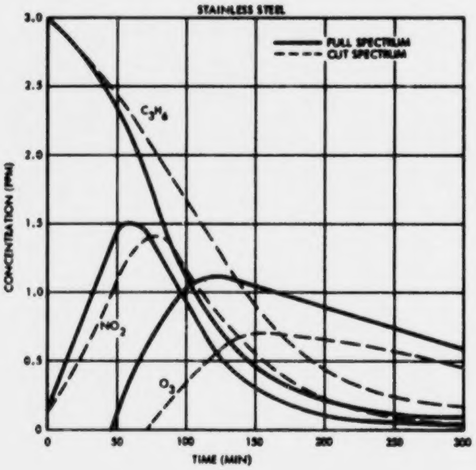

Fig. 3-4 Composite Photochemical Test Results for Stainless Steel Surfaces

Table 3-2

EFFECTS BY MATERIAL

(1) NO_2 FORMATION PARAMETERS

Effect	① NO_2 Rate				② NO_2 T_{max}				③ NO_2 Dose				⑱ NO_2 Dose Factor			
	Alum	Pyrex	Teflon	S.S.	Alum	Pyrex	Teflon	S.S.	Alum	Pyrex	Teflon	S.S.	Alum	Pyrex	Teflon	S.S.
m	13.1	10.0	8.63	25.4	106	131	154	70	176	178	219	153	39.0	39.2	48.7	34.5
A	0.35	-0.7	-0.26	13.5*	–	37.2*	-19.1*	-22.5*	14†	85*	-47*	- 4	2.5	16.7*	-10.5*	-0.7
B	4.42†	5.3†	2.77	9.3*	-38.5*	-74.2*	-67.5*	-28.0*	-32*	-76*	-70*	-41*	-7.7*	-10.3*	-16.1*	-9.0*
C	-1.38	0.5	-1.71	-10.3*	8.0	- 3.2	16*	20.5*	10	-24*	- 2	14†	1.7	- 6.0*	- 1.8	4.2*
AB	-1.65	0.4	-0.09	3.1	6.0	-30.7	3	1.0	-10	-41	14	- 4	-2.5	-10.5	4.2	-1.2
AC	1.50	-1.5	-0.58	- 1.7	- 7.5	- 4.7	9	- 0.5	0.2	-29	11	4	-0.6	- 5.0	2.1	0.2
BC	-1.38	1.2	-0.06	- 0.6	4.0	- 6.2	7	- 8.0	- 5	21	15	- 6	-0.8	2.7	3.3	-2.7
ABC	0.10	-1.2	0.13	- 1.4	4.5	18.2	-12	1.0	1	33	- 7	- 1	0.5	6.0	- 1.5	-0.4
s		2.60				7.35				8.43				1.93		
10%		3.87				11.0				12.6				2.88		
1%		5.33				15.1				17.3				3.96		

Effect	⑳ NO_2 FWHM				㉑ Crossover Time				㉒ = ② - ㉑				⑰ NO Rate			
	Alum	Pyrex	Teflon	S.S.	Alum	Pyrex	Teflon	S.S.	Alum	Pyrex	Teflon	S.S.	Alum	Pyrex	Teflon	S.S.
m	99	103	125	86	56	78	82	38	50	58	70	36	8.71	8.55	7.20	14.4
A	6.2	27*	-19*	- 9†	- 1.7	12.5*	0.7	-14.0*	1.7	26.0*	-25.7*	- 8*	-0.08	- 2.06†	0.59	3.8*
B	-32.7*	-59*	-69*	-31*	-17.2*	-35.5*	-26.2*	-13.5*	-21.2*	-38.5*	-35.7*	-14*	2.60†	4.61*	2.45†	4.8*
C	1.2	- 9	9†	11	5.2	4.5	13.7	13.0*	2.2	- 7.5*	7.7*	8	-0.13	1.23	- 0.16	-1.9†
AB	0.7	-23	17	- 1	4.7	- 9.5	1.2	2.0	1.2	-20.5	6.7	- 1	-0.24	0.38	- 0.01	0.4
AC	- 5.2	-11	11	1	- 5.7	1.5	7.2	- 1.5	- 1.7	- 6.0	6.2	1	0.78	- 0.92	- 0.30	-0.3
BC	0.7	2	2	- 5	3.7	- 6.5	- 0.2	- 4.0	0.2	1.5	1.2	- 4	-0.23	1.56	- 0.06	0.7
ABC	2.2	15	- 3	- 1	2.7	6.5	- 4.2	1.5	1.7	13.5	-14.2	- 1	0.09	- 1.29	0.33	-0.2
s		4.83				4.18				2.91				1.29		
10%		7.20				6.23				4.33				1.92		
1%		9.90				8.57				5.97				2.69		

*Significant at 1% Level.
†Significant at 10% Level.

Table 3-2 (Cont.)

(2) OZONE PARAMETERS

Effect	④ Ozone Max Rate				⑤ Ozone Avg. Rate				⑥ Max Ozone Conc				⑦ Ozone T_{Max}			
	Alum	Pyrex	Teflon	S.S.	Alum	Pyrex	Teflon	S.S.	Alum	Pyrex	Teflon	S.S.	Alum	Pyrex	Teflon	S.S.
m	24.7	24.7	21.3	21.2	4.08	3.60	3.12	5.68	1.00	0.93	1.03	0.90	172	189	230	137
A	-9.7*	-8.5*	-1.4	-8.2*	- 0.66*	- 1.35*	0.20	- 0.01	- 0.14*	- 0.12*	-0.06	- 0.26	6	-58*	-31*	-18*
B	7.7*	8.2*	11.2*	10.8*	1.61*	2.18*	1.92*	3.35*	0.04	0.09*	0.20*	0.40*	-56*	-98*	-89*	-45*
C	0.9	4.5†	2.4	0.4	- 0.08	0.56*	0.16	- 1.05*	0.08*	0.13*	0.15*	0.05†	8	- 2	12†	25
AB	-3.7	4.4	-5.6	-1.9	- 0.21	0.01	- 0.11	- 0.01	0.02	- 0.01	-0.06†	- 0.03	2	-43	15	1.2
AC	-2.0	1.0	-1.2	-0.1	0.25	- 0.05	- 0.21	- 0.05	–	0.03	-0.04	- 0.02	- 9	-15	7	- 4
BC	-1.1	-0.4	-2.4	-0.5	- 0.13	0.39	- 0.20	0.02	–	0.01	-0.05	0.01	4	- 1	1	-10
ABC	0.9	-1.0	-0.5	1.1	–	- 0.56	0.08	0.01	–	- 0.03	–	0.02	3	27	8	4
s	2.66				0.258				0.033				8.05			
10%	3.97				0.385				0.049				12.0			
1%	5.45				0.529				0.068				16.5			

Effect	⑯ Max Pan Conc				㉓ = ⑦ - ㉑				⑧ Ozone Dose				⑲ Ozone Dose Factor			
	Alum	Pyrex	Teflon	S.S.	Alum	Pyrex	Teflon	S.S.	Alum	Pyrex	Teflon	S.S.	Alum	Pyrex	Teflon	S.S.
m	0.35	0.14	0.29	0.23	116	115	148	103	156	126	131	157	34.3	27.8	28.6	34.1
A	-0.05	0.04	-0.10*	-0.03	8.5†	46.0*	-30.5*	- 4	-22.0*	-48*	4.0	-29*	- 5.4*	-12.5*	1.9	- 6.4*
B	-0.11*	0.02	0.19*	0.01	-39.0*	-62.0*	-62.5*	-31*	38.0*	61*	94.5*	48*	7.9*	12.3*	20.6*	10.8*
C	0.03	-0.02	0.12*	0.02	2.5	- 6.5	- 1.0	11*	5.5	26*	9.5	- 4	0.9	4.2*	0.8	- 3.0†
AB	0.09	0.03	-0.12	0.07	- 3.0	-34.0	14.5	–	-11.0	15	21.0	-12	- 2.7	2.0	- 3.6	–
AC	-0.02	–	-0.06	0.01	- 3.5	-16.5	- 0.5	- 3	10.5	9	14.5	2	1.8	2.9	- 3.4	–
BC	0.04	0.03	0.03	0.03	1.0	5.5	0.5	- 6	- 8.5	3	11.5	8	- 1.7	- 0.7	- 2.5	0.8
ABC	-0.06	-0.01	-0.02	–	1.0	20.5	- 4.5	2	6.5	-13	8.0	3	1.5	- 3.1	1.7	0.6
s	0.039				4.86				8.51				1.68			
10%	0.058				7.24				12.7				2.50			
1%	0.080				9.96				17.4				3.44			

*Significant at 1% Level.
†Significant at 10% Level.

Table 3-2 (Cont.)

(3) PROPYLENE PARAMETERS

Effect	⑨ HC Final Conc.				⑩ HC T 0.75				⑪ HC T 0.5				⑫ HC T 0.25			
	Alum	Pyrex	Teflon	S.S.	Alum	Pyrex	Teflon	S.S.	Alum	Pyrex	Teflon	S.S.	Alum	Pyrex	Teflon	S.S.
m	0.16	0.26	0.26	0.15	94	117	124	64	133	157	180	97	166	189	218	133
A	0.05	0.15*	-0.10*	-0.03	- 3	27*	–	-21*	3	44*	-15*	-22*	8	45*	-19*	-18*
B	-0.06†	- 0.19*	-0.24*	-0.09*	-28*	-56*	-38*	-20*	-43*	-76*	-70*	-34*	-48*	-80*	-84*	-45*
C	–	- 0.10*	-0.02	–	9	- 3	11	22*	12†	- 8	6	19*	7	-15*	4	19*
AB	-0.01	- 0.06	0.04	0.04	9	-18	- 4	4	7	-25	3	7	6	-26	6	4
AC	-0.01	- 0.10	0.04	-0.04	- 3	-11	–	-11	- 7	- 9	7	- 7	-10	-14	7	-11
BC	0.04	0.04	0.08	-0.02	9	4	- 1	- 9	7	- 1	4	- 9	7	5	7	-11
ABC	0.03	0.06	-0.08	0.02	- 8	18	–	7	- 2	22	- 8	3	2	26	- 9	5
s		0.039				8.34				6.85				6.76		
10%		0.058				12.4				10.2				10.1		
1%		0.080				17.1				14.0				13.9		

Effect	⑬ HC Max. Rate				⑭ HC Av. Rate				⑮ Max. Ald			
	Alum	Pyrex	Teflon	S.S.	Alum	Pyrex	Teflon	S.S.	Alum	Pyrex	Teflon	S.S.
m	21.8	23.6	15.9	23.9	11.5	10.1	8.2	16.2	0.87	0.70	0.75	0.76
A	-3.7†	-10.2*	4.0*	0.5	-0.85	- 2.2*	0.6	4.5*	- 0.13	- 0.40*	- 0.01	- 0.02
B	6.6*	13.5*	8.2*	9.2*	4.04*	- 5.3*	3.6*	5.8*	- 0.08	0.11	0.06	0.01
C	-0.8	0.9	2.2	1.4	-1.52	1.1	- 0.3	- 3.0*	- 0.10	–	- 0.02	- 0.06
AB	0.8	- 0.5	1.1	-0.4	-0.88	1.0	0.1	0.3	- 0.06	- 0.09	–	- 0.07
AC	2.9	0.8	-1.0	0.1	1.3	- 0.5	0.1	–	- 0.04	- 0.01	- 0.06	0.04
BC	1.2	- 0.2	0.3	1.3	-1.06	- 1.4	- 0.5	0.6	0.04	0.07	- 0.02	0.02
ABC	-0.8	2.0	0.6	-0.2	0.53	–	0.5	- 0.3	- 0.06	- 0.03	- 0.05	- 0.10
s			1.94			1.06					0.135	
10%			2.89			1.58					0.201	
1%			3.98			2.17					0.277	

*Significant at 1% Level.
†Significant at 10% Level.

For example, consider the following data for NO_2 time-to-maximum for Teflon surfaces:

Run No.	A	B	C	Time
38	+	+	+	121
34, 35	+	+	-	103
42	-	+	+	142
43, 44	-	+	-	115
36, 39	+	-	+	192
37	+	-	-	162
40	-	-	+	193
41	-	-	-	205

Effect A is $[(121-142) + (103-115) + (192-193) + (162-205)]/4 = -19.1$

Effect B is $[(121-192) + (103-162) + (142-193) + (115-205)]/4 = -67.5$, etc.

Note the efficiency with which each data point is utilized. This is characteristic of full factorial experimental designs. Selected conditions were replicated, to provide data on reproducibility to determine whether effects are "real" or are due to random deviation in chamber behavior. In this analysis, these replicates are averaged to allow the orthogonal data treatment just described.

Deviations between replicates were used to obtain s, the estimated standard deviation of the parameter. For all four materials and 23 parameters, pooling of the deviations is justified. The significance levels are then calculated from the t value for the number of degrees of freedom and s. The "effects" found are compared to the 1-percent and 10-percent significance levels in data interpretation.

Practical considerations required that the experimental plan be conducted for each material and each S/V level as a subgroup. A time trend analysis (Appendix B, page B-10) was thus conducted, to see if systematic drift was present in the experiment. Three sets of replicates are available, immediate reruns, reruns differing by more than 1 and less than 15 run numbers, and a complete rerun of the first material used in the experiment (run number differing by more than 50). Both the Rank Sum Test and the Sign Test show no evidence of drift, either within each material tested, or on the basis of material block-to-material block.

3.1 DETAILED STATISTICAL ANALYSIS

A detailed statistical analysis of the raw data was performed. The ground rule was that all photochemical runs submitted for analysis were used. The experimenter was free to declare a run invalid on the basis of physical grounds, such as equipment failure, undue deviation from desired initial conditions, suspected off-calibration instrumentation, or new material subject to aging effects. The analysis results are given in Appendix B in some detail and are summarized here.

3.1.1 Covariate Analysis

The covariate analysis considered the following initial conditions: $\%NO_2$, HCinit, NO_X, HC/NO_X, NO_2 and T_{adj} as covariates, where:

$\%NO_2$ = percent of NO_2 in initial NO_X
HC Init = initial propylene concentration, ppm
NO_X = initial NO_X concentration, ppm
HC/NO_X = ratio of propylene/NO_X initially
NO_2 = initial concentration of NO_2, ppm
T_{adj} = correction factor to NO_2 time-to-maximum to account for deviation in $\%NO_2$ from desired value of 10%

As a single covariate correction, $\%NO_2$ or T_{adj}, were very similar in effectiveness in increasing R^2 (Appendix B, page B-23). As the $\%NO_2$ correction is based purely on statistical grounds, and as T_{adj} was based purely on observation of the photochemical behavior, this is gratifying. The result further emphasizes the importance of considering initial $\%NO_2$ when correlating smog chamber results. For most of the materials and the run parameters, the increase in R^2 obtained by including covariate correction terms beyond $\%NO_2$ and HC Init was insignificant. Therefore the bulk of the statistical analysis was conducted on the raw data as corrected by these two covariate correction factors.

3.1.2 Principal Components

The 23 parameters used to describe each photochemical run are very strongly interrelated (See Tables B5-2 through B5-4 of Appendix B.) In particular a single "TIME" value can be used to represent the following: 1/NO_2 Rate, NO_2 Time to Max, 1/Ozone Avg. Rate, Ozone Time to Max, HC Time 0.5, 1/HC Avg. Rate, 1/NO Rate, NO_2 FWHM, and Crossover Time. Time to 75% HC disappearance correlates very well with 50% disappearance time (about .98) and time to 25% disappearance correlates almost as well (.95). These are the parameters that form the principal component called TIME, as defined in Table B5-5. It was also found that a combination of NO_2 and Ozone Doses and Dose Factors can be used, rather than each separately. These are the principal component called DOSE. The maximum rates and concentrations form another pair of principal components. These two combine HC Max. Rate, HC Final Conc., Ozone Max. Rate, and Ozone Max. Conc. by two different linear combinations, and are called MISC I and MISC II.

These four principal components were studied as run results themselves. In particular, cross plots of the four, taken two at a time, were prepared and the effects of S/V, Spectrum, and Cleaning noted. The patterns obtained were quite regular.

3.1.3 Effects by Materials

Models were formulated for each of the 23 parameters for each material separately, as well as for the material-to-material contrast. These models differ from the orthogonalized analysis just reported in using all the replicates as separate data points, not averaging. An effects-by-materials table was then prepared, and is given in Table 3-3. This table was calculated from results of the analysis of variance within each material using the Doolittle Matrix Inversion Method. For Table 3-3, s is the square root of the unexplained variability (experimental error), which differs significantly for each material. Table 3-3 differs from Table 3-2 in (1) using all replicates as separate data points, not averaging; and (2) using the covariate adjusted data.

Effects are declared significant at the 10% or 1% level using similar criteria to those used for Table 3-2. The results of the two analysis methods are very similar, which further reinforces the statement that the data is of sufficiently high quality and validity as to support models which can be used for reconcilliation of data from other smog chambers, and as the basis for

TABLE 3-3

Effects by Material

Effect	1 1/NO_2Rate				2 NO_2T_{max}				3 NO_2 Dose			
	Alum	Pyrex	Teflon	S.S.	Alum	Pyrex	Teflon	S.S.	Alum	Pyrex	Teflon	S.S.
m	.077	.107	.114	.043	100.9	126.7	147.2	66.2	177.5	178.0	220.1	155.5
A	-.007	.012†	.005	-.021*	.833	41.1†	-20.6†	-18.5*	15.0	82.0*	-46.3*	-5.08
B	-.026†	-.058†	-.042*	-.018*	-36.8†	-71.1†	-67.4	-26.1*	-33.8†	-74.5*	-72.5*	-40.6*
C	.009	.004	.025*	.021*	9.17	-.624	16.9†	19.4*	9.46	-24.5*	-1.50	14.6*
AB	.012	-.008†	0.0	.002	7.17	-25.1†	2.63	-.875	-11.8	-42.5*	16.0†	-3.58
AC	-.007	.014†	.012†	-.005†	-4.83	-5.87	10.9	.625	-1.54	-31.5*	11.0	2.58
BC	.005	-.013†	-.002	-.007†	3.83	-6.12	9.13	-6.12†	-3.71	16.5*	18.7	-6.92
ABC	.008	.006	-.005	.003	4.83	20.6†	-11.9†	.625	-2.71	32.0*	-7.75	.083
s	.016	.0016	.0049	.0043	12.5	3.54	7.92	4.86	10.4	0	7.37	6.64
10%	.025	.007	.007	.005	19.2	15.3	11.9	5.46	16.0	.00003	11.1	7.45
1%	.061	.070	.018	.009	47.7	154.3	29.5	11.7	39.7	.0003	27.4	14.2

Effect	18 NO_2Dose Factor				20 NO_2 FWHM				21 Crossover Time			
	Alum	Pyrex	Teflon	S.S.	Alum	Pyrex	Teflon	S.S.	Alum	Pyrex	Teflon	S.S.
m	39.1	39.3	48.8	34.7	99.8	102.8	124.8	86.4	51.1	68.9	75.2	29.5
A	2.90†	16.6*	-10.5†	-.600	6.04	26.9†	-19.1*	-9.04*	-1.29	13.2	.625	-12.1*
B	-7.67*	-18.2*	-16.2*	-8.95*	-33.3†	-59.4†	-69.6*	-31.5*	-15.5†	-33.7†	26.1*	-12.1*
C	1.84	-5.85*	-1.68	4.25*	.960	-9.87†	-8.88†	11.8*	5.79	5.25	13.1*	11.6*
AB	-2.47†	-10.3*	4.40	-1.35	.208	-22.1†	17.6*	-.800	6.04	7.25†	1.13	.917
AC	-.596	-5.25*	2.20	.150	5.54	-11.6†	10.87†	.542	-3.71	.750	8.88*	-.417
BC	-.529	2.45*	3.45	-2.70†	.791	1.13	2.88	-4.96†	3.46	-7.25†	1.62	-3.43
ABC	.178	5.95*	-1.58	- .300	1.29	15.4†	-3.38	-.708	2.96	7.25†	-3.63†	.583
s	1.38	0	3.46	1.30	9.36	2.12	3.90	2.49	8.35	1.41	2.20	2.54
10%	2.12	.000007	5.19	1.46	14.4	9.16	5.85	2.80	12.8	6.10	3.30	2.85
1%	5.27	.000007	12.9	2.79	35.7	92.4	14.5	5.34	31.9	61.5	8.19	5.44

TABLE 3-3

Effects by Material (Continued)

Effects	23 = 7 - 21				8 Ozone Dose				19 Ozone Dose Factor			
	Alum	Pyrex	Teflon	S.S.	Alum	Pyrex	Teflon	S.S.	Alum	Pyrex	Teflon	S.S.
m	116.6	114.9	147.1	103.3	151.8	128.8	129.6	160.7	33.3	28.1	28.7	35.7
A	8.17†	46.6†	-31.6*	-2.67	-19.9†	-52.1†	7.36†	-28.3*	-4.89†	-13.1†	2.01	-6.60*
B	-38.7*	-62.1†	-62.9*	-30.9*	35.2†	62.9&	88.7*	48.2*	7.54*	12.6†	20.0*	10.8*
C	2.83	-5.62	- .125	11.17†	2.20	24.2†	10.9†	-3.54	.192	3.66	1.21	-1.05
AB	-3.67	-31.4†	14.3*	-1.17	-14.6	17.7†	-18.2*	-11.9†	-3.06†	1.89	-3.54†	-2.96†
AC	-3.17	-16.9†	-.375	-2.58	5.45	3.52	-12.4†	.858	.892	2.13	-3.36†	-1.72
BC	.667	4.38	.875T	-5.23	-9.35	4.42	-4.09	8.01†	-1.84	-.087	-1.84	-.421
ABC	.667	21.1†	-4.38*	1.92	-4.60	-12.5	7.83†	4.81	-.342	-2.81	1.69	-.445
s	3.30	2.12	.407	5.94	10.6	3.68	4.19	6.63	1.66	.919	1.44	1.98
10%	5.08	9.16	.610	6.67	16.3	15.9	6.28	7.45	2.55	3.97	2.16	2.22
1%	12.6	92.4	1.51	12.7	40.5	160.4	15.6	14.2	6.34	40.1	5.36	4.24

Effects	9 HC Final Conc				10 HC T 0.75				11 HCT 0.5			
	Alum	Pyrex	Teflon	S.S.	Alum	Pyrex	Teflon	S.S.	Alum	Pyrex	Teflon	S.S.
m	.159	.254	.269	.151	88.4	110.0	118.2	60.4	128.4	150.9	171.9	93.2
A	.048	.147†	-.092†	-.039	-3.17	29.0	1.38	-18.7*	4.35	47.6†	-15.1†	-18.4*
B	-.073	-.198†	-.245*	-.089†	-26.8†	-55.0†	-33.9†	-20.4*	-40.2*	75.6†	-70.6*	34.6*
C	-.008	-.127†	-.025	.006	9.17	-4.0	10.9	20.2*	12.2	-6.62	7.62	17.6*
AB	-.013	-.087†	.045	.052	9.17	-16.0	-1.87	4.04	8.75	-18.9	3.38	4.62
AC	-.018	-.098†	.025	-.044	-1.83	-10.0	.875	-9.29†	-4.75	-8.87	8.62	-3.62
BC	.043	.047	.085†	-.024	8.83	2.0	1.62	-8.54†	6.25	-2.12	6.12	-7.38†
ABC	.023	.067†	-.088†	.026	-8.17	20.0	-.218	4.96	-1.75	24.6	-7.88	.138
s	.050	.014	.025	.052	9.10	9.90	10.5	5.61	9.96	9.19	5.79	4.11
10%	.077	.061	.037	.058	14.0	42.8	15.7	6.30	15.3	39.7	8.68	5.74
1%	.191	.610	.093	.111	34.7	431.5	39.1	12.0	38.0	400.5	21.6	11.0

TABLE 3-3

Effects by Material (Continued)

Effect	17 1/NO Rate				4 1/Ozone Max Rate				5 1/Ozone Avg. Rate			
	Alum	Pyrex	Teflon	S.S.	Alum	Pyrex	Teflon	S.S.	Alum	Pyrex	Teflon	S.S.
m	.114	.127	.139	.069	.044	.046	.051	.052	.251	.313	.350	.182
A	.004	.040†	-.013	-.016*	.017†	.023†	-.006†	.022*	.028	.155†	-.039†	-.004
B	-.032†	-.069†	-.053*	-.026*	-.012	-.022†	-.028*	-.027*	-.098*	-.217†	-.228*	-.117*
C	.002	-.007	.003	.018*	.002	-.012†	-.011†	-.001	-.011	-.067†	-.048*	.041*
AB	.010	-.025†	.003	.004	.002	-.014†	.014†	-.006†	-.003	-.108†	.038†	.003
AC	-.007	.004	.011	0.0	.004	-.008	.007†	.002	-.018	-.047†	.020†	.003
BC	.001	-.009	0.0	-.007†	.002	.008	.011†	.001	.002	.024	.048*	-.026†
ABC	.006	.014	-.009	0.0	0.0	.008	-.003	-.003	.019	.073†	-.037†	-.004
s	.0089	.0037	.0103	.0048	.0105	.0021	.0033	.0034	.021	.007	.012	.013
10%	.014	.016	.015	.005	.016	.009	.005	.004	.032	.030	.018	.015
1%	.034	.161	.038	.010	.040	.092	.012	.007	.080	.305	.045	.028

Effect	6 Max Ozone Conc.				7 Ozone T_{max}				16 Max Pan Conc			
	Alum	Pyrex	Teflon	S.S.	Alum	Pyrex	Teflon	S.S.	Alum	Pyrex	Teflon	S.S.
m	1.01	.943	1.02	.921	167.3	183.6	221.9	132.4	.365	.143	.291	.251
A	-.139*	-.125†	-.061	-.246*	7.08	61.2†	-31.4†	-14.9†	-.050	.039	-.098†	-.027
B	.044†	.110	.197*	.207*	-54.1*	-95.3†	-88.8*	-43.7*	-.122†	.026	.172*	.013
C	.079†	.150†	.159*	.048*	9.42	-.250	13.4†	23.2*	.030	-.014	.138†	.022
AB	.001	.010	-.051†	-.046*	3.42	-38.2†	15.9†	-.458	.078†	-.001	-.108†	.058†
AC	-.001	.010	-.034†	-.014	-6.08	-16.2	8.62	-2.04	-.030	-.021	-.053	.002
BC	.004	-.005	-.041†	.013	4.08	-2.75	2.62	-8.29†	.032	-.004	.047	-.018
ABC	.014	-.035	.006	.036†	3.60	28.3†	-8.13	3.46†	-.088†	-.011	-.023	.007
s	.021	.028	.019	.021	11.1	4.24	8.75	7.06	.037	.0495	.038	.032
10%	.032	.121	.028	.024	17.1	18.3	13.1	7.93	.057	.214	.057	.036
1%	.080	1.22	.071	.045	42.4	184.8	32.6	15.1	.141	2.16	.141	.069

TABLE 3-3

Effects by Material (Continued)

Effect	12 HC T 0.25				13 1/HC Max Rate				14 1/HC Avg. Rate			
	Alum	Pyrex	Teflon	S.S.	Alum	Pyrex	Teflon	S.S.	Alum	Pyrex	Teflon	S.S.
m	160.8	185.3	210.9	129.8	.048	.050	.069	.044	.090	.106	.124	.064
A	8.32	54.0†	-19.4†	-14.5*	.009	.026*	-.021†	.001	.001	.037†	-.014†	-.015†
B	-46.0*	-84.5†	-83.6*	-45.3*	-.015†	-.031*	-.036*	-.017*	-.024†	-.059†	-.058*	-.025*
C	8.37	-9.50	5.12	17.3*	.002	0.0	-.012	-.002	.007	-.011	.002	.014*
AB	7.13	-26.0	6.12	2.46	-.004	-.008*	.005	0.0	.004	-.020	.003	.005†
AC	-7.63	-8.00	8.37	-7.46†	-.006	-.002†	.012	.001	-.007	-.008	.005	-.004†
BC	6.88	-1.50	8.62†	-9.71†	-.002	0.0	.005	0.0	.001	.002	.008†	-.007*
ABC	2.88	23.0	-9.13†	3.54	.004	-.003†	-.006	0.0	.002	.019	-.008†	.002
s	10.1	9.90	5.61	5.31	.007	.0001	.009	.003	.010	.006	.005	.003
10%	15.5	42.8	8.51	5.96	.010	.0004	.013	.003	.015	.026	.007	.003
1%	38.6	431.5	20.9	11.4	.027	.004	.003	.006	.038	.262	.019	.007

Effect	15 Max. Ald				22 = 2 - 21			
	Alum	Pyrex	Teflon	S.S.	Alum	Pyrex	Teflon	S.S.
m	.880	.719	.773	.774	49.9	57.8	69.5	36.6
A	-.126†	-.027	-.034	.020	1.75	26.3†	-23.3*	-7.54*
B	-.069	.142	.064	.015	-21.3*	-38.3*	-36.0*	-14.3*
C	.001	.047	.001	-.068	3.25	-6.37†	8.50*	8.04*
AB	-.064	-.023	-.006	-.097	.750	-18.6†	6.75*	-1.54
AC	-.024	-.048	-.029	.060	-1.75	-6.63†	6.75*	.792
BC	.039	.062	-.021	.044	.250	.625	1.50†	-3.46†
ABC	-.056	-.125	-.041	-.103	1.25	13.4†	-14.3*	-.204
s	.066	.042	.091	.106	4.32	.707	.577	2.46
10%	.102	.182	.136	.119	6.64	3.06	.865	2.76
1%	.252	1.831	.339	.227	16.5	30.8	2.15	5.72

further eluciation of the photochemical reaction mechanism.

3.2 MATERIAL DIFFERENCES

The four materials may be grouped in terms of increasing NO_2 formation rate: Teflon, Pyrex, aluminum, stainless steel. Pyrex and aluminum are similar in behavior for most parameters. Other reactivity manifestations such as times to NO_2 maximum, 50 percent propylene destruction, and NO_2 dose follow the same order. Figures 3-1 to 3-4 provide a better understanding of material differences than word description, but also see the means by material in Tables 3-2 and 3-3.

3.3 EFFECTS OF FACTORS

Of the three independent variables studied, the spectral change (Effect B) caused the largest change in behavior. Table 3-4 gives the significant effects count for the four materials and the three variables. Spectral distribution was significant at the 1% level (one chance in 100 that it was really not significant) for nearly all 23 parameters for all four materials. The notable exception was NO_2 formation rate, in which case spectrum was significant at the 1% level only for stainless steel, and at the 10% level for aluminum and Pyrex, and not significant for Teflon. Recall that all runs were performed at constant k_d. Maximum ozone concentration was strongly affected for the Teflon and stainless steel, which are the two materials with highest ozone levels, as shown in Table 3-5 below. Spectrum is significant at the 1% level for all but aluminum.

For all four materials, the cutoff spectrum consistently and clearly slowed the reaction relative to the full spectrum. Table 3-6 shows the ratio of cut to full spectrum for several "reactivity" measures.

S/V ratio (Effect A) was next in importance in affecting smog chamber behavior. Pyrex results were influenced by S/V to a larger degree than were the other materials. Cleaning had its largest effect for stainless steel, and Pyrex. These counts of significant effect are somewhat misleading, in that some of the calculated run parameters, such as NO_2 Time Max. and Ozone Max. Conc. are of greater practical importance than others. As just shown in Table 3-5, Teflon S/V hardly affects Ozone Max Conc., and the general picture is that S/V is of less importance for Teflon than for, say, aluminum. To make such judgments, the run graphs, which are given in Appendix A, should be consulted.

Table 3-4
SIGNIFICANT EFFECTS BY MATERIAL

Material	S/V Significant at 1%	S/V Significant at 10%	Spectrum Significant at 1%	Spectrum Significant at 10%	Cleaning Significant at 1%	Cleaning Significant at 10%
Aluminum	5	3	18	3	1	1
Pyrex	20	1	20	1	9	2
Teflon	12	-	20	1	4	2
Stainless Steel	14	1	21	-	13	4

Table 3-5
MAXIMUM OZONE CONCENTRATIONS (PPM)

	Aluminum	Pyrex	Teflon	Stainless Steel
Averages				
All runs	1.00	.93	1.03	.90
Full Spectrum	1.02	.98	1.13	1.10
Cut Spectrum	.98	.89	.93	.70
High S/V	.93	.87	1.00	.77
Low S/V	1.07	.99	1.06	1.03
Vacuum Clean	1.04	1.00	1.11	.92
Purge Clean	.96	.87	.96	.88

Table 3-6
CUT/FULL SPECTRUM RATIO

	Teflon	Pyrex	Aluminum	Stainless Steel
NO_2 T_{max} 1	1.58	1.78	1.54	1.49
Ozone T_{max} 7	1.49	1.68	1.47	1.39
50% Propylene Destruction 11	1.50	1.64	1.47	1.43

3.4 OZONE DECAY RESULTS

One parameter frequently used as a measure of chamber cleanliness is the ozone half-life in the smog chamber. Measurements were made of the ozone half-life in the chamber each time a new set of surface materials was installed, and when the S/V was changed. The conditions were: temperature, 95°F; relative humidity, 55°F dewpoint; total HC as methane, <0.1 ppm. The initial ozone concentration was 1 to 2 ppm. These tests were usually conducted in conjunction with the vacuum chamber off-gassing that was used as the final cleaning step after installing the new material. Ozone decay was determined in the dark and for the illuminator (full spectrum configuration) at its nominal 6,500-W power output (decay in the light). Results are shown in Table 3-7. Ozone decayed fastest in the presence of stainless steel surfaces and most slowly in the presence of Pyrex. It should be recognized that ozone decay behavior is a function of previous conditioning as well as material and configuration, and, by itself, has been the subject of several research investigations such as Sabersky (Ref. 19).

Table 3-7

OZONE HALF-LIFE STUDY

Configuration	Half-Life in Dark (min)	Half-Life in Light (min)
Base Chamber	430	180
Aluminum High S/V	270	210
Aluminum Low S/V	340	215
Pyrex High S/V	360	300
Pyrex Low S/V	340	275
Teflon High S/V	295	200
Teflon Low S/V	350	270
Stainless Steel High S/V	160	100
Stainless Steel Low S/V	190	120

The correlation coefficient for the ozone half-life and the calculated run parameters is given in Table 3-8. The full spectrum data averaged over both cleaning methods was used, which gives a sample size of eight. Several of the run parameters show a significant correlation at the 5% level (1 chance in 20 that it really is not significant) and several more at the 10% significance level. The correlation coefficient is usually higher for ozone half-life in the dark than in the light. This result implies that it may in some way be possible to correlate smog chamber behavior using ozone decay in the dark as the link between chambers. However note the poor correlation for Ozone Max. Conc. and ozone half-life.

3.5 RELATIVE HUMIDITY EFFECTS

A number of tests were conducted at lower relative humidity than the standard condition. These were done for the purpose of obtaining additional insight into the mechanisms that might be operative to cause the spectral effects and to obtain experimental data on this effect for which opposite results have been obtained by different groups (Ref. 15). The resulting data is briefly summarized in Table 3-9. Appendix A gives the run graphs and the complete run parameter calculation results. Decreasing the dew point slowed the photochemical reaction for the stainless steel and aluminum surfaces. This is in accordance with Altshuler and Bufalini hypothesis (Reference 15) that lower dew point allows more active wall sites, which lowers the free radical concentration in the gas phase, leading to decreased reactivity. Maximum ozone concentration increased for all three materials studied.

For Teflon surfaces, which gave the slowest reacting system studied, a decrease in dew point increased the reaction rate. The three data points taken do not show a monotonic trend. Whether this is caused by experimental error or by some trend turnaround between 17 and -20°F dew point has not been established. The latter hypothesis is favored by the author.

For all materials and all spectral conditions, the steady state ozone concentration is higher as the dew point is decreased. The humidity effect occurs for both spectral conditions. This implies that the spectral effect is not due to $O(^1D)$.

Table 3-8

CORRELATION OF OZONE HALF-LIFE WITH RUN PARAMETERS AVERAGED OVER CLEANING

Variable	Correlation of Half-Life in Light	Correlation of Half-Life in Dark
NO_2TM	.775	.792
HCT 50	.739	.750
O_3TM	.579	.629
FWHM	.346	.436
XTIME	.806	.825
1/Oz Avgr	.797	.812
1/HC Avgr	.726	.767
$1/NO_2R$	.795	.824
1/NO RATE	.741	.780
NO_2 DOSE	.411	.480
NO_2 DF	.307	.399
O_3 DOSE	-.373	-.226
O_3DF	-.423	-.275
$1/O_3$ MAX R	-.270	-.417
1/HC MAX R	.296	.300
O_3 MAX C	.122	.256
HCFC	.703	.539
PAN Max	-.078	.002
HCT 75	.767	.793
HCT 25	.712	.718
NO_2XT	.629	.655
O_3XT	.195	.275
ALD Max	.119	.343
TIME	.730	.759
DOSE	-.414	-.403
Max 1	.009	.141
Max 2	.349	.437
Sample Size	8	8
Significant Correlation (5%)	.707	.707
(10%)	.621	.621

Table 3-9
RELATIVE HUMIDITY VARIATION EFFECTS

Material	S/V	Spectrum	Dewpoint (°F)	NO_2 Time to Max Min	HC T. 50	Ozone Max Conc. (ppm)	Run No.
Alum	Low	Full	55	76	92	1.04	75
Alum	Low	Full	22	86	113	1.16	76
Alum	High	Full	55	86	113	.94	69 & 85
Alum	High	Full	19	105	126	1.00	89
Alum	High	Cut	55	117	145	.84	82 & 84
Alum	High	Cut	14	155	182	.94	88
Stainless	Low	Full	55	60	81	1.14	61 & 66
Stainless	Low	Full	22	60	77	1.14	64
Stainless	Low	Full	-20	80	105	1.23	65
Stainless	Low	Cut	55	81	112	.87	60 & 67
Stainless	Low	Cut	-12	115	135	1.06	68
Stainless	High	Full	55	39	69	.83	51, 52, 58
Stainless	High	Full	12	57	83	.90	59
Teflon	Low	Full	55	118	142	1.08	46
Teflon	Low	Full	17	67	93	1.20	47
Teflon	Low	Full	-20	77	106	1.31	49
Teflon	Low	Cut	55	205	230	.80	41
Teflon	Low	Cut	15	190	210	1.03	48

3.6 BUTANE RUNS

A series of tests were conducted using the n-butane/NO_x system. The major objectives of these tests were to determine if the spectral effect and S/V effect were detectable in this low reactivity paraffinic hydrocarbon system. It was felt this would help to establish the generality of the effects. The butane-NO_x system has been investigated by Altshuler (Ref. 16). Appreciable oxidant production occurs at a restricted range of values of the HC/NO_x ratio of about 5-10 (molar basis). The oxidant production vs HC/NO_x ratio curves for butane show sharp peaks, in contrast to similar curves for propylene as the hydrocarbon. The condition chosen for this study was 3 ppm butane and 0.6 ppm NO_x, for a HC/NO_x ratio of 5 (molar basis). At this ratio, Altshuler obtained about 0.25 ppm "oxidant" (ozone) and 15% hydrocarbon consumption after six hours irradiation.

Irradiation conditions for the butane runs were the same as for the propylene runs, (95°F, 25% relative humidity, approximately 10% initial NO_2 in NO_x) but the system was run for six hours, rather than five. Two materials, Teflon and aluminum, were tested at two S/V values each. The single cleaning technique of purge cleaning was used.

Results are summarized in Table 3-10. (Appendix A gives the run graphs and the run parameter calculation listing.) The full spectrum results were comparable to those of Altshuler. The average butane consumption was 16%, considering the dilution correction, which was made individually for each run. The average peak ozone concentration was 0.23 ppm, and the ozone concentration appeared to be still slowly increasing at the six hour end-of-run time. Time to NO_2 maximum averaged 253 minutes. S/V ratio had major effects on NO_2 Max Time, % HC Disappearance and for Teflon on Ozone Max. Conc.

TABLE 3-10

Butane Effects by Materials*

Effect	1 NO_2 Rate		2 NO_2 T_{max}		3 NO_2 Dose		18 Dose Factor	
	Alum	Teflon	Alum	Teflon	Alum	Teflon	Alum	Teflon
m	2.11	2.00	125	267	138	132	63	61
A	.43	.25	-1.5	-95	28	6	13	5
B	1.33	.75	19.5	-50	40	44	20	18
AB	-.47	.01	-1.5	40	-3	9	-1	5

Effect	20 Crossover Time		22 = 2 - 21		23 = 360 - 21		17 NO Rate	
	Alum	Teflon	Alum	Teflon	Alum	Teflon	Alum	Teflon
m	132	127	179	141	228	233	1.50	1.52
A	-38	-22	31	-73	38	22	.33	-.11
B	-54	-42	-43	-8	55	42	.60	.09
AB	3	-6	-10	46	-3	6	-.08	.32

Effect	4 Ozone Max Rate		5 Ozone Avg Rate		6 Max Ozone Conc.		8 Ozone Dose	
	Alum	Teflon	Alum	Teflon	Alum	Teflon	Alum	Teflon
m	.72	.84	.19	.26	.14	.13	11	12
A	-.05	.61	-.03	.24	.02	.07	3	5
B	1.38	1.08	.36	.42	.20	.18	18	12
AB	-.12	.01	-.04	.14	-.02	.03	1	9

Effect	19 Ozone Dose Factor		13 HC Max Rate		14 HC Avg Rate		% HC Disappearance*	
	Alum	Teflon	Alum	Teflon	Alum	Teflon	Alum	Teflon
m	5.1	5.5	1.9	2.2	1.0	.84	14	13
A	1.6	1.8	.05	2.7	.99	-.11	10.3	2
B	7.9	5.0	.53	1.6	.32	.69	-1.4	7
AB	.2	4.1	-.60	-1.1	.21	-1.1	-.3	-11

*Those parameters that are inappropriate or poorly defined are omitted from this table, i.e. NO_2 FWHM, Max PAN concentration, Max. Ald. Conc., HCT .75, HCT .5, HCT .25. Ozone T_{max} was 360 minutes for all runs. Rather than tabulate HC Final Conc., the loss of butane - after dilution correction - is tabulated as % HC Disappearance.

The cut spectrum drastically lowered ozone production (the average ozone maximum concentration for the cut spectrum condition was 0.04 ppm) and increased the time to NO_2 maximum to an average of 328 minutes. Conclusions drawn from this small number of tests are somewhat tentative but are stated here: (1) the cut spectrum condition has the same effect in butane/NO_x as in propylene/NO_x of slowing the photochemical reaction system (2) S/V remains as an important variable in affecting the photochemistry; (3) measurable amounts of acetaldehyde (about 0.2 ppm) and PAN (about 3 ppb) were detected in two of the eight runs. These were both the high S/V aluminum runs.

3.7 Background Reactivity Runs

For each material at high S/V, background reactivity tests were made, both at the initial use of the material, and at the end of the material block investigation. Conditions for these tests were standard except that the chamber charge was 0.1 ppm of NO_x and no hydrocarbon was charged. The average maximum ozone concentration for those tests was less than 0.02 ppm, and the NO_2 formation rate was about 0.2 ppb/min. There was little observable difference between the results before or after the block of photochemical runs.

3.8 "Virgin Surface" Effect

For the metallic materials, the initial photochemical run gave a different kinetic picture than did the second or third replicate at the same constant condition. These initial runs have not been used in the data analysis. For aluminum, the "fresh" surface gave a faster reaction than did the sebsequent runs. For stainless steel, the initial run was slower than the subsequent runs. These effects have not been analyzed in any detail, but are present.

The "fresh" surfaces referred to had been through the standard cleaning technique of acetone or trichloroethylene cleaning, followed by several distilled water rinses, followed by overnight or longer hold at 2 microns or less pressure at about 100° F. Then the ozone decay studies were performed. This involved exposure to 1 to 3 ppm of ozone for usually

3 days continuously. Then the background reactivity run was performed, which involved irradiation with 0.1 ppm NO_x in the system. Evidently, metallic smog chamber surfaces do not stabilize until being exposed to at least one full scale photochemical run. Cleaning as performed by this project did not degrade the stability of the Teflon or aluminum surfaces. Cleaning appears to be affecting the stainless steel surfaces, and may be affecting the Pyrex.

3.9 NITROGEN BALANCE

It is commonly believed that prior to NO_2 peak, NO and NO_2 are the only nitrogen compounds present in the photochemical reaction system at measurable concentrations (say greater than 0.05 ppm). In fact only recently has the chemiluminescent method made direct measurement of NO possible. In this project, the Saltzman NO_2 (after accounting for instrument lag time) and the chemiluminescent NO are taken as correct measurements. Using this ground rule, the NO, NO_2, NO_x stoichiometry can be studied. The ratio of NO_2 at peak NO_2 to initial NO_x is shown in Table 3-11. It is observed that the ratio is significantly affected by S/V for Pyrex.

Such "excess NO_2" behavior has been observed by other smog chamber operators but to our knowledge has not been discussed in the literature. It seems to occur with "fast" photochemical systems. The behavior may indicate that the Saltzman NO_2 readings includes a response to a species other than NO_2.

Another disconcerting observation is the apparent non-stoichiometric behavior of NO_2 and NO during the first few minutes of irradiation. In this interval NO_2 builds up while NO decreases at a lesser rate. This induction period effect causes parameter 17 (NO disappearance rate) to be smaller than parameter 1, the NO_2 formation rate. Table 3-12 gives the ratio of NO_2 rate to NO rate. Material does significantly affect this ratio, in the sense that the fastest photochemical material-stainless steel – gives the highest ratio. The ratio is sensitive to cleaning technique for all the materials studied, and is also sensitive to S/V for stainless steel.

Table 3-11

NO_2 at Maximum/NO_x Initially

	Material			
Run Condition	Stainless Steel	Alum.	Pyrex	Teflon
+++	.99	1.08	1.02	1.05
++-	1.05	1.05	1.08	1.03
-++	.99	1.08	.86	1.12
-+-	1.00	1.07	.92	1.15
+-+	1.05	1.08	1.03	.93
+--	.98	.99	1.19	1.00
--+	.93	.98	.81	1.05
---	.95	.95	.83	1.13

Averages

All Runs	1.00	1.04	.97	1.06
S/V High	1.02	1.05	1.08	1.00
Low	.97	1.02	.86	1.11
Spectrum Full	1.01	1.07	.97	1.09
Cut	.99	1.00	.97	1.03
Cleaning Vacuum	.99	1.06	.93	1.04
Purge	1.00	1.02	1.00	1.08

Table 3-12

NO_2 Rate Divided by NO Rate

Run Condition	Stainless Steel	Alum.	Pyrex	Teflon
+++	1.74	1.39	1.24	1.01
++-	2.35	1.64	1.39	1.28
-++	1.24	1.44	1.06	1.19
-+-	1.61	1.68	1.10	1.35
+-+	1.71	1.28	1.23	1.05
+--	2.03	1.70	1.45	1.22
--+	1.20	1.31	1.07	1.16
---	1.77	1.39	1.04	1.40

Averages

All Runs	1.71	1.48	1.20	1.22
Full Spectrum	1.74	1.54	1.20	1.25
Cut Spectrum	1.68	1.42	1.20	1.20
High S/V	1.96	1.50	1.33	1.14
Low S/V	1.46	1.46	1.07	1.28
Cleaning Vacuum	1.47	1.36	1.15	1.10
Purge	1.94	1.60	1.25	1.31

It is generally acknowledged that nitrogen balance in smog chambers is somewhat unsatisfactory. We observe that this lack of balance is not restricted to the post-NO_2 peak time, (at which time nitric acid formation is usually invoked), but includes the early period. An additional complication in interpreting this data is the effect of the delay time between sampling the reactants in the illuminated chamber and analysis. The rapid reaction between 0_3 and NO in the dark to form NO_2 reduces the apparent concentrations of these two species. Instrument response times also affect the indicated concentrations. The NO_2 instrument has a rise time of about 10 minutes, while for the chemi-luminescent NO and 0_3 instruments, the rise times are about 3 seconds. The NO_2 readings were corrected by subtracting 10 minutes from the time of each reading. This compensates for the time lag while ignoring the integration effect. The dark time before sampling has been calculated at about 9.6 seconds. For an 0_3, NO rate constant of 29.5 ppm^{-1} min^{-1}, kt is equal to 4.46 ppm^{-1}. At this value, 0_3 and NO would react and not co-exist at concentrations above about 0.1 ppm. It thus appears that the calculated dark time is too high or that the 0_3 and NO instruments give high readings. The latter hypothesis is rejected on the basis of (1) pre- and post-run zero checks frequently, showing zeros within 0.02 ppm of the anticipated 0.00 value; (2) experiments in which excess NO was added to the chamber at the end of the photochemical run (lights off) and 0_3 was recorded at about 0.02 ppm (accuracy of 0_3 meter zero confirmed); and (3) the normal check reading at the end of each photochemical run (lights off) which gives a condition of excess 0_3 in the chamber and which did give an NO reading of about 0.02 ppm (accuracy of NO meter zero confirmed).

Additional effort in NO and NO_2 monitoring techniques, such as gas-phase titration of NO with 0_3 (thus establishing NO by the decrease in 0_3), and in linking NO_2 and NO monitoring by using the NO_x mode of a chemiluminescent detector would be useful in resolving these problems. It is believed that to start resolving these questions, monitoring of the nitrogen species also must be accomplished by a technique sensitive to more than NO and NO_2. Such monitoring may be in-chamber or with a few seconds sampling time delay. Two promising methods are long path length IR or Fourier Transform Spectrometry, or by time derivative spectroscopy. Either seem well suited.

Section 4
DISCUSSION

4.1 General Observations

The large effect of spectral distribution on photochemical reaction systems – at the same intensity as measured by k_d – has not previously been reported. However, some literature data are available that suggest that such an effect is not only present but may be general. Altshuler and Cohen (Ref. 5) reported a factor of 2 to 3 times higher NO_2 formation rates for tests in Teflon vs. Mylar containers. This difference was attributed to the difference in k_d of 0.35 to 0.4 min^{-1} for Teflon vs. 0.25 to 0.3 min^{-1} for the Mylar. The substantial difference in light below 330 nm for the two materials was noted, but not further discussed. This differential rate was observed for some 16 hydrocarbons, ranging in reactivity from 1, 3, 5 trimethylbenzene and 1, 2, 3, 5 tetramethylbenzene at the high reactivity end, to ethylbenzene and toluene at the low reactivity end.

Table 4-1 gives a "Mylar/Teflon" spectral effect for time to NO_2 maximum calculated from Altshuler's data, after normalizing by the ratio of 0.275/0.325 to account for the difference in k_d. Glasson and Tuesday (Ref. 6) give experimental data that show that NO_2 formation rate is linear with k_d for a variety of hydrocarbons. Such a linear factor is also suggested by Niki et al. (Ref. 7) as applicable to the early stages of the photochemical reaction. The difference in transmission characteristics for the Teflon vs. the Mylar containers results in a cut/full spectral distribution somewhat similar to that used in the present study. The spectral effect factor for propylene was 1.65.

A similar treatment of that data for oxygenates yields the following "Mylar/Teflon" spectral effect: formaldehyde 5.9, acetaldehyde 3.5, proprionaldehyde 3.9, acrolein 2.9, ethanol 1.6.

Table 4-1

"MYLAR/TEFLON" SPECTRAL EFFECT*

Hydrocarbon	Ratio of NO_2—T_{max}
Ethylene	2.93
Propylene	1.65
Isobutene	1.81
Toluene	1.76
Ethylbenzene	>2.7
1,2-dimethylbenzene	1.46
1,3-dimethylbenzene	1.32
1,4-dimethylbenzene	2.20
1,2-methylethylbenzene	1.74
1,3-methylethylbenzene	1.96
1,4-methylethylbenzene	2.29
1,3,5-trimethylbenzene	2.00
1,2-diethylbenzene	2.05
1,3-diethylbenzene	1.67
1,4-diethylbenzene	2.06
1,2,3,5-tetramethylbenzene	1.92

---

*Calculated from Ref. 5.

Bufalini et al. (Ref. 8) have reported that photooxidation of formaldehyde in the presence of NO_2 proceeded more rapidly at k_d of 0.14 min^{-1} with sunlamps than at 0.32 min^{-1} with blacklamps. This is an obvious result of the photodisintegration by the shorter wavelength light from the sunlamps. The time ratio for 50 percent consumption of formaldehyde, corrected for the k_d ratio, is 1.6 for the blacklamp/sunlamp distribution. For an irradiation without NO_2, the corrected time ratio for 37 percent consumption is 2.7.

4.2 NO_2 Photolysis Distribution

The distribution of NO_2 photolysis events versus wavelength has been calculated for several spectral distributions. For this calculation, the wavelength interval between 290 and 410 nm is considered. Absorption coefficient (Ref. 9) and quantum yield (Ref. 10) for NO_2 are tabulated at 10-nm intervals in this interval. These multiplied by each other and by the number of photons in the 10-nm wavelength interval gives the total NO_2 photolysis rate. This total rate divided into the events in each 10-nm band gives the fractional distribution of NO_2 photolysis events, or shows how the same k_d occurs for different spectra. Figure 4-1 gives the results.

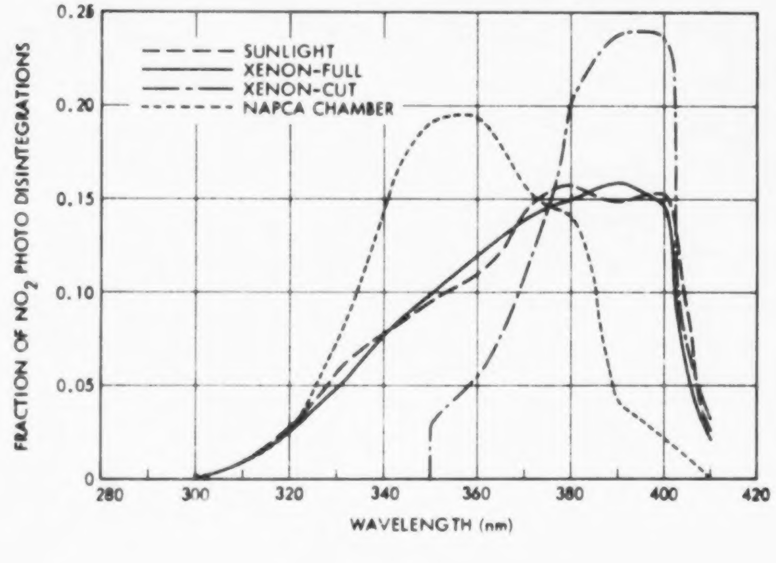

Fig. 4-1 Distribution of NO_2 Photodisintegrations for Various Spectra

The sunlight curve is for high noon in Los Angeles or Stanford, Conn. (two distributions averaged)(Refs. 11, 12); the xenon-full and xenon-cut are for the spectra used in this study, as previously shown in Fig. 2-6. The NAPCA chamber curve is for the spectral distribution given by Korth et al. (Ref. 13), which is one of the few reported chamber spectra in the literature.

The xenon-full NO_2 disintegration spectral distribution does indeed closely match the sunlight curve, over the entire wavelength interval. The NAPCA chamber distribution is probably typical of chambers illuminated by fluorescent tube combinations, and shows that the wavelength band from 335 to 365 nm is overemphasized (relative to the sunlight distribution), while the 385 – 410 nm band is underrepresented. This disparity is frequently unrecognized in discussing the application of smog chamber data to atmospheric simulation.

It is clear that the spectral distribution of light provided a smog chamber influences the photochemical reaction observed. In particular, the NO_2 photodisintegration rate (k_d or its equivalent k_1) does not sufficiently characterize the light conditions.

4.3 Possible Mechanisms

There are two major effects demonstrated by the experimental work that are not well accounted for in present-day photochemical reaction system kinetic modeling studies. These are: (1) the spectral effect and (2) the material and S/V effects (in fact, chamber wall effects usually are not included in such models.) An effort is presently underway to examine the propylene/NO_x system reactions by an updated kinetic model and to determine those mechanisms that best suit the experimental findings. This analysis is being submitted for publication to Environmental Science and Technology as "Interpretations of Smog Chamber Design Effects," P. S. Connell, R. J. Jaffe, and H. S. Johnston. The model accommodates up to 200 elementary reactions and 50 species, and is intended to include all important elementary reactions. It is well known that there are a number of reactions in the system that are spectrally sensitive. These are listed as follows.

		Effective Wavelength (nm)
(1)	$HONO + h\nu \longrightarrow HO + NO$	300–390
(2)	$HCHO + h\nu \longrightarrow H + HCO$	290–360
(2a)	$HCHO + h\nu \longrightarrow H_2 + CO$	300–370
(3)	$CH_3\,CHO + h\nu \longrightarrow CH_3 + HCO$	300–350
(3a)	$CH_3\,CHO + h\nu \longrightarrow CH_4 + CO$	300–350
(4)	$H_2O_2 + h\nu \longrightarrow 2\,HO$	300–370
(5)	$O_3 + h\nu \longrightarrow O_2(^1\Delta g) + O(^1D)$	290–310
(5a)	$O\,(^1D) + H_2O \longrightarrow 2\,HO$	

The mechanism and rate constants for which no experimental evidence exists are drawn largely from the modelling work of Demerjian, Kerr, and Calvert; and Niki, Daby and Weinstock. When available, CIAP rate constants were used as well as more recent experimental work. The photolytic constants for nitrous acid and for the production of $O(^1D)$ were developed from recent studies at the University of California of cross section and quantum yield by R. Graham, R. A. Cox (nitrous acid) and J. Girman (unpublished study of $O(^1D)$ production).

For the full spectrum data, the sunlight cross sections and yields have been used, after normalizing for intensity by the k_d ratios. The cut spectrum distribution and photolytic data have been used to assign new rate constants for the above reactions. Nothing else in the model was changed. The resulting comparison of cut/full spectrum conditions gives a ratio for time to NO_2 maximum of 1.37 to 1.81, depending upon the initial nitrous acid concentration. The midpoint of about 1.6 agrees well with the experimental data from this project, and from Altshuler's 1963 work.

The responsible reactions were identified by replacing individual full-spectrum 'j' values with the corresponding cut-spectrum values, one by one. The largest effect was observed for nitrous acid, followed by, in order, formaldehyde, acetaldehyde, and hydrogen peroxide. The production of $O(^1D)$ in the photolysis of ozone appears to be unimportant in the smog chamber. Table 4-2 gives the ratio of the cut spectrum to full spectrum time to NO_2 maximum considering the change for each species, individually.

Table 4-2

SPECTRAL EFFECT ON TIME TO NO_2 MAXIMUM CAUSED BY EACH SPECIES

Species	Ratio of Times for Cut/Full Spectrum
Nitrous Acid	1.50
Formaldehyde	1.26
Acetaldehyde	1.17
Hydrogen Peroxide	1.12
$O_3 \rightarrow O(^1D)$	1.00

The observed surface effect is that 'active' surfaces, such as stainless steel, speed the smog reaction in comparison to inert surfaces, such as Teflon. The net contribution of heterogeneous reactions must not be in the direction of radical quenching but catalysis of initiating or chain propagating processes. By examination of propene destruction data as a function of photons absorbed by NO_2, it was found that the stainless steel effect is one of increased initial effective quantum yield. The important identified heterogeneous reactions are (1) the formation of nitric acid by the reaction of N_2O_5 with absorbed water and (2) the wall dependent formation of nitrous acid. Unpublished work in two cells, one of quartz and the other of quartz and stainless steel, shows that the stainless steel surface promotes the rate of formation of nitrous acid by a factor of about a thousand (as observed in the gas phase). Since the photolysis of nitrous acid has been seen to be an important initiator, its rate of formation and concentration at the beginning of the irradiation time are significant parameters in determining the overall rate of the smog reaction.

4.4 Background Reactivity Runs

The background reactivity runs were performed to determine whether the cleaning techniques had removed trace amounts of reactive species. Tests were conducted, in which about 0.1 ppm of NO_x was charged to the chamber and NO, NO_2 and O_3 monitored. The results are summarized in Table 4-3.

Table 4-3

BACKGROUND REACTIVITY RESULTS

Material and Conditions	O_3 Maximum (ppm)	NO_2 Formation Rate (ppb/min)
Aluminum – Post Runs – High S/V	0.012	0.2
Aluminum – Post Runs – Low S/V	0.014	0.2
Pyrex – Pre Runs – High S/V	0.024	0.3
Pyrex – Post Runs – High S/V	0.012	0.2
Teflon Pre Runs – High S/V	0.014	0.3
Teflon Post Runs – High S/V	0.020	0.2

The NO_2 formation rate of 0.2 to 0.3 ppb/min agrees well with the reported rate for similar background runs conducted by the University of North Carolina using a 6000 ft^3 Teflon outdoor smog chamber (Ref. 17). For those tests the NO charge was 0.2 ppm, contrasted to the 0.1 ppm charge used with this chamber. Thus this 100-fold smaller chamber has a background NO_2 formation rate about 4 times higher. There is no indication of residual reactive species upon comparing the tests conducted at the start and at the end of a test series.

4.5 Ozone Decay Results

The ozone decay results indicate that the stability of ozone in the presence of the various materials is greatest for pyrex, followed in order by teflon, aluminum, and stainless steel. Ozone decay time in the light is 0.4 to 0.8 of the value measured in the dark. Ozone decay rate is usually considered to be a measure of the cleanliness of the chamber. Recently Dodge and Hecht (Ref. 18) analyzed ozone decay data from the University of California, Riverside evacuable smog chamber. Ozone half life in the dark was 501 min, and in the light 260 min. The difference in half lives could be accounted for by ozone photolysis, so the conclusion was that stability of ozone in the light is not a good measure of chamber contamination. Conditioning effects do occur in ozone half life determination. Such effects were observed in this study and have been reported by Sabersky (Ref. 19). Such conditioning effects probably reflect removel of surface contaminants by the ozone.

Section 5

RECONCILIATION OF CAPI-6 DATA

The Coordinating Research Council Project CAPI-6 (Techniques for Irradiation Chamber Studies) generated data from some ten smog chambers. A group of round-robin tests were conducted using these ten chambers as follows: (1) irradiation of seven different hydrocarbons with nitrogen oxide; (2) replicate runs to establish reproducibility using the propylene-nitrogen oxide system, and (3) a reactant concentration study in which 3 ppm propylene was reacted with 3, 1.5, and 0.5 ppm nitrogen oxides (Ref. 2). Table 5-1 gives the chamber characteristics. The wide variation in chamber size, materials, lighting conditions and type of lights is notable.

It is not surprising that these 10 chambers should give different values for the photochemical run parameters. The run parameters reported for the 3 ppm propylene/ 1.5 ppm NO system are given by Table 5-2. The variation between chambers was about a factor of two or three, as shown below:

Parameter	Minimum (Laboratory)	Maximum (Laboratory)
NO_2 Formation Rate (ppb/min)	18 (A, F, J)	42 (C, D)
Time to NO_2 Max. (min)	30 (I)	73 (A)
NO_2 Dose (ppm-min.)	76 (H, J)	296 (E)
Oxidant Max. Conc. (ppm)	.46 (D)	1.4 (C)
Time to Oxidant Max. (min)	90 (G)	>360 (E)
Oxidant Dosage (ppm-min)	57 (D)	240 (H)
Propylene Final Conc. (ppm)	.01 (B, F, G, H, I)	0.66 (E)
Propylene Half Time (min)	54 (B)	104 (A, E)
Propylene Max. Rate (ppb/min)	12 (E)	41 (B)

The analysis described below has shown that the observed differences in chamber behavior can largely be accounted for by variations in chamber lighting, chamber materials S/V, chamber volume, and initial conditions. To obtain this normalization of chamber behavior, a combined photochemical and statistical approach was used, in which the experimental data from the factorial experiment was used along with the CAPI data. This provided a data base with sufficient variation in materials and k_d effects to obtain

Table 5-1 Chamber Characteristics

	A	B	C	D	E	F	G	H	I	J
Volume, ft^3	298	335	6.7	14	2.9	116	1140	64	1.8	610
Surface Area, ft^2	450	330	22.4	65.8	14.2	147	1300	92	7.1	479
S/V, $ft.^{-1}$	1.5	1.0	3.35	4.6	4.9	1.25	1.15	1.44	3.9	0.78
Surface Material, %:										
Stainless Steel	67			53		56				
Aluminum		45					43	64		79
Nickel					90					
Glass			84	29			57			
Pyrex	33				10			32	99	
Teflon			16	18					1	21
Tedlar		55				44				
Light Intensity-k_d	.37	.4	.4	.42	.16	.36	.6*	.49	.2	.3**
Lighting System:										
Internal	X			X	X		X			
External		X	X			X		X	X	X
Black Lights	X	X	X	X	X	X	X	X	X	X
Blue Lights	X	X				X		X		X
Sunlamps	X	X						X		X
Ozone Decomposition:										
T 1/2, dark, hr.	10	10***	18.5	3.5	NA	6	7	12	56	8
T 1/2, light, hr.	2.2	7***	5.5	0.85	NA	1.5	4	3	9	1.5

NA = Not Available

* Private communication, J. Shikiya to R. J. Jaffe, 4-25-75.

** Calculated from data supplied in private communication, D. Miller to R. J. Jaffe, 4/11/75.

*** Calculated from reported loss in 3 1/2 hours.

Table 5-2 CRC-APRAC Irradiation Chamber Comparison - Study III
Propylene Reactivity Comparison: 3 ppm Propylene - 1.5 ppm NO

Laboratory	A	B	C	D	E	F	G	H	I	J
Initial Concentrations										
Propylene, ppm	3.0	3.06	3.10	3.15	3.03	2.94	3.0	3.0	3.0	3.05
NO_x, ppm	1.53	1.49	1.86	1.49	1.50	1.55	1.5	1.5	1.5	1.60
NO_2, ppm	0.12	0.09	0.38	0.13	0.18	0.14	0.16	0.06	0.06	0.03
NO_2 Formation										
NO_2 Formation Rate, ppb/min	18	33	42	42	20	18	28	23	38	18
Time to NO_2 Maximum, min	73	35	34	32	85	71	50	56	30	58
NO_2 Dosage, ppm-min	118	149*	210	110	296*	159	109*	76	87	77
Oxidant Formation										
Maximum Rate, ppb/min.	22	37	20	13	2.5	16	27	42	25*	27
Average Rate, ppb/min.	6	12	13	5	2.0	6	7	9	11	5.8
Maximum Concentration, ppm	1.1	1.3	1.4	0.46	0.7	1.0	1.0	1.2	0.8	0.8
Time to Maximum, min.	135	93	175	82	>360*	>300*	90	106	124	93
Oxidant Dosage, ppm-min	195	173*	317	57	103	203	185*	240	65	114
Propylene Disappearance										
Final Concentration, ppm	0.11	0.01	0.02	0.40	0.66	0.01*	0.01	0.01	0.01*	0.10
$T_{0.75}$, min	79	39	29	30	56	61	48	44	31	74
$T_{0.5}$, min	104	54	55	71	104	90	69	68	60	92
$T_{0.25}$, min	140	78	76	118	159	136	95	89	88	113
Maximum Rate, ppb/min	25	41	33	17	12	21	31	35	26	38
Average Rate, ppb/min	14	28	29	20	11	18	21	22	25	16
Maximum CH_2O, ppm		2.0		1.5		1.5		2.4	2.8	0.9
Maximum PAN, ppm		0.28						0.47		

*These values were determined by personal communication with the experimenter or calculated from other tests conducted for CAPI-6.

model equations for the various run parameters that are high enough in R^2 that they are believed to be realistic.

5.1 CAPI-6 DATA HANDLING

The seven materials shown in Table 5-1 were reduced to four by grouping similar materials. Stainless steel was used for both stainless steel and nickel; Pyrex was used for both Pyrex and glass; and Teflon was used for both Teflon and Tedlar. These groupings were made in consideration of the known similarities in surface properties of the materials, which leads to the expectation that effects of the paired materials are close enough to justify the pairings. Cleaning technique used for the CAPI-6 chambers was not systematically varied. Some chambers used overnight purges at elevated temperature, and some used vacuum offgassing techniques. It was thus not possible to treat cleaning as an independent variable.

Light intensity for the chambers was reported as k_d. The types of lamps used were also reported. Basically two systems were used. Chambers A, B, F, H, and J used a combination of sunlamps, black lamps and blue lamps. The mix used for the lamps varied somewhat from chamber to chamber. The other chambers used black lights only. The factorial experiment results showed that light at wavelengths below 340 nm was proportionally more important in speeding the smog reaction than was light at higher wavelength. To account for this effect, the regressions were carried out to group chambers A, B, F, H, and J and chambers C, D, E, G, and I as having two separate k_d effects. That is, it was assumed that the combination-lamp chambers had the same spectral effectivity and that the black lamp chambers could have a different spectral effectivity.

5.2 FACTORIAL EXPERIMENT DATA HANDLING

The factorial experiment, as described in Sections 2 and 3, resulted in data for the photochemical run parameters for a total of 32 chambers, as obtained from four materials times 2 S/V values times 2 spectral conditions times 2 cleaning conditions.

The full spectrum condition is the one that is closest to the CAPI spectral distribution and was the one used. As the CAPI data was gathered from chambers that used a variety of cleaning conditions, the average of the two cleaning techniques was selected from the factorial experiment results. This gave run parameters for eight chambers. Data for a ninth chamber was also available. The ninth chamber was the baseline, empty Pyrex chamber with no added surface materials. The photochemical runs for all these chambers were conducted at k_d of 0.3 min^{-1}.

5.3 MULTIPLE REGRESSION RESULTS

The nine factorial experiment runs and the ten CAPI runs formed the 19 point array analyzed in the multiple regression. Twelve independent variables have been included in the regression model:

Aluminum S/V, ft^{-1}
Stainless Steel S/V, ft^{-1}
Pyrex S/V, ft^{-1}
Teflon S/V, ft^{-1}
Chamber Volume, ft^3
Initial HC, ppm
NO_x, ppm
NO_2, ppm
% NO_2 in NO_x
HC/NO_x Ratio
k_d ACT, min^{-1}
k_d ADJ, min^{-1}

These were selected based on the results obtained in Appendix B, for correlating the factorial experiment; and on the previously discussed basis that k_d and spectrum combined would give a better fit than a single k_d. Thus k_d is entered in two ways: k_d ACT is the actual k_d for the factorial experiment runs and the CAPI chambers A, B, F, H, and J but zero for the remaining CAPI chambers; and k_d ADJ is the actual k_d for CAPI chambers C, D, E, G, and I, and zero for the remaining chambers.

Running multiple regressions (using the BMD 03R multiple regression program developed at the University of California at Los Angeles) with the twelve independent variables, the prediction equations and R^2 values for the nine run parameters considered are as found in Table 5-3. It should be noted that the R^2 value is the percentage of the observed variability which is accounted for by the independent variables, and ranges from 75.5% to 89.7%. While the R^2 values are not particularly high when considering the number of data points and the number of independent variables, it is encouraging that they are as high as they are. Tables 5-4, 5-5, and 5-6 give the results of the multiple regression prediction equation; the residuals, and the normalized residuals. The normalized residual (Table 5-6) is the residual divided by the respective parameter standard deviation. For 16 of the 19 chambers, the normalized residual is less than 3, indicating satisfactory fit of the data. It should also be noted that the normalized residuals are well distributed among the 19 chambers, with the possible exceptions of oxidant maximum concentration and oxidant dose, for which the factorial experiment results form extremes.

To find whether the double entry of k_d (to allow for spectral differences) was advantageous, the full model was changed so as to include only a single k_d term, that term being the actual k_d for each chamber. The 10 other variables were unchanged. Table 5-7 gives the R^2 comparisons of the dual and single k_d models.

The R^2 values show a decrease from the dual k_d model to the single k_d model for all parameters except those dealing with NO_2, and the HCT 50, indicating that the dual k_d allowing for a spectral effect is beneficial in the parameters. Through the decrease is small for some of the remaining parameters (notably O_3TM), it is expected that the decrease in R^2 is caused by the removal of a needed term, rather than merely because fewer independent variables were used (the drop in R^2, with the possible exception of O_3TM, is large when considering that the number of independent variables is being decreased by only one variable, or by 8.3%). The insensitivity of the NO_2 parameters to use of a second k_d is not surprising, as k_d is a measure of NO_2 photolysis rate, and the regression equation fit can be satisfied by a single value of k_d.

Table 5-3 Results of Multiple Regression with Full Model

	Run Parameters								
	1 $1/NO_2R$	2 NO_2TM	3 NO_2DOSE	6 $O_3MAX\ C$	7 O_3TM	8 O_3DOSE	9 HCFC	11 HCT50	13 1/HC MAX RATE
R^2	77.1	81.7	81.9	79.5	75.5	89.7	80.8	79.1	79.4
VOL	-0.00001	-0.01601	-0.01544	0.00026	-0.13341	0.01296	-0.00022	-0.01981	-0.00004
ALUM	-0.00847	-7.27405	-20.19029	0.01021	-42.08414	11.49137	-0.03204	-10.85161	-0.00890
SS	-0.01019	-5.25568	-10.46144	-0.06142	-0.47079	4.31745	0.03437	-8.74458	-0.00152
PYR	-0.00488	0.74252	-29.32697	-0.01558	-36.58080	2.44492	-0.04372	-1.72086	-0.00808
TEF	0.01233	9.04682	0.80514	-0.01325	-16.99710	-8.28517	0.00475	10.06901	-0.00032
k_dACT	-0.07332	-32.96704	-454.05908	0.40104	-367.24854	383.83301	-0.70153	-82.51172	-0.07654
HC INIT	0.45600	306.51807	541.18042	-4.11157	1887.50269	-1035.93994	2.20197	450.18188	0.37821
NO_x	-0.61969	-321.92065	-1205.93994	3.86622	-3732.97095	1284.81372	-1.87708	-474.81421	-0.59283
NO_2	-1.65762	-2985.35156	1857.54834	20.30347	-1741.55469	2178.25098	-10.29309	-3070.67969	-0.85324
$\%NO_2$	0.02811	49.98193	-19.47304	-0.29726	33.22971	-28.72931	0.16763	51.20485	0.01431
HC/NO_x	-0.72429	-642.34033	-746.38794	5.79683	-3714.80566	1124.15088	-2.73319	-764.72607	-0.59400
k_dADJ	-0.07619	-48.49976	-354.90674	-0.50213	-167.00391	169.23122	-0.17421	-76.15112	0.00219
CONST.	1.07049	887.02930	1945.75562	-4.14520	7652.95703	-1055.64429	1.94828	976.24683	1.01017

Table 5-4 Run Parameters Predicted From Multiple Regression

	Run Parameters								
CHAMBER	1 $1/NO_2R$	2 NO_2TM	3 NO_2DOSE	6 O_3MAX C	7 O_3TM	8 O_3 DOSE	9 HCFC	11 HCT 50	13 1/HC MAX R
A	0.04817	64.82300	134.57764	1.07269	178.30469	194.35645	0.08407	86.34229	0.03662
B	0.04834	44.87793	128.94653	1.18542	75.31641	174.26685	0.00542	72.57080	0.02752
C	0.02762	38.33400	218.17624	1.38206	193.38986	311.96899	0.03499	59.17482	0.03338
D	0.03124	39.53026	137.78392	0.56036	124.83102	78.74800	0.39399	72.22748	0.06411
E	0.03897	67.17046	252.26547	0.63516	306.89258	98.14925	0.54406	93.41737	0.07476
F	0.06735	88.22900	162.14966	1.06523	255.85547	210.57935	0.13546	109.20288	0.05041
G	0.03072	45.75050	96.66560	0.97474	66.25079	176.73207	0.01566	66.97267	0.02878
H	0.02641	36.34375	43.86914	1.15695	68.58984	228.58740	-0.08510	53.11987	0.02109
I	0.02676	32.52100	83.43175	0.75248	110.87657	55.03642	0.06837	63.61304	0.03675
J	0.05841	62.74487	101.96338	0.90188	132.15234	127.10132	0.08473	92.28516	0.02855
ALUM HIGH	0.06896	91.20044	171.86060	1.01108	159.29297	177.17993	0.16738	114.23608	0.04070
ALUM LOW	0.06726	90.33032	159.92212	1.00162	141.39063	155.28076	0.16867	116.46240	0.04363
SS HIGH	0.03252	58.73291	154.96045	0.97268	126.53906	167.74487	0.22869	79.93945	0.03891
SS LOW	0.05560	82.96143	159.56519	0.96508	167.26953	159.12183	0.21037	107.34180	0.04654
TEF HIGH	0.09679	111.74316	176.66138	1.11413	179.79688	169.14233	0.09115	136.82568	0.04569
TEG LOW	0.08533	109.72583	164.71191	1.03559	173.36719	171.64917	0.15595	135.88403	0.04661
PYR LOW	0.06025	100.73438	124.99365	1.10186	157.36719	197.83032	0.04414	118.20264	0.03563
PYR HIGH	0.06835	87.68359	139.77075	0.92530	105.60156	143.60522	0.15816	120.57324	0.03444
PYR BASE	0.05655	77.47168	171.57568	1.19648	159.61328	186.08130	0.07348	101.50000	0.04077

Table 5-5 Run Parameters Residuals from Multiple Regression

Run Parameters

CHAMBER	1 $1/NO_2R$	2 NO_2TM	3 NO_2DOS	6 O_3MAX C	7 O_3TM	8 O_3DOS	9 HCFC	11 HCT 50	13 1/HC MAX R
A	-0.00743	-8.17700	+16.57764	-0.02731	+43.80469	-0.64355	-0.02593	-17.65771	-0.00338
B	+0.01804	+9.87793	-20.05347	-0.10458	-17.68359	+1.26685	-0.00458	+18.57080	+0.00352
C	+0.00382	+4.33400	+8.17624	-0.01794	+18.38986	-5.03101	+0.01499	+4.17482	+0.00338
D	+0.00744	+7.53026	+27.78392	+0.10036	+42.83102	+21.74800	-0.00601	+1.22748	+0.00511
E	-0.01103	-17.82954	-42.73453	-0.06484	-53.10742	-4.85075	-0.11594	-10.58263	-0.00824
F	+0.01175	+17.22900	+3.14966	+0.06523	-44.14453	+7.57935	+0.12546	+19.20288	+0.00241
G	-0.00498	-4.24950	-12.33440	-0.02526	-23.74921	-7.26793	+0.00566	-2.02733	-0.00322
H	-0.01709	-19.65625	-32.13086	-0.04305	-37.41016	-11.41260	-0.09510	-14.88013	-0.00791
I	+0.00046	+2.52100	-3.56825	-0.04752	-13.12343	-9.96358	+0.05837	+3.61304	-0.00125
J	+0.00281	+4.74487	+24.96338	+0.10182	+39.15234	+13.10132	-0.01527	+0.28516	+0.00555
ALUM HIGH	+0.00086	+1.20044	+9.86060	+0.05108	+10.29297	+19.17993	+0.00738	-2.76392	-0.00130
ALUM LOW	+0.00456	+7.33032	+1.92212	-0.07838	+1.39063	-35.71924	+0.05867	+10.46240	+0.00563
SS HIGH	+0.00642	+12.73291	+26.96045	+0.10268	+21.53906	+6.74487	+0.11869	+7.93945	+0.00391
SS LOW	+0.00950	+16.96143	+22.56519	-0.19492	+45.26953	-41.87817	+0.11037	+20.34180	+0.01154
TEF HIGH	-0.00361	-0.25684	+8.66138	+0.04413	+2.79688	-0.85767	-0.01885	-2.17432	+0.00169
TEF LOW	-0.01187	-18.27417	-35.28809	-0.14441	-19.63281	-15.35083	-0.01405	-14.11597	-0.01139
PYR LOW	+0.01915	+10.73438	+6.99365	+0.04186	+25.36719	+25.83032	-0.06586	+12.20264	+0.00763
PYR HIGH	-0.00765	-9.31641	-22.22925	+0.01530	-42.39844	+3.60522	-0.05184	-6.42676	-0.00556
PYR BASE	-0.02135	-17.52832	+10.57568	+0.22648	-0.36872	+34.08130	-0.08652	-27.50000	-0.00823

Table 5-6 Normalized Residuals from Multiple Regression

Run Parameters

	1	2	3	6	7	8	9	11	13	
CHAMBER	$1/NO_2R$	NO_2TM	NO_2DOS	O_3MAX C	O_3TM	O_3DOS	HCFC	HCT 50	1/HC MAX R	Average of Absol. Value
A	-1.11	-1.14	+2.72	-1.24	+5.62	-.10	-.74	-2.43	-.70	1.76
B	+2.69	+1.37	-3.29	-4.75	-2.27	+.20	-.13	+2.56	+.73	2.00
C	+.57	+.60	+1.34	-.82	+2.36	-.80	+.43	+.58	+.70	.91
D	+1.11	+1.05	+4.55	+4.56	+5.50	+3.45	-.17	+.17	+1.06	2.40
E	-1.65	-2.48	-7.01	-2.95	-6.82	-.77	-3.31	-1.46	-1.72	3.13
F	+1.75	+2.39	+.52	+2.97	-5.67	+1.20	+3.58	+2.65	+.50	2.36
G	-.74	-.59	-2.02	-1.15	-3.05	-1.15	+.16	-.28	-.67	1.09
H	-2.55	-2.73	-5.27	-1.96	-4.80	-1.81	-2.72	-2.05	-1.65	2.84
I	+.07	+.35	-.58	-2.16	-1.68	-1.58	+1.67	+.50	-.26	.98
J	+.42	+.66	+4.09	+4.63	+5.03	+2.08	-.44	+.04	+1.16	2.06
ALUM HIGH	+.13	+.17	+1.62	+2.32	+1.32	+3.04	+.21	+.38	-.27	1.05
ALUM LOW	+.68	+1.02	+.32	-3.56	+.18	-5.67	+1.68	+1.44	+1.17	1.75
SS HIGH	+.96	+1.77	+4.42	+4.67	+2.76	+1.07	+3.39	+1.09	+.81	2.33
SS LOW	+1.42	+2.36	+3.70	-8.86	+5.81	-6.65	+3.15	+2.80	+2.40	4.13
TEF HIGH	-.54	-.04	+1.42	+2.01	+.36	-.14	-.54	-.30	+.35	.63
TEF LOW	-1.77	-2.54	-5.78	-6.56	-2.52	-2.44	-.40	-1.94	-2.37	2.93
PYR LOW	+2.86	+1.49	+1.15	+1.90	+3.26	+4.10	-1.88	+1.68	+1.59	2.21
PYR HIGH	-1.14	-1.29	-3.64	+.70	-5.44	+.57	-1.48	-.89	-1.16	1.81
PYR BASE	-3.19	-2.43	+1.73	+10.29	-.05	+5.41	-2.47	-3.79	-1.71	3.45
AVERAGE OF ABSOLUTE VALUE	1.33	1.39	2.90	3.58	3.39	2.22	1.50	1.42	1.11	2.09

Table 5-7

COMPARISON OF R^2 FROM DUAL AND SINGLE k_d MODELS

Run Parameters	Dual k_d Model (%)	Single k_d Model (%)
$1/NO_2R$	77.1	77.1
NO_2 TM	81.7	81.6
NO_2 DOS	81.9	80.2
O_3MAX D	79.5	69.1
O_3TM	75.5	70.7
O_3 DOSE	89.7	81.6
HC FC	80.8	74.0
HCT 50	79.1	79.1
1/HC MAX R	79.4	61.8

To determine how good a fit could be obtained with fewer independent variables, the Hocking-LaMotte regression algorithm was used. In employing this algorithm, k_d ACT and k_d ADJ were forced into the model, and the remaining terms allowed to enter as needed. The resulting range in R^2 was from 60.1 to 86.3%. Table 5-8 gives the results. Interesting items to note are that of nine possible times, % NO_2 enters eight times (accompanied by NO_2 seven of these times), that stainless steel S/V enters five times, and that chamber volume enters only once. Another approach to a limited number of variables data fit was to force into the model the two k_d values, the four material S/V values and the % NO_2. This gave R^2 of 51 to 79.5%.

From these multiple regressions, it is seen that most of the variability between the chambers is due to some or all of the measured variables. Improvements might be made by using cross products of various variables, or by using a more refined measurement of the spectral effectiveness. These procedures were not attempted at this time due to the relatively small number of data points in comparison with the cross products.

Table 5-8 Reduced Multiple Regression Models

	1	2	3	6	7	8	9	11	13
	$1/NO_2R$	NO_2TM	NO_2DOS	O_3MAX C	O_3TM	O_3DOSE	HCFC	HCT 50	1/HC MAX R
R^2	66.1	74.5	78.6	70.8	60.1	86.3	70.7	75.4	67.2
VOL	-	-	-	-	-	-	-	-	-.00003
ALUM	-	-	-9.50805	-	-	-	-	-	-
SS	-.00699	-	-	-.03980	34.26399	-	.07321	-6.46031	-
PYR	-	-	-19.07977	-	-	-	-	-	-.00596
TEF	.01450	10.30616	-	-	-	-	-	14.12842	-
k_dACT	-.05018	-38.93828	-365.99365	.96338	-196.48689	373.43481	-.58105	-99.00389	-.08840
HC INIT	-	-	-	-1.04420	-	-313.43384	-	-	-
NO_x	-	-	-	-	-616.49585	-	-	368.80396	-
NO_2	-.52186	-1085.55029	-	6.08616	-	2058.18018	-2.00685	-2858.43530	-.32312
$\%NO_2$	.01009	31.46994	8.60604	-.08095	-	-26.41008	.03853	47.56219	.00587
HC/NO_x	-	-212.43953	-	-	-921.18018	-	-	-	-
k_dADJ	-.08556	-81.42564	-302.70654	.29652	-216.76044	189.46100	-.37457	-115.42805	-.02825
CONST	.05215	469.45679	211.33298	3.80398	2967.64429	957.28271	.18939	-468.91699	.06889
R^2*	60	53.7	79.5	61.7	54.9	67.4	70.4	51	61.1

*Based on k_dACT and k_dADJ, the four material S/Vs, and % NO_2.

5.4 NORMALIZATION FOR k_d EFFECTS

The effect of variations in light intensity in smog chamber experiments is complex. It is possible to use a photochemical smog simulation model and vary the light intensity. One such simulation is reported by Niki (Ref. 7), for the propylene (2.23 ppm)/NO (0.97 ppm) system at 90° F and 50% relative humidity. He found that the NO_2 formation rate and the time to NO_2 maximum were nearly linear with light intensity, but that the run parameters that characterize later stages of the reaction are not. Thus the propylene half time ratio was 1.67, and the ratio of ozone maximims is "much less than a factor of two," for a reduction in k_d of a factor of two. The data of Altshuler (Ref. 5) show a ratio of ozone maximum concentration of about two, for a reduction in light intensity of a factor of three in light intensity. It would not be surprising to find an interaction of chamber material and size with light intensity effect.

One experiment was conducted to compare the effect of k_d on the run parameters. The empty baseline Pyrex chamber was used, and tests made at k_d of 0.4 and 0.3 min^{-1}. The data obtained is given in Table 5-9. If the parameter were linearly proportional to k_d, the ratio of the values would be 1.33 (or 1.33^{-1} for those parameters that decrease for an increase in k_d). The difference between the experimental data and the linearly proportional assumption is shown by the last column of Table 5-9, which gives the ratio of the experimental data to 1.33. To account for the variation in k_d among the CAPI chamber, an adjustment factor defined as the product of the ratio of k_d of the chamber divided by 0.4 times the experimental data divided by 1.33 ratio was used These run parameters are shown in Table 5-10, with the notation AA, DA, EA, etc. A linear proportional adjustment of the run parameters is also shown in the table. These values are noted as AL, DL, EL, etc. These normalized data were used in a stepwise regression of the CAPI data (as discussed below), but did not result in a satisfactory fit of the data. It appears that k_d effects cannot be accounted for by either adjustment method. It would be interesting to use a propylene/NO_x photochemical simulation model to predict the run parameters for a range of k_d values from 0.16 to 0.6 min^{-1}, and to compare those results with experimental data.

Table 5-9 Effect of k_d Variation

Parameter	k_d0.4	k_d0.3	Ratio .4/.3	Exper Ratio/1.33
1. NO_2Rate	22.5	12.8	1.752	1.31
2. NO_2T MAX	65	95	1.462^{-1}	1.10
3. NO_2DOSE	127	161	1.267^{-1}	.950
4. O_3MAX Rate	31.5	25.5	1.235	.926
5. O_3 Avg. Rate	7.78	4.11	1.893	1.420
6. O_3 Max Conc.	1.25	.97	1.290	.968
7. O_3T Max	120	160	1.333^{-1}	1.000
8. O_3Dose	246	152	1.623	1.22
9. HC Final Conc.	.10	.16	1.60^{-1}	1.20
10. HC T.75	52	88	1.692^{-1}	1.27
11. HC T.50	82	129	1.466^{-1}	1.10
12. HC T.25	111	162	1.459^{-1}	1.10
13. HC Max Rate	25.4	20.3	1.253	.94
14. HC Avg. Rate	18.1	11.2	1.619	1.21
15. Ald Max	1.15	.75	1.530	1.15
16. PAN Max	.37	.38	1.01^{-1}	.757
17. NO Rate	11.3	7.44	1.512	1.13
18. NO_2DF	28.3	36.9	1.267^{-1}	.930
19. O_3DF	30.4	34.7	1.125^{-1}	.843
20. FWHM	68	92	1.353^{-1}	1.02
21. Cross Time	38	58	1.526^{-1}	1.14
22. NO_2XT	27	37	1.370^{-1}	1.03
23. O_3XT	82	102	1.240^{-1}	.930

Table 5-10 CAPI Chambers Adjusted to k_d of 0.4

		AA	AL	B	C	DA	DL	EA	EL	FA	FL	GA	GL	HA	HL	IA	IL	JA	JL
1.	NO_2Rate	19.9	19.5	33	42	39.6	40	59.4	50	25	20	16.9	18.7	18.6	18.8	87.9	76	31.5	23.9
2.	NO_2Time	67	67.5	35	34	33.6	33.6	35	34	62	69.3	77.5	75	69.9	68.6	14.3	15	39.7	43.5
3.	NO_2Dose	110	109	149	210	116	116	122	118	150	143	161	164	92.3	93.1	44.6	43.5	60.8	57.8
4.	O_3MR	34.7	23.8	37	20	12.4	12.4	5.98	6.25	17.5	17.8	18.6	18.0	34.6	34.3	48.3	50	33.3	35.9
5.	O_3AR	6.69	6.49	12	13	4.67	4.67	6.26	5.00	8.82	6.66	4.09	4.67	6.82	7.34	26.6	22	11.0	7.71
6.	O_3MC	1.18	1.19	1.3	1.4	.44	.44	1.72	1.75	1.11	1.10	.67	.67	.98	.98	1.58	1.6	1.03	1.06
7.	O_3TM	125	125	93	175	86.1	86.1	144	144	270	270	135	135	130	130	62	62	69.8	69.8
8.	O_3DOSE	214	211	173	317	53.7	543	292	258	252	226	115	123	188	196	144	130	185	152
9.	HCFC	.10	.10	.01	.02	.42	.42	.26	.26	.008	.01	.016	.015	.013	.012	.005	.005	.06	.08
10.	HC25	71.6	73.1	39	29	31.9	31.5	19.2	22.4	46.9	54.9	78.5	72	56.6	53.9	14.7	15.5	43.7	55.5
11.	HC50	95.5	96.2	54	55	74.6	74.6	39.2	41.6	80	81	107	104	84.9	83.3	28.9	30	62.8	69
12.	HC75	129	130	78	76	124	124	60	63.6	120	122	147	143	111	109	41.9	44	77.5	84.8
13.	HCMR	26.9	27.0	41	33	16.2	16.2	28.9	30	21.8	23.3	21.1	20.7	28.9	28.6	50.4	52	47.6	50.5
14.	HCAR	15.4	15.1	28	29	18.9	19.0	31	27.5	22.1	20.0	13.1	14.0	17.3	18.0	55.3	50	25.9	21.3

5.5 COMPUTATIONS USING NORMALIZED CAPI DATA

An attempt was made to utilize the prediction formula coefficients given in Tables B3-1 and B4-3 of Appendix B. These equations were obtained from the factorial experiment, and apply to a k_d of 0.3 min^{-1}, and to addition of each material at the noted S/V to a base S/V of 1.4 ft^{-1} of Pyrex. Because of this structure of the factorial experiment, it is not possible to use the prediction formulas directly in analyzing the CAPI data. The factorial experiment chamber conditions that most closely resemble each CAPI chamber was determined as found in Table 5-11. There were 16 factorial experiment condition combinations to choose from (four materials times two S/V values times two cleaning techniques) in matching each CAPI chamber. The prediction equation was then used to predict the CAPI results which would be expected after adjusting for the initial conditions of initial percent NO_2 in NO_x and hydrocarbon content.

Tables 5-12, 5-13 and 5-14 exhibit the predicted values, the residuals (or differences) of the predicted values and the actual CAPI results after adjustment for k_d, and the normalized residuals, respectively. The normalized residuals for any CAPI chamber averaged from 2.23 to 8.41, indicating lack of agreement between the factorial experiment and the CAPI data. This lack of agreement is not too surprising when the range of k_d extrapolation required, the spectral effect, and the need to obtain material effects in the factorial experiment against a constant background of 1.4 ft^{-1} of Pyrex are considered. The generally poor predictive ability of the factorial equations point out the desirability of the multiple regression approach of Section 5.3 It is recommended that the coefficients given by Table 5-3 be used to compare results of various smog chambers.

5.6 CORRELATION COEFFICIENTS

The correlation coefficients between the parameters studied are given by Table 5-15. The first entry in each column is for the correlation among the CAPI chambers after adjusting for k_d variations and the initial condition covariates. The second entry is for the factorial experiment results, after adjusting for initial condition covariates. The differences between the pairs are possible indications that the two sets of experimental data are in some sense different. The two parameters that are troublesome in this are ozone dose and hydrocarbon final concentration.

The correlation coefficients between the run parameters and the ozone half lives are given in Table 5-16. Ozone half-life data was not available for Chamber E. The halflife for Chamber I seemed unusually long, and a correlation was performed that omitted that chamber. The correlation coefficients obtained in the factorial experiment are also shown. The differences show that ozone half-life by itself cannot be used to characterize smog chambers.

Table 5.11

Material, Spectrum, S/V and Cleaning for CAPI Chambers

Chamber	Material	Spectrum	S/V	Cleaning
A	Pyrex	Full	low	Purge
B	Aluminum	Full	low	Purge
C	Teflon	Full	hi	Vacuum
D	Stainless Steel	Full	hi	Vacuum
E	Pyrex	Full	hi	Vacuum
F	Aluminum	Full	low	Purge
G	Teflon	Full	low	Purge
H	Aluminum	Full	low	Purge
I	Stainless Steel	Full	hi	Vacuum
J	Stainless Steel	Full	low	Purge

Table 5-12

Predicted CAPI Run Parameters

Chamber	Run Parameters 1/NO_2R 1	NO_2TM 2	NO_2DOS 3	O_3MAXC 6	O_3TM 7	O_3DOSE 8	HCFC 9	HCT50 11	1/HC MAX R 13
A	.0726	82.76	135.6	.981	123.5	165.6	.1519	132.1	.0263
B	.0604	75.87	154.7	1.053	131.3	183.8	.0705	95.9	.0376
C	.1044	112.03	165.8	1.135	173.2	174.3	.1085	163.8	.0375
D	.0333	52.16	138.0	.890	111.6	162.9	.1095	75.8	.0359
E	.0788	97.21	148.8	1.003	144.0	155.6	.1159	89.6	.0451
F	.0604	75.87	154.7	1.053	131.3	183.8	.0705	95.9	.0376
G	.0806	112.50	196.6	1.101	178.0	173.8	.1289	105.4	.0635
H	.0604	75.87	154.7	1.053	131.3	183.8	.0705	95.9	.0376
I	.0333	52.16	138.0	.890	111.6	162.9	.1095	75.8	.0359
J	.0355	55.59	134.3	1.143	108.7	204.9	.0753	75.2	.0367

Table 5-13

Residuals from Predicted vs Normalized CAPI Parameters

Run Parameters

Chamber	1/NO_2R 1	NO_2TM 2	NO_2DOS 3	O_3MAXC 6	O_3TM 7	O_3DOSE 8	HCFC 9	HCT50 11	1/HC MAX R 13
A	.0160	3.3	-16.3	.067	-32.5	-1.3	.0109	15.29	-.0227
B	.0352	42.5	-53.2	.039	21.0	41.3	.0545	38.67	.0046
C	.0508	47.2	-103.3	.107	-79.9	-49.9	-.1075	69.40	-.0045
D	.0068	13.1	-22.3	.565	2.8	113.2	-.4375	-17.0	-.0491
E	.0528	52.5	-9.3	-.3162	-47.4	-39.2	-.2281	34.8	.0001
F	.0036	-7.6	-40.8	.2268	-219.8	8.5	.0435	-2.6	-.0194
G	.0138	15.5	-24.6	.5908	2.1	78.3	.1059	-28.9	-.0005
H	.0109	3.3	18.7	.2778	-22.7	21.0	.0405	5.6	-.0064
I	.0473	60.1	62.4	-.3680	57.4	63.0	.0425	86.5	.0136
J	.0055	70.3	42.2	.2160	38.9	70.5	-.0437	5.19	.0107

Table 5-14

Normalized Residuals from Predicted vs Normalized CAPI Parameters

	Run Parameter									Average of
Chamber	1/NO$_2$R 1	NO$_2$TM 2	NO$_2$DOS 3	O$_3$MAXC 6	O$_3$TM 7	O$_3$DOSE 8	HCFC 9	HCT50 11	1/HCMAX2 13	Absolute Value
A	2.39	0.46	-2.67	3.05	-4.17	-0.21	0.31	2.11	-4.73	2.23
B	5.25	5.90	-8.72	1.77	2.70	6.56	1.56	5.33	0.96	4.31
C	7.58	6.56	-16.93	4.86	-10.26	-7.92	-3.07	9.56	-0.94	7.52
D	1.01	1.82	-3.66	25.68	0.36	17.97	-12.50	-2.34	-10.23	8.40
E	7.88	7.29	-1.52	-14.37	-6.08	-6.22	-6.52	4.79	0.02	6.08
F	0.54	1.06	-6.69	10.04	-28.22	1.35	1.24	-0.36	-3.83	5.93
G	2.06	2.29	-4.03	26.85	0.27	12.43	3.03	-3.98	-0.10	6.12
H	1.63	0.46	3.07	12.63	-2.91	3.33	1.16	0.77	-1.75	3.08
I	7.06	8.35	10.23	-16.73	7.37	10.00	1.21	11.91	2.83	8.41
J	0.82	2.82	6.92	13.00	4.99	11.19	-1.25	1.13	2.23	4.93
Average of Absolute Value	3.62	3.70	6.44	12.90	6.73	7.72	3.18	4.23	2.76	5.70

Table 5-15

CORRELATION COEFFICIENTS OF RUN PARAMETERS

	1 NO_2 Rate		2 NO_2 T Max		3 NO_2 Dose		6 O_3 Max Conc		7 O_3 T Max		8 O_3 Dose		9 HC Final Conc		11 HC T50		13 HC Max Rate
1																	
2	.982	.933															
3	.639	.611	.588	.843													
6	-.457	-.033	-.447	-.047	.193	-.209											
7	.654	.852	.679	.970	.650	.913	-.013	-.147									
8	.267	-.652	.233	-.753	.319	-.742	.674	.656	.555	-.801							
9	-.220	.672	-.196	.780	-.191	.755	-.313	-.394	-.208	.805	-.439	-.811					
11	.938	.922	.929	.990	.568	.852	-.680	-.118	.486	.971	-.037	-.786	-.005	.810			
13	.447	.608	.495	.785	.376	.871	-.782	-.326	.317	.858	-.456	-.799	.590	.755	.657	.794	

Table 5-16 Correlation Coefficients of Run Parameters and Ozone Half-Lives

		FACTORIAL EXPERIMENT DATA		CAPI CHAMBERS, EXCLUDING E			
				CAPI	ORIG	CAPI	ADJ
		Light	Dark	Light	Dark	Light	Dark
1	1/NO_2R	.795	.824	-.583	-.385	-.555	-.732
2	NO_2 TM	.775	.792	-.621	-.451	-.543	-.682
3	NO_2 DOS	.411	.480	.151	-.156	.011	-.437
6	O_3 MAX C	.122	.256	.359	-.047	.706	.701
7	O_3 TM	.579	.628	-.152	-.027	-.295	-.361
8	O_3 DOSE	-.373	-.226	.003	-.266	.159	.064
9	HCFC	.703	.539	-.519	-.315	.524	-.307
11	HCT 50	.739	.750	-.713	-.381	-.642	-.763
13	1/HC MAX R	.296	.300	-.315	-.153	-.588	-.561
	Sample Size	8	8	9	9	9	9

		CAPI CHAMBERS EXCLUDING E AND I			
		CAPI	ORIG	CAPI	ADJ
		Light	Dark	Light	Dark
1	1/NO_2R	-.513	-.233	-.006	.241
2	NO_2 TM	-.506	-.195	-.087	.084
3	NO_2 DOS	.514	.513	.656	.445
6	O_3 MAX C	.782	.830	.527	.706
7	O_3 TM	-.164	.078	-.005	.188
8	O_3 DOSE	.533	.864	.372	.815
9	HCFC	-.549	-.517	-.577	-.575
11	HCT 50	-.741	-.403	-.235	-.104
13	1/HC MAX R	-.317	-.123	-.427	-.531
	Sample Size	8	8	8	8

Section 6
RECOMMENDATIONS

Further investigations are recommended, as outlined below:

a. Conduct a similar set of tests for another hydrocarbon/NO_x system, such as m-xylene/NO_x. This will indicate whether the observed spectral effects are general, as the range of organic species from unreactive aliphatic (butane), reactive olefin (propylene), and reactive aromatic (m-xylene) will then be available. Also use of a range of compounds from unreactive gas to polar high-boiling liquid may show differing cleaning effects.

b. Perform further studies of the spectral effect, by varying the cutoff wavelength. By use of Teflon rather than Pyrex chamber faces, the amount of light at wavelengths below 320 nm can be substantially increased. Evidently this lower wavelength light is disproportionately important in smog photochemistry. A second new spectrum to investigate is one that has a cutoff between the 320 and 350 nm spectra just investigated. Having available spectral effect data for four cutoffs, it is then possible to obtain an important function for the wavelength range.

c. Investigate light intensity effects by a set of tests at 67 percent and 200 percent of the light intensity previously used. It is theoretically stated that initial behavior of the photochemical system is linear with light intensity, but how late smog manifestations, such as ozone maximum concentration and PAN build-up, vary is not well known. Such data will also be helpful in applying chamber data to the atmospheric diurnal intensity variation.

d. Searching for explanations of persistent anomalies in smog chamber behavior would be productive. Among such anomalies not well understood at present are the occurence of peak NO_2 concentrations greater than initial NO_x charged (for fast reacting systems such as propylene); the initial induction period in NO disappearance; and the entire nitrogen balance. One technique for such an investigation would be to utilize an alternative detection method for the nitrogen species to correlate with the Saltzman NO_2 and the chemiluminescent NO. Time Derivate Spectroscopy is such a technique, and arrangements may be made for such a spectrometer.

e. Ozone production from low levels of hydrocarbons and nitrogen oxides is a subject of increasing practical interest, and could be investigated well using these facilities. The effect of carbon monoxide in such a system is not well known. "Background" runs with say 0.1 ppm NO and 100 ppm CO would be of great interest.

REFERENCES

1. Coordinating Research Council, Individual Hydrocarbon Reactivity Measurements: State-of-the-Art, CRC Report No. 398, New York, Jun 1966
2. D. B. Wimmer, "Factors Affecting Reactions in Environmental Chambers," Coordinating Research Council Inc., Air Pollution Research Advisory Committee Symposium, Chicago, May 1971
3. R. J. Jaffe, Factors Affecting Reactions in Environmental Chambers, Phase I, LMSC-A997745, 20 May 1972
4. O. L. Davies (ed.), The Design and Analysis of Industrial Experiments, Ch. 7, "Factorial Experiments," p. 247, Hafner Publishing Co., New York 1956
5. A. P. Altshuler and I. R. Cohen, "Structural Effects on the Rate of Nitrogen Dioxide Formulation in the Photooxidation of Organic Compound-Nitric Oxide Mixtures in Air," Int. J. Air Wat. Poll., Vol. 7, 1963, p. 787
6. W. A. Glasson and C. S. Tuesday, "Hydrocarbon Reactivity and the Kinetics of the Atmospheric Photooxidation of Nitric Oxide," J. Air Pollution Control Assoc., Vol. 20, 1970, p. 239
7. H. Niki, E. E. Daby, and B. Weinstock, "Mechanisms of Smog Reactions," Advan. Chem., Vol. 13, 1972, p. 16
8. J. J. Bufalini, B. W. Gay, and K. L. Brubaker, "Hydrogen Peroxide Formation From Formaldehyde Photo Oxidation and Its Presence in Urban Atmospheres," Env. Sci. Tech., Vol. 6, 1972, p. 816
9. P. A. Leighton, Photochemistry of Air Pollution, Academic Press, 1961
10. R. J. Gordon, in National Air Pollution Control Administration Pub. 999-AP-38
11. R. C. Hirt et al., Ultraviolet Spectral Energy Distributions of Natural Sunlight and Accelerated Test Light Sources, J. Opt. Soc. Am., Vol. 50, 1960, p. 706
12. J. S. Nader, in National Air Pollution Control Administration Pub. 999-AP-38
13. M. W. Korth, A. H. Rose, and R. C. Stahman, "Effects of Hydrocarbon to Oxides of Nitrogen Ratios on Irradiated Auto Exhaust," Part I, J. Air Pollution Control Assoc., Vol. 14, 1964, p. 168

14. R. J. Jaffe, et al., Factors Affecting Reactions in Environmental Chambers, Phase III, LMSC-D401598, 28 April 1974

15. A. P. Altshuler and J. J. Bufalini, "Photochemical Aspects of Air Pollution, A Review," Env. Sci. Tech. Vol. 5, No. 1, 1971, p. 39

16. A. P. Altshuler, et al., "Photochemical Reactivities of n-Butane and Other Paraffinic Hydrocarbons," J. Air Pollution Control Assoc., Vol. 19, No. 10, 1969, p. 787

17. H. Jeffries, et al., "Photochemical Conversion of NO to NO_2 by Hydrocarbons in an Outdoor Chamber," Air Pollution Control Association, paper 75-16.2, June 1975

18. M. C. Dodge and T. A. Hecht, "Ozone Decay in Irradiated Smog Chambers," submitted to Environmental Letters, June 1975

19. R. H. Sabersky, et al., "Concentration, Decay Rate, and Removal of Ozone," Env. Sci. Tech., Vol. 7, 1973, p. 347

Appendix A
PHOTOCHEMICAL RUN DATA

A.1 Propylene Graphs

Photochemical run data are given in this appendix in several forms – plots of NO, NO_2, ozone, and propylene vs irradiation time, and tabulations of the calculated run parameters as defined in Table 3-1. Data at 10 or 15 minute intervals are available for acetaldehyde and PAN, but only the maximum for these species is reported in the tables. The materials order is aluminum, Pyrex, Teflon, and stainless steel. Eight run graphs are shown for each material. These are for the eight combinations of S/V, spectrum, and cleaning investigated, and are arranged in sequence as follows:

S/V	Spectrum	Cleaning
High	Full	Vac
High	Full	Purge
Low	Full	Vac
Low	Full	Purge
High	Cut	Vac
High	Cut	Purge
Low	Cut	Vac
Low	Cut	Purge

For each material and variable combination, the average of the replicates of the individual runs is given. Pages A-4 to A-11 give these run graphs.

A.2 Propylene Data Tabulation

Initial condition variations affect some of the run parameters rather strongly. Two methods were used to account for initial conditions. One was based on photochemical observations, and one on statistical methods. The photochemical observation method accounted for the initial percentage of NO_2 in the NO_x. As previously suggested, on both theoretical and experimental grounds (Niki, Ref. 7, and B. Dimitriades, Bureau of Mines RI 7433), this is accounted for by a linear extrapolation along the time axis to the standard reference starting condition of 10 percent NO_2 content in NO_x. The tabulated run data show this adjustment as the column T ADJ. For the runs used in the effects analysis, the largest value of T ADJ is 14 minutes. Pages A-12 to A-17 give the data. The statistical analysis considered additional covariates and supported this adjustment method. Appendix B discusses those analyses. Pages A-18 to A-22 give the covariate adjusted data.

It will be noted that two complete sets of experiments were performed for aluminum surfaces. Changes were made in the instrumentation after runs 3 to 6 in the test sequence. These changes made the set of runs between run 69 and run 85 better suited for the effects analysis. In addition, as experience in operating the smog chamber accumulated, better control of initial conditions were obtained. The data accumulated in the later set of aluminum runs is preferable for the reasons just mentioned, and are the ones used in the figures. Both the original runs and the reruns are tabulated for the aluminum surfaces.

Run graphs showing the relative humidity effect are given on pages A-23 to A-30. Run graphs for the butane runs are given on pages A-31 and A-32.

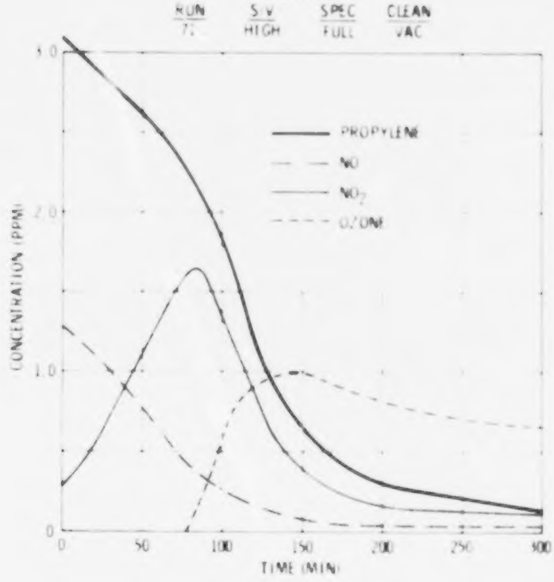

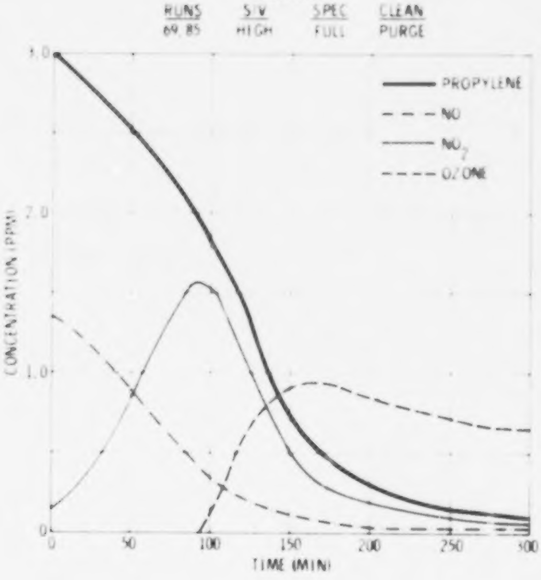

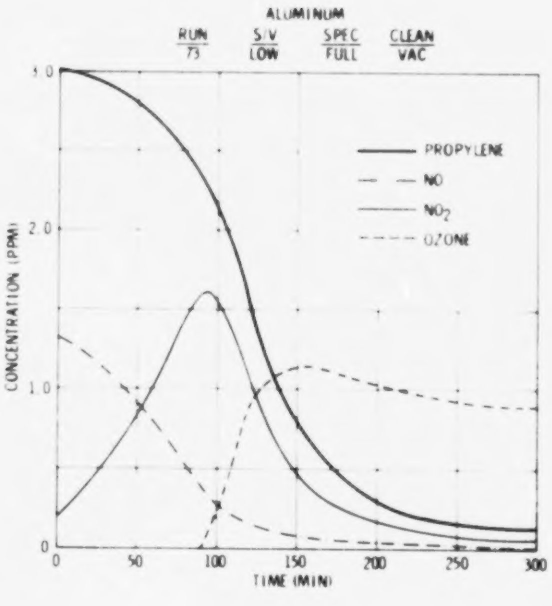

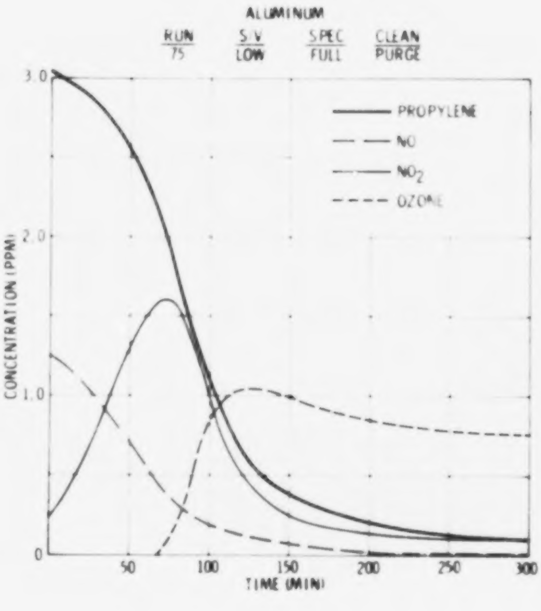

Preceding page blank

ALUMINUM

RUN	S/V	SPEC	CLEAN
81	HIGH	CUT	VAC

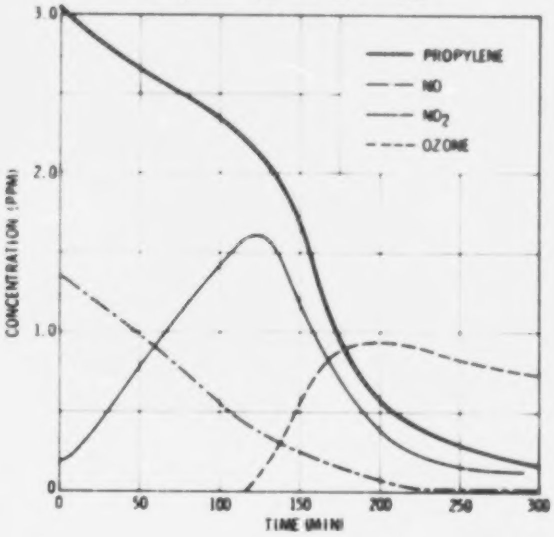

ALUMINUM

RUNS	S/V	SPEC	CLEAN
70, 82, 84	HIGH	CUT	PURGE

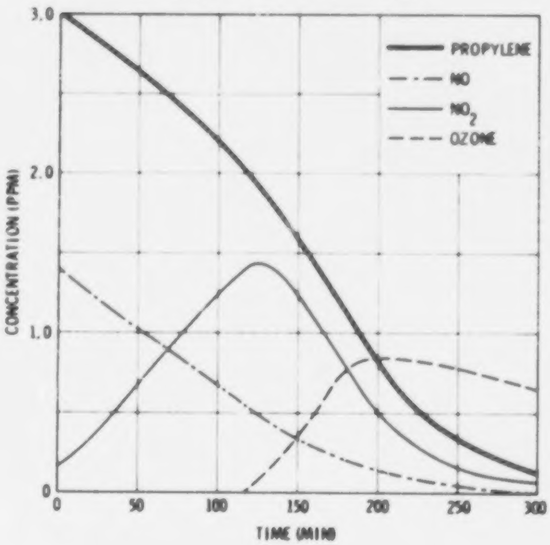

ALUMINUM

RUN	S/V	SPEC	CLEAN
74	LOW	CUT	VAC

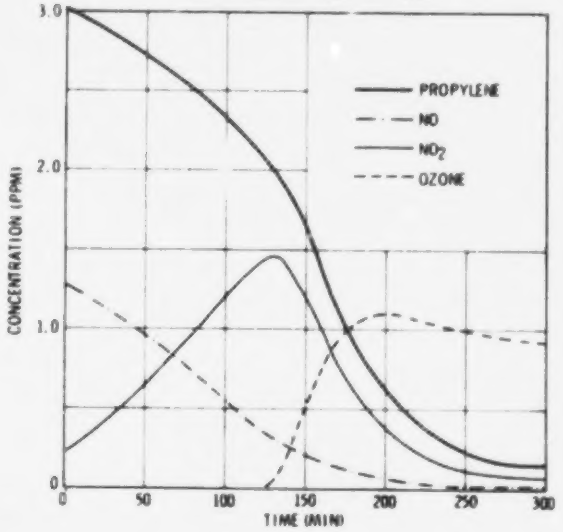

ALUMINUM

RUN	S/V	SPEC	CLEAN
72	LOW	CUT	PURGE

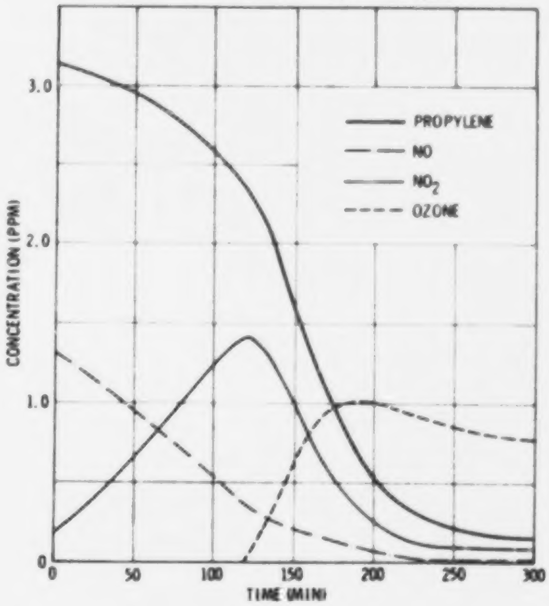

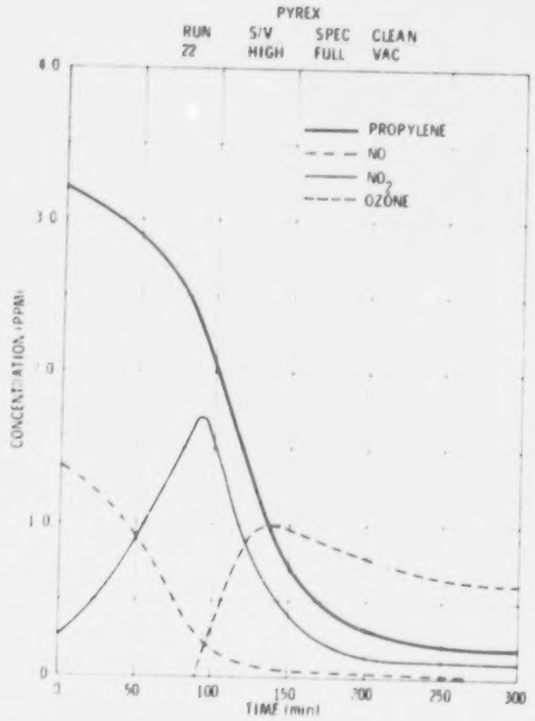
PYREX
RUN 22
S/V HIGH
SPEC FULL
CLEAN VAC
PROPYLENE
NO
NO_2
OZONE
CONCENTRATION (PPM)
0
1.0
2.0
3.0
4.0
0
50
100
150
200
250
300
TIME (min)

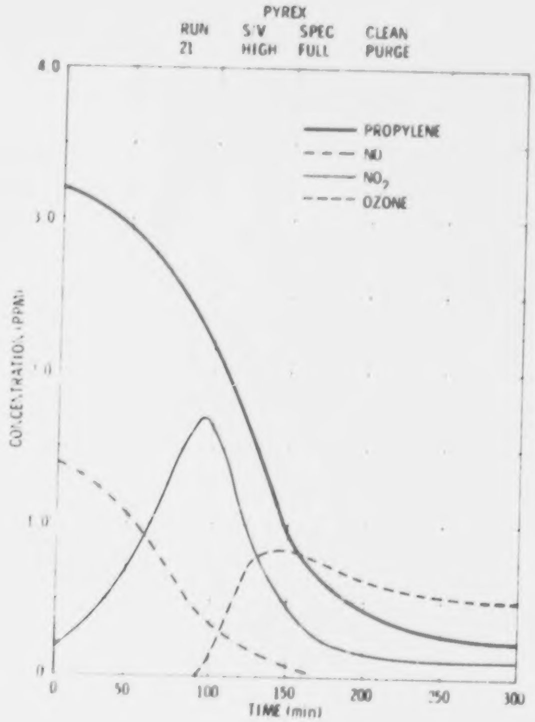
PYREX
RUN 21
S/V HIGH
SPEC FULL
CLEAN PURGE
PROPYLENE
NO
NO_2
OZONE
CONCENTRATION (PPM)
0
1.0
2.0
3.0
4.0
0
50
100
150
200
250
300
TIME (min)

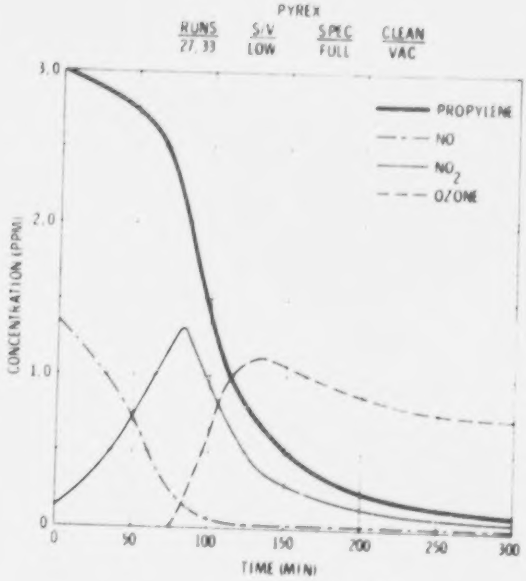
PYREX
RUNS 27, 33
S/V LOW
SPEC FULL
CLEAN VAC
PROPYLENE
NO
NO_2
OZONE
CONCENTRATION (PPM)
0
1.0
2.0
3.0
0
50
100
150
200
250
300
TIME (MIN)

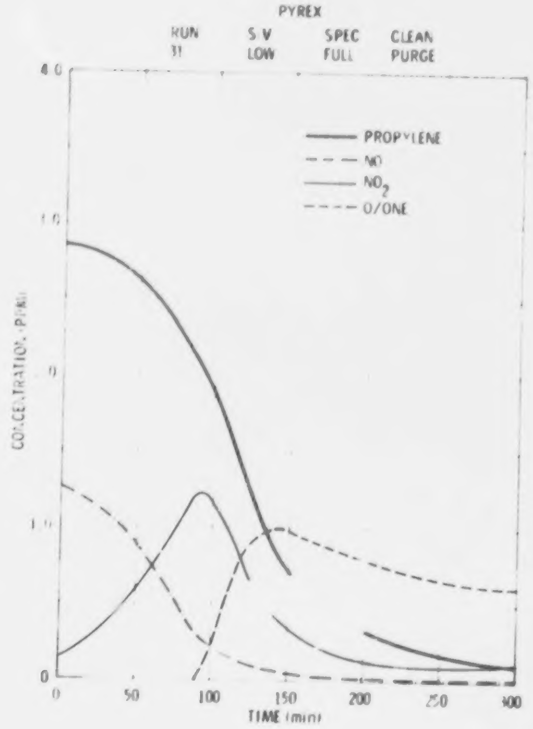
PYREX
RUN 31
S/V LOW
SPEC FULL
CLEAN PURGE
PROPYLENE
NO
NO_2
OZONE
CONCENTRATION (PPM)
0
1.0
4.0
0
50
100
150
200
250
300
TIME (min)

PYREX

RUN	S/V	SPEC	CLEAN
26	HIGH	CUT	VAC

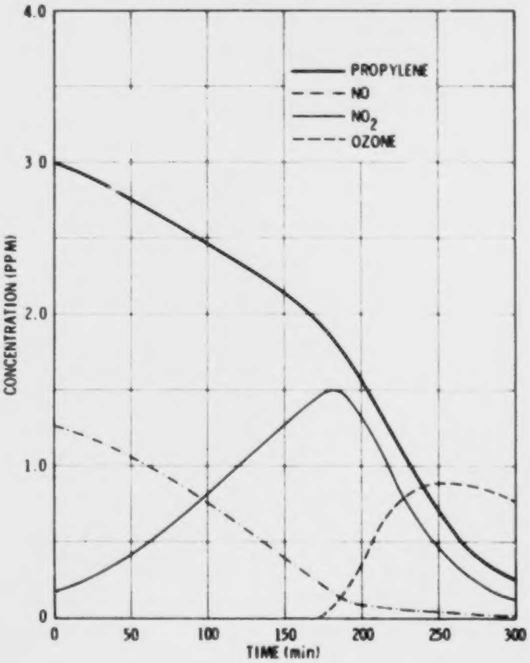

PYREX

RUN	S/V	SPEC	CLEAN
25	HIGH	CUT	PURGE

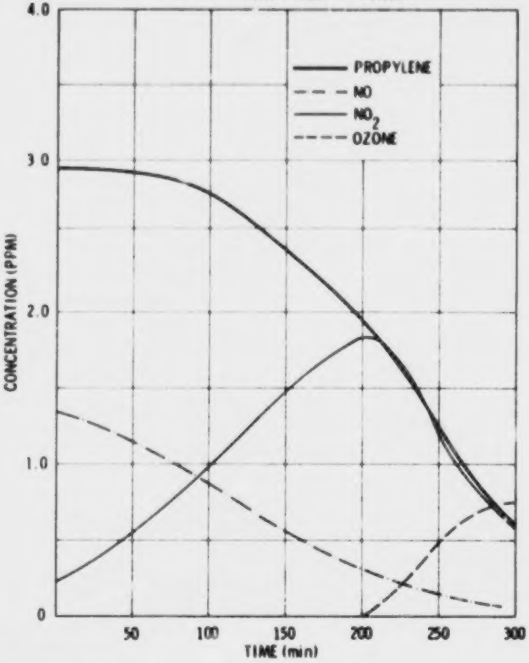

PYREX

RUN	S/V	SPEC	CLEAN
30	LOW	CUT	VAC

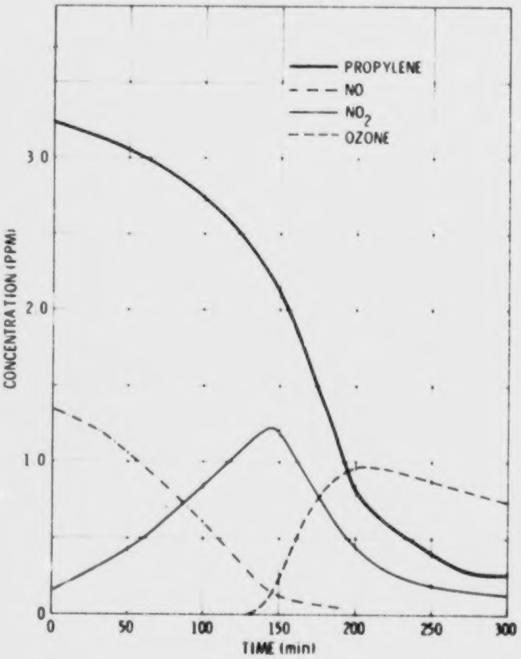

PYREX

RUN	S/V	SPEC	CLEAN
32	LOW	CUT	PURGE

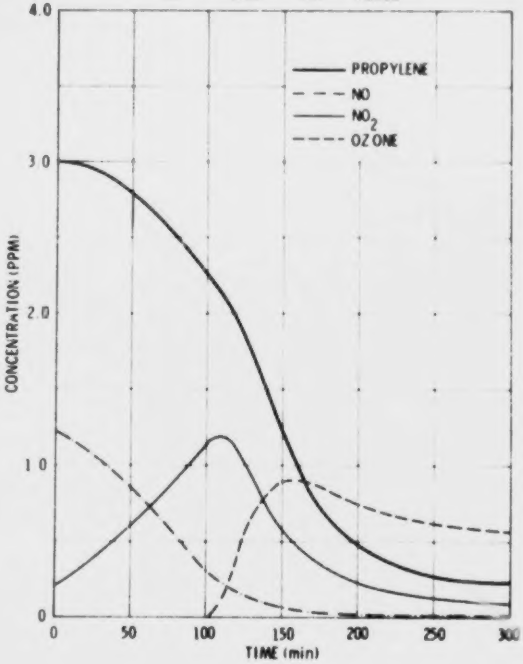

TEFLON

RUN	S/V	SPEC	CLEAN
38	HIGH	FULL	VAC

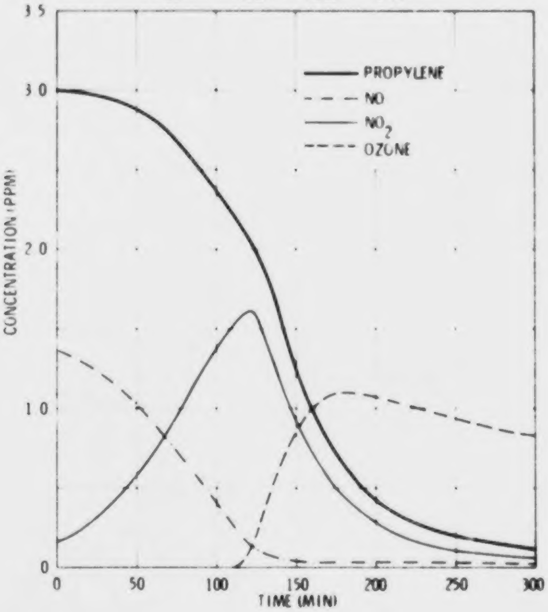

TEFLON

RUNS	S/V	SPEC	CLEAN
34, 35	HIGH	FULL	PURGE

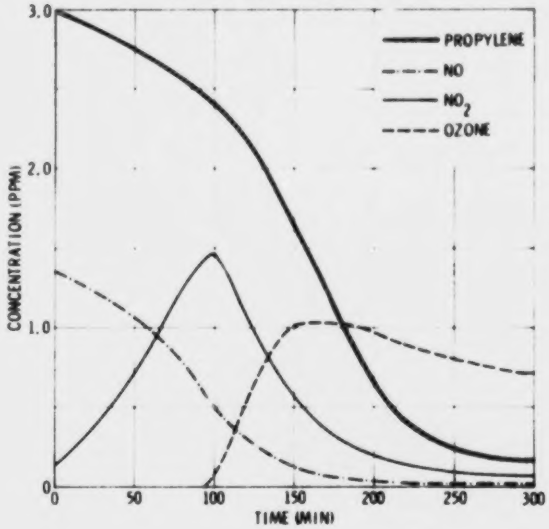

TEFLON

RUN	S/V	SPEC	CLEAN
42	LOW	FULL	VAC

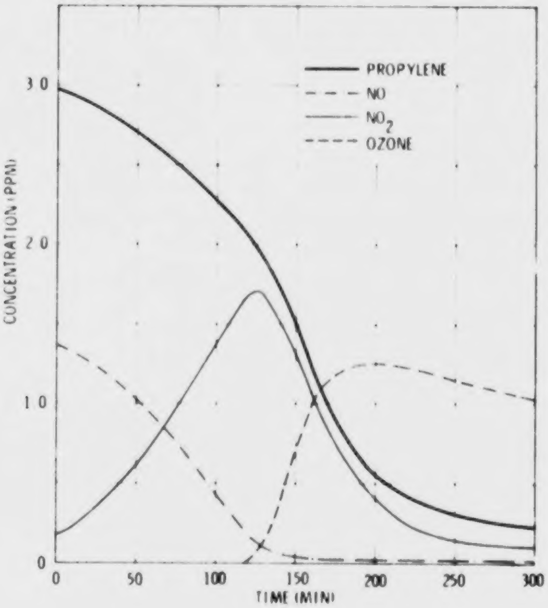

TEFLON

RUNS	S/V	SPEC	CLEAN
43, 44	LOW	FULL	PURGE

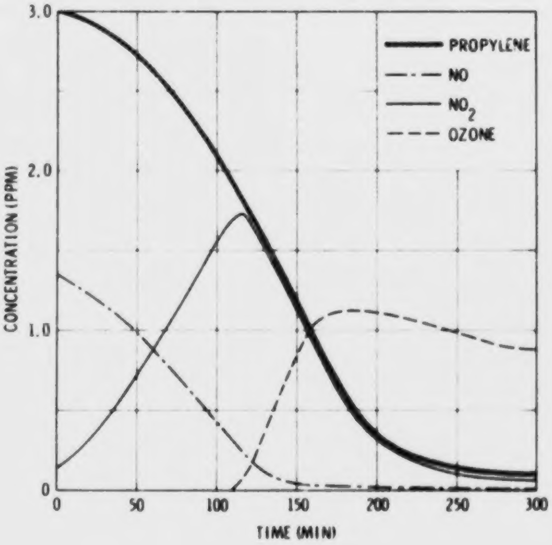

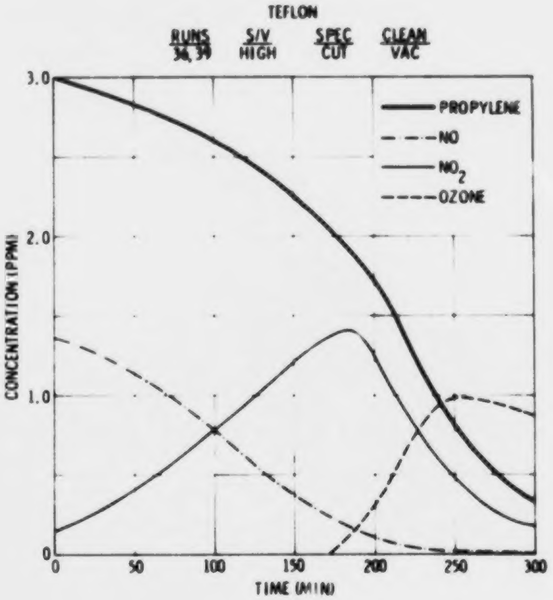
TEFLON
RUNS 36, 39
S/V HIGH
SPEC CUT
CLEAN VAC
PROPYLENE
NO
NO_2
OZONE
CONCENTRATION (PPM)
3.0
2.0
1.0
0
0
50
100
150
200
250
300
TIME (MIN)

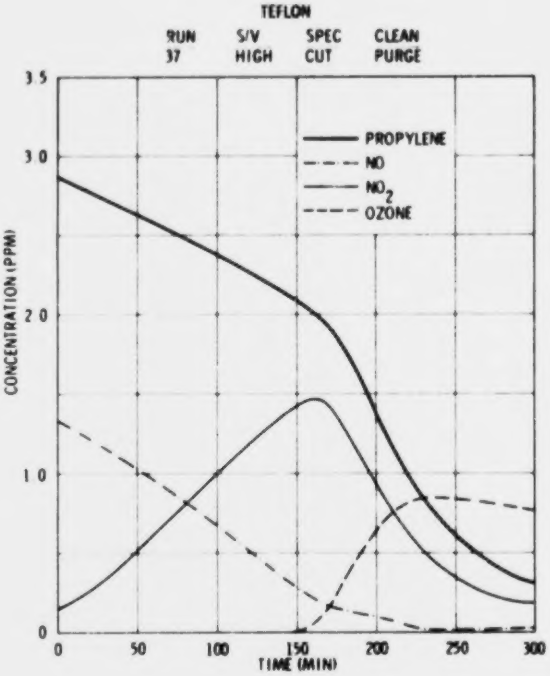
TEFLON
RUN 37
S/V HIGH
SPEC CUT
CLEAN PURGE
PROPYLENE
NO
NO_2
OZONE
CONCENTRATION (PPM)
3.5
3.0
2.0
1.0
0
0
50
100
150
200
250
300
TIME (MIN)

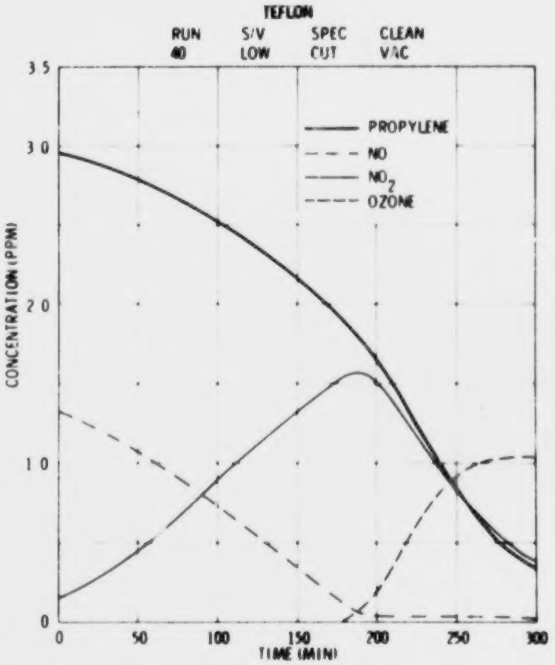
TEFLON
RUN 40
S/V LOW
SPEC CUT
CLEAN VAC
PROPYLENE
NO
NO_2
OZONE
CONCENTRATION (PPM)
3.5
3.0
2.0
1.0
0
0
50
100
150
200
250
300
TIME (MIN)

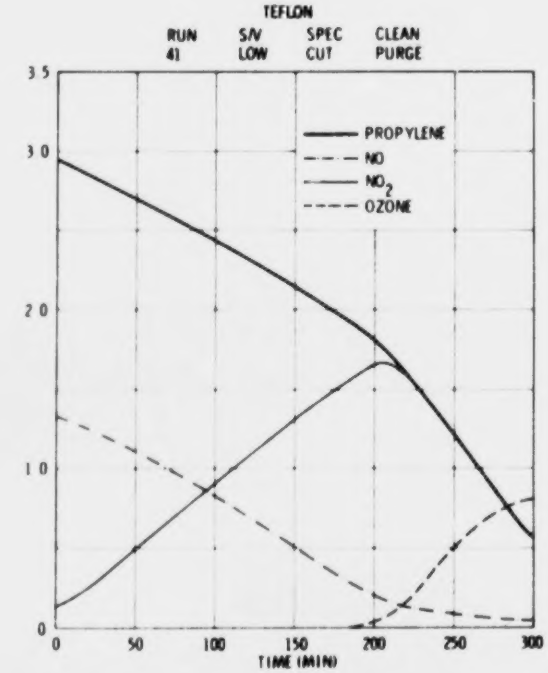
TEFLON
RUN 41
S/V LOW
SPEC CUT
CLEAN PURGE
PROPYLENE
NO
NO_2
OZONE
3.5
3.0
2.0
1.0
0
0
50
100
150
200
250
300
TIME (MIN)

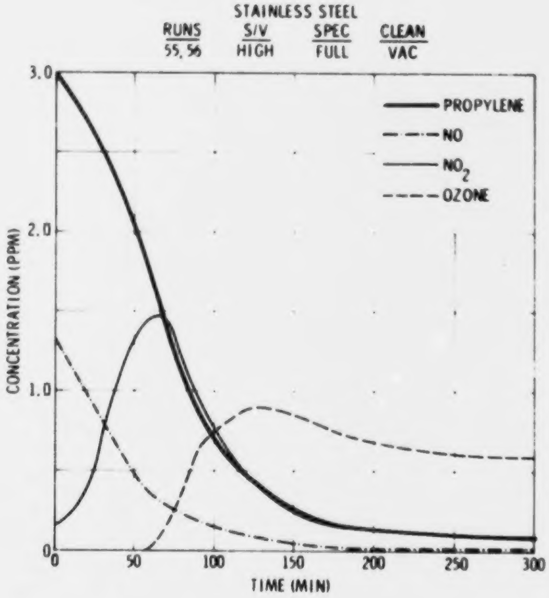
STAINLESS STEEL
RUNS 55, 56
S/V HIGH
SPEC FULL
CLEAN VAC
PROPYLENE
NO
NO_2
OZONE
CONCENTRATION (PPM)
3.0
2.0
1.0
0
TIME (MIN)
0
50
100
150
200
250
300

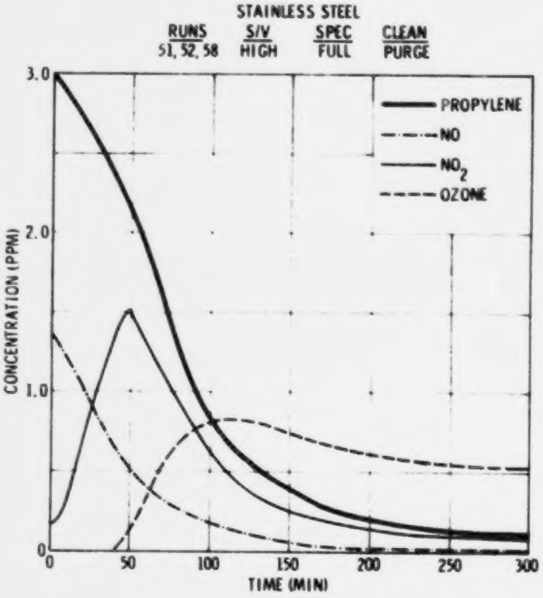
STAINLESS STEEL
RUNS 51, 52, 58
S/V HIGH
SPEC FULL
CLEAN PURGE
PROPYLENE
NO
NO_2
OZONE
CONCENTRATION (PPM)
3.0
2.0
1.0
0
TIME (MIN)
0
50
100
150
200
250
300

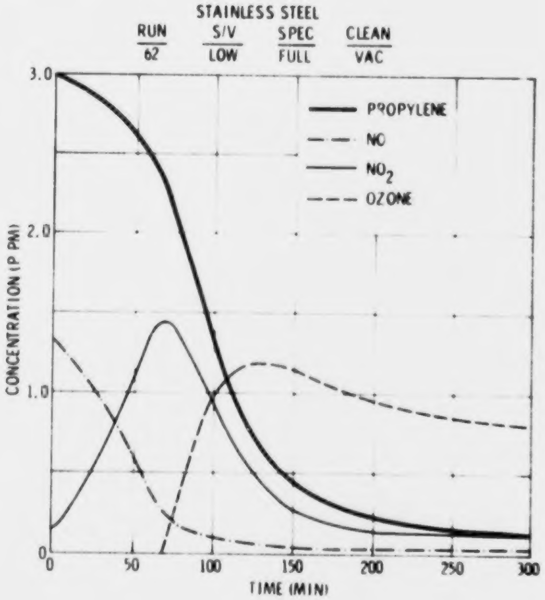
STAINLESS STEEL
RUN 62
S/V LOW
SPEC FULL
CLEAN VAC
PROPYLENE
NO
NO_2
OZONE
CONCENTRATION (P PM)
3.0
2.0
1.0
0
TIME (MIN)
0
50
100
150
200
250
300

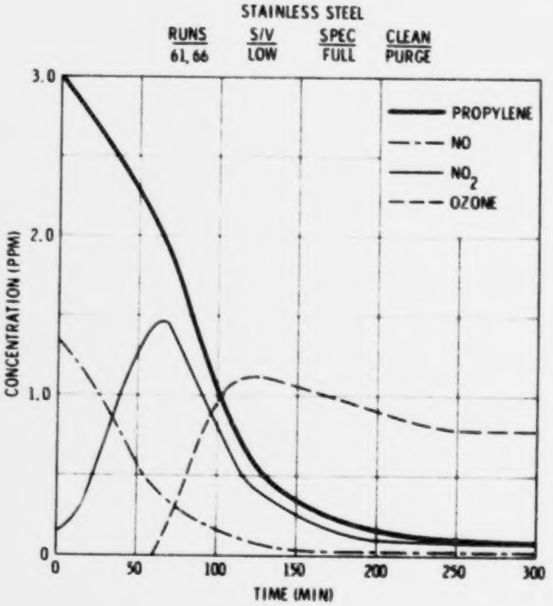
STAINLESS STEEL
RUNS 61, 66
S/V LOW
SPEC FULL
CLEAN PURGE
PROPYLENE
NO
NO_2
OZONE
CONCENTRATION (PPM)
3.0
2.0
1.0
0
TIME (MIN)
0
50
100
150
200
250
300

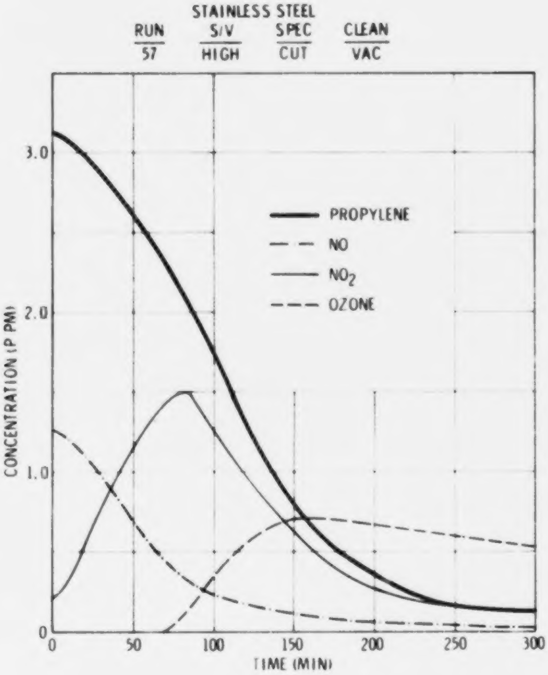
STAINLESS STEEL
RUN
57
S/V
HIGH
SPEC
CUT
CLEAN
VAC
PROPYLENE
NO
NO$_2$
OZONE
CONCENTRATION (P PM)
3.0
2.0
1.0
0
0
50
100
150
200
250
300
TIME (MIN)

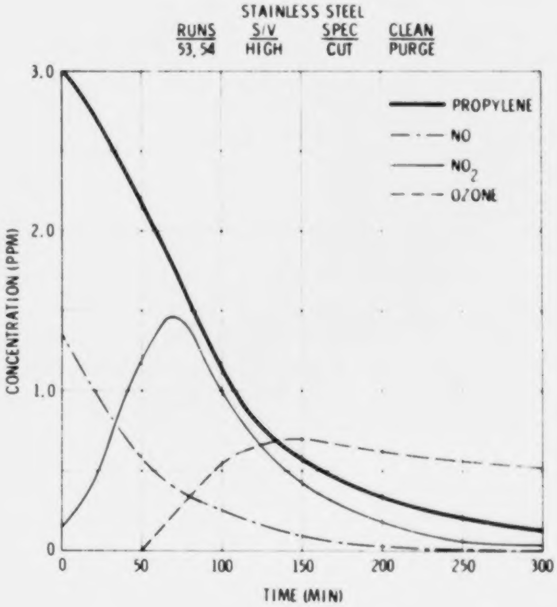
STAINLESS STEEL
RUNS
53, 54
S/V
HIGH
SPEC
CUT
CLEAN
PURGE
PROPYLENE
NO
NO$_2$
OZONE
CONCENTRATION (PPM)
3.0
2.0
1.0
0
0
50
100
150
200
250
300
TIME (MIN)

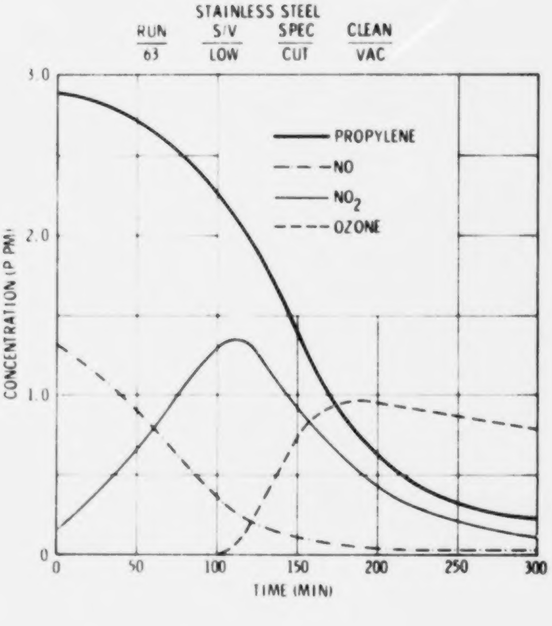
STAINLESS STEEL
RUN
63
S/V
LOW
SPEC
CUT
CLEAN
VAC
PROPYLENE
NO
NO$_2$
OZONE
CONCENTRATION (P PM)
3.0
2.0
1.0
0
0
50
100
150
200
250
300
TIME (MIN)

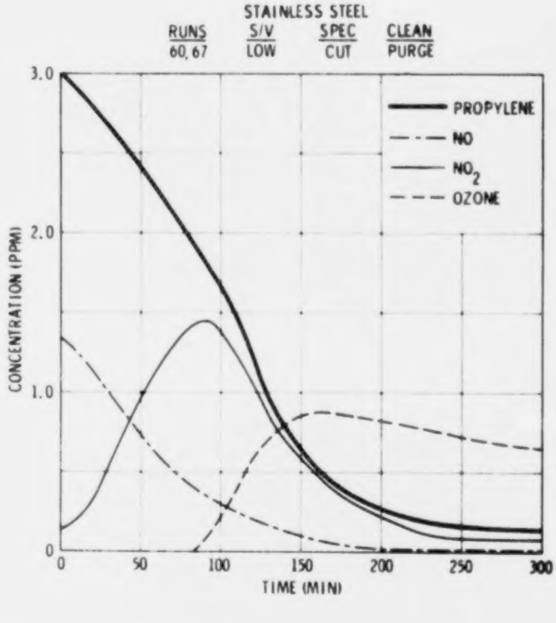
STAINLESS STEEL
RUNS
60, 67
S/V
LOW
SPEC
CUT
CLEAN
PURGE
PROPYLENE
NO
NO$_2$
OZONE
CONCENTRATION (PPM)
3.0
2.0
1.0
0
0
50
100
150
200
250
300
TIME (MIN)

TITLE- ALUM

	RUNINO	STOV	SPEC	CLEAN	HCINIT	NOX	NO2	PCNO2	TADJ	HCNOX	① NO2R
1#	3.0	1	1	1	3.17	1.52	.22	14.5	9	2.09	15.10
2#	71.0	1	1	1	3.10	1.52	.25	16.4	12	2.00	14.00
3#	4.0	1	1	-1	3.05	1.54	.29	18.8	17	1.98	15.80
4#	4.5	1	1	-1	2.90	1.41	.29	20.6	21	2.06	13.00
5#	69.0	1	1	-1	3.04	1.47	.21	14.3	8	2.07	14.70
6#	85.0	1	1	-1	2.94	1.49	.13	8.7	-2	1.97	16.00
7#	10.0	-1	1	1	2.96	1.51	.31	20.5	20	1.96	15.80
8#	11.0	-1	1	1	3.03	1.43	.22	15.4	11	2.12	13.20
9#	73.0	-1	1	1	3.00	1.47	.14	9.5	0	2.02	13.80
10#	12.0	-1	1	-1	2.98	1.51	.11	7.3	-8	1.97	13.10
11#	12.5	-1	1	-1	2.83	1.67	.36	19.2	18	1.69	15.50
12#	75.0	-1	1	-1	3.06	1.45	.19	13.1	6	2.11	18.10
13#	6.0	1	-1	1	2.81	1.59	.31	19.5	28	2.04	10.10
14#	81.0	1	-1	1	3.04	1.49	.14	9.4	-2	2.04	12.60
15#	5.0	1	-1	-1	2.98	1.33	.12	9.0	0	2.24	8.40
16#	70.0	1	-1	-1	2.88	1.47	.17	11.6	4	1.96	8.78
17#	82.0	1	-1	-1	3.07	1.49	.17	11.4	4	2.06	13.70
18#	84.0	1	-1	-1	2.96	1.41	.14	8.5	0	2.10	11.10
19#	9.0	-1	-1	1	2.94	1.49	.33	22.1	35	1.97	7.79
20#	74.0	-1	-1	1	3.02	1.46	.16	12.3	6	2.07	9.23
21#	7.0	-1	-1	-1	2.84	1.42	.22	15.5	16	2.00	9.28
22#	8.0	-1	-1	-1	2.92	1.36	.19	14.0	12	2.15	8.03
23#	72.0	-1	-1	-1	3.00	1.46	.15	10.3	0	2.15	10.60

TITLE- ALUM

	RUN2NO	② NO2TM	③ NO2DOS	④ O3MAXR	⑤ O3AVGR	⑥ O3MAXC	⑦ O3TM	⑧ O3DOSE	⑨ HCFC	⑩ HCT75
1#	3.0	79	142	22.8	4.46	.82	129	135	.05	70
2#	71.0	94	165	21.3	4.55	1.00	152	165	.18	86
3#	4.0	77	142	32.5	5.84	1.04	122	165	.10	69
4#	4.5	81	128	30.9	5.53	1.05	121	158	.10	64
5#	69.0	83	152	21.9	4.48	.94	143	144	.14	76
6#	85.0	88	166	22.1	4.23	.93	148	158	.10	82
7#	10.0	81	145	30.3	6.09	1.15	140	200	.19	81
8#	11.0	86	146	37.3	5.54	1.12	131	190	.15	83
9#	73.0	91	160	35.6	5.18	1.13	149	181	.12	91
10#	12.0	92	159	31.7	5.38	1.14	137	189	.13	85
11#	12.5	92	168	28.9	5.31	1.04	138	193	.14	91
12#	75.0	76	157	34.7	5.47	1.04	131	201	.10	63
13#	6.0	125	178	19.2	3.24	.92	190	133	.15	101
14#	81.0	118	211	17.4	3.29	.94	198	140	.18	104
15#	5.0	107	123	17.6	2.72	.77	165	114	.35	96
16#	70.0	144	200	18.0	2.71	.90	219	112	.31	107
17#	82.0	114	206	22.1	3.02	.84	189	133	.22	103
18#	84.0	120	186	13.8	2.73	.83	210	121	.27	88
19#	9.0	145	176	23.0	2.74	.92	205	116	.31	148
20#	74.0	136	188	26.2	3.48	1.10	206	147	.16	111
21#	7.0	124	159	22.8	3.32	.91	176	127	.27	128
22#	8.0	125	140	26.7	3.38	.96	177	135	.28	132
23#	72.0	120	172	21.2	3.52	1.02	190	137	.17	116

TITLE- ALUM		⑪	⑫	⑬	⑭	⑮	⑯	⑰	⑱	⑲
	RUN3NO	HCT50	HCT25	HCMAXR	HCAVGR	ALDMAX	PANMAX	NORATE	NO2DF	O3DF
1#	3.0	100	127	27.4	15.80	.60	.56	12.50	31.1	28.5
2#	71.0	122	152	24.9	12.30	.70	.31	10.10	35.5	35.5
3#	4.0	99	131	25.1	15.40	.55	1.10	14.20	31.6	36.7
4#	4.5	105	132	23.1	14.70	.51	1.10	12.20	30.3	37.3
5#	69.0	108	143	22.0	13.60	.72	.38	10.50	33.6	31.8
6#	85.0	118	149	22.9	12.50	.83	.29	8.70	35.9	34.2
7#	10.0	109	141	24.8	13.20	.59	.13	12.80	32.1	44.2
8#	11.0	111	143	27.2	13.30	.60	.17	11.10	34.0	44.3
9#	73.0	120	146	25.7	12.20	1.00	.35	9.56	35.5	40.2
10#	12.0	119	142	27.0	12.80	.50	.30	11.00	35.1	41.7
11#	12.5	118	145	26.3	11.50	.54	.33	11.80	33.5	38.5
12#	75.0	92	124	27.4	16.60	.86	.20	10.80	34.7	44.4
13#	6.0	148	184	18.3	10.30	.77	.23	9.93	37.3	27.9
14#	81.0	153	185	17.0	9.67	.86	.35	7.88	46.0	30.5
15#	5.0	137	190	17.8	10.70	.73	.32	9.03	30.9	28.5
16#	70.0	165	211	13.2	8.10	.94	.37	6.70	45.6	25.6
17#	82.0	144	186	18.2	10.10	.92	.33	7.70	45.2	29.2
18#	84.0	147	194	14.8	9.89	.82	.26	6.90	43.1	28.0
19#	9.0	180	210	23.6	7.54	.49	.18	7.36	39.4	26.0
20#	74.0	161	195	17.9	8.87	.90	.45	7.04	42.1	32.9
21#	7.0	159	204	21.0	8.37	.52	.16	8.77	37.3	29.8
22#	8.0	160	203	21.6	8.63	.58	.14	7.82	34.3	33.1
23#	72.0	151	182	23.7	10.10	.98	.50	7.62	38.5	30.6

TITLE- ALUM		⑳	㉑	㉒	㉓
	RUN4NO	FWHM	XTIME	NO2XT	O3XT
1#	3.0	73	43	36	86
2#	71.0	86	52	42	100
3#	4.0	66	44	33	78
4#	4.5	70	47	34	74
5#	69.0	89	44	39	99
6#	85.0	85	49	39	99
7#	10.0	74	43	38	97
8#	11.0	67	49	37	82
9#	73.0	82	52	39	97
10#	12.0	72	52	40	85
11#	12.5	73	48	44	90
12#	75.0	77	40	36	91
13#	6.0	110	66	59	124
14#	81.0	115	58	60	140
15#	5.0	89	64	43	101
16#	70.0	126	76	68	143
17#	82.0	110	56	58	138
18#	84.0	131	63	57	147
19#	9.0	117	82	63	123
20#	74.0	117	73	63	133
21#	7.0	101	64	60	112
22#	8.0	97	71	54	106
23#	72.0	109	63	57	127

TITLE- PYREX

	RUN1NO	STOV	SPEC	CLEAN	HCINIT	NOX	NO2	PCNO2	IADJ	HCINOX	① NO2R
1#	22	1	1	1	3.22	1.68	.27	16.1	12	1.92	12.80
2#	21	1	1	-1	3.20	1.57	.17	10.8	0	2.04	13.50
3#	27	-1	1	1	2.94	1.55	.18	11.6	5	1.90	13.50
4#	33	-1	1	1	3.00	1.52	.16	10.5	0	1.97	15.00
5#	31	-1	1	-1	2.84	1.39	.14	10.1	0	2.04	10.10
6#	26	1	-1	1	2.98	1.44	.18	12.5	7	2.07	6.25
7#	25	1	-1	-1	2.95	1.54	.21	13.6	10	1.92	7.26
8#	30	-1	-1	1	3.23	1.50	.16	10.7	2	2.15	7.58
9#	32	-1	-1	-1	3.00	1.43	.20	14.0	11	2.10	8.10

TITLE- PYREX

	RUN2NO	② NO2TM	③ NO2DOS	④ O3MAXR	⑤ O3AVGR	⑥ O3MAXC	⑦ O3TMAX	⑧ O3DOSE	⑨ HCFC	⑩ HCT75
1#	22	99	163	28.8	4.19	.98	152	152.9	.16	98
2#	21	95	161	24.7	3.85	.84	143	127.5	.26	89
3#	27	78	116	36.3	6.56	1.16	122	187.7	.08	70
4#	33	79	114	32.9	6.13	1.11	125	190.0	.11	81
5#	31	102	122	28.8	4.58	.98	140	156.0	.13	87
6#	26	192	225	17.7	2.17	.92	267	80.7	.30	149
7#	25	212	332	10.6	1.49	.73	310	41.5	.64	185
8#	30	147	161	28.5	3.02	.97	207	127.8	.26	133
9#	32	121	144	25.6	3.36	.91	166	126.5	.24	111

TITLE- PYREX

	RUN3NO	⑪ HCT50	⑫ HCT25	⑬ HCMAXR	⑭ HCAVGR	⑮ ALDMAX	⑯ PANMAX	⑰ NORATE	⑱ NO2DF	⑲ O3DF
1#	22	130	159	26.8	12.00	.70	.15	10.30	32.0	30.3
2#	21	125	157	23.3	12.30	.68	.15	9.72	34.2	27.1
3#	27	88	117	34.0	16.40	.96	.11	12.70	24.8	43.4
4#	33	98	128	34.6	15.10	.88	.16	14.20	24.8	41.1
5#	31	120	150	36.8	11.70	.77	.13	9.19	29.1	37.4
6#	26	210	235	12.0	6.67	.64	.14	5.07	52.1	19.9
7#	25	249	295	12.1	5.20	.68	.18	5.00	72.0	9.0
8#	30	172	203	22.9	8.92	.57	.12	7.10	35.9	28.4
9#	32	148	183	20.6	9.52	.65	.12	7.81	33.6	29.5

TITLE- PYREX

	RUN4NO	⑳ FWHM	㉑ XTIME	㉒ NO2XT	㉓ O3XT
1#	22	74	61	42	91
2#	21	77	55	40	88
3#	27	63	50	28	72
4#	33	66	50	29	75
5#	31	77	60	42	80
6#	26	138	106	86	161
7#	25	176	100	114	210
8#	30	115	89	59	118
9#	32	100	73	48	93

TITLE- TEFLON

	RUN1NO	STOV	SPEC	CLEAN	HCINIT	NOX	NO2	PCNO2	TADJ	HCINOX	① NO2H
1#	38	1	1	1	3.00	1.52	.16	10.5	0	1.97	8.72
2#	34	1	1	-1	2.82	1.38	.13	9.4	-2	2.04	11.30
3#	35	1	1	-1	2.86	1.50	.15	14.7	14	1.91	11.10
4#	42	-1	1	1	2.97	1.54	.18	11.7	5	1.93	9.52
5#	43	-1	1	-1	2.98	1.52	.15	14.5	13	1.96	11.60
6#	44	-1	1	-1	3.03	1.47	.15	13.6	10	2.06	10.50
7#	36	1	-1	1	2.99	1.63	.17	10.4	0	1.84	6.19
8#	39	1	-1	1	2.96	1.45	.17	11.7	7	2.04	5.91
9#	37	1	-1	-1	2.86	1.48	.15	10.1	0	1.93	8.11
10#	40	-1	-1	1	2.96	1.49	.17	11.4	5	1.99	6.87
11#	41	-1	-1	-1	2.96	1.47	.14	9.5	-2	2.01	7.56

TITLE- TEFLON

	RUN2NO	② NO2TM	③ NO2DOS	④ O3MAXR	⑤ O3AVGR	⑥ O3MAXC	⑦ O3TMAX	⑧ O3DOSE	⑨ HCFC	⑩ HCT75
1#	38	121	176	22.5	4.04	1.10	183	166.0	.12	109
2#	34	102	151	23.6	4.33	1.04	168	166.0	.09	95
3#	35	104	167	24.8	4.09	1.04	174	181.0	.12	102
4#	42	142	205	31.3	4.08	1.25	200	189.0	.22	112
5#	43	116	203	32.9	4.08	1.12	176	189.0	.08	105
6#	44	113	188	26.2	3.90	1.10	195	180.0	.15	98
7#	36	180	217	20.2	2.42	1.01	260	94.8	.32	136
8#	39	203	228	19.6	2.25	.98	267	97.0	.32	166
9#	37	162	223	15.7	2.28	.85	237	97.9	.30	139
10#	40	193	267	16.4	2.33	1.05	295	93.0	.34	147
11#	41	205	303	10.8	1.67	.80	298	50.0	.56	136

TITLE- TEFLON

	RUN3NO	⑪ HCT50	⑫ HCT25	⑬ HCMAXR	⑭ HCAVGR	⑮ ALDMAX	⑯ PANMAX	⑰ NORATE	⑱ NO2DF	⑲ O3DF
1#	38	143	174	23.6	10.20	.70	.31	8.61	38.6	36.4
2#	34	133	161	21.3	10.50	.74	.25	8.86	36.4	40.0
3#	35	134	169	21.7	10.30	.95	.23	8.77	36.5	39.5
4#	42	156	190	18.8	9.05	.82	.61	7.99	44.3	39.8
5#	43	143	175	13.4	10.30	.79	.39	8.67	44.3	39.6
6#	44	144	177	18.7	10.20	.73	.34	7.86	42.4	39.8
7#	36	205	246	12.7	6.81	.70	.25	6.24	44.4	19.4
8#	39	224	262	14.0	6.11	.72	.21	5.33	52.9	21.0
9#	37	197	241.	13.1	6.70	.72	.18	6.65	50.1	22.0
10#	40	217	263	12.0	6.39	.73	.25	5.92	59.8	19.8
11#	41	230	282	8.5	5.80	.72	.12	5.41	68.6	11.3

TITLE2 TEFLON

	RUN4NO	⑳ FWHM	㉑ XTIME	㉒ NO2XT	㉓ O3XT
1#	38	90	78	43	105
2#	34	86	58	42	110
3#	35	91	63	41	111
4#	42	84	73	70	127
5#	43	93	63	53	122
6#	44	102	60	53	122
7#	36	143	107	85	157
8#	39	142	107	85	157
9#	37	140	82	58	155
10#	40	165	96	97	199
11#	41	190	94	111	204

TITLE- SSTEEL

	RUN1NO	STOV	SPEC	CLEAN	HCINIT	NOX	NO2	PCNO2	TADJ	HCNOX	① NO2R
1#	55	1	1	1	3.19	1.48	.15	10.1	0	2.16	33.5
2#	56	1	1	1	3.04	1.52	.18	11.8	0	2.00	29.1
3#	51	1	1	-1	3.09	1.42	.15	10.6	0	2.18	49.2
4#	52	1	1	-1	3.11	1.43	.15	10.5	0	2.17	45.7
5#	58	1	1	-1	2.86	1.49	.17	11.4	0	1.92	41.3
6#	62	-1	1	1	3.02	1.46	.15	10.3	0	2.07	17.8
7#	61	-1	1	-1	2.98	1.50	.16	10.7	0	1.99	26.8
8#	66	-1	1	-1	3.06	1.48	.16	10.8	0	2.07	24.4
9#	57	1	-1	1	3.11	1.44	.17	11.8	0	2.16	21.0
10#	53	1	-1	-1	3.05	1.49	.16	10.7	0	2.05	35.3
11#	54	1	-1	-1	3.24	1.52	.17	11.2	2	2.13	26.4
12#	63	-1	-1	1	2.88	1.44	.13	9.0	0	2.00	10.8
13#	60	-1	-1	-1	3.02	1.55	.18	11.6	3	1.95	21.2
14#	67	-1	-1	-1	3.00	1.53	.18	11.8	3	1.96	19.2

TITLE- SSTEEL

	RUN2NO	② NO2TM	③ NO2DOS	④ O3MAXR	⑤ O3AVGR	⑥ O3MAXC	⑦ O3TMAX	⑧ O3DOSE	⑨ HCFC	⑩ HCT75
1#	55	51	133	23.2	6.77	.88	115	162	.10	51
2#	56	53	134	20.9	6.87	.91	110	169	.11	49
3#	51	38	121	22.2	8.16	.81	90	159	.10	44
4#	52	37	116	21.6	8.04	.82	95	146	.15	39
5#	58	43	133	19.5	7.50	.85	110	164	.14	44
6#	62	73	139	31.1	6.86	1.18	130	200	.10	71
7#	61	58	135	32.9	8.00	1.12	110	194	.08	50
8#	66	63	134	31.7	7.70	1.15	120	210	.12	58
9#	57	86	186	12.5	3.43	.69	163	118	.14	71
10#	53	53	157	12.6	4.72	.68	135	130	.17	48
11#	54	65	164	13.3	4.40	.71	137	133	.20	64
12#	63	111	181	20.0	3.50	.96	190	136	.27	111
13#	60	81	174	16.5	4.34	.85	153	147	.11	61
14#	67	80	158	19.6	4.50	.89	143	147	.27	64

TITLE- SSTEEL

	RUN3NO	⑪ HCT50	⑫ HCT25	⑬ HCMAXR	⑭ HCAVGR	⑮ ALDMAX	⑯ PANMAX	⑰ NORATE	⑱ NO2DF	⑲ O3DF
1#	55	73	103	33.0	21.5	.60	.23	17.90	30.0	36.4
2#	56	77	107	26.7	19.3	.74	.27	18.10	29.4	32.0
3#	51	71	104	26.3	22.1	.55	.23	18.80	28.3	37.4
4#	52	64	100	26.9	23.5	.85	.25	20.00	27.1	39.1
5#	58	71	104	28.3	19.7	.91	.26	19.40	29.8	36.8
6#	62	94	124	29.8	15.7	.82	.21	14.30	31.8	45.7
7#	61	79	110	25.4	18.8	.79	.18	16.80	30.0	43.0
8#	66	82	113	28.8	18.2	.82	.26	15.00	30.2	47.3
9#	57	112	155	19.9	13.7	.81	.20	12.30	43.0	27.4
10#	53	86	132	18.5	17.6	.79	.16	16.00	35.0	29.1
11#	54	97	146	20.5	16.3	.71	.13	14.20	35.9	29.1
12#	63	148	190	18.7	9.2	.61	.29	9.03	41.9	31.6
13#	60	111	146	19.3	13.3	.79	.23	12.00	37.3	31.7
14#	67	113	148	18.5	12.9	.89	.28	11.00	33.7	31.5

```
TITLE= SSTEEL ⑳     ㉑       ㉒      ㉓
      RUN4NO FNRM-XTIME NO2XT O3XT
1#        55    70    25    26    90
2#        56    67    26    27    84
3#        51    60    17    21    78
4#        52    61    17    20    78
5#        58    64    18    25    92
6#        62    78    38    35    92
7#        61    75    27    31    83
8#        66    69    31    32    89
9#        57   107    40    46   123
10#       53    88    23    30   112
11#       54    89    29    36   108
12#       63   113    59    52   131
13#       60   100    38    43   115
14#       67    97    40    40   103
```

Covariate Adjusted Data

		ALUMINUM								
RUN NO	S/V	SPEC	CLEAN	HCINIT	NOX	NO2	%NO2	TADJ	HC/NOX	NO2R
71	2	2	2	3.10	1.52	.25	16.4	12.	2.00	12.50
69	2	2	1	3.04	1.47	.21	14.3	8.	2.07	15.31
85	2	2	1	2.94	1.49	.13	8.7	-2.	1.97	18.38
73	1	2	2	3.00	1.47	.14	9.5	0.	2.02	14.68
75	1	2	1	3.06	1.45	.19	13.1	6.	2.11	18.18
81	2	1	2	3.04	1.49	.14	9.4	-2.	2.04	13.79
70	2	1	1	2.88	1.47	.17	11.6	4.	1.96	9.40
82	2	1	1	3.07	1.49	.17	11.4	4.	2.06	14.04
84	2	1	1	2.76	1.41	.14	8.5	0.	2.10	12.52
74	1	1	2	3.02	1.45	.16	12.3	6.	2.07	9.10
72	1	1	1	3.00	1.46	.15	10.3	0.	2.15	11.11

		ALUMINUM							
RUN NO	NO2TM	NO2DOS	O3MAXR	O3AVGR	O3MAXC	O3TMAX	O3DOSE	HCEC	HCT75
71	93.	163.	20.24	4.75	1.00	151.	148.9	.16	92.
69	80.	152.	21.37	4.69	0.94	140.	150.1	.13	72.
85	80.	171.	23.15	4.46	0.94	140.	160.3	.11	76.
73	85.	164.	37.17	5.40	1.14	143.	182.6	.12	86.
75	72.	154.	33.78	5.12	1.05	127.	190.6	.30	58.
81	114.	215.	17.66	3.44	0.96	194.	142.3	.19	93.
70	136.	201.	18.45	2.78	0.99	211.	107.2	.33	101.
82	109.	209.	22.03	3.22	0.86	184.	129.9	.21	96.
84	110.	192.	14.16	2.88	0.84	200.	125.0	.28	90.
74	130.	187.	26.11	3.38	1.10	200.	137.6	.16	105.
72	115.	175.	21.55	3.68	1.03	185.	136.1	.17	111.

		ALUMINUM							
RUN NO	HCT50	HCT25	HCMAXR	HCAVGR	ALDMAX	PANMAX	NORATE	NO2DE	O3DE
71	121.	151.	23.53	12.29	.73	.29	9.41	35.9	32.5
69	108.	140.	21.51	12.32	.73	.37	10.18	33.9	33.4
85	110.	141.	23.70	13.12	.81	.32	8.99	36.2	33.8
73	114.	140.	25.91	12.32	1.00	.38	10.73	35.9	39.9
75	89.	120.	26.53	14.73	.99	.29	11.27	34.2	42.1
81	168.	180.	16.86	10.15	.88	.39	8.25	46.4	30.2
70	159.	203.	13.61	8.61	.90	.36	7.12	45.5	26.6
82	139.	180.	17.83	10.37	.95	.35	8.12	45.5	28.1
84	137.	184.	15.04	10.62	.81	.29	7.42	43.4	28.1
74	155.	189.	17.76	9.06	.91	.46	7.13	41.8	30.8
72	146.	177.	23.81	10.44	.98	.52	7.95	38.7	30.0

		ALUMINUM		
RUN NO	FWHM	XTIME	NO2XT	O3XT
71	85.	50.	42.	100.
69	89.	41.	39.	99.
85	86.	42.	39.	99.
73	93.	46.	40.	98.
75	77.	36.	36.	92.
81	116.	53.	61.	141.
70	126.	69.	67.	142.
82	110.	50.	59.	139.
84	132.	53.	57.	147.
74	117.	67.	63.	133.
72	110.	58.	57.	127.

Covariate Adjusted Data

PYREX

RUN NO	S/V	SPEC	CLEAN	HCINIT	NOX	NO2	TNO2	TADJ	HC/NOX	NO2R
22	2	2	2	3.22	1.68	.27	16.1	12.	1.92	11.67
21	2	2	1	3.20	1.57	.17	10.8	0.	2.04	13.55
27	1	2	2	2.94	1.55	.18	11.6	5.	1.90	15.75
33	1	2	2	3.00	1.52	.15	10.5	0.	1.97	16.13
31	1	2	1	2.84	1.39	.14	10.1	0.	2.04	11.06
26	2	1	2	2.98	1.44	.18	12.5	7.	2.07	6.31
25	2	1	1	2.95	1.54	.21	13.6	10.	1.92	7.54
30	1	1	2	3.23	1.50	.16	10.7	2.	2.15	7.70
32	1	1	1	3.00	1.43	.20	14.0	11.	2.10	8.29

PYREX

RUN NO	NO2TM	NO2DOS	O3MAXR	O3AVGR	O3MAXC	O3TMAX	O3DOSE	HCSC	HCT75
22	103.	157.	26.25	4.57	1.00	152.	153.0	.13	93.
21	95.	164.	23.98	4.22	0.98	143.	133.1	.24	95.
27	70.	117.	37.59	7.03	1.16	114.	198.9	.09	63.
33	75.	117.	33.78	6.57	1.12	120.	193.7	.11	77.
31	94.	125.	30.96	4.63	0.97	132.	158.5	.15	82.
26	195.	225.	17.76	2.23	0.92	260.	80.4	.30	142.
25	206.	330.	10.60	1.52	0.72	302.	44.4	.64	178.
30	145.	164.	27.40	3.28	1.01	205.	134.2	.23	127.
32	113.	142.	25.19	3.63	0.90	158.	130.2	.24	103.

PYREX

RUN NO	HCT50	HCT25	HCMAXR	HCAVGR	ALDMAX	PANMAX	NORATE	NO2DF	O3DF
22	131.	159.	23.92	11.59	.78	.15	10.03	32.0	30.3
21	124.	155.	21.51	11.90	.75	.20	10.09	34.7	27.4
27	80.	109.	35.46	18.28	.94	.11	14.15	25.0	42.8
33	93.	123.	34.84	15.80	.88	.19	15.29	25.0	41.5
31	111.	142.	41.67	12.84	.72	.13	9.77	29.1	37.9
26	203.	248.	12.05	6.93	.63	.14	5.25	52.1	18.7
25	241.	287.	12.22	5.43	.66	.16	5.05	71.5	10.0
30	170.	199.	20.92	8.77	.65	.11	7.41	36.4	28.7
32	141.	176.	20.53	10.06	.65	.11	8.15	33.5	29.9

PYREX

RUN NO	FWHM	XTIME	NO2XT	O3XT
22	73.	58.	43.	93.
21	78.	52.	42.	90.
27	63.	43.	28.	72.
33	66.	45.	29.	75.
31	77.	54.	41.	79.
26	138.	99.	86.	161.
25	176.	93.	113.	209.
30	116.	85.	61.	121.
32	100.	66.	48.	93.

Covariate Adjusted Data

	TEFLON									
RUN NO	S/V	SPEC	CLEAN	HCINIT	NOX	NO2	%NO2	TADJ	HC/NOX	NO2R
38	2	2	2	3.00	1.52	.16	10.5	0.	1.97	9.09
34	2	2	1	2.92	1.39	.13	9.4	-2.	2.04	12.45
35	2	2	1	2.86	1.50	.15	14.7	14.	1.91	12.74
42	1	2	2	2.97	1.54	.18	11.7	5.	1.93	10.25
43	1	2	1	2.98	1.52	.15	14.5	13.	1.96	12.99
44	1	2	1	3.03	1.47	.15	13.6	10.	2.06	11.38
36	2	1	2	2.99	1.63	.17	10.4	0.	1.84	6.39
39	2	1	2	2.96	1.45	.17	11.7	7.	2.04	6.20
37	2	1	1	2.86	1.48	.15	10.1	0.	1.93	9.69
40	1	1	2	2.95	1.49	.17	11.4	5.	1.90	7.27
41	1	1	1	2.96	1.47	.14	9.5	-2.	2.01	7.84

	TEFLON								
RUN NO	NO2TM	NO2DOS	O3MAXR	O3AVGR	O3MAXC	O3TMAX	O3DOSE	HCEC	HCT75
38	117.	179.	22.94	4.23	1.11	178.	169.7	.12	105.
34	92.	155.	25.25	4.35	1.03	160.	169.6	.12	91.
35	92.	162.	25.06	4.18	1.01	163.	165.2	.13	93.
42	136.	206.	31.95	4.26	1.25	193.	185.1	.23	105.
43	107.	199.	32.26	4.28	1.11	167.	177.0	.08	96.
44	111.	185.	25.71	4.13	1.10	188.	170.3	.14	90.
36	175.	220.	20.58	2.49	1.02	255.	98.6	.32	132.
39	194.	229.	19.98	2.32	0.98	258.	92.2	.33	157.
37	154.	226.	16.26	2.30	0.84	229.	100.6	.32	134.
40	195.	268.	16.61	2.41	1.05	287.	90.1	.35	140.
41	200.	307.	10.98	1.70	0.81	293.	54.8	.57	132.

	TEFLON								
RUN NO	HCT50	HCT25	HCMAXR	HCAVGR	ALDMAX	PANMAX	NORATE	NO2DF	O3DF
38	138.	169.	23.70	10.52	.70	.33	9.03	38.8	35.8
34	124.	153.	23.09	11.38	.68	.25	9.35	36.4	40.7
35	123.	159.	22.88	11.53	.90	.19	9.50	36.4	37.5
42	149.	183.	19.01	9.51	.91	.61	8.43	44.3	40.0
43	135.	167.	13.42	10.99	.78	.37	8.74	44.1	39.2
44	137.	170.	18.45	10.71	.74	.33	8.15	42.2	38.7
36	200.	241.	12.77	6.97	.70	.27	6.45	44.6	19.8
39	214.	253.	14.16	6.41	.71	.21	5.58	52.9	21.2
37	189.	233.	13.61	7.03	.67	.18	6.94	50.1	22.5
40	209.	255.	12.12	6.66	.72	.26	6.10	59.9	20.0
41	224.	276.	8.58	5.93	.71	.14	5.54	68.8	11.9

	TEFLON			
RUN NO	FWHM	XTIME	NO2XT	O3XT
38	90.	73.	43.	105.
34	87.	52.	41.	109.
35	90.	54.	40.	109.
42	84.	66.	70.	127.
43	93.	55.	52.	121.
44	102.	58.	53.	122.
36	143.	102.	85.	157.
39	142.	98.	85.	157.
37	140.	76.	57.	154.
40	165.	88.	97.	199.
41	191.	89.	111.	204.

Covariate Adjusted Data

STAINLESS STEEL

RUN NO	S/V	SPEC	CLEAN	HCINIT	NOX	NO2	%NO2	TADJ	HC/NOX	NO2R
55	2	2	2	3.19	1.48	.15	10.1	0.	2.16	36.10
56	2	2	2	3.04	1.52	.18	11.8	0.	2.00	29.85
51	2	2	1	3.09	1.42	.15	10.6	0.	2.18	57.14
52	2	2	1	3.11	1.43	.15	10.5	0.	2.17	52.08
58	2	2	1	2.86	1.49	.17	11.4	0.	1.92	52.36
62	1	2	2	3.02	1.46	.15	10.3	0.	2.07	19.46
61	1	2	1	2.98	1.50	.16	10.7	0.	1.99	30.58
66	1	2	1	3.06	1.48	.16	10.8	0.	2.07	26.75
57	2	1	2	3.11	1.44	.17	11.8	3.	2.16	19.84
53	2	1	1	3.05	1.49	.16	10.7	0.	2.05	40.00
54	2	1	1	3.24	1.52	.17	11.2	2.	2.13	27.25
63	1	1	2	2.88	1.44	.13	9.0	0.	2.00	12.18
60	1	1	1	3.02	1.55	.18	11.6	3.	1.95	22.42
67	1	1	1	3.01	1.53	.18	11.8	3.	1.96	20.66

STAINLESS STEEL

RUN NO	NO2TH	NO2DOS	O3MAXP	O3AVGR	O3MAXC	O3TMAX	O3DOSE	HCEC	HCT75
55	49.	137.	22.78	8.22	0.92	113.	168.9	.08	45.
56	52.	135.	20.98	7.19	0.92	109.	170.8	.11	47.
51	35.	124.	22.17	9.43	0.83	87.	163.6	.09	40.
52	35.	119.	21.51	9.43	0.85	92.	151.1	.14	34.
58	38.	134.	20.16	7.31	0.83	105.	164.3	.16	42.
62	69.	142.	31.75	7.55	1.19	125.	204.3	.17	66.
61	54.	137.	33.90	8.58	1.13	106.	197.1	.09	46.
66	60.	137.	31.85	8.59	1.17	117.	213.9	.11	54.
57	93.	187.	12.39	3.64	0.71	160.	120.7	.13	66.
53	50.	160.	12.63	5.04	0.70	132.	134.0	.17	44.
54	65.	166.	13.00	5.03	0.75	136.	138.6	.17	59.
63	101.	186.	21.05	3.64	0.96	180.	141.0	.29	104.
60	76.	175.	16.56	4.46	0.86	148.	148.9	.11	59.
67	75.	159.	19.72	4.89	0.89	138.	148.3	.27	53.

STAINLESS STEEL

RUN NO	HCT50	HCT25	HCMAXP	HCAVGR	ALDMAX	PANMAX	NORATE	NO2DF	O3DF
55	70.	100.	29.76	20.89	.67	.28	19.89	30.5	36.9
56	76.	106.	26.18	19.27	.75	.29	18.66	29.5	32.1
51	68.	101.	25.32	22.32	.58	.26	20.58	28.6	37.8
52	61.	97.	25.58	23.47	.89	.29	22.12	27.5	39.5
58	66.	100.	30.67	21.93	.86	.25	20.62	29.7	37.1
62	89.	119.	29.59	16.39	.83	.24	15.53	32.0	46.2
61	74.	105.	25.71	19.96	.78	.20	18.19	30.1	43.4
66	79.	110.	28.01	18.52	.84	.29	15.97	30.5	47.6
57	109.	152.	19.12	13.55	.85	.22	12.33	43.2	27.5
53	82.	128.	18.21	18.02	.81	.19	17.21	35.2	29.5
54	96.	144.	18.80	15.58	.79	.18	14.77	36.4	29.3
63	137.	180.	19.65	9.95	.57	.31	9.86	42.1	32.4
60	106.	141.	19.19	13.85	.80	.24	12.85	37.4	31.9
67	108.	143.	18.48	13.48	.89	.29	11.42	33.9	31.6

STAINLESS STEEL

RUN NO	FWHM	XTIME	NO2XT	O3XT
55	71.	20.	28.	92.
56	67.	24.	27.	85.
51	61.	13.	22.	79.
52	62.	13.	21.	80.
58	64.	15.	24.	91.
62	79.	33.	36.	93.
61	75.	23.	31.	83.
66	69.	27.	33.	90.
57	107.	36.	47.	124.
53	88.	19.	31.	113.
54	90.	25.	38.	111.
63	114.	50.	52.	130.
60	100.	33.	43.	115.
67	97.	35.	40.	103.

Covariate Adjusted Data

ORIGINAL ALUMINUM

RUN NO	S/V	SPEC	CLEAN	HCINIT	NOX	NO2	%NO2	TADJ	HC/NOX	NO2R
3	2	2	2	3.17	1.52	.22	14.5	9.	2.09	15.82
4	2	2	1	3.05	1.54	.29	18.8	17.	1.98	15.60
4.5	2	2	1	2.90	1.41	.29	20.6	21.	2.05	13.40
10	1	2	2	2.96	1.51	.31	20.5	20.	1.96	16.64
11	1	2	2	3.03	1.43	.22	15.4	11.	2.12	15.38
12	1	2	1	2.98	1.51	.11	7.3	-8.	1.97	14.58
12.5	1	2	1	2.83	1.67	.36	19.7	18.	1.69	15.06
6	2	1	2	2.81	1.59	.31	19.5	28.	2.04	11.30
5	2	1	1	2.98	1.33	.12	9.0	0.	2.24	9.07
9	1	1	2	2.94	1.49	.33	22.1	35.	1.97	7.87
7	1	1	1	2.84	1.42	.22	15.5	16.	2.00	10.22
8	1	1	1	2.92	1.36	.19	14.0	12.	2.15	8.57

ORIGINAL ALUMINUM

RUN NO	NO2TM	NO2DOS	O3MAXP	O3AVGP	O3MAXC	O3TMAX	O3DOSE	HCEC	HCT75
3	78.	141.	21.60	4.96	0.84	128.	138.3	.02	55.
4	75.	137.	29.59	5.89	1.02	120.	163.9	.08	65.
4.5	76.	121.	28.82	5.25	1.00	117.	154.6	.10	61.
10	78.	139.	27.93	5.65	1.11	138.	199.5	.18	78.
11	82.	143.	35.46	5.72	1.11	127.	192.9	.14	78.
12	88.	166.	34.12	5.79	1.16	133.	192.5	.14	82.
12.5	86.	164.	28.01	4.95	0.98	132.	169.4	.15	88.
6	130.	173.	18.93	3.35	0.86	175.	136.6	.16	89.
5	99.	128.	18.08	2.86	0.78	157.	120.3	.36	99.
9	130.	169.	21.37	2.89	0.97	191.	121.3	.30	136.
7	112.	157.	22.94	3.41	0.87	164.	128.4	.29	119.
8	115.	139.	26.74	3.51	0.94	167.	144.2	.29	122.

ORIGINAL ALUMINUM

RUN NO	HCT50	HCT25	HCMAXR	HCAVGR	ALDMAX	PANMAX	NORATE	NO2DF	O3DF
3	99.	125.	25.06	15.34	.66	.57	14.97	31.1	33.2
4	98.	130.	24.15	15.60	.57	1.04	12.97	31.7	37.6
4.5	102.	130.	23.64	15.75	.47	1.00	12.08	30.4	38.7
10	108.	140.	24.75	13.93	.57	.04	11.98	32.2	45.7
11	108.	138.	26.53	13.76	.61	.15	11.36	34.1	45.6
12	114.	137.	27.70	13.18	.49	.35	11.51	35.6	41.3
12.5	114.	141.	28.17	12.80	.48	.24	11.95	33.8	36.6
6	134.	171.	19.31	11.96	.70	.13	10.48	37.4	32.1
5	128.	181.	18.02	11.38	.72	.35	9.81	31.2	29.2
9	158.	198.	23.64	8.42	.47	.07	7.34	40.0	29.5
7	148.	194.	22.22	9.30	.46	.11	9.18	37.4	31.4
8	150.	194.	22.22	9.35	.55	.11	9.22	34.2	35.0

ORIGINAL ALUMINUM

RUN NO	FWHM	XTIME	NO2XT	O3XT
3	73.	39.	37.	87.
4	65.	42.	32.	77.
4.5	58.	45.	32.	71.
10	72.	42.	36.	95.
11	66.	45.	37.	82.
12	73.	47.	41.	86.
12.5	71.	46.	41.	87.
6	109.	54.	56.	121.
5	90.	56.	44.	101.
9	115.	70.	61.	121.
7	100.	55.	58.	110.
8	97.	62.	53.	105.

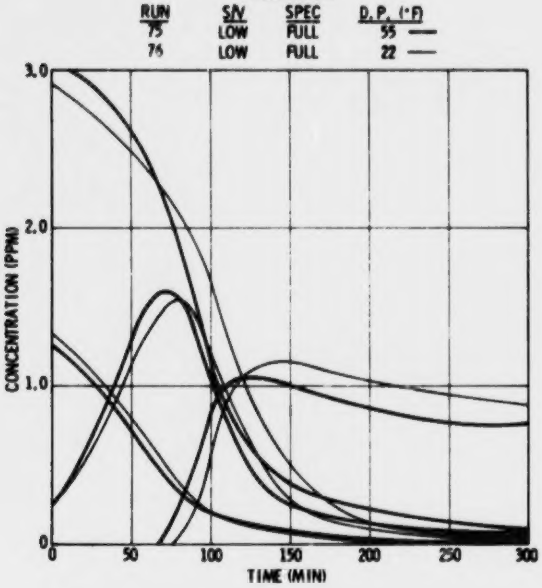
RELATIVE HUMIDITY EFFECT
ALUMINUM

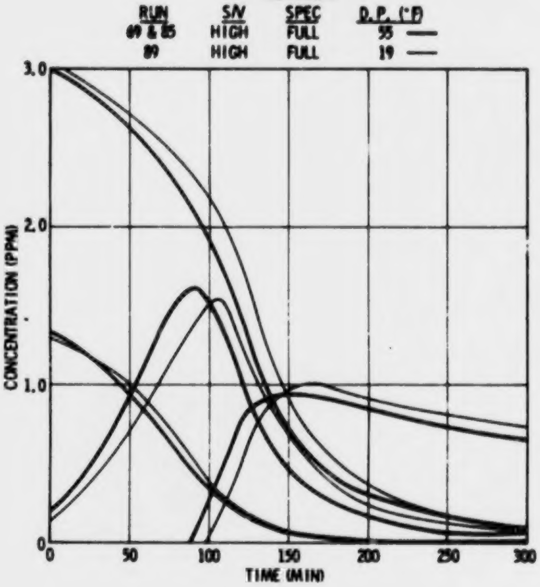
RELATIVE HUMIDITY EFFECT
ALUMINUM

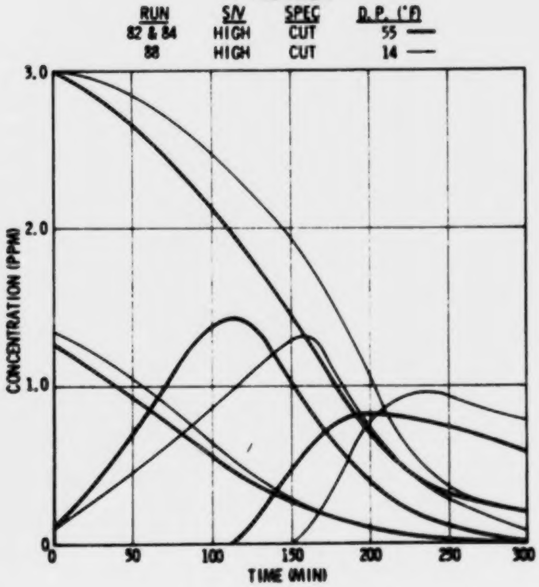
RELATIVE HUMIDITY EFFECT
ALUMINUM

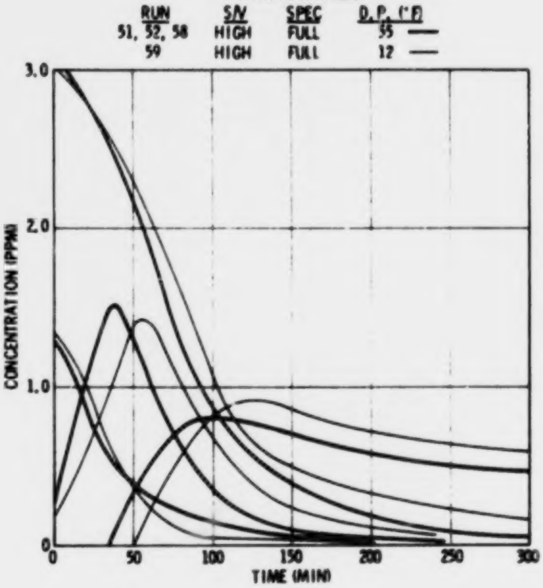
RELATIVE HUMIDITY EFFECTS
STAINLESS STEEL

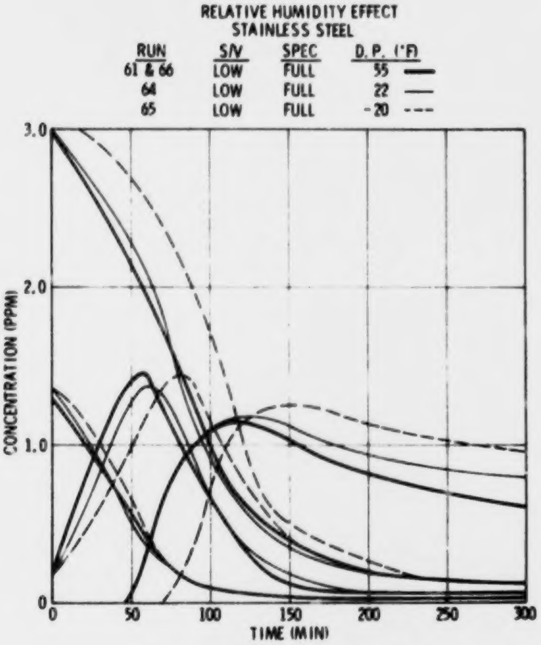
RELATIVE HUMIDITY EFFECT
STAINLESS STEEL
RUN
S/V
SPEC
D.P. (°F)
61 & 66
LOW
FULL
55
64
LOW
FULL
22
65
LOW
FULL
-20
3.0
2.0
1.0
0
CONCENTRATION (PPM)
0
50
100
150
200
250
300
TIME (MIN)

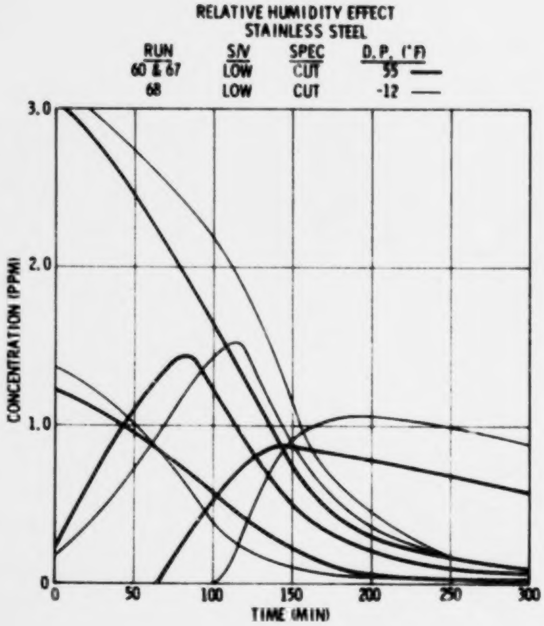
RELATIVE HUMIDITY EFFECT
STAINLESS STEEL
RUN
S/V
SPEC
D.P. (°F)
60 & 67
LOW
CUT
55
68
LOW
CUT
-12
3.0
2.0
1.0
0
CONCENTRATION (PPM)
0
50
100
150
200
250
300
TIME (MIN)

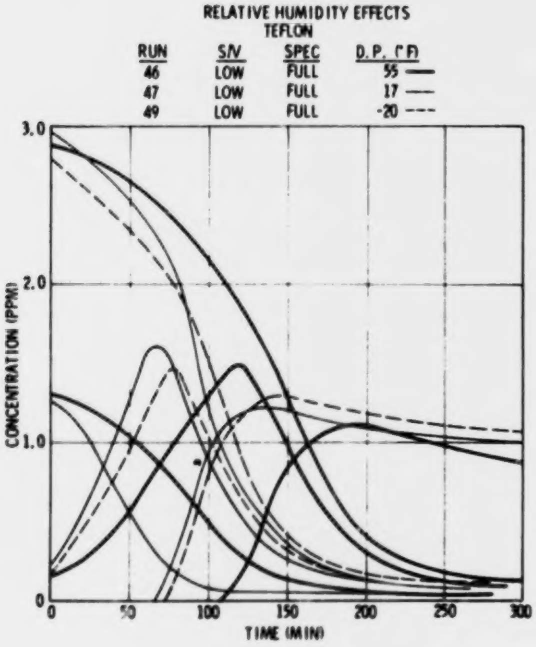
RELATIVE HUMIDITY EFFECTS
TEFLON
RUN
S/V
SPEC
D.P. (°F)
46
LOW
FULL
55
47
LOW
FULL
17
49
LOW
FULL
-20
3.0
2.0
1.0
0
CONCENTRATION (PPM)
0
50
100
150
200
250
300
TIME (MIN)

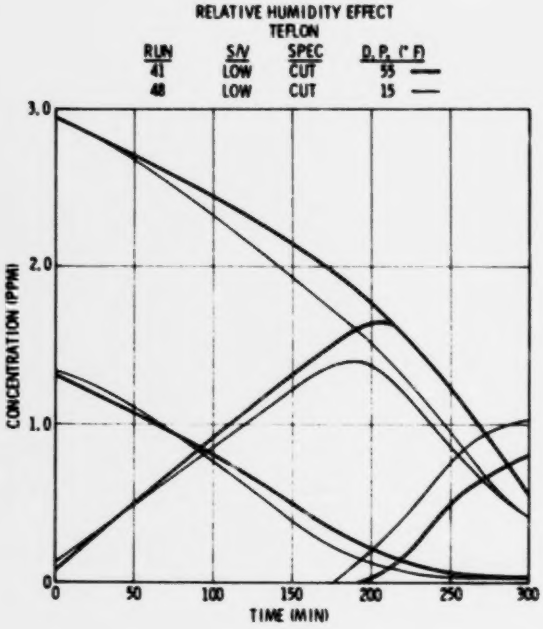
RELATIVE HUMIDITY EFFECT
TEFLON
RUN
S/V
SPEC
D.P. (°F)
41
LOW
CUT
55
48
LOW
CUT
15
3.0
2.0
1.0
0
CONCENTRATION (PPM)
0
50
100
150
200
250
300
TIME (MIN)

BUTANE/NO_X
ALUMINUM

RUN	S/V	SPEC
86B	HIGH	FULL

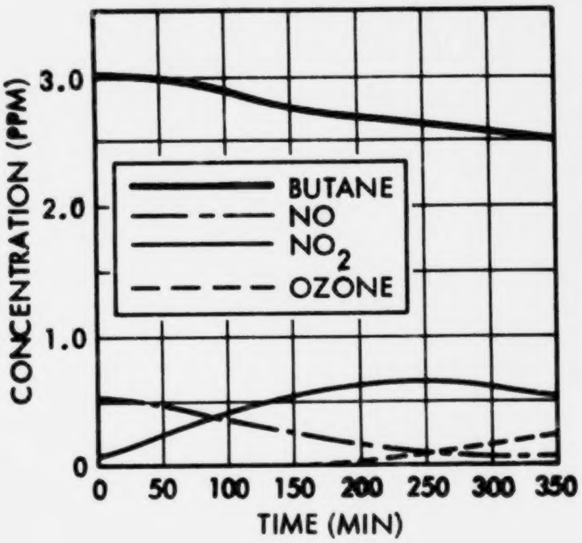

BUTANE/NO_X
ALUMINUM

RUN	S/V	SPEC
87B	HIGH	CUT

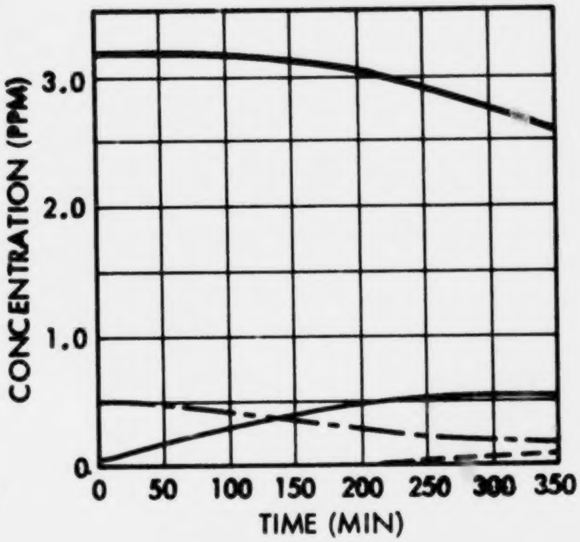

BUTANE/NO_X
ALUMINUM

RUN	S/V	SPEC
79B	LOW	FULL

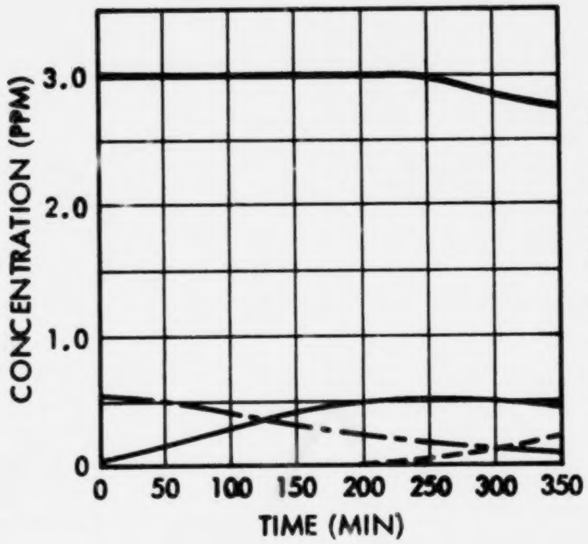

BUTANE/NO_X
ALUMINUM

RUN	S/V	SPEC
80B	LOW	CUT

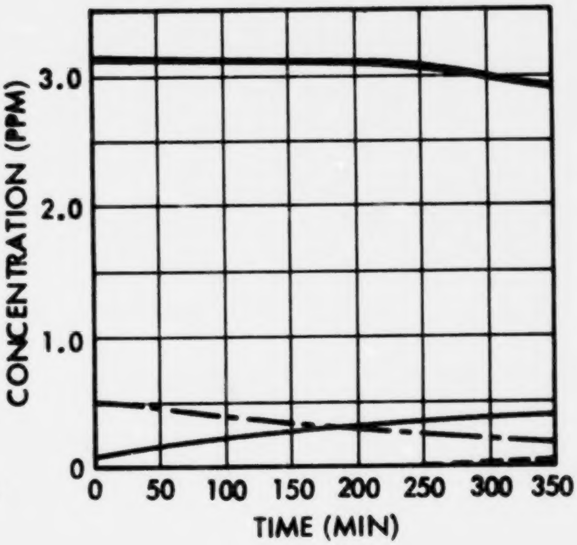

BUTANE/NO$_X$
TEFLON

RUN	S/V	SPEC
95B	HIGH	FULL

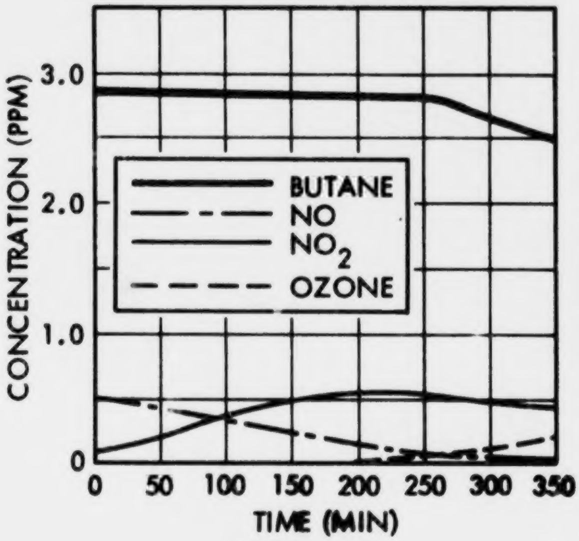

BUTANE/NO$_X$
TEFLON

RUN	S/V	SPEC
96B	HIGH	CUT

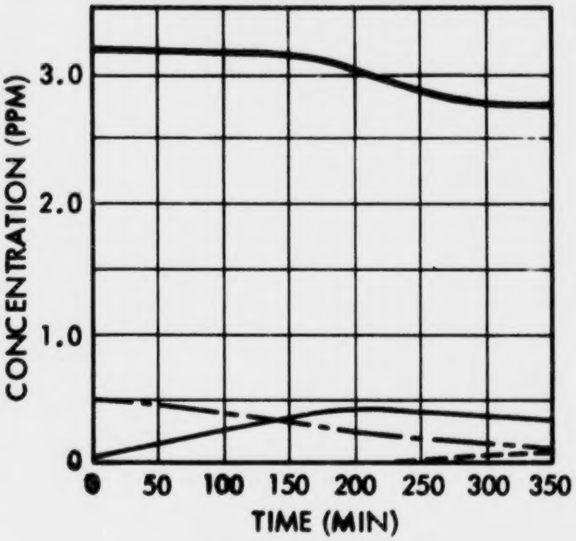

BUTANE/NO$_X$
TEFLON

RUN	S/V	SPEC
94B	LOW	FULL

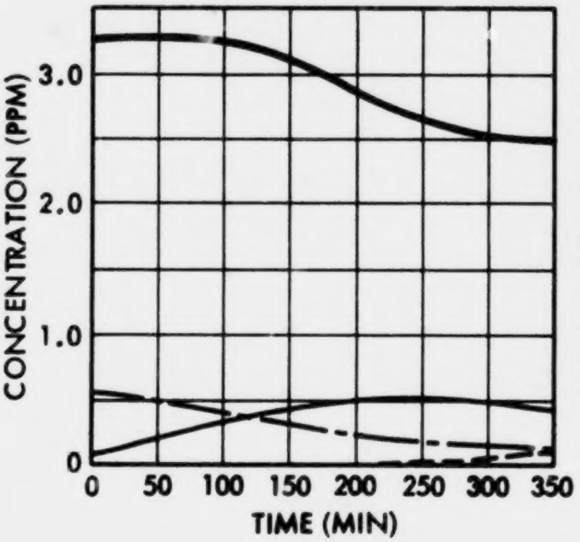

BUTANE/NO$_X$
TEFLON

RUN	S/V	SPEC
93B	LOW	CUT

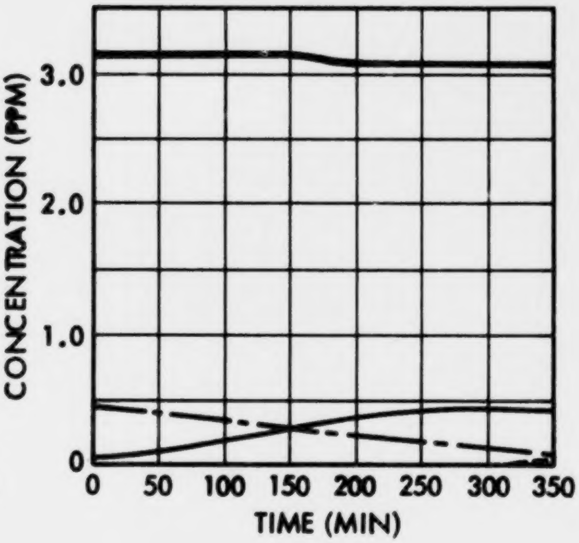

Appendix B

STATISTICAL ANALYSIS

Prepared by Ken W. Last and Michael W. Reeder

1.0 INTRODUCTION AND OVERVIEW

1.1 The analysis has been complicated by a number of problems commented upon separately below. There have been a number of opportunities to choose among several alternative methods of analysis. In the body of the report we have tried to show not only what was done (in the way of analysis), but have also tried to indicate the reasoning that led to the choices selected.

1.2 The analysis establishes that initial conditions are important. In particular, initial HC and % NO_2 were found to be most effective in standardizing the data. NO_x also contributed when the data was viewed in a Multivariate-all the parameter taken together fashion, or when certain materials were considered alone (i.e., Pyrex). One might well speculate that different correction factors for initial conditions should be developed for cut spectrum vs. full spectrum or for the various materials, however, there simply is not sufficient data to pursue this point. The corrections for initial conditions which were developed are given in Table B3-1.

1.3 Among the effects, that of spectrum dominates virtually every parameter. S/V is also important in a number of parameters, while cleaning is less important. These effects are not consistent across materials although the spectral effect is so large that it is clearly visible even in the midst of the interactions with materials. The analysis across materials is summarized in Tables B4-5 thru B4-9. Note that cleaning has a substantially greater effect in stainless steel than in any of the other materials. One other notable feature of the data is the repeated occurrence of a significant Material-Spectrum-S/V interaction: interpreted as meaning that the effect of spectrum depends upon the S/V ratio, however, the form of this dependence not consistent across materials. This results generally from an increased sensitivity under cut spectrum conditions. When the runs are full spectrum, the system is "fast" and subsidiary effects are washed out, whereas, when the system is run with cut spectrum the system slows down and other effects have an opportunity to exert their influence.

After applying several tests which would indicate drift, the conclusion drawn is that there is no compelling evidence of drift either within each block of material (excluding the original set of aluminum runs) or from material block to material block.

1.4 There are very strong interrelationships among the 23 parameters which tie together NO_x, ozone and HC. Thus, when the system is "fast" it is fast with respect to all three. Substantially fewer than 23 parameters are adequate to describe the system. The 21 parameters involving NO_x ozone and HC can be reduced to four which contain the great majority of the information represented by the original 21.

Of the four "principal components" two stand out in particular. The first of these represents "time" – i.e., time to max value, time to decay a fixed fraction, etc. In addition, "time" also represents rates as well. The second component represents "dose", the integral under the curve. These two principal components are quite highly correlated which indicates that concentration patterns are consistent with the time effects in response to changes in chamber conditions. Two other components complete the set, but these are both less consistent and more obscure in their interpretation. The analysis reported in Table B5-15 provides a summary of the effects of S/V, spectrum and cleaning material by material which is, in effect, an overview of the results for the 21 parameters (excluding ALD MAX and PAN MAX).

1.5 There are a number of anomolous characteristics of the data; runs which seem inconsistent. In particular, run 25 on pyrex and run 41 on Teflon standout as unusual. Also run 42 on stands out with respect to PAN MAX . These runs can have a profound influence upon the analysis and we have tended to analyze without deleting them and then to conduct some informal analyses which indicate what their effects may be.

1.6 We have been particularly troubled by the possibility that the results of the program may be confounded by the presence of drifts introduced by aging, instrumental errors, etc. The form of the experimental design is such that the program is especially vulnerable to such drifts. In particular, a steady trend would tend to be confused with a S/V effect.

2.0 BACKGROUND

2.1 The Experimental Design

Three variables - S/V ratio, spectra, and cleaning method - each at two levels, were combined into a complete 2x2x2 factorial experiment for each of four materials (aluminum, pyrex, teflon, stainless steel). In addition, upon completion of these materials, a complete rerun of the aluminum runs was conducted.

Certain of the combinations were repeated to provide a measure of reproducibility, while others were repeated at the convenience of the experimenter.

The order in which the experiments was conducted was not randomized. The possible consequences of not running the experiments in random order are discussed in Section 2.7 below.

2.2 The Data

The basic data for each run consists of a set of initial conditions (initial HC, NO_x, NO_2) together with (nearly continuous) graphs of NO_x, NO_2, Ozone, Propylene, Acetaldehyde, and PAN. From these graphs are derived a set of 23 parameters as defined in Section 3 of the body of the report. These parameters are intended to summarize the time-wise behavior of the photochemical system. Indeed, through the use of the parameter set it is possible to generate graphs which appear to be good approximations to the originals. Note, however, that within the framework of the present statistical analysis no systematic effort has been addressed to evaluating better summary measures or toward modeling the chemical system in a direct fashion. Rather, the major emphasis has been directed towards analysis of the parameters as defined. Note that, of the 23 parameters, 13 are strongly involved with time.

2.3 Covariates

While a careful effort was made to provide each experimental trial with the same starting conditions, so that observed changes could be attributed only to the deliberately introduced variations in the experimental design, some variation in these conditions did occur.

In order to remove this extraneous source of variability, an analysis of covariance was performed. The intent of the analysis is to adjust each trial to standard initial conditions (using a linear relation) in a manner which best aides in clarifying the other effects.

Early in the program it was observed that initial NO_2 could be used as a basis for standardizing "time" within the system — that is, sliding the continuous graphs so as to bring the early NO_2 values into coincidence, seems to bring replicates into coincidence across the entire time axis as regards the occurrence of peaks, etc. Such an adjustment to the same percentage content of NO_2 in the NO_x has been previously suggested after both theoretical and experimental consideration of the photochemistry (Dimitriades, Ref. 14 and Niki, Ref. 7). The results incorporating a time adjustment were reported thereafter as the basic parameter set.

In this analysis, we have returned to the unadjusted data and let the covariance analysis "find" the adjustment. This analysis resulted in comparable data as is shown in Table B2-1. This table compares the standard deviations calculated from replicates for each data set. Generally, it can be seen that the covariate set is superior. One must recognize that the covariance corrections are limited by the very nature of the derived parameters. Some of the parameters represent pure times and provide no particular problem. Others, however, involved time nonlinearly. For example, the calculation of dose involves integrating under a curve until a fixed time index and the consequence of sliding the index can be expected to influence the derived parameter in a nonlinear fashion.

TABLE B2-1

PARAMETER		Est. Std. Dev. As Initially Corrected	Est. Std. Dev. Using Covariate Correction
1*	NO_2 Rate	.0091	.0082
2	NO_2 Time Max	7.35	4.54
3	NO_2 Dose	8.43	8.02
4*	Ozone Max Rate	.0057	.0108
5*	Ozone Avg. Rate	.0115	.0145
6	Ozone Max. Conc.	.033	.038
7	Ozone Time Max.	8.05	7.61
8	Ozone Dose	8.51	7.65
9	HC Final Conc.	.039	.039
10	HC Time .75	8.34	7.01
11	HC Time .5	6.85	6.13
12	HC Time .25	6.76	6.30
13*	HC Max Rate	.0057	.0052
14*	HC Avg. Rate	.0062	.0053
15	Max Ald.	.135	.0817
16	Max PAN	.039	.042
17*	NO Rate	.0104	.0070
18	NO_2DF	1.93	1.90
19	Ozone DF	1.68	2.10
20	NO_2FWAM	4.83	4.72
21	Crossover Time	4.18	4.19
22	2-21	2.91	2.50
23	7-21	4.87	4.63

* Based on reciprocals.

The point is, ideally, the covariates would be used to adjust the graphs to standard conditions and then the derived parameters would be read from the graphs. Actually the procedure used attempts, linearly, to adjust the parameters and cannot help but be less effective than it might be otherwise.

One of the judgemental decisions which had to be made in performing this analysis was whether or not to conduct the multivariate analysis of variance and covariance on the data as originally adjusted or upon the raw data (with the attendant risk of nonlinearities). The analysis reported in Section 3, led to the expectation that the covariance on unadjusted data would be fairly successful, and this together with the favorable comparison in Table B2-1, has led us to base the bulk of the present analysis upon the raw (unadjusted) data, and to use covariance analysis to introduce any corrections needed.

2.4 The Unbalanced Design and Its Consequences

One major advantage in analyzing data from a "balanced" experimental design is the orthogonality of the resultant estimates: each estimate stands alone and is not changed, when the underlying model is changed. For example, the estimate of the effect of changing the S/V ratio is the same whether or not the model includes an estimate of the effect of changing the method of cleaning. With unbalanced data this feature is lost and generally the estimates depend upon what terms are in the model. Moreover, the sums of squares attributed to particular effects (used in forming tests of significance), depend on the order in which they are considered. As a consequence, the testing of hypotheses concerning the significance of the various effects is greatly complicated.

An "orthogonalized" analysis has been reported in the body of the report. This analysis avoids the complexities of an unbalanced analysis by averaging replicates and then proceeding as if only a single result were available at each trial. Such a procedure sacrifices some efficiency and invalidates (to a moderate extent) the formal tests of hypothesis. It does, however, enjoy the important advantage of simplicity and ease of interpretation. So much so, that in this Appendix results are again presented in this form, in addition to the results from the more formally correct unbalanced analysis.

2.5 Principal Comments

One of the basic goals of the current statistical analysis has been to clarify and illuminate the data. It is difficult (if not impossible) to visualize 23 dimensions. Yet, examining the variables one at a time can be misleading since it fails to exploit the rather strong system structure from which the parameters are all derived.

A fairly common technique used to reduce the dimensions without losing the structure is the technique of principal components. Here the object is to "economize in the number of variates" by seeking linear combinations of the original variates which account for most of the variation.

Section 5 presents the results of such a reduction in dimensions, from the original 23 down to four.

2.6 Outliers

This data set is rather sensitive to anomalies since the bulk of the trials were performed only once.

There are a number of trials where the data as represented by one or more parameters might be considered unusual. For example, the unusually high values of PAN max on Run 42 (teflon).

Our policy throughout the program has been the following: If the experimenter during the course of a run felt a physical or chemical grounds that the results were invalid, he was free to supress the data. Once, however, the data was reported for analysis, then that data could be modified only upon the basis of formal justification, i.e., it was presumed valid unless proved otherwise. As a consequence of this policy, we have been reluctant to throw out data even when the statistical analysis makes us suspicious that it is, in some sense, anomalous.

Note, however, that in reporting the results of the analysis of the four derived principal parameters in Section 5.3, two runs (No. 25 on Pyrex and No. 41 on Teflon) have been suppressed. In each case these were extremely slow runs with cut spectra. Sequentially in time, Run 25 was the first cut spectrum run for Pyrex while Run 41 was fifth (final) run for cut spectrum on Teflon.

In both materials the cut spectrum runs appear to exhibit a time trend — becoming faster in Pyrex; becoming slower in Telfon.

We can only speculate about the source of the evident discrepancy of these runs. Note, however, that no explanation has been advanced as to why any "drift" such as lamp or filter aging, or instrumental bias should cause a striking increase in one material and an opposite effect in the other —

particularly when nothing of a similar character is seen in the other materials. Moreover, as is seen in Section 5.3, the data, after suppressing these runs, exhibits substantial regularity as regards the effects of S/V, spectrum, and cleaning. One possibility is that the underlying photochemical reactions begin to undergo a basic change in character when things get slow enough and that other factors which are not even being considered in the variable set become important.

2.7 Time Trends

In forming the experimental design for this program it was found expedient to omit the usual randomization of the order in which the experiments were to be performed. This was a consequence of the fact that changing materials involves rebuilding the smog chamber and that changing the surface to volume ration (for a given material) involves a partial rebuilding and resealing of the chamber. Initially this led to a design in which all runs for a given material were to be performed in a block. Moreover all runs for a given surface to volume ratio would also be run as a block. Subject to these constraints, the following randomization steps could still be performed.

1. Randomize the order in which the materials were run.
2. Within each material block, randomize the order in which the S/Vs were run (i.e., all high runs then all low or visa versa).
3. Within each material-S/V block, randomize the order in which the four runs comprising the block were run.

In addition the very limited number of repeats were scheduled so as to represent each of the following conditions:

a. An immediate rerun.

b. A rerun without the chamber seal being broken, i.e., a rerun within the same S/V block, but not an immediate rerun.

c. A rerun within the same material block, but after a S/V change,

and finally,

d. A rerun after a material change.

During the initial runs (which were, coincidently, high S/V full spectrum runs) it was noted that it seemed to take several runs to achieve stable behavior and that this problem might be attributed to a "virgin surface effect". This being the case it seemed prudent to start the runs with all the material in the chamber exposed to the highest light intensity. Thus, the randomization was further restricted in that within each material block the first S/V block was invariably at high S/V and, within each high S/V block the initial runs were at full spectrum.

The end result has been that the experimental design is quite vulnerable to drift or other time trends. If such trends were present they would tend to be confused (confounded) with the estimated S/V effects within materials and with the material to material comparisons. This weakness in the design was recognized and a decision was made to proceed using insofar as possible, experimental controls (calibrations, frequent K_d checks, etc.) to prevent any drift from arising.

Fortunately, in the course of the program, the experimental procedures achieved an increase in efficiency which permitted an increased amount of replication to the extent that the replicates can be used to form a judgment as to the existance of drift during the program.

There are a number of ways in which an analysis might be undertaken which addresses the question of drift.

One possibility is to undertake, material by material, a stepwise regression to examine which variables are important in the sense that they provide a good fit to the observed data. This was done and revealed that run sequence provided, in a number of cases, a superior fit to that which resulted when this variable was excluded. In addition, it was noted that whenever run sequence entered the model, S/V was omitted. Also, it was found that when the models were revised to force S/V into the model and to add run sequence only if it significantly enhanced the fit beyond what S/V had contributed, that no significant additional enhancement resulted.

Thus, this analysis was inconclusive in that we were left in a position of finding either run sequence or S/V (but not both) to be important. Rather than pursue this analysis further, an alternate has been used.

The hypothesis to be tested concerns the presence of a steady drift over run sequence. If such drift were present, then runs which are duplicates (except for sequence) might be expected to differ by an amount which grows steadily as a function of the separation overtime. Our attention is then focused upon an examination of the differences between replicate pairs as a function of run sequence separation.

Note that the time separations of replicates tend to fall into three basic groups:

(1) Immediate reruns - $(\Delta = 1)$. There are nine such

4-4A	Aluminum
7-8	Aluminum
10-11	Aluminum
12-12A	Aluminum
34-35	Teflon
43-44	Teflon
51-52	Stainless
53-54	Stainless
55-56	Stainless

(2) Sequence numbers differing by more than 1 but less than 20 $(1 < \Delta < 20)$.

There are ten such*.

27-33	Pyrex
26-39	Teflon
51-58	Stainless
52-58	Stainless
60-67	Stainless
61-66	Stainless
70-82	Aluminum (Rerun)
70-84	Aluminum (Rerun)
69-85	Aluminum (Rerun)
82-84	Aluminum (Rerun)

---

*A complication in application of these tests has been the triplets formed by runs 51, 52 and 58 and by runs 70, 82 and 84. Clearly we are not justified in using three pairs (one of the three differences is simply the sum of the other two differences). We have avoided this problem by dropping the middle value, thus leaving in the replicate, the difference involving the largest run sequence separation.

(3) Long term replicates: A complete rerun of the aluminum block.

There are two basic data sets. First the data incorporating the NO_2 time adjustment, and second, the unadjusted data after incorporation of the covariate corrections. In addition, as will be seen below, we have some reason to be less confident of the initial runs on aluminum and, the analysis has been redone, dropping these pairs.

In the analysis, we concentrate on the differences between duplicate pairs since this provides a direct basis for comparison. In the absence of drift, these pairs should be distributed around a central value of zero. If there is drift then the pairs separated further apart in time (or sequence) could be expected to center about a value, different than zero and increasing in absolute magnitude as the separation increases. Note, however, that the long term replicates group 3 all involve only one material, aluminum, and that each set of runs, (initial aluminum, replicate aluminum) were fairly compact in time. One might anticipate in this case a different kind of drift than which might occur during a single series. Thus, we distinguish two types of drift, drifts within a compact series on runs on a given material, and drifts from material to material, or series to series.

The drifts within materials can be studied using the shorter term replicates, groups 1 and 2, while the drifts across materials or series can be studied by comparing the mean values across materials and especially between the initial aluminum set and the final replicate aluminum set.

2.7.1 Drifts within Material

If there is a drift within material then the replicates with longer separations, group 2, should be centered around a different value than those of group 1. Hence we test the hypothesis that both sets are centered about the same central value. The test used is the rank sum test using the value of T^1 defined as follows: Arrange the two samples (of differences) in order of size, and assign rank scores to the individual observations, score 1 for the smallest, 2 for the next smallest, etc. Then T^1 is the sum of the ranks of the observations in the smaller of the two sets. Using tables, (Reference B-1), we reject the hull hypothesis (no drift) if the calculated score is significantly large or significantly small where the critical values are selected to provide a probability of approximately 0.05 of falling in each tail (10% overall).

The rank sums calculated in this manner are shown in Tables B2-2, B2-3 and B2-4.

For the adjusted data only one parameter (13-HC Max Rate) qualifies as significant. For the covariate corrected data three parameters qualify as significant. These are: 1-NO_2 Rate; 21-Crossover Time; and 23-Ozone Time Max to Crossover Time. For the covariate corrected data, omitting early aluminum runs, two parameters (19-Ozone DF and 21-Crossover Time) qualify as significant.

Here, after applying a test which would declare significance about 10% of the time when no time trend is present, we have found in the case of the covariate corrected data, three parameters which may be displaying drift or trend. This is just about what would be expected to occur by chance if no trend were present in any parameter.

TABLE B2-2

Rank Sum and Sign Test Results for Adjusted Data

PARAMETER		1	2	3	4	5	6
Rank Sum		47	49.5	58	66	59	58
Sign Test	+	11	3	7	9	11	7
	0		1				1
	-	4	11	8	6	4	7

PARAMETER		7	8	9	10	11	12
Rank Sum		49	51	52.5	48.5	50.5	53
Sign Test	+	5	4	3	4	2*	2*
	0		1	22	1	1	1
	-	10	10	10	10	12	12

PARAMETER		13	14	15	16	17	18
Rank Sum		39.5	61.5	62	56	57	49
Sign Test	+	4	12	6	7	9	8
	0				1		
	-	11	3*	9	7	6	7

PARAMETER		19	20	21	22	23
Rank Sum		52	57	63.5	58.5	45
Sign Test	+	5	7	4	5	5
	0	1		1	3	3
	-	9	8	10	7	7

Critical values for rank sum are 41 and 71
Critical values for sign test are 2 when N = 12, 13 or 14
Critical values for sign test are 3 when N = 15

TABLE B2-3

Sign Test Results for Covariate Corrected Data

PARAMETER		1	2	3	4	5	6
Rank		72*	55.5	45.5	56	57	59
	+	4	3	7	6	4	7
Sign Test	0	0	2	2	1	2	4
	-	11	10	6	8	9	4

PARAMETER		7	8	9	10	11	12
Rank		52.5	54.5	53	44.5	54.5	58
	+	6	10	3	3	3	3
Sign Test	0	1	0	2	1	22	2
	-	8	5	10	11	10	10

PARAMETER		13	14	15	16	17	18
Rank		59	54	55	57.5	54	49.5
	+	8	5	6	8	4	7
Sign Test	0	1	0	0	2	1	2
	-	6	10	9	5	10	6

PARAMETER		19	20	21*	22	23*
Rank		45	58.5	73*	55	40*
	+	9	8	3*	5	6
Sign Test	0	0	0	0	4	3
	-	6	7	12	6	6

Critical Values for Rank Sum are 41 and 71
Critical Values for Sign Test are 2 when N = 12, 13, 14
Critical Values for Sign Test are 3 when N = 15

TABLE B2-4

Covariate Corrected Data (Original Alum Omitted)

PARAMETER		1	2	3	4	5	6
Rank Sum		15.5	22	27	23	25	21
	+	3	2	4	4	2	5
Sign Test	0	0	2	2	1	2	3
	-	8	7	5	6	7	3

PARAMETER		7	8	9	10	11	12
Rank Sum		21.5	20.5	23.5	28.5	23.5	17
	+	3	7	2	2	3	2
Sign Test	0	1	0	1	0	0	0
	-	7	4	8	9	8	9

PARAMETER		13	14	15	16	17	18
Rank Sum		24	22.5	23.5	22.5	25	26.5
	+	6	3	4	6	3	4
Sign Test	0	0	0	0	1	1	2
	-	5	8	7	4	7	5

PARAMETER		19	20	21	22	23
Rank Sum		35*	21	14*	22.5	31
	+	7	5	2	4	3
Sign Test	0	0	0	0	2	3
	-	4	6	9	5	5

Critical values for rank sum are 15 and 33.
Critical values for sign test is 1 for N = 9, 10 or 11.

Next, we test the null hypothesis that the central value of the differences is zero. If this were true, then there would be equal chance for each difference to be either positive or negative (a difference of zero is excluded). Letting r represent the smaller of the counts of positive or negative differences then the null hypothesis is rejected if r is too small. In particular using Table A-10a (Ref. B-1) we select r such that there is approximately a 10% chance of falling in the critical region if the null hypothesis is true.

The counts are also shown in Tables B2-2 to B2-4. For the adjusted data three parameters show significant counts. These are 11-HCT. 5, 12 HCT. 25, and 14-HC Avg. Rate. For the covariate corrected data, one parameter (21-Crossover Time) shows a significant count. For the covariance corrected data, omitting early aluminum, no parameter shows a significant count. As was the case with the rank sum test, the number of parameters qualifying as significant is approximately what would be expected to occur by chance if no trend were present.

In only one case (21-Crossover Time) do both tests qualify. In this case the majority of the differences are negative implying a down trend with sequence. However, the rank score is significant on the high end implying that the differences show an increasing trend, so that the two results are inconsistent.

All in all, the conclusion drawn is that there is no compelling evidence of drift. Note also that the Pyrex and Teflon runs at cut spectrum seem to show a time trend (See Fig. B5-2 and B5-3 for both "time" and "dose" parameters). However for Pyrex the trend appears to be for faster runs with increasing sequence number while for Teflon the trend appears to be just the reverse (towards slower runs with increasing sequence number).

2.7.2 Material to Material Time Drift Analysis

Next, we consider whether there is any indication of a long term drift from material block to material block. First note that there is .no evident pattern in the block means arranged in sequential order. Table B2-5 presents the means parameter by parameter based on the orthogonalized analysis. In that table there are 17 parameters which appear to follow a steady upwards or downward progression starting with the original aluminum block and continuing thru Pyrex (the second material run) and Teflon (the third). This pattern is not continued thru the stainless steel runs, where, of the 17, only two parameters continue the trend. These are 4-Ozone Max. Rate and 14-Max. Ald.

Of greater interest is the comparison between the original aluminum block and the rerun block. This is material contrast two reported in Table B4-4. From that table it can be seen that for 8 of the parameters a significant difference is found and in 6 additional parameters a significant Material-S/V interaction is found. Evidently these two sets are not consistent with regard to their individual means or the S/V effect or (in two cases) both. This can be interpreted as evidence of drift. However, a comparison of the two sets indicates substantial inconsistencies between points which would be replicates except for drift.

Now that we have seen how highly correlated the various "time" parameters are, it can be seen that to a large extent these tests are redundant -- testing for the same thing over and over -- so that it is no surprise that a small number of the tests show significance.

Table B2-5

MEANS BY MATERIAL

TIME →

Parameter	Alum (Original)	Pyrex	Teflon	S.S.	Alum (Repeat)
1	11.65	10.00	8.63	25.38	13.12
2	104.2	130.9	154.2	70.20	105.8
3	151.5	178.0	219.0	152.8	176.1
4	25.4	24.7	21.3	21.2	24.7
5	4.15	3.60	3.12	5.68	4.08
6	0.95	0.93	1.03	0.90	1.00
7	157	189	230	137	172
8	147	126	131	157	156
9	0.19	0.26	0.26	0.15	0.16
10	97.6	116.6	124.4	64.2	93.6
11	131.2	156.5	179.5	96.8	132.9
12	166.2	188.8	218.2	133.4	165.9
13	23.1	23.6	15.9	23.9	21.8
14	11.66	10.13	8.18	16.16	11.52
15	0.597	0.696	0.752	0.758	0.870
16	0.37	0.14	0.29	0.23	0.35
17	10.81	8.55	7.20	14.36	8.71
18	34.1	39.2	48.7	34.5	39.0
19	32.9	27.8	28.6	34.1	34.3
20	87.2	102.8	124.9	85.8	99.4
21	57.7	78.2	81.6	38.2	56.2
22	46.2	57.5	69.9	35.8	49.6
23	99.4	114.5	147.5	102.6	116.2

As regards long term drift -- based on looking for trends from material to material and especially as regards the original versus the rerun aluminum, there are some important conclusions: 1. There is a definite change in parameter 15 (Max Ald) due to a change in the analytical method. 2. There is a similar change in parameter 16 (Max PAN) for similar reasons. In particular the values reported for runs 3, 4 and 4A are very different for corresponding runs on the aluminum reruns. Moreover, the two sets original versus rerun aluminum are generally inconsistent. 3. There are inconsistencies (already reported in the Phase II final report) between the original and rerun of aluminum, which are definitely not resolved by the introduction of the covariate corrections. This latter point is further examined in the next paragraph.

A tentative explanation is that during the initial aluminum runs there was a run sequence effect, equivalent to an experience factor. It is our considered judgment that the early aluminum runs should be dropped from consideration on the basis that a learning process was taking place and that several changes in procedure were instituted during these runs. It is felt (but cannot be established statistically) that the system had stabilized by the time these runs were completed.

It must, however, be acknowledged that the best available evidence to unravel the confounded effects of run sequence and S/V reveals a substantial inconsistency in the S/V effect in two sets of aluminum runs.

Note, however, that the materials which exhibit the extremes as regards the four principal components are Teflon and stainless with aluminum and Pyrex in between. Since Teflon and stainless were adjacent in time with Pyrex and aluminum both before and after, then it is clear that the possible drift is not overwhelming material properties. Nothing more can really be said because of the inconsistency between the early and late and late aluminum runs, without postulating a different kind of drift in the two places.

2.8 Computer Program

Many times it is felt that a manual massage of experimental data presents insight into the data that might be overlooked if the data were analyzed by an impersonal computer. True as this may be, it is often the case that the immensity of the analysis demands computer usage, and such was the situation with many of the analyses of the smog chamber data. A computer program, entitled the Modified Abbreviated Doolittle (MAD) program, was therefore used in this study.

MAD is a generalized analysis program developed by the Brigham Young University Department of Statistics, which is capable of analyzing balanced and unbalanced univariate and multivariate analysis of variance and covariance problems as well as univariate regression problems. These analyses can also be performed in the presence of missing cells. The algorithm which is incorporated within the MAD program is an open ended algorithm allowing for expansion to handle forms of analyses which can be based upon construction of a X'X matrix. The X'X is then partitioned according to user control into blocks containing the various analysis of variance terms and covariates, or the independent variables with the dependent variables. The Abbreviated Doolittle Operations are then performed on this particular ordering of the X'X matrix, with those variables not specified by the user being ignored.

3.0 COVARIANCE ANALYSIS

Fundamental to the study of the smog chamber data is a study of those parameters which might be considered as covariates. Through such a study, the desireability of including the covariates in a descriptive model can be determined. Six parameters were considered as likely candidates for inclusion as covariates: HCint, NO_2, NO_X, $\%NO_2$, TADJ*, and HC/NO_X These six parameters were studied separately and in various combinations to determine their effect on the 23 dependent variables. The covariate effects were determined for the dependent variables in both univariate and multivariate models(ALD Max and PANmax were excluded from the multivariate study).

3.1 Univariate Covariance Results

The results of the covariate study on the univariate variables indicated that two covariates were generally useful in explaining data variation and that the remaining covariates were not generally of additional value. The two useful covariates in order of their relative importance were $\%NO_2$ and HCint. The adjustment coefficients for these two covariates are given in Table B3-1. The data, as corrected by these factors, is given in Appendix A of this report.

Two approaches were used to determine the fact that $\%NO_2$ and HCint were of value, both of which invoked the usual analysis of covariance assumptions. The first approach was to eliminate NO_2 and TADJ from the list of covariates (on the basis of a preliminary investigation) and to test the effects of all possible combinations of the remaining four covariates after accounting for

---

*TADJ represents that amount of time adjustment introduced in forming the adjusted data set.

TABLE B3-1

Univariate Covariate Adjustment Coefficient

Dependent Variable	HC Init	% NO_2
NO_2TM	-18.148	-2.2342
HCT50	-17.013	-2.4526
O3TM	-17.198	-2.2818
FWHM	-1.0533	.23104
XTIME	-3.2832	-2.4154
1/O3AVGR	.067834	-.0054873
1/HCAVGR	-.025843	-.0014754
1/NO_2R	-.018421	-.0023856
1/NO_2RATE	-.0020981	-.0025264
NO_2DOSE	-2.1619	1.4064
NO_2DF	-1.4307	.098329
O_3DOSE	-12.326	1.8671
O_3DF	.19986	.20911
1/O_3MAXR	-.0090996	-.00039398
1/HCMAXR	-.018591	-.000099554
O_3MAXC	-.15294	.0046785
HCFC	.12951	.0016781
PANMAX	-.15136	.010004
HCT75	2.4908	-2.1539
HCT25	-12.212	-2.4416
NO_2XT	-7.3887	.19681
O_3XT	-10.464	.18141
ALDMAX	-.34816	.00025681

a model of the four main effects (Materials, S/V, Spectrum, and cleaning) and all but two of the two-way interactions. Using the reduction in sum of squares approach to determine the effect of the covariate groups after the model, the results were arrived at. The second approach was to use the same model of main effects and interactions, and the reduction sum of squares, but to allow all six covariates to enter in a forward selection procedure analogous to the forward selection procedure used in Regression Analysis.

The results of the two approaches were in agreement in the univariate covariance studies.

3.2 Multivariate Covariance Results

Using the two approaches described above, the dependent variables (excluding ALD max and PAN max) were studied in a multivariate analysis to determine the effect of the covariates. As opposed to the univariate results, three covariates were found to be useful in the multivariate description of the data. The first approach (that of eliminating NO_2 and TADJ) resulted in the selection of HCint, NO_X, and $\%NO_2$ as jointly useful covariates, NO_X being added to the univariate covariate set. The second approach, however, exchanged TADJ for $\%NO_2$ to conclude the set should be HCint, NO_X, and TADJ. While the two results appear to differ. such is not the case. Both sets are effectively the same, since $\%NO_2$ and TADJ are highly correlated with a coefficient of .9579. Table B3-2 gives the adjustment factors associated with the first set of covariates (HCint, NO_X, and $\%NO_2$), and Table B3-3 presents the results of each step of the multivariate forward approach.

TABLE B3-2

MULTIVARIATE COVARIATE ADJUSTMENT COEFFICIENTS

Dependent Variable	HC Init	NO_x	% NO_2
NO_2TM	-47.281	-9.975	-2.170
HCT50	-46.155	4.019	-2.462
O_3TM	-75.241	5.024	-2.848
FWHM	-38.021	8.494	-.2197
XTIME	-11.965	-8.251	-2.270
1/O_3AVGR	-.0905	-.0091	-.0074
1/HCAVGR	-.0563	-.0114	-.0015
1/NO_2R	-.0225	-.0681	-.0015
1/NORATE	-.0355	-.0658	-.0019
NO_2DOSE	-71.297	118.25	-.4304
NO_2DF	-16.073	1.495	-.0683
O_3DOSE	23.464	18.987	1.881
O_3DF	6.189	-20.859	.4407
1/O_3MAXR	-.0264	.0126	-.0009
1/HCMAXR	-.0295	-.0034	-.0003
O_3MAXC	-.0955	-.0616	.0063
HCFC	-.0710	-.0606	-.0025
HCT75	-19.472	-4.067	-1.998
HCT25	-47.829	-28.033	-2.474
NO_2XT	-33.787	12.999	-.0869
O_3XT	-61.863	20.286	-.6164

TABLE B3-3

Results of Covariate Multivariate Forward Approach

Covariate	HC Init	NO_x	NO_2	% NO_2	Tadj	HC/NO_x	DF	F = .05
Covariate Alone								
"F"	5.982	37.797	8.015	10.385	13.268	7.454	21,15	2.33
Covariate After NO_x								
"F"	5.566	-	5.654	8.274	12.247	3.667	21,14	2.39
Covariate After NO_x and Tadj								
"F"	5.139	-	0.894	0.865	-	3.789	21,13	2.46
Covariate After NO_x, Tadj, and HC Init								
"F"	-	-	0.806	0.809	-	1.438	21,12	2.54
Covariate After NO_x, Nadj, HC Init, HC/NO_x, and % NO_x								
"F"	-	-	0.789	-	-	-	21,10	2.77

3.3 Comparison of Covariate Corrected Data to Adjusted Data

Upon completion of the experiment, the experimenter adjusted the data to a common basis of initial conditions. The analyses reported in this present work have been performed on the original data prior to the experimenter's adjustment. An effort has been made to compare this original data corrected by covariates to the experimenter's adjusted data. To do this, both sets of data have been univariately analyzed according to the same model, and the R^2 values therefrom compared. The R^2 values thus attained for each of the 23 dependent variables are represented in Table B3-4 along with the sign of the difference. The data with the higher R^2 values is the preferred data as the higher R^2 indicates that more of the variation has been accounted for by the adjustment. In all but one case, the covariate adjustment is superior to the experimenter's adjustment with the one exception being, understandably, Ozone DF. As such, the analyses were continued using this covariate corrected data. The experimenters adjustment, based solely on $\%NO_2$ was typically 1 or 2 percent lower in R^2.

4.0 ANALYSIS OF VARIANCE

Having determined the significant covariates for the univariate and multivariate models, attention was focused on the models themselves. The basic model investigated was

$$Y_{ijklm} = \mu + \sum \beta X_{ijklm} + M_i + A_j + B_k + C_l + MA_{ij} + MB_{ik} + AB_{jk} + MAB_{ijk} + MC_{il} + AC_{jl} + \epsilon_{ijklm}$$

where β was an adjustment factor for the appropriate covariate X, M was materials (i = 1, . . . , 5, with original and rerun aluminum considered as two materials), A was S/V (j = 1, 2), B was Spectrum (k = 1, 2), and C was

TABLE B3-4

Comparison of Covariate Corrected Data to Adjusted Data

Dependent Variable	R^2- Covariate Corrected Data		R^2 - Adjusted Data	Diff
NO_2TM	95.9	(96.1)*	94.9	+
HCT50	96.3	(96.4)	95.5	+
O_3TM	95.7	(95.9)	94.2	+
FWHM	93.7	(93.9)	92.7	+
XTIME	96.2	(96.3)	95.8	+
$1/O_3AVGR$	92.1	(93.5)	91.6	+
1/HCAVGR	95.3	(95.9)	93.2	+
$1/NO_2R$	94.6	(95.6)	94.4	+
1/NORATE	95.3	(96.3)	93.8	+
NO_2DOSE	88.3	(90.6)	87.3	+
NO_2DF	90.0	(90.6)	88.5	+
O_3DOSE	93.6	(94.7)	92.6	+
O_3DF	91.9	(95.0)	92.8	-
$1/O_3MAXR$	82.5	(85.3)	79.9	+
1/HCMAXR	92.8	(93.3)	90.9	+
O_3MAXC	92.8	(95.2)	91.3	+
HCFC	78.9	(82.6)	78.3	+
PANMAX	87.1	(88.5)	82.6	+
HCT75	93.4	(93.9)	92.9	+
HCT25	96.5	(96.8)	95.5	+
NO_2XT	91.9	(92.1)	90.3	+
O_3XT	93.2	(93.6)	91.0	+
ALDMAX	77.8	(80.7)	74.2	+

MODEL: $Y = \mu + M + A + B + MA + MB + AB + C + MC + \epsilon$

*( ) = R^2 with all six covariates considered

cleaning (l = 1, 2). All main effects were considered fixed, with contrasts used given in Table B4-1. This model was analyzed in two ways: first as a univariate model for each of the 23 dependent variables, and secondly, as a 21 variable multivariate model.

TABLE B4-1

CONTRASTS USED IN THE ANALYSES OF VARIANCE

Contrast	Material				
	Original Aluminum	Pyrex	Teflon	Stainless Steel	Rerun Aluminum
1	-1	-1	-1	4	-1
2	-1	0	0	0	1
3	0	-1	1	0	0
4	-1	1	1	0	-1

Contrast	Condition	
	S/V Low	S/V High
S/V	-1	1
	Cut	Full
Spectrum	-1	1
	Purge Clean	Vacuum Clean
Clean	-1	1

Interactions formed by appropriate products of above.

4.1 Results of Univariate Analysis

The univariate analysis resulted in a preponderance of material, spectrum, material by S/V, and material by spectrum effects. These four terms were significant for at least 22 of the 23 dependent variables. The three-way interaction of material x S/V x spectrum was surprisingly more prevalent than either the S/V or cleaning main effects, though none of these effects appeared in even half of the cases. Table B4-2 shows those terms which were of statistical significance for each dependent variable.

Three different considerations were made in determining significance. These considerations were necessitated by the imbalancing of the data, which resulted in nonorthogonal sums of squares. The first consideration was to test each term against the error in the order specified by the model of Section 4.0. The second consideration was to test each term using the method of weighted squares of means. Thirdly, each term was tested after adjusting only for the mean. In each consideration, each term was tested against the error mean square, which remained constant for all three considerations. The results of these three approaches were then compared, with the final results given above and in Table B4-2. Prediction coefficients for the complete model are given in Table B4-3. These prediction coefficients apply to the data after it has been adjusted for HCint and $\%NO_2$.

The material effect and material interactions each were composed of four degrees of freedom. As each degree of freedom was defined by a material contrast (see Table B4-1), these contrasts were further investigated. Since there were no missing cells and due to the basic orthogonality of the contrasts, each degree of freedom is directly interpretable from the contrasts. Hence,

TABLE B4-2

Significance of Effects & Interactions on Univariate Data Given HC Init and % NO_2

	M	A	B	MA	MB	AB	MAB	C	MC	AC	BC
NO_2TM	X		X	X	X		X	X			
HCT50	X		X	X	X			X			
O_3TM	X		X	X	X		X	X			
FWHM	X		X	X	X		X		X		
XTIME	X		X	X	X			X			
1/O_3ANGR	X	X	X	X	X				X		
1/HCANGR	X		X	X	X						
1/NO_2R	X		X	X	X		X	X	X		
1/NO RATE	X		X	X	X		X				
NO_2 DOSE	X		X	X	X						
NO_2 DF	X		X	X	X		X		X		
O_3DOSE	X	X	X	X	X	X					
O_3 DF	X	X	X	X	X	X					
1/O_3MAXR	X	X	X	X	X		X	X			X
1/HCMAXR	X	X	X	X	X						
O_3MAXC	X	X	X	X	X	X		X	X		
HCFC	X		X	X	X					X	
PANMAX	X	X	X	X	X	X	X		X	X	
HCT75	X		X	X	X			X			
HCT25	X		X	X	X						
NO_2XT	X		X	X	X		X				
O_3XT	X		X	X	X		X				
ALDMAX	X				X	X					
Total	23	7	22	22	23	5	9	8	6	2	1

TABLE B4-3

Univariate Prediction Coefficients for Covariate Adjusted Data

Term	NO_2TM	HCT50	O_3TM	FWHM	XTIME	$1/O_3AVGR$	1/HCAVGR	$1/NO_2R$	1/NORATE
CONSTANT	107.29	133.64	170.96	100.07	55.158	.2690	.0934	.0854	.1089
MAT 1	-10.311	-10.172	-9.654	-3.459	-6.440	-.0220	-.0073	-.0106	-.0100
MAT 2	2.752	2.109	9.148	7.055	.2316	.0008	.0030	-.0041	.0096
MAT 3	10.410	10.741	19.481	11.019	3.435	.0178	.0089	.0043	.0065
MAT 4	18.791	17.187	21.960	10.278	10.225	.0396	.0138	.0138	.0136
S/V	-.5319	.3122	1.407	.1149	-.2989	.0151	-.0003	-.0013	.0001
SPEC	-23.809	-26.266	-32.929	-22.772	-10.649	-.0793	-.0197	-.0192	-.0214
MAT 1 x S/V	-2.242	-2.322	-2.238	-1.197	-1.408	-.0049	-.0017	-.0021	-.0020
MAT 2 x S/V	3.368	5.995	4.618	2.733	1.296	.0049	.0052	.0004	.0059
MAT 3 x S/V	-15.542	15.962	-23.300	-11.662	-3.453	-.0483	-.0120	-.0025	-.0136
MAT 4 x S/V	4.013	5.893	4.209	.4843	2.551	.0097	.0055	.0039	.0051
MAT 1 x SPEC	2.843	2.436	2.971	1.855	1.197	.0065	.0020	.0026	.0021
MAT 2 x SPEC	-1.850	-.8047	-3.157	-.5144	-.4773	.0078	.0011	.0029	-.0009
MAT 3 x SPEC	.7315	1.144	1.441	-2.877	1.884	-.0045	0.0	.0041	.0047
MAT 4 x SPEC	-8.881	-8.643	-10.813	-7.958	-3.632	-.0277	-.0080	-.0041	-.0072
S/V x SPEC	-1.362	.3043	-2.286	-.4999	.0514	-.0081	-.0002	.0010	-.0003
MAT 1 x S/V x SP	.1935	.4254	.3660	.0459	.0725	.0025	.0006	-.0001	.0006
MAT 2 x S/V x SP	.0341	.0588	.1241	-.9418	.4588	-.0005	-.0011	.0002	.0001
MAT 3 x S/V x SP	6.530	4.941	12.910	9.442	1.496	.0352	.0055	.0009	.0064
MAT 4 x S/V x SP	-3.900	-3.699	-3.034	-1.054	-1.621	-.0078	-.0035	-.0031	-.0046
CLEANING	4.799	3.287	5.673	.1613	3.530	-.0081	.0012	.0054	.0009
MAT 1 x CL	1.153	1.265	1.458	1.376	.5363	.0067	.0013	.0012	.0012
MAT 2 x CL	.9111	2.075	-.799	-2.004	1.026	-.0041	.0014	.0022	-.0002
MAT 3 x CL	5.283	4.346	4.088	.5853	2.479	.0071	.0039	.0060	.0034
MAT 4 x CL	.6221	-1.666	-.7803	-3.159	1.623	-.0123	-.0017	.0028	-.0008
S/V x CL	.2663	-.9434	-1.170	-.0716	.1823	-.0035	-.0016	.0002	-.0004
SPEC x CL	-1.042	-1.082	-1.668	-1.109	-1.104	.0027	-.0003	-.0022	-.0025

TABLE B4-3 (Continued)

Term	NO_2 DOSE	NO_2DF	O_3 DOSE	O_3DF	$1/O_3$MAXR	1/HCMAXR	O_3MAXC	HCFC	PANMAX
CONSTANT	175.72	39.167	144.18	32.120	.0469	.0513	.9678	.2037	.2750
MAT 1	-5.107	-1.138	4.281	.8797	.0012	-.0018	-.0111	-.0136	-.0054
MAT 2	14.542	2.430	.4174	-1.020	.0006	.0024	.0358	-.0153	.0158
MAT 3	19.965	4.566	.0629	.2885	.0025	.0093	.0412	.0078	.0708
MAT 4	17.799	3.625	-10.626	-2.824	.0029	.0066	.0055	.0443	-.0666
S/V	3.052	.4806	-11.578	-2.717	.0064	.0024	-.0680	.0010	.0248
SPECTRUM	-22.917	-5.413	27.926	5.852	-.0100	-.0108	.0718	-.0776	.0453
MAT 1 x S/V	-1.510	-.2272	-.6670	-.1251	.0011	-.0005	-.0135	-.0052	-.0113
MAT 2 x S/V	6.860	1.484	-.4817	-.2603	.0016	.0009	-.0081	.0267	-.1136
MAT 3 x S/V	-31.924	-6.797	14.965	3.740	-.0073	-.0115	.0170	-.0572	-.0338
MAT 4 x S/V	3.850	.7314	-.6073	-.1963	-.0011	-.0015	.0083	.0102	-.0504
MAT 1 x SPEC	.9097	.3246	-1.210	-.1188	-.0007	.0007	.0071	.0105	-.0093
MAT 2 x SPEC	-5.709	-1.072	-.5213	.2679	.0002	-.0015	-.0287	.0223	-.1169
MAT 3 x SPEC	-.4611	.3276	6.632	1.931	-.0020	-.0019	.0222	-.0154	.0354
MAT 4 x SPEC	-13.221	-2.971	9.404	2.263	-.0034	-.0053	.0131	-.0259	-.0061
S/V x SPEC	-4.893	-.9605	-4.099	-.9143	-.0005	-.0013	-.0116	-.0061	.0273
MAT 1 x S/V x SPEC	.7581	.0893	-.6160	-.1249	-.0005	.0003	-.0041	.0067	.0003
MAT 2 x S/V x SPEC	-1.027	-.6885	1.378	-.0915	.0013	-.0004	.0128	.0040	-.0349
MAT 3 x S/V x SPEC	14.899	3.6650	-8.340	-1.293	.0070	.0029	-.0146	.0321	-.0242
MAT 4 x S/V x SPEC	-1.363	-.4994	3.559	.4434	-.0001	.0003	-.0027	.0011	-.0518
CLEANING	.8486	.0362	3.678	.4211	-.0022	-.0012	.0426	-.0200	-.0038
MAT 1 x CLEAN	1.528	.4799	-1.073	-.2530	.0003	0.0	-.0033	.0051	.0047
MAT 2 x CLEAN	.4972	.0615	1.076	.0895	-.0011	.0003	.0255	.0130	.0661
MAT 3 x CLEAN	6.048	1.146	-3.991	-.6963	.0005	-.0026	.0009	.0290	.0391
MAT 4 x CLEAN	-4.860	-1.272	3.917	.4579	-.0030	-.0012	.0306	-.0095	.0405
S/V x CLEAN	.1190	-.2251	-.4989	-.6088	.0006	.0002	-.0071	-.0213	-.0214
SPEC x CLEAN	-.2531	-.1840	.3944	-.2772	.0021	.0005	-.0057	.0158	-.0054

TABLE B4-3 (Continued)

Term	HCT75	HCT25	NO_2XT	O_3XT	ALDMAX
CONSTANT	93.168	169.10	51.915	115.98	.7396
MAT 1	-8.270	-9.909	-3.849	-3.188	.0083
MAT 2	-.7944	.9236	2.462	9.290	.1496
MAT 3	4.224	13.186	6.172	16.111	.0092
MAT 4	12.380	18.641	8.079	11.821	.0006
S/V	-1.891	1.676	-.8581	1.530	-.0049
SPECTRUM	-17.610	-31.478	-12.955	-22.397	.0126
MAT 1 x S/V	-1.798	-2.129	-.7359	-.7426	.0010
MAT 2 x S/V	6.091	6.317	2.162	3.527	-.0632
MAT 3 x S/V	-7.265	-18.650	-12.559	-19.437	.0047
MAT 4 x S/V	7.734	5.333	.8928	1.664	-.0070
MAT 1 x SPEC	2.114	2.577	1.521	1.893	-.0016
MAT 2 x SPEC	2.034	1.165	-1.096	-2.475	-.0036
MAT 3 x SPEC	4.094	.1084	.2755	-.3139	-.0209
MAT 4 x SPEC	-4.088	-8.875	-4.578	-7.147	.0399
S/V x SPEC	.2231	-.9889	-1.132	-2.543	-.0235
MAT 1 x S/V x SPEC	.2173	.3740	.0921	.4048	-.0021
MAT 2 x S/V x SPEC	-.1019	.2718	-.4210	-.4622	.0079
MAT 3 x S/V x SPEC	3.105	7.273	6.294	11.389	.0071
MAT 4 x S/V x SPEC	-4.494	-3.576	-1.652	-1.291	.0133
CLEANING	3.581	1.650	1.724	1.857	.0031
MAT 1 x CLEAN	1.478	1.552	.5325	.9005	-.0099
MAT 2 x CLEAN	2.187	2.532	-.1801	-1.861	-.0129
MAT 3 x CLEAN	4.062	4.555	4.180	1.562	-.0142
MAT 4 x CLEAN	-.4469	-1.082	-.3419	-2.268	.0004
S/V x CLEAN	-2.021	-2.035	.3865	-1.552	-.0022
SPEC x CLEAN	-.7448	-.0371	-.8231	0.7057	.0188

the first material degree of freedom compares stainless steel with the average of the other materials. The second degree of freedom compares the original aluminum to the redone aluminum, the third, pyrex to teflon, and the fourth, the average aluminum to the average of the pyrex and teflon. The material interactions follow the basic pattern. The significance of these individual degrees of freedom is shown in Table B4-4. Of particular concern was the comparison of the aluminums, wherein 8 of the 23 variables indicated a significant difference.

With such profound material effects and interactions are shown in Table B4-4, it was thought that a univariate analysis by materials might be of value, as the various terms could then be considered separately from the material interactions. A study was thus performed which, after adjusting for the covariates HCint and $\%NO_2$, checked the need of additional covariates and then studied the model of $Y_{ijkl} = \mu + \sum \beta X_{ijkl} + A_i \; B_j + AB_{ij} + C_k + AC_{ik} + BC_{jk} + \epsilon_{ijkl}$

with the same term explanations as in Section 4.0.

The original aluminum data, studied in this new context, required no additional covariates after HCinit and $\%NO_2$. Spectrum, S/V, and spectrum by cleaning were generally significant, though no consistent pattern in the model was detected.

The Pyrex analysis helped explain the need for NO_x as a covariate in the multivariate analysis (see Section 3.2). Though the error had only 1 degree of freedom, NO_X was significant after HCinit and $\%NO_2$ nearly 20% of the time. The model, however, was analyzed ignoring this NO_X covariate, with the result of S/V and spectrum being the predominately significant terms.

TABLE B4-4

Significance of Univariate Material Contrasts Given HC Init and % NO_2

	MAT				MAT x S/V				MAT x SPEC				MAT x S/V x SPEC				MAT x CLEAN			
	1	2	3	4	1	2	3	4	1	2	3	4	1	2	3	4	1	2	3	4
NO_2TM	X		X	X	X		X	X	X			X			X	X			X	
HCT50	X		X	X	X	X	X	X	X			X				X				
O_3TM	X	X	X	X	X		X	X	X			X			X					
FWHM	X	X	X	X			X		X			X			X		X			X
XTIME	X		X	X	X			X	X			X				X				
1/O_3AVGR	X			X			X		X			X			X		X			X
1/HCAVGR	X		X	X	X	X	X	X	X			X				X	X			
1/NO_2R	X	X		X	X			X	X			X				X			X	
1/NORATE	X	X	X	X	X	X	X	X	X			X				X				
NO_2DOSE	X	X	X	X			X					X			X					
NO_2DF	X	X	X	X			X			X		X			X		X			X
O_3DOSE	X			X			X				X	X								X
O_3DF	X			X			X				X	X								
1/O_3MAXR	X				X		X		X			X	X		X					X
1/HCMAXR	X		X	X			X					X								
O_3MAXC	X		X		X		X		X	X								X		X
HCFC	X			X		X	X		X			X								
PAN MAX			X	X	X	X	X	X		X				X	X	X		X	X	X
HCT75	X			X		X	X	X	X			X				X				
HCT25	X		X	X	X	X	X	X	X			X			X	X				
NO_2XT	X		X	X			X		X			X			X				X	
O_3XT	X	X	X	X			X		X	X		X			X					
ALDMAX	X	X				X						X								
TOTAL	21	8	15	20	11	8	20	10	16	4	2	21	1	1	11	9	4	2	4	7
Overall Term Significant	23				22				23				9				6			

X Indicates Significance

The Teflon data required no new covariates after HCinit and %NO_2. Spectrum, S/V, and the S/V by spectrum interaction were the most significant, with an occasional cleaning effect and cleaning effect interaction.

Cleaning appeared as a significant term in the stainless steel analysis, along with S/V and spectrum. No additional covariates were required.

The rerun aluminum differed from the original in that only spectrum was significant in the rerun aluminum.

A major difficulty in this "by material" study was the lack of error degrees of freedom, thus a limited power for detecting significance. Hence a failure to declare a term significant in no way implies an absolute lack of significance. With this understanding, Tables B4-5 to B4-9 summarize the above "by materials" analyses.

4.2 Results of Multivariate Analysis

The multivariate data, adjusted for HC Init, TADJ, and NO_2, showed most of the terms of the model of Section 4 to be significant, when the three methods of Section 4.1 were considered. Only S/V by spectrum, S/V by cleaning, and spectrum by cleaning failed to be significant at $\alpha = .05$. Table B4-10 presents an abbreviated MANOVA in which the numerator and denominator degrees of freedom and associated "F" is given for each term, where the "F" is calculated from Wilk's U. (Analogous univariate tables were deemed impractical for the analyses of Section 4.1, due to the large number of such tables which would be required). Though a multivariate "by materials" study would be of great interest, such a study was not possible due to limited error degrees of freedom.

TABLE B4-5

Univariate Original Aluminum Analysis, After HC Init and % NO_2

	NO_x	S/V	SPEC	S/VxSPEC	CLEAN	S/V x CLEAN	SPECxCLEAN
NO_2TM		X	X				X
HCT50		X	X	X			X
O_3TM		X	X				X
FWHM			X		X		X
XTIME		X	X				
$1/O_3AVGR$			X				
1/HCAVGR		X	X	X			
$1/NO_2R$			X				
1/NORATE		X	X			X	
NO_2DOSE		X				X	X
NO_2DF		X	X				X
O_3DOSE			X				
O_3DF			X				
$1/O_3MAXR$			X				
1/HCMAXR		X	X	X			X
O_3MAXC			X				
HCFC		X	X		X	X	
PAN MAX		X	X	X	X	X	X
HCT75		X	X	X			
HCT25		X	X	X		X	
NO_2XT		X	X		X	X	X
O_3XT		X	X		X		
ALDMAX		X		X			
TOTAL	0	16	21	7	5	6	9

X Indicates Significant Term

TABLE B4-6

Univariate Pyrex Analysis After HC Init and % NO_2

	NO_x	S/V	SPEC	S/V x SPEC	CLEAN	S/V x CLEAN	SPEC x CLEAN
NO_2TM		X	X				
HCT50		X	X				
O_3TM		X	X				
FWHM		X	X				
XTIME		X	X				
1/O_3AVGR		X	X				
1/HCAVGR		X	X				
1/NO_2R		X	X			X	X
1/NORATE	X	X	X			X	
NO_2DOSE	X	X	X				
NO_2DF	X	X	X			X	
O_3DOSE		X	X		X		
O_3DF		X	X				
1/O_3MAXR		X	X				
1/HCMAXR	X	X	X			X	
O_3MAXC		X	X		X		
HCFC		X	X		X		
PAN MAX							
HCT 75		X	X				
HCT 25		X	X				
NO_2XT		X	X				
O_3XT			X				
TOTAL	4	21	22	0	3	4	1

TABLE B4-7

Univariate Teflon Analysis, After HC Init and % NO_2

	NO_x	S/V	SPEC	S/V x SPEC	CLEAN	S/V x CLEAN	SPEC x CLEAN
NO_2TM			X				
HCT50			X				
O_3TM		X	X				
FWHM		X	X	X	X	X	
XTIME			X		X	X	
1/O_3AVGR			X				
1/HCAVGR			X				
1/NO_2R		X	X		X	X	
1/NORATE			X				
NO_2DOSE		X	X	X			X
NO_2DF		X	X				
O_3DOSE			X	X			
O_3DF			X	X			
1/O_3MAXR			X	X			X
1/HCMAXR		X	X				
O_3MAXC		X	X	X		X	X
HCFC		X	X	X			
PAN MAX		X	X	X			
HCT 75			X				
HCT 25			X				
NO_2XT			X				
O_3ST		X	X	X			
ALDMAX							
TOTAL	0	9	22	8	3	4	3

X Indicates Significance

TABLE B4-8

Univariate Stainless Steel Analysis, After HC Init and % NO_2

	NO_2	S/V	SPEC	S/V x SPEC	CLEAN	S/V x CLEAN	SPEC x CLEAN
NO_2TM		X	X		X		
HCT 50		X	X		X		X
O_3TM		X	X		X		
FWHM		X	X		X		X
XTIME		X	X		X		X
$1/O_3AVGR$	X	X	X				
1/HC AVGR		X	X		X		X
$1/NO_2R$		X	X		X		
1/NORATE		X	X		X		X
NO_2DOSE		X	X		X		
NO_2DF		X	X		X		
O_3DOSE		X	X	X			
O_3DF		X	X	X			
$1/O_3MAXR$		X	X				
1/HC MAXR			X				
O_3MAXC		X	X	X	X		
HCFC			X				
PAN MAX				X			
HCT 75		X	X		X	X	
HCT 25		X	X		X	X	X
NO_2XT		X	X		X		X
O_3XT		X	X		X		X
ALDMAX							
TOTAL	1	18	21	4	15	2	7

X Indicates Significance

TABLE B4-9

Univariate Rerun Aluminum Analysis, After HC Init and % NO_2

	NO_x	S/V	SPEC	S/V x SPEC	CLEAN	S/V x CLEAN	SPEC x CLEAN
NO_2TM			X				
HCT50			X				
O_3TM			X				
FWHM			X				
XTIME			X				
1/O_3AVGR		X	X				
1/HCAVGR			X				
1/NO_2R			X				
1/NORATE			X				
NO_2DOSE		X	X				
NO_2DF		X	X	X			
O_3DOSE		X	X				
O_3DF		X	X	X			
1/O_3MAXR	X	X					
1/HCMAXR			X				
O_3MAXC		X	X		X		
HCFC			X				
PANMAX			X				
HCT 75			X				
HCT 25			X				
NO_2XT			X				
O_3XT	X	X	X				
ALDMAX							
TOTAL	2	8	20	2	1	0	0

X Indicates Significance

TABLE B4-10

Abbreviated MANOVA, Given HC Init, TADJ, and NO_x

Term	Numerator df	Denominator df	"F"
MATERIALS	84	30	9.097**
S/V	21	7	13.836**
SPECTRUM	21	7	50.200**
MAT x S/V	84	30	4.993**
MAT x SPEC	84	30	3.320**
S/V xSPEC	21	7	2.003
MAT x S/V x SPEC	84	30	1.714*
CLEAN	21	7	3.895*
MAT x CLEAN	84	3	1.800*
S/V x CLEAN	21	7	1.395
SPEC x CLEAN	31	7	0.841

*Indicates Significance at $\alpha = 0.5$

**Indicates Significance at $\alpha = .01$

5.0 PRINCIPAL COMPONENTS

5.1 Selection

Tables B5-1 to B5-3 present the correlation matrix of the 23 parameters derived from the raw data, the adjusted data and the data after the covariate correction (for HC init and %NO_2) respectively. In each case the order of the parameters has been organized so that highly correlated parameters are adjacent to each other.

Rather than using the reported values of the rate parameters, the inverse values have been used. This was done because it was noted that the correlations between these rates and the time parameters increased when this transformation was made. The cross plots show a non-linear relation as typified by Fig. B5-1.

Generally, all three correlation matrices are similar although there is a slight tendency for the values in Table B5-3 to be higher.

There is a remarkable regularity among the first 13 parameters - they are very highly correlated with each other. So much so that we are led to believe that to a major extent they are all reflective of a single underlying "TIME" parameter of the system irregardless of materials, S/V, spectrum or cleaning.

There is a similar linkage between parameters 8 and 19 and between parameters 3 and 18. This is as would be expected since these are in each case standardized versions of one another.

Also all four (3/18 and 8/19) exhibit similar correlations with the 13 time parameters.

	2	21	10	11	12	7	20	23	22	5	14	17	1	8	19	3	18	4	13	6	9	16
2																						
21	961																					
10	957	937																				
11	991	944	968																			
12	978	921	947	992																		
7	973	912	913	976	979																	
20	901	792	824	919	938	955																
23	876	750	798	893	915	954	968															
22	947	835	879	944	944	951	934	932														
5	921	843	869	938	959	945	945	916	915													
14	983	924	961	992	987	969	920	895	944	939												
17	968	942	935	970	959	953	885	858	904	916	961											
1	939	963	934	926	907	868	771	704	830	814	914	913										
8	-750	-670	-686	-783	-826	-800	-853	-808	-763	-900	-778	-754	-652									
19	-753	-670	-684	-782	-815	-801	-849	-811	-772	-890	-772	-744	-635	974								
3	841	695	761	853	855	895	901	945	920	870	859	812	632	-729	-766							
18	863	720	786	877	887	917	925	961	931	898	885	844	670	-761	-769	986						
4	416	287	324	463	538	556	674	686	508	681	470	421	224	-792	-781	622	643					
13	808	696	675	820	855	867	899	905	853	864	824	791	655	-791	-787	864	889	665				
6	037	046	-011	-103	-185	-139	-293	-261	-109	-372	-105	-079	052	655	621	-191	-214	-777	-294			
9	774	666	748	805	841	790	824	792	824	881	822	749	674	-810	-791	654	780	638	756	-391		
16	-161	-185	-226	-177	-199	-184	-197	-163	-114	-213	-189	-226	-140	171	176	-081	-087	-226	-080	221	-260	

TABLE B5-1

Correlation Coefficients for Unadjusted Data

Table B5-2

CORRELATION COEFFICIENT FOR ADJUSTED DATA

	2	10	11	12	7	22	20	23	21	5	14	1	17	8	19	3	18	4	13	6	9
2																					
10	.953																				
11	.991	964																			
12	.977	942	991																		
7	.971	902	974	979																	
22	.971	881	956	960	971																
20	.895	.800	.911	.938	.958	934															
23	.863	768	880	910	953	932	968														
21	971	951	955	925	910	787	798	745													
5	867	843	891	900	874	830	846	798	844												
14	916	922	929	912	875	844	789	745	919	918											
1	767	784	747	705	672	647	551	477	830	767	892										
17	829	820	847	829	804	773	742	704	817	880	907	781									
8	-714	-642	-746	-785	-764	-757	-842	-783	-627	-754	-568	-306	-534								
19	-732	-656	-762	-795	-782	-779	-848	-800	-644	-781	-782	-345	-563	974							
3	847	754	861	878	914	923	907	952	726	-770	-735	-498	-693	-718	-732						
18	859	766	873	894	926	929	926	963	733	-776	-740	-496	-706	-743	-764	987					
4	354	263	409	478	505	460	642	650	223	523	269	056	312	-783	-782	560	574				
13	800	621	762	800	811	780	840	858	630	764	689	414	681	702	-723	826	834	625			
6	016	.022	-079	-154	-126	-119	-306	-276	091	-277	-060	-319	.020	663	637	-227	-242	805	400		
9	785	745	814	850	814	847	846	816	686	-694	-662	-414	-588	-819	-811	802	815	-557	-673	-368	

	2	10	11	12	7	22	20	23	21	5	14	1	17	8	19	3	18	4	13	6	9
2																					
10																					
11																					
12			TIME																		
7																					
22																					
20																					
23																					
21																					
5	924	863	940	956	950	941	957	923	844												
4	989	959	993	989	967	953	910	882	938	942		$\frac{1}{\text{RATE}}$									
1	946	940	929	899	869	837	755	687	986	799	916										
17	955	914	962	949	948	920	889	860	923	912	950	896									
8										-881	-746	-600	-715								
19										-884	-756	-599	-722								
3										907	862	645	830								
18										920	878	668	853								
4	379	266	423	500	531	514	680	694	222	658	438	160	405	-777	-772	648	662				
13	838	642	802	838	864	856	902	909	681	859	806	629	787	-756	-769	886	902	664			
6										-354	-809	.121	-094					-777	-290		
9										891	839	652	762					636	762		

	2	10	11	12	7	22	20	23	21	5	14	1	17	8	19	3	18	4	13	6	9	16
2																						
10	951																					
11	989	964																				
12	976	941	990																			
7	969	899	970	975																		
22	958	880	954	957	972																	
20	888	800	904	930	955	934																
23	859	765	873	901	952	933	966															
21	967	945	950	921	899	868	780	726														
5	920	866	938	960	942	932	941	905	839													
14	983	957	993	988	969	955	914	883	933	948												
1	933	934	921	899	852	823	740	664	979	811	903											
17	966	931	969	957	947	924	878	843	937	911	965	910										
8	-752	-678	-786	-830	-800	-790	-856	-807	-655	-891	-794	-652	-747									
19	-749	-661	-776	-811	-800	-788	-848	-811	-651	-871	-781	-621	-731	970								
3	842	746	851	860	913	917	906	953	706	875	865	611	820	-742	-776							
18	860	770	872	887	927	930	925	961	723	901	887	648	847	-770	-774	986						
4	375	667	420	500	525	508	662	677	208	638	439	169	368	-771	-774	631	640					
13	785	633	794	835	858	848	892	898	666	850	802	608	769	-799	-799	871	887	667				
6	-047	-019	-117	-201	-146	-141	-312	-276	065	-371	-135	-032	-078	656	619	-208	-233	-785	-326			
9	780	750	809	852	805	829	830	796	681	890	833	671	762	-810	-777	754	784	619	754	-393		
16	-137	-203	-154	-176	-155	-139	-202	-166	-120	-186	-179	-122	-130	-125	-139	-105	-098	-183	-070	186	-280	
15	-156	-247	-191	-174	-.061	-098	-018	046	-200	-135	-179	-266	-108	135	065	022	-035	040	-000	093	-178	-002

TABLE B5-3

Correction Coefficients for Covariate Adjusted Data

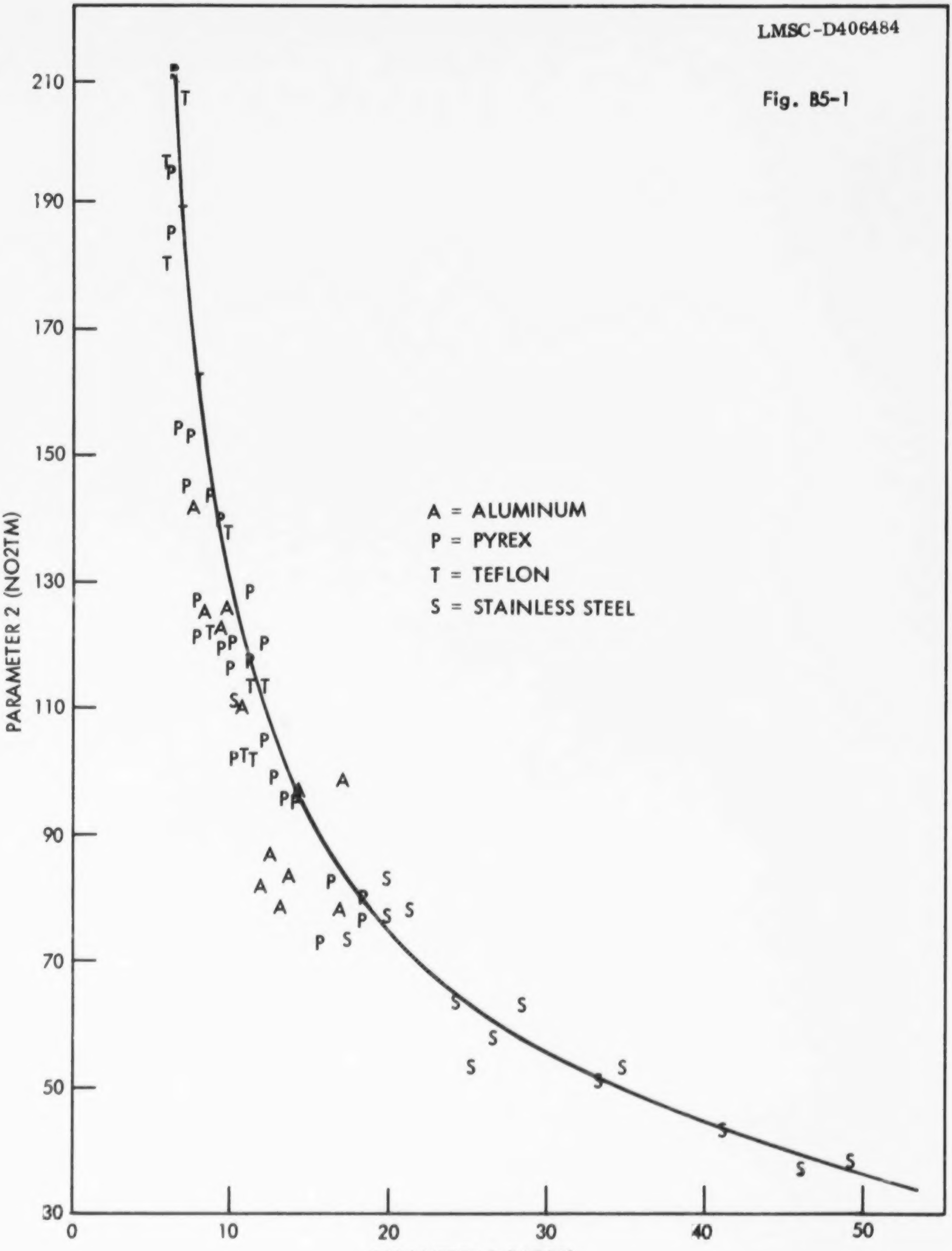
Fig. B5-1
A = ALUMINUM
P = PYREX
T = TEFLON
S = STAINLESS STEEL
PARAMETER 2 (NO2TM)
PARAMETER 1 (NO2R)
210
190
170
150
130
110
90
70
50
30
0
10
20
30
40
50

Finally it is notable that parameters 15 and 16 are largely uncorrelated with each other and with any other parameters.

Thus, we are led to expect that the full 23 parameter set might be well approximated by a reduced set involving:

1 or more components representing "TIME"
1 or more components representing "DOSE"
1 or more components representing the set consisting of 4, 13, 6 and 9 plus possibility parameters 15 and 16.

Prior to forming the principal components it was necessary to consider how the variables should be scaled with respect to each other. To this end, the total variances across the full set were compared parameter by parameter against the variances of replicate observations (prior to covariate adjustment). These ratios shown in Table B5-4, were quite similar with the exception of parameter 15, where the ratio was quite low - indicating that, since the error variance was comparable to the total variance, there was no point in considering this parameter further. Thus parameter 15 was dropped from further consideration.

It is reassuring to see the relatively uniform value of this ratio for the other parameters, since it is indicative of good experimental practice.

5.2 Calculation

In forming the principal components, each parameter value was divided by its "error" standard deviation and the principal components were extracted from covariance matrices of these standardized values.

TABLE B5-4

Ratio of Mean Variation to Error Variation

PARAMETER	T (OVERALL)	TIME (ERROR)	RATIO
2	42.896	7.35	5.836
10	33.149	8.34	
11	43.650	6.84	3.372
12	46.967	6.76	
7	52.069	8.05	6.468
20	29.649	4.83	6.139
21	23.168	4.18	5.543
(22)	20.764	2.91	
(23)	32.338	4.86	
	Inverse Avg Rate		
5	.1140	.01149	9.922*
14	.0343	.00623	5.506
1	.0372	.00914	4.070
17	.0394	.01043	3.778
	DOSE		
3	42.943	8.43	5.094
18	9.480	1.93	4.912
8	37.146	8.51	4.365
9	8.269	1.68	4.922
	Inverse Max Rate & Concentrations		
4	.0159	.00567	2.804
13	.0174	.00565	3.080
6	.1340	.033	4.061
9	.1120	.039	2.872
	PAN MAX		
16	.194	.039	4.974
	ALD MAX		
15	.135	.135	1.000

5.2.1 Time

In the case of the 13 time parameters -

1, 2, 5, 7, 10, 11, 12, 14, 17, 20, 21, 22, 23

we have a certain amount of redundancy. For example parameters 22 and 23 are linear combination of others in the set. Also, parameters 10, 11 and 12 are really three related readings from the same (HC) curve. Hence, it was decided to use a reduced set to derive the principal components. This set consisted of parameters:

1, 2, 5, 7, 12, 14, 17, 20, and 21

The linear combination of these variables which has maximum variance has the following coefficients respectively:

.32, .34, .33, .34, .34, .34, .34, .31, .32

This linear combination accounts for 92.6% of the variance of the original set. The next best combination, orthogonal to this, would account for less than 4% additional. Hence it appears that the "time" variation is well represented by a single principal component. Note that the coefficients are all very nearly 1/3 which means that the principal "time" component is essentially just the average of the 9 individual time parameters.

5.2.2 Dose

For the 4 dose parameters the derived coefficient vector was

8 - - .49
19 - - .51
3 - + .49
18 - + .51

This linear combination accounts for 85% of the total variation of the set. The next best component, orthogonal to this accounts for an additional 14% and might prove useful. However, mainly for simplicity, we have chosen to use only the first component, which is equivalent to the average of 3 and 18 minus the average of 8 and 19.

5.2.3 MISC I and MISC II

For the 5 remaining parameters the principal component was derived using initially all 5 and then, again, dropping parameter 16. This was done because parameter 16 has exhibited some anomalies (Runs 3, 4, and 4A on aluminum, and Run 42 on Teflon).

It was found that the relative weights among the other four parameters were similar in both cases and that 16 did not appear to particular contribute to the desired econimization and it was decided to treat it separately.

The first principal component for the other four parameters was

4 - .56
13 - .48
6 - -.43
9 - .50

This linear combination accounts for 67.7% of the total variation - the next component, orthogonal to this accounts for an additional 22% and it was decided to include this. The second principal components weights are:

4: -.23
13: .54
6: .73
9: .35

The first component is simply the sum of 4 + 13 + 9 minus 6.

The second component has no ready interpretation. Henceforth these two components are called MISC I and MIS II respectively.

Thus, at some potential sacrifice in sensitivity the original 23 parameter set has been reduced to four: (Because of the time drift, Section 2, PAN Max was not further considered.) "TIME", "DOSE", MISC I, MISC II. The transformation used to obtain these parameters is given in Table B5-5. A listing of the four variables is given in Table B5-6. Time sequential plots of these new parameters are presented in Figs. B5-2 thru B5-5.

With only four parameters to keep track of, it is relatively easy to form scatter diagrams of pairs of parameters, material by material, and this is presented in the next section, material by material.

5. 3 Results and Interpretation

5. 3. 1 Stainless Steel

Figures B5-6 to B5-11 present scatter plots of the 4 parameters, two at a time. The experimental conditions for each run are also indicated as follows:

	S/V	Spectrum	Cleaning
+ + +	High	Full	Vacuum
+ + -	High	Full	Purge
- + +	Low	Full	Vacuum
- + -	Low	Full	Purge
+ - +	High	Cut	Vacuum
+ - -	High	Cut	Purge
- - +	Low	Cut	Vacuum
- - -	Low	Cut	Purge

TABLE B5-5

Transformations Used In Obtaining Principal Components

$$\text{TIME} = \frac{\text{NO}_2\text{TM}}{3(7.35)} + \frac{\text{HCT.50}}{3(6.85)} + \frac{\text{O}_3\text{TM}}{3(8.05)} + \frac{\text{FWHM}}{3(4.83)}$$

$$+ \frac{\text{XTIME}}{3(4.18)} + \frac{1}{\text{O}_3\text{AVG R}(3)(.012)} + \frac{1}{\text{HC AVG R}(3)(.006)}$$

$$+ \frac{1}{\text{NO}_2\text{R}(3)(.009)} + \frac{1}{\text{NO R }(3)(.01)}$$

$$\text{DOSE} = \frac{\text{O}_3\text{DOSE}}{2(8.51)} + \frac{\text{O}_3\text{DF}}{2(1.68)} - \frac{\text{NO}_2\text{DOSE}}{2(8.43)} - \frac{\text{NO}_2\text{DF}}{2(1.93)}$$

$$\text{MISC I} = \frac{\text{O}_3\text{MAXR}}{2(.0057)} + \frac{\text{HC MAX R}}{2(.0057)} - \frac{\text{O}_3\text{ MAX C}}{2(.033)} + \frac{\text{HCFC}}{2(.039)}$$

$$\text{MISC II} = -\frac{\text{O}_3\text{MAX R}}{4.545(.0057)} + \frac{\text{HC MAX R}}{1.852(.0057)} + \frac{\text{O}_3\text{MAX C}}{1.37(.033)} + \frac{\text{HCFC}}{2.857\ (.039)}$$

Where all variables were originally adjusted for HC Init and % NO_2 as in Table B3-1.

Table B5-6
PRINCIPAL COMPONENTS VALUES

REDONE ALUMINUM

RUN NO	S/V	SPEC	CLEAN	HCINIT	NOX	NO2	%NO2	TADJ	HC/NOX
71	2	2	2	3.10	1.52	.25	16.4	12.	2.00
69	2	2	1	3.04	1.47	.21	14.3	8.	2.07
85	2	2	1	2.94	1.49	.13	8.7	-2.	1.97
73	1	2	2	3.00	1.47	.14	9.5	0.	2.02
75	1	2	1	3.06	1.45	.19	13.1	6.	2.11
81	2	1	2	3.04	1.49	.14	9.4	-2.	2.04
70	2	1	1	2.88	1.47	.17	11.6	4.	1.96
82	2	1	1	3.07	1.49	.17	11.4	4.	2.06
84	2	1	1	2.96	1.41	.14	8.5	0.	2.10
74	1	1	2	3.02	1.46	.16	12.3	6.	2.07
72	1	1	1	3.00	1.46	.15	10.3	0.	2.15

REDONE ALUMINUM

RUN NO	TIME	DOSE	MISC 1	MISC 2
71	42.87	-0.55	-5.04	25.68
69	40.22	0.96	-4.39	24.56
85	40.24	-0.04	-5.34	24.11
73	40.00	3.58	-9.99	28.91
75	35.23	5.73	-8.85	26.46
81	53.00	-7.42	-2.06	26.28
70	61.92	-10.09	1.95	27.52
82	51.63	-8.21	-1.43	24.47
84	55.60	-6.92	2.89	24.67
74	58.24	-4.67	-6.32	29.62
72	52.60	-3.48	-5.67	26.50

Table B5-6
PRINCIPAL COMPONENTS VALUES (Cont.)

ORIGINAL ALUMINUM

RUN NO	S/V	SPEC	CLEAN	HCINIT	NOX	NO2	%NO2	TADJ	HC/NOX
3	2	2	2	3.17	1.52	.22	14.5	9.	2.09
4	2	2	1	3.05	1.54	.29	18.8	17.	1.98
4.5	2	2	1	2.90	1.41	.29	20.6	21.	2.06
10	1	2	2	2.96	1.51	.31	20.5	20.	1.96
11	1	2	2	3.03	1.43	.22	15.4	11.	2.12
12	1	2	1	2.98	1.51	.11	7.3	-8.	1.97
12.5	1	2	1	2.83	1.67	.36	19.2	18.	1.69
6	2	1	2	2.81	1.59	.31	19.5	28.	2.04
5	2	1	1	2.98	1.33	.12	9.0	0.	2.24
9	1	1	2	2.94	1.49	.33	22.1	35.	1.97
7	1	1	1	2.84	1.42	.22	15.5	16.	2.00
8	1	1	1	2.92	1.36	.19	14.0	12.	2.15

ORIGINAL ALUMINUM

RUN NO	TIME	DOSE	MISC 1	MISC 2
3	35.60	0.69	-4.91	20.75
4	34.19	4.48	-7.83	25.90
4.5	35.87	5.55	-7.12	25.69
10	36.74	8.74	-7.83	28.62
11	36.61	7.59	-9.24	28.29
12	38.29	4.53	-10.04	29.21
12.5	38.68	1.77	-6.68	25.01
6	49.87	-2.37	-1.78	23.32
5	49.98	0.08	2.52	23.61
9	60.95	-4.48	-1.52	24.14
7	51.73	-2.11	-1.69	24.43
8	53.29	2.08	-3.30	26.22

ORIGINAL ALUMINUM

Table B5-6

PRINCIPAL COMPONENTS VALUES (Cont.)

PYREX

RUN NO	S/V	SPEC	CLEAN	HCINIT	NOX	NO2	%NO2	TADJ	HC/NOX
22	2	2	2	3.22	1.68	.27	16.1	12.	1.92
21	2	2	1	3.20	1.57	.17	10.8	0.	2.04
27	1	2	2	2.94	1.55	.18	11.6	5.	1.90
33	1	2	2	3.00	1.52	.16	10.5	0.	1.97
31	1	2	1	2.84	1.39	.14	10.1	0.	2.04
26	2	1	2	2.98	1.44	.18	12.5	7.	2.07
25	2	1	1	2.95	1.54	.21	13.6	10.	1.92
30	1	1	2	3.23	1.50	.16	10.7	2.	2.15
32	1	1	1	3.00	1.43	.20	14.0	11.	2.10

PYREX

RUN NO	TIME	DOSE	MISC 1	MISC 2
22	44.38	0.41	-6.48	25.78
21	43.07	-2.74	-2.52	24.42
27	31.12	11.01	-11.61	28.11
33	33.26	10.32	-10.45	27.34
31	41.84	5.64	-7.84	23.83
26	79.12	-16.55	2.13	28.73
25	93.19	-32.54	12.74	25.78
30	62.22	-2.73	-4.96	27.53
32	52.43	-0.55	-2.81	25.14

Table B5-6

PRINCIPAL COMPONENTS VALUES (Cont.)

RUN NO	TEFLON S/V	SPEC	CLEAN	HCINIT	NOX	NO2	%NO2	TADJ	HC/NOX
38	2	2	2	3.00	1.52	.16	10.5	0.	1.97
34	2	2	1	2.82	1.38	.13	9.4	-2.	2.04
35	2	2	1	2.86	1.50	.15	14.7	14.	1.91
42	1	2	2	2.97	1.54	.18	11.7	5.	1.93
43	1	2	1	2.98	1.52	.15	14.5	13.	1.96
44	1	2	1	3.03	1.47	.15	13.6	10.	2.06
36	2	1	2	2.99	1.63	.17	10.4	0.	1.84
39	2	1	2	2.96	1.45	.17	11.7	7.	2.04
37	2	1	1	2.86	1.48	.15	10.1	0.	1.93
40	1	1	2	2.96	1.49	.17	11.4	5.	1.99
41	1	1	1	2.96	1.47	.14	9.5	-2.	2.01

RUN NO	TEFLON TIME	DOSE	MISC 1	MISC 2
38	51.05	0.25	-7.75	27.95
34	44.79	3.45	-6.80	26.44
35	45.30	1.83	-6.30	26.11
42	52.39	-0.91	-8.63	33.49
43	47.35	-1.16	-6.54	31.13
44	50.40	-0.38	-6.71	29.22
36	76.34	-12.92	-0.22	30.98
39	80.05	-15.56	-0.01	29.39
37	70.43	-13.78	3.22	26.04
40	79.27	-20.17	1.10	31.86
41	88.83	-29.27	13.25	30.56

Table B5-6

PRINCIPAL COMPONENTS VALUES (Cont.)

```
     STAINLESS STEEL
RUN NO   S/V SPEC CLEAN   HCINIT   NOX     NO2   %NO2   TADJ   HC/NOX
   55      2   2     2     3.19   1.48    .15   10.1     0.     2.16
   56      2   2     2     3.04   1.52    .18   11.8     0.     2.00
   51      2   2     1     3.09   1.42    .15   10.6     0.     2.18
   52      2   2     1     3.11   1.43    .15   10.5     0.     2.17
   58      2   2     1     2.86   1.49    .17   11.4     0.     1.92
   62      1   2     2     3.02   1.46    .15   10.3     0.     2.07
   61      1   2     1     2.98   1.50    .16   10.7     0.     1.99
   66      1   2     1     3.06   1.48    .16   10.8     0.     2.07
   57      2   1     2     3.11   1.44    .17   11.8     3.     2.16
   53      2   1     1     3.05   1.49    .16   10.7     0.     2.05
   54      2   1     1     3.24   1.52    .17   11.2     2.     2.13
   63      1   1     2     2.88   1.44    .13    9.0     0.     2.00
   60      1   1     1     3.02   1.55    .18   11.6     3.     1.95
   67      1   1     1     3.00   1.53    .18   11.8     3.     1.96
```

```
     STAINLESS STEEL
RUN NO      TIME      DOSE   MISC 1   MISC 2
   55      25.54      4.87    -6.12    22.56
   56      26.88      3.94    -4.98    23.11
   51      21.45      6.10    -4.00    21.17
   52      21.21      6.45    -3.58    21.97
   58      23.55      5.05    -3.31    20.97
   62      31.84      9.04   -11.02    29.21
   61      26.51      8.57    -9.97    28.35
   66      28.06     10.71   -10.43    29.04
   57      42.24     -7.01     2.58    18.71
   53      30.77     -1.96     3.34    19.15
   54      34.16     -2.42     2.23    20.19
   63      50.19     -4.01    -2.20    26.83
   60      38.75     -1.83    -1.75    22.62
   67      38.37     -0.07    -0.83    25.28
```

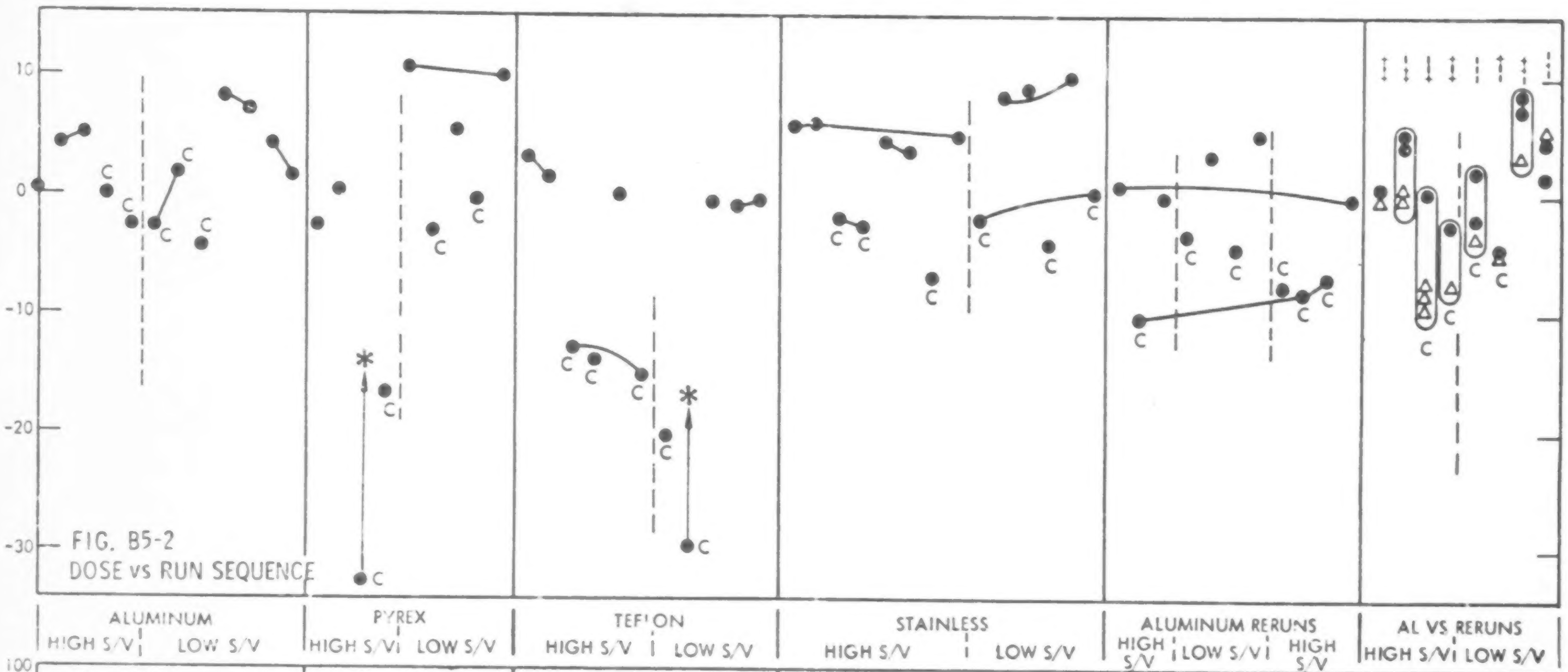

FIG. B5-2
DOSE vs RUN SEQUENCE

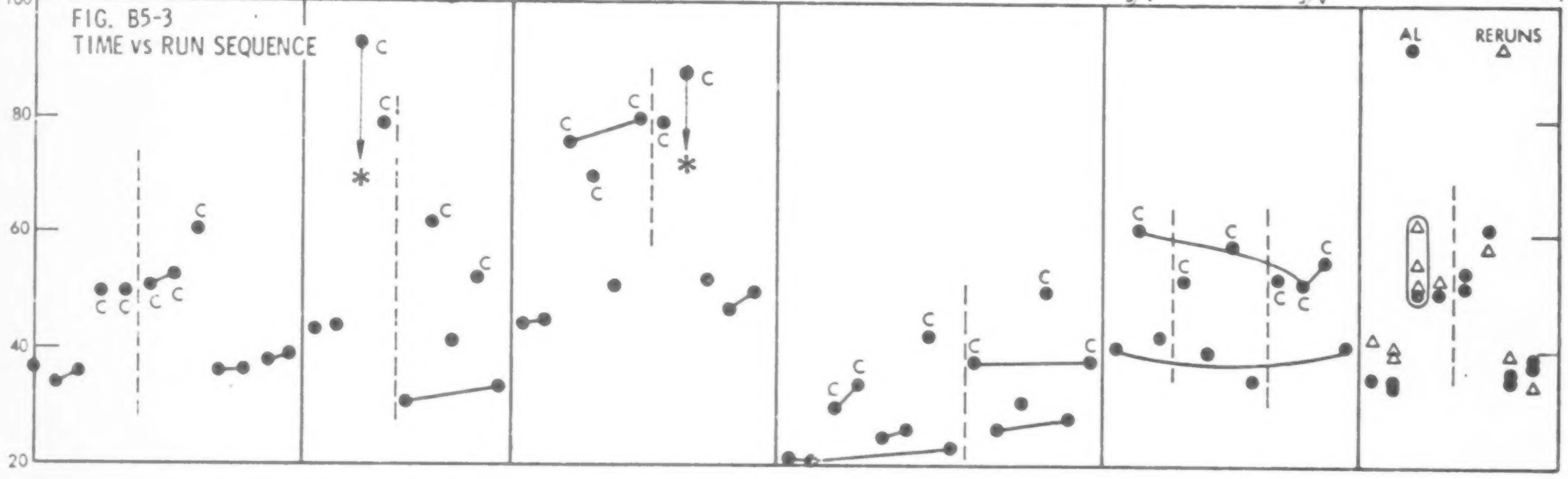

FIG. B5-3
TIME vs RUN SEQUENCE

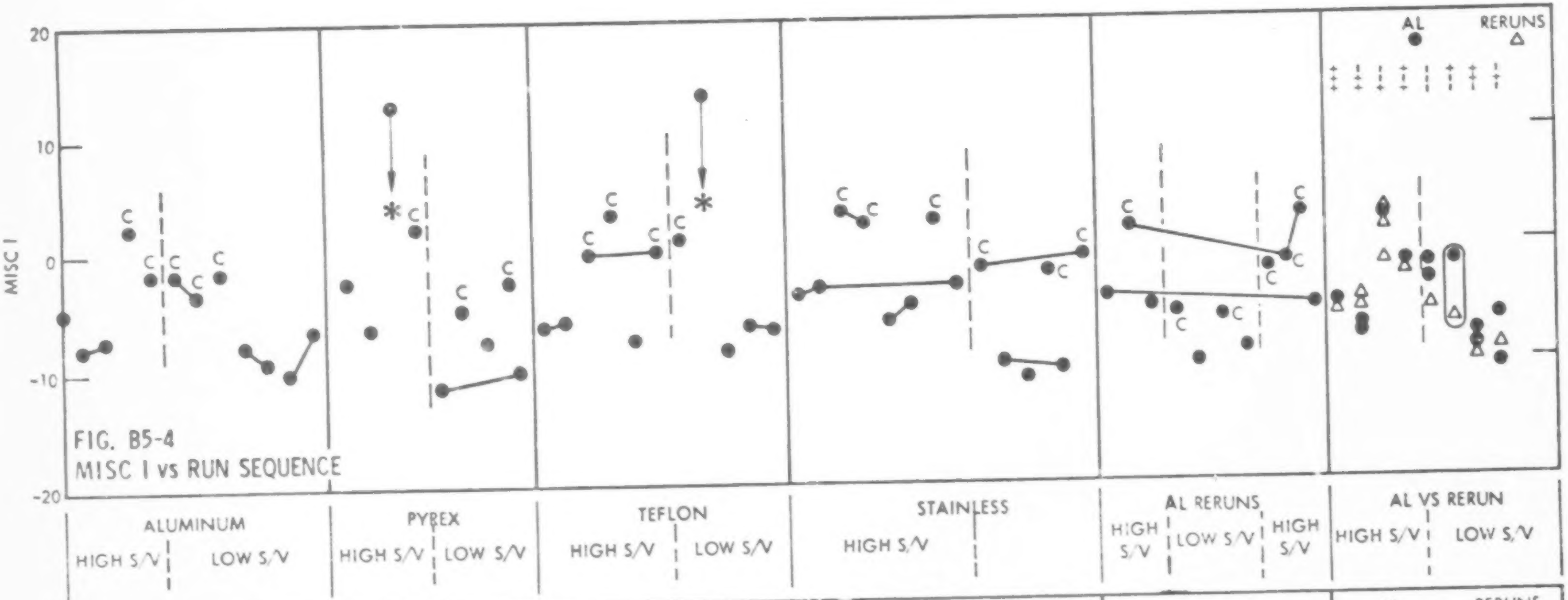
FIG. B5-4
MISC I vs RUN SEQUENCE

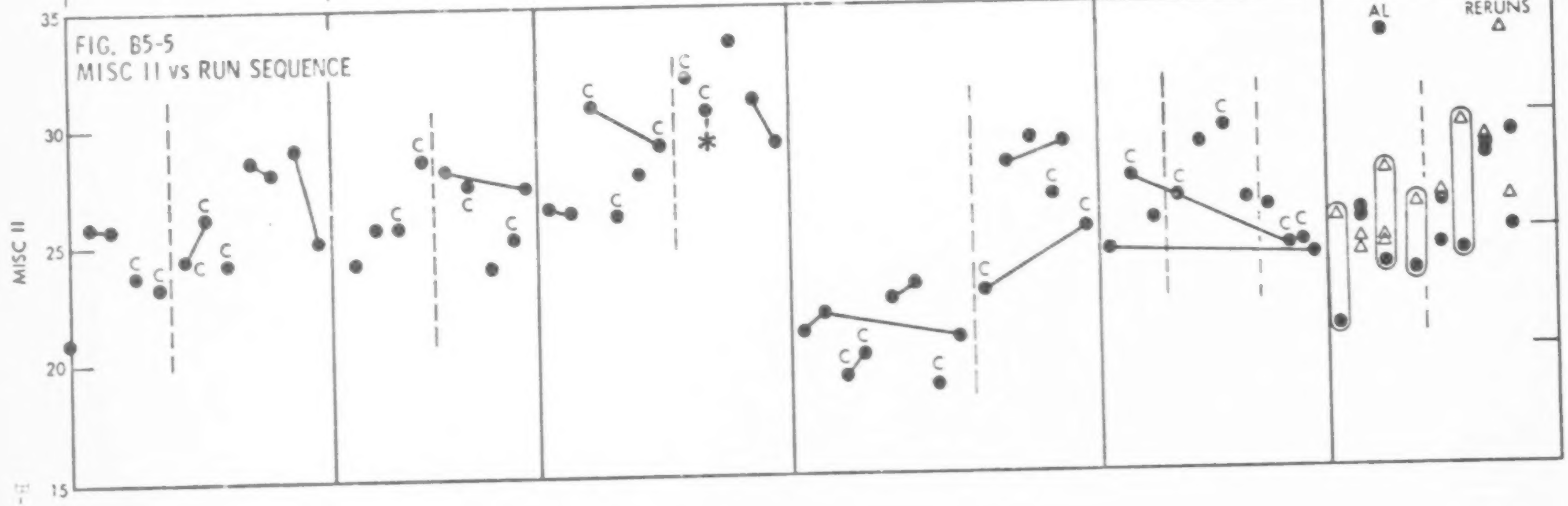
FIG. B5-5
MISC II vs RUN SEQUENCE

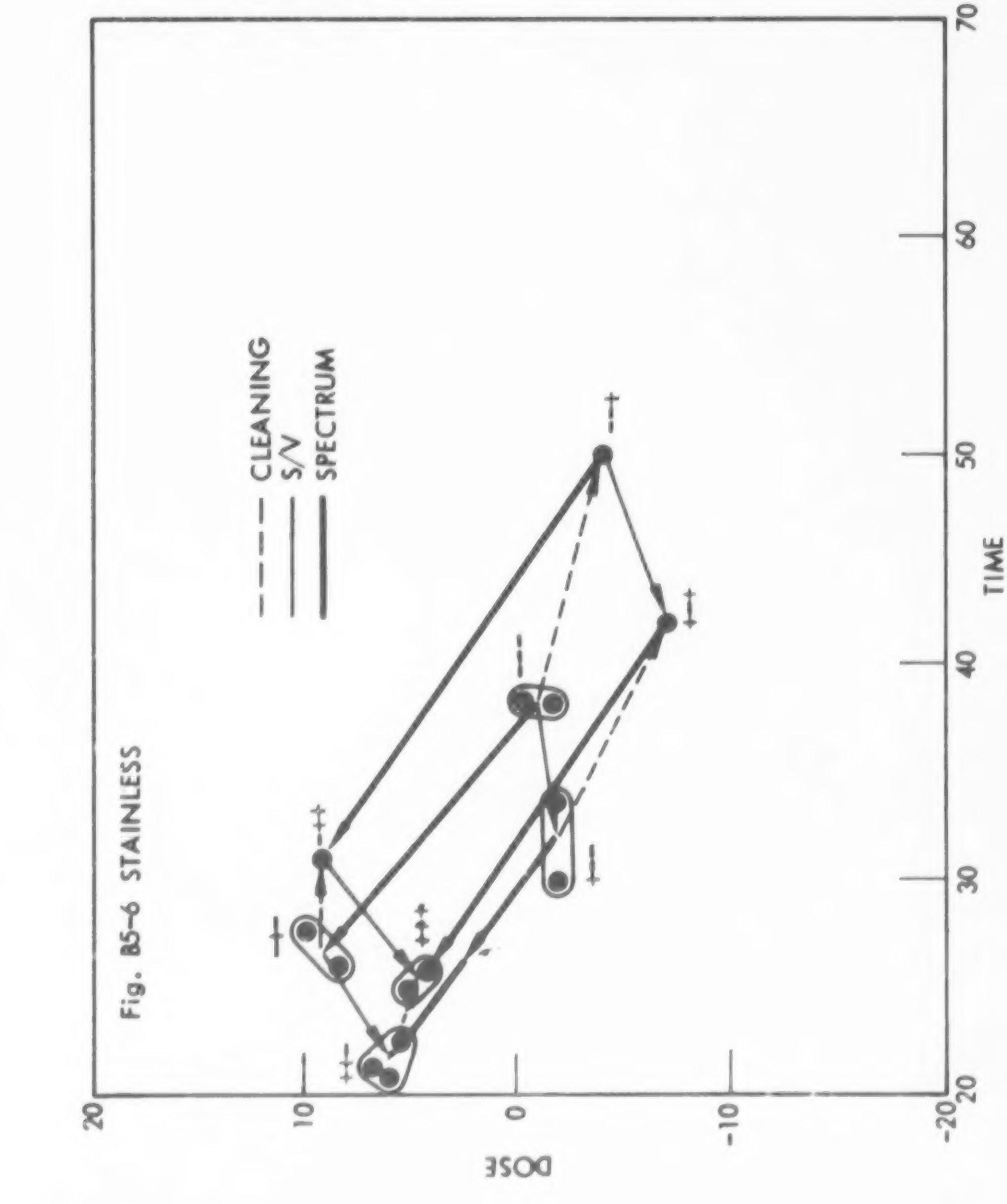

Fig. B5-6 STAINLESS

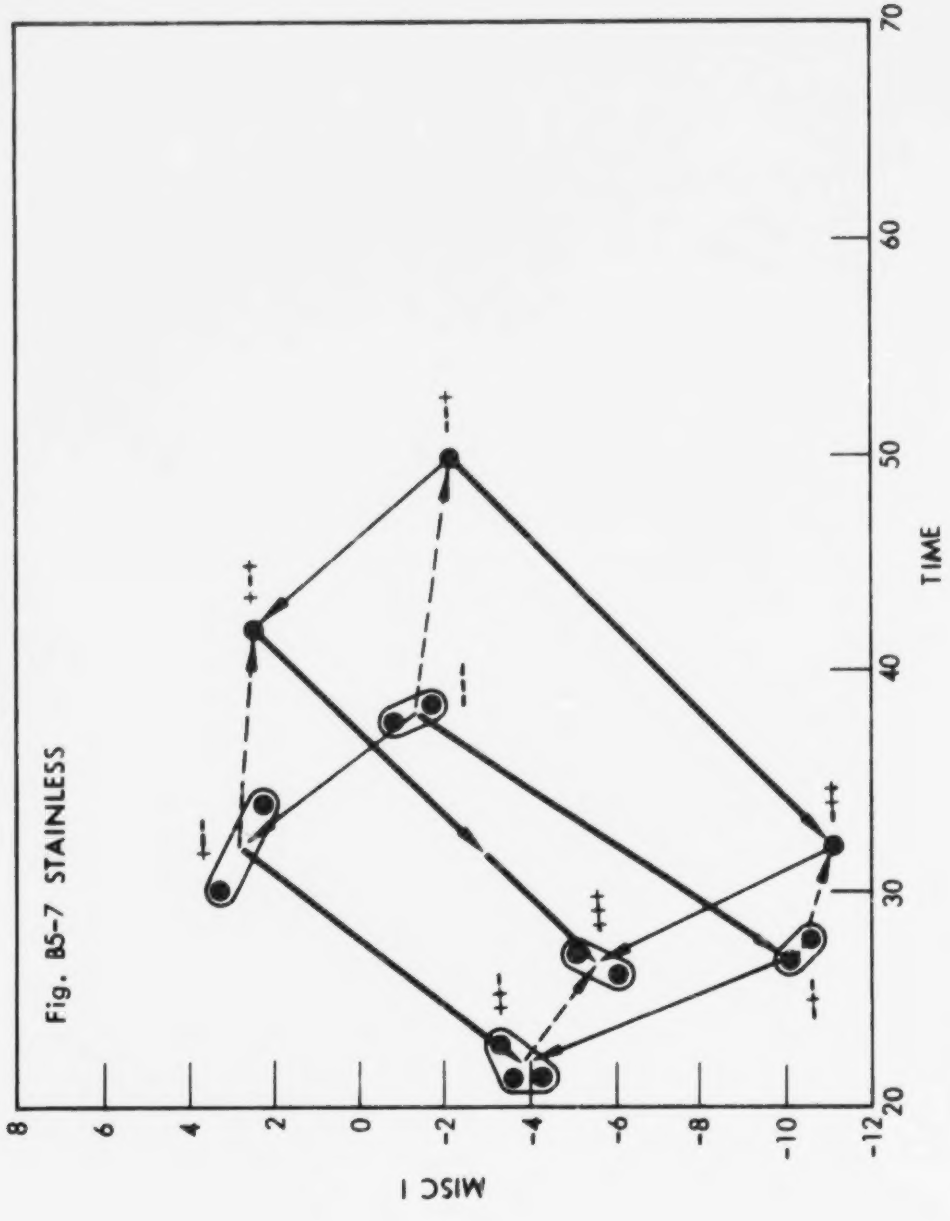

Fig. B5-7 STAINLESS

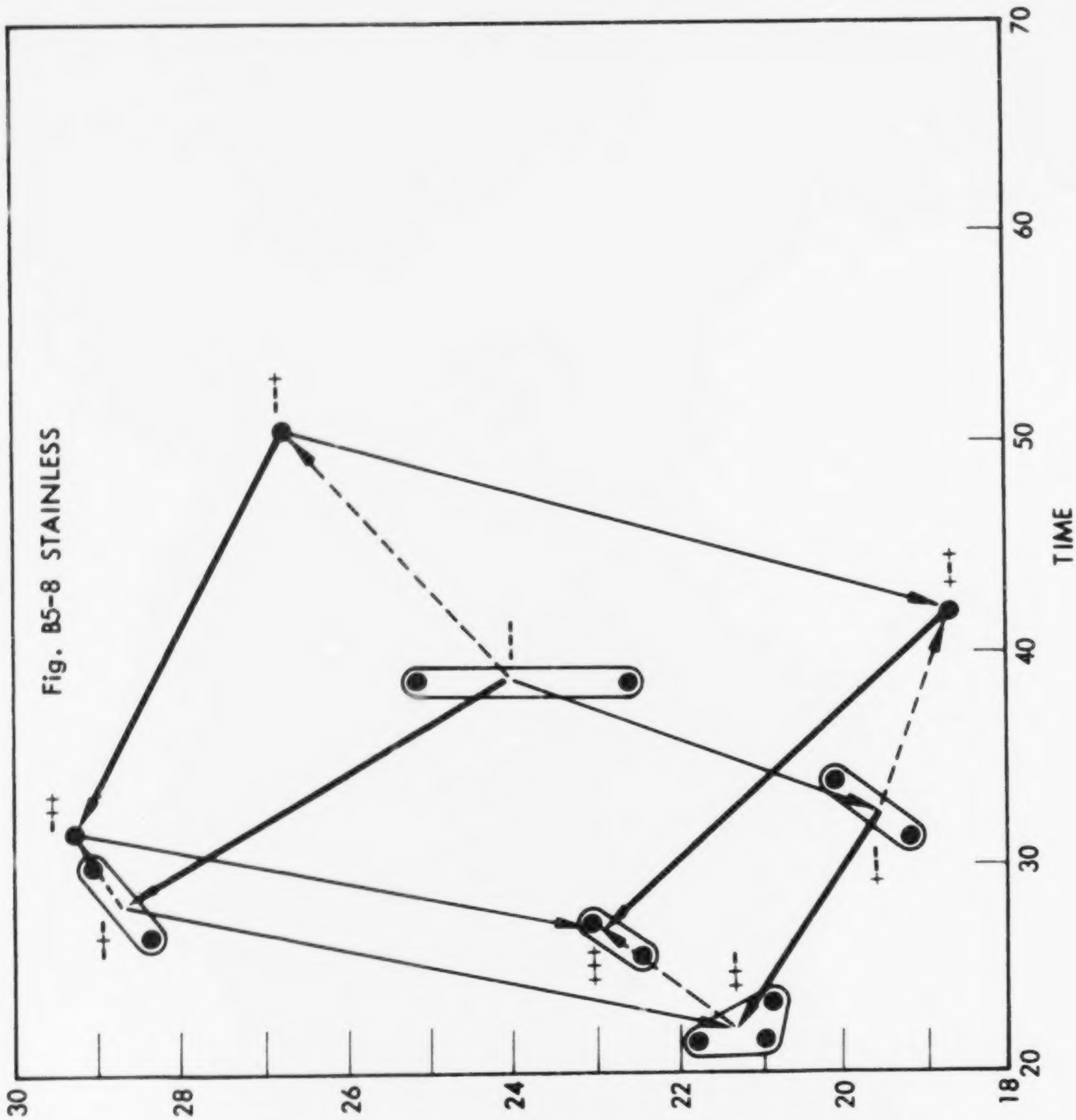

Fig. B5-8 STAINLESS

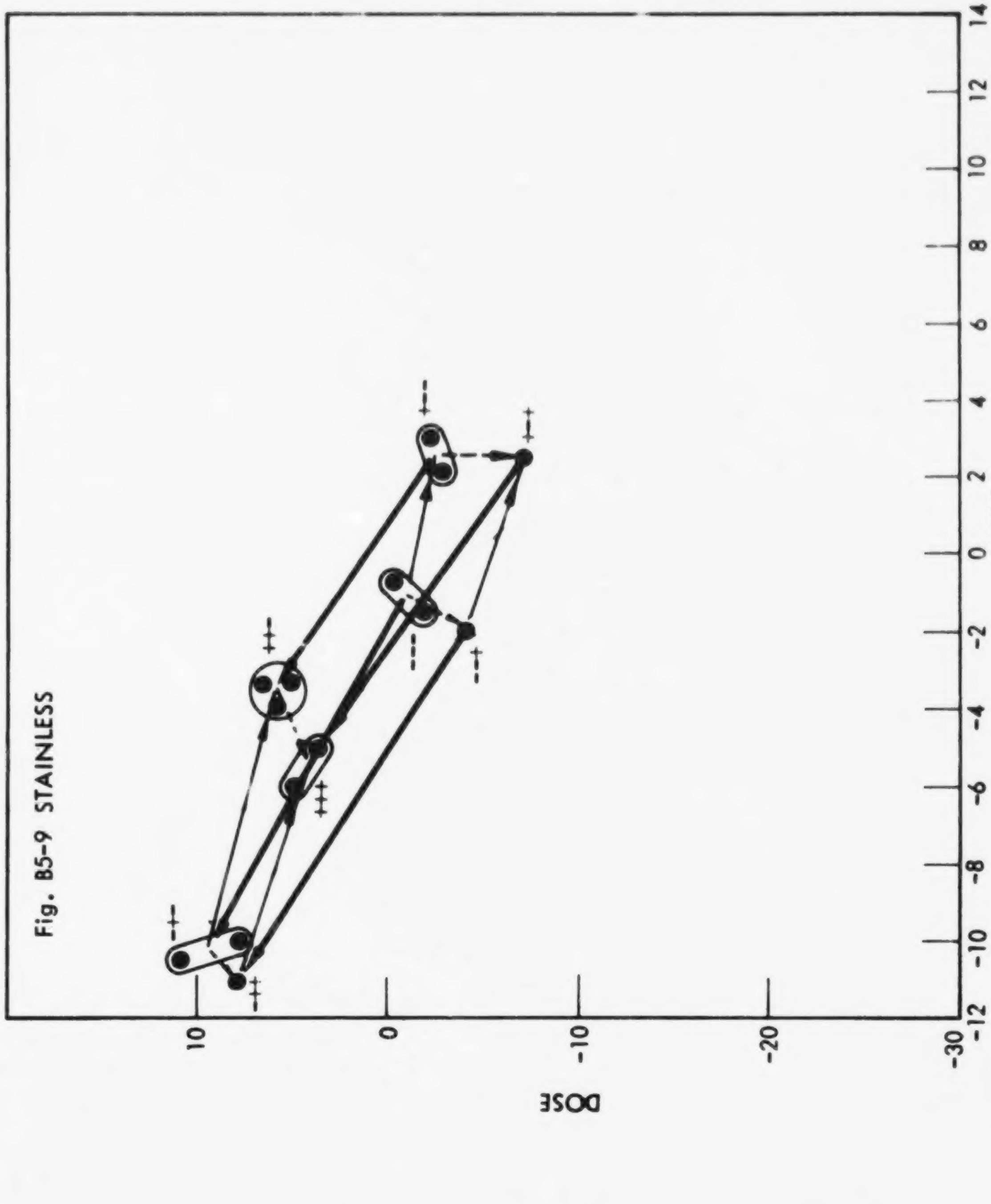

Fig. B5-9 STAINLESS

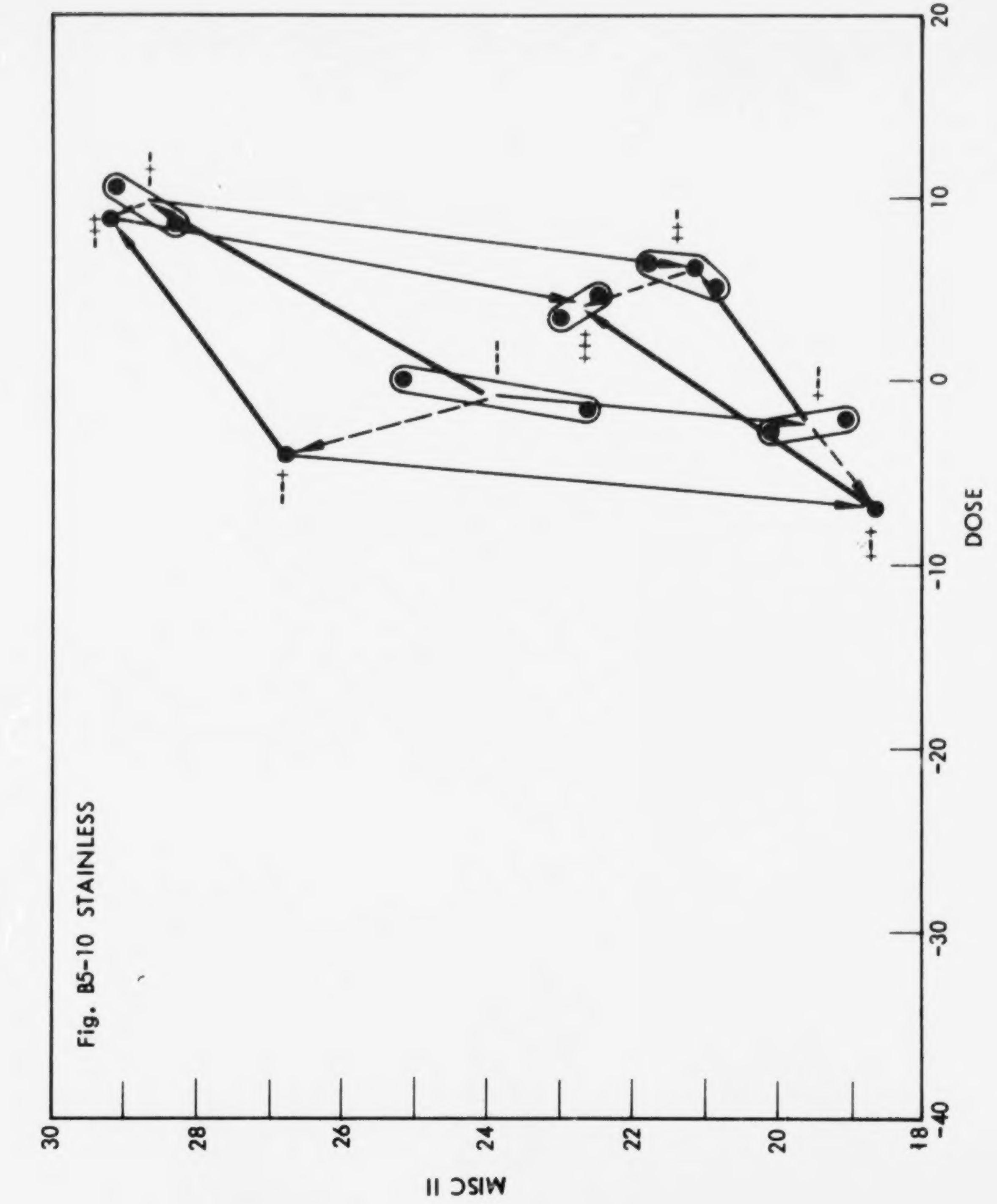

Fig. B5-10 STAINLESS

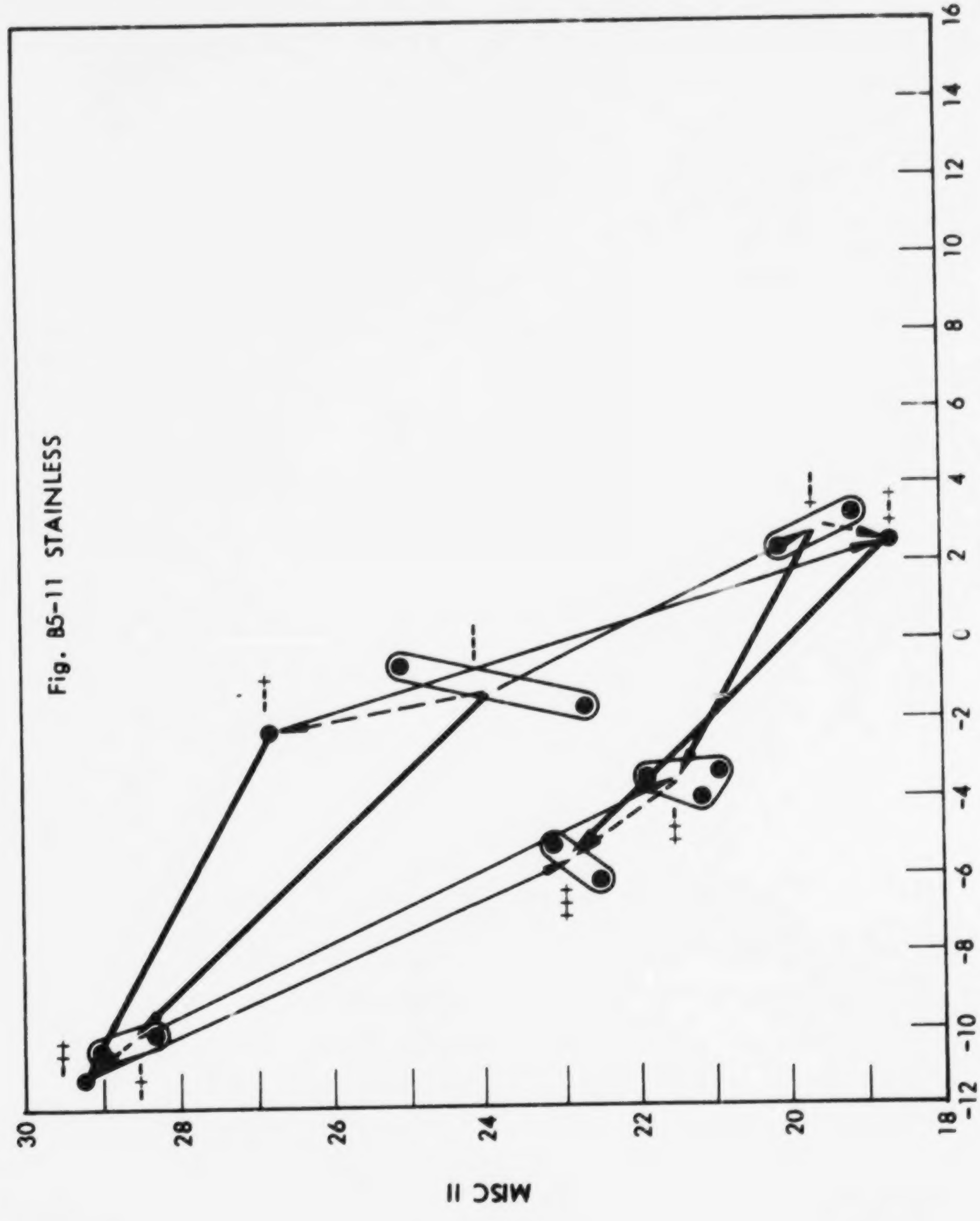

Fig. B5-11 STAINLESS

Thus, for example (+ - +) indicates a run with High S/V, cut spectrum, and vacuum cleaning.

On each plot, pairs of runs which differ in only one of the three variables have been connected by arrows which run from the "minus" to the "plus". If all of the variables has a consistent effect then the arrows will be parallel for each pair which differs in the same variable. Thus, a very regular additive model produces a diagram which looks like a three dimensional box.

It is notable that such is the case for all six pictures.

Hence the "orthonalized" analysis presented in Table B5-7 shows very little interaction for any of the parameters.

5.3.2 Teflon

Figure B5-12 thru B5-17 present plots in the same manner as was done for stainless steel. Here however the pattern is substantially less regular due almost entirely to the data from Run 41.

We are led to speculate about the validity of this run. It is one of the slowest runs experienced during the program. Moreover it, together with run 25 on Pyrex is largely responsible for the initial concern over time trend. Jumping ahead we note that while run 41 was the final run at cut spectrum - possibly implying a degradation with lamp and filter age - leading to decreased time; run 25 was the first run at cut spectrum for pyrex where the apparent trend is in the opposite direction. Thus there does not seem to be any consistent trend which might explain the discrepancy. Note also that Run 41 seems to be discrepant in all 4 parameters.

	TIME				DOSE			
	S.S.	Teflon	Pyrex	Alum	S.S.	Teflon	Pyrex	Alum
MEAN	33.88	62.22	52.91	46.97	1.85	-8.00	-2.48	-1.74
A=S/V	-6.18	-2.08	11.47	.94	-3.16	3.42	-11.48	-3.81
B=SPECTRUM	-13.72	-25.76	-25.07	-14.78	10.78	16.60	11.95	8.11
C=CLEANING	7.49	6.01	3.14	3.11	-2.49	-1.54	.86	-1.05
AB	.85	-.51	-4.76	3.02	-1.04	-1.13	-2.16	-.39
AC	.61	.88	3.07	-2.09	- .66	.10	.56	.37
BC	-2.97	-1.26	-7.31	.59	1.45	.28	3.22	-.53
ABC	.32	.37	2.41	1.03	.22	-1.23	-.37	-.30

	MISC I				MISC II			
	S.S.	Teflon	Pyrex	Alum	S.S.	Teflon	Pyrex	Alum
MEAN	-3.56	-2.67	-3.69	-5.66	23.91	29.31	26.12	26.54
A=S/V	5.23	- .26	5.94	4.90	-6.52	-3.40	.12	-2.66
B=SPECTRUM	-8.08	-9.44	-6.55	-3.85	3.24	.32	-1.11	-.40
C=CLEANING	-.97	-2.36	-2.60	-1.19	.98	3.12	2.65	2.16
AB	.80	.74	-1.01	-.42	-.32	-1.33	-.80	-.02
AC	-.10	.09	-.12	-.29	-.72	-.22	-.49	-.63
BC	-.41	.76	-.79	.53	.02	-.63	-.27	-.26
ABC	-.45	.31	-.26	.77	1.20	-.61	-.77	.08

TABLE B5-7 Material Effects for Principal Components

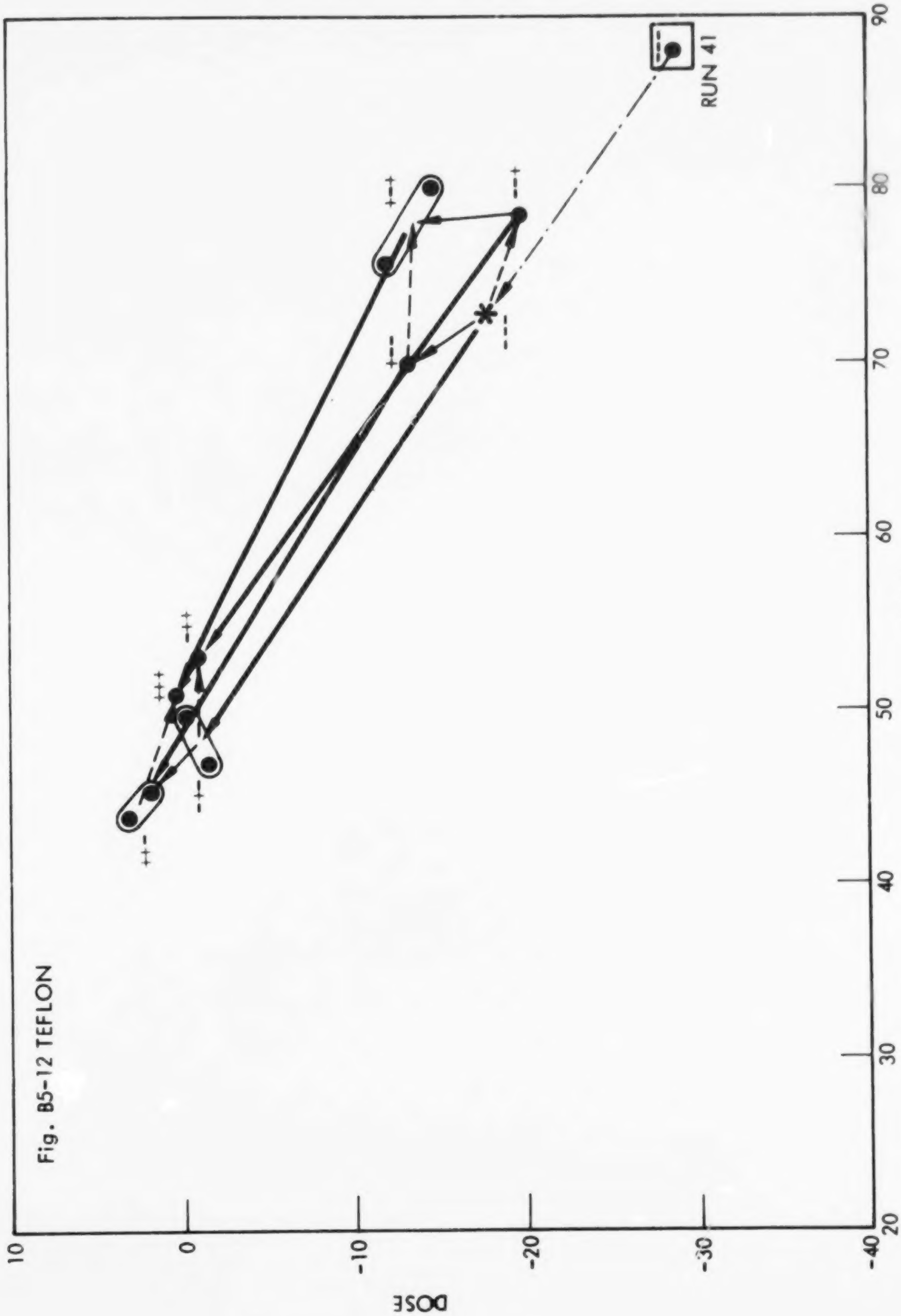

Fig. B5-12 TEFLON

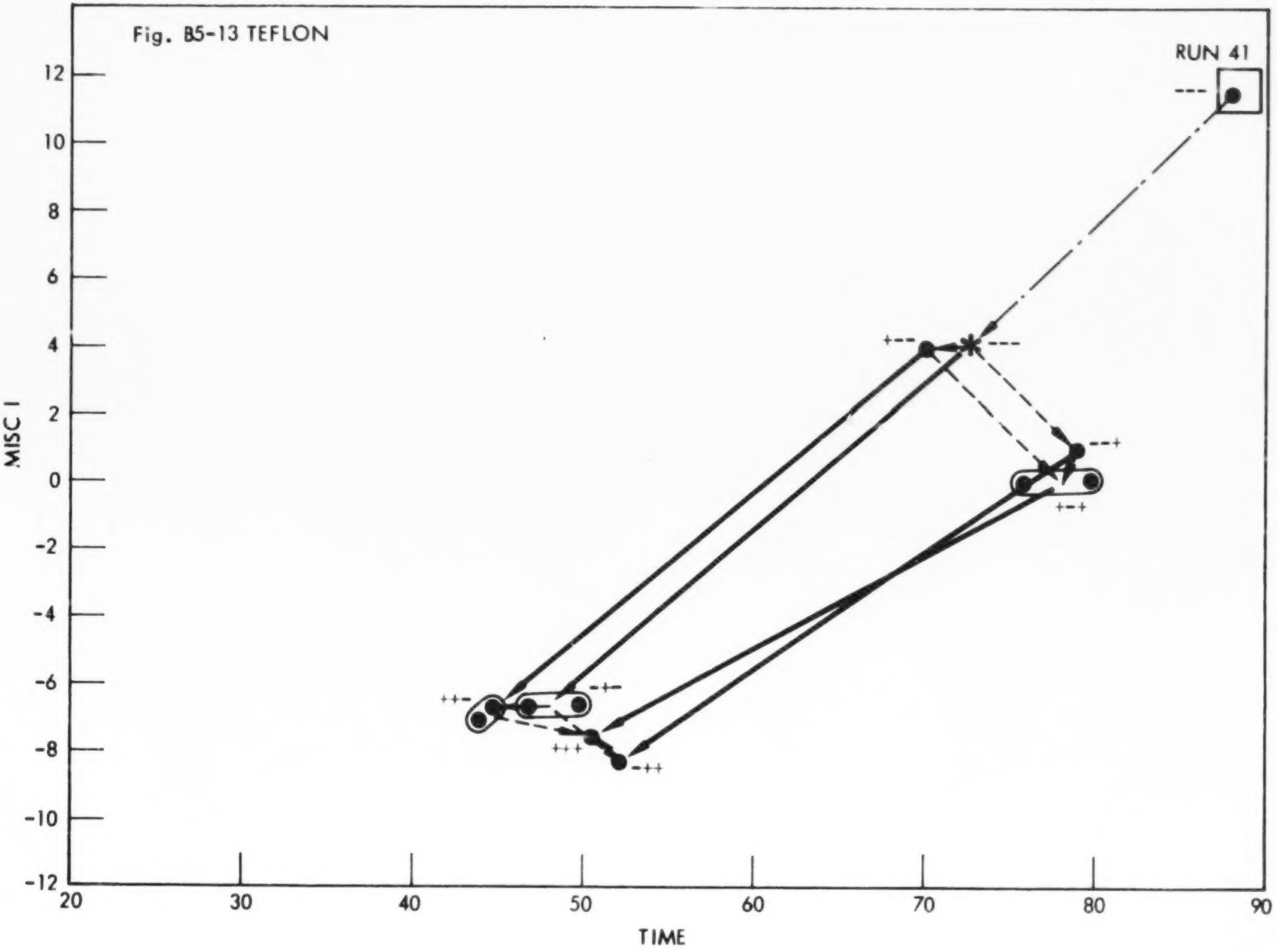
Fig. B5-13 TEFLON

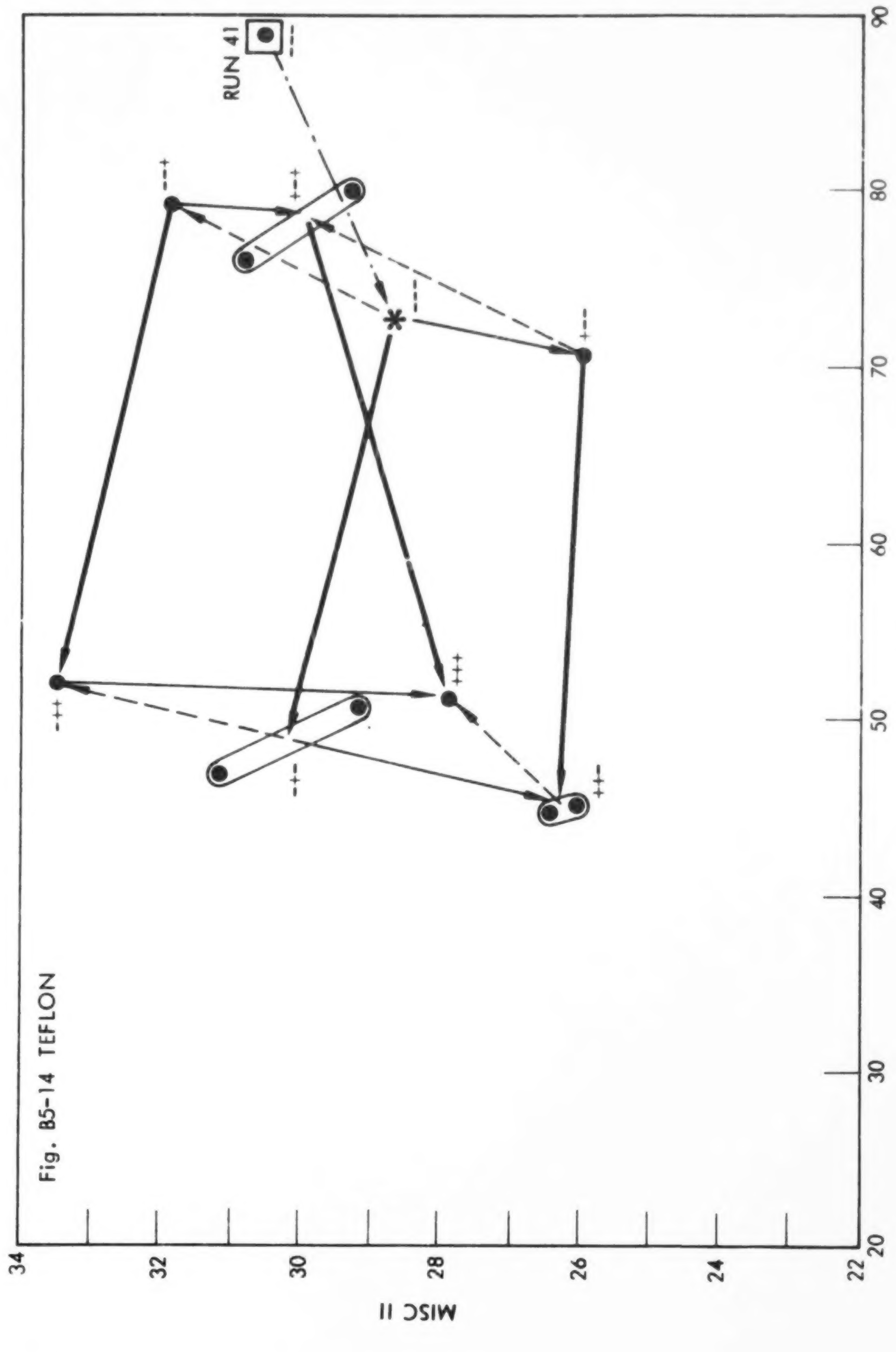

Fig. B5-14 TEFLON

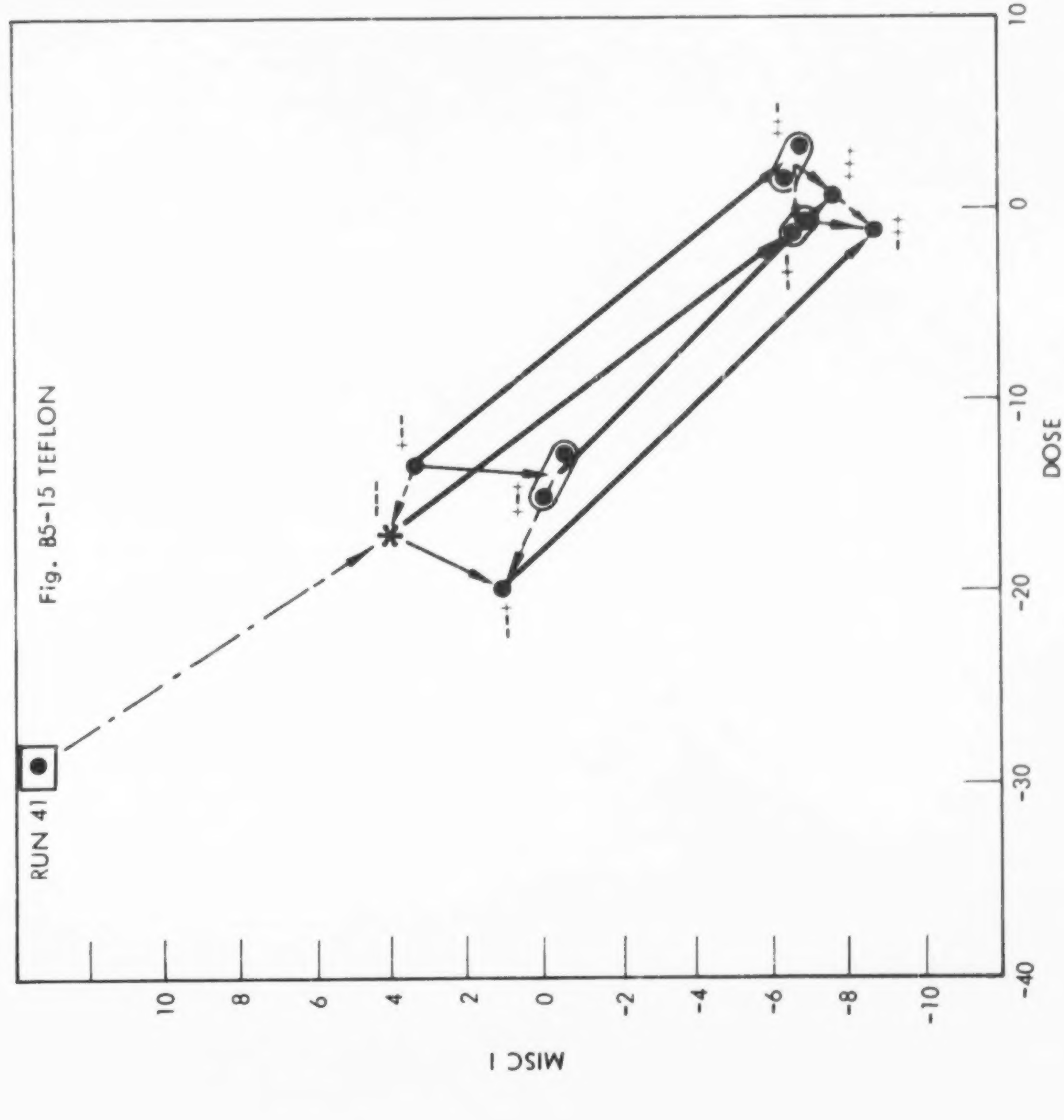

Fig. B5-15 TEFLON

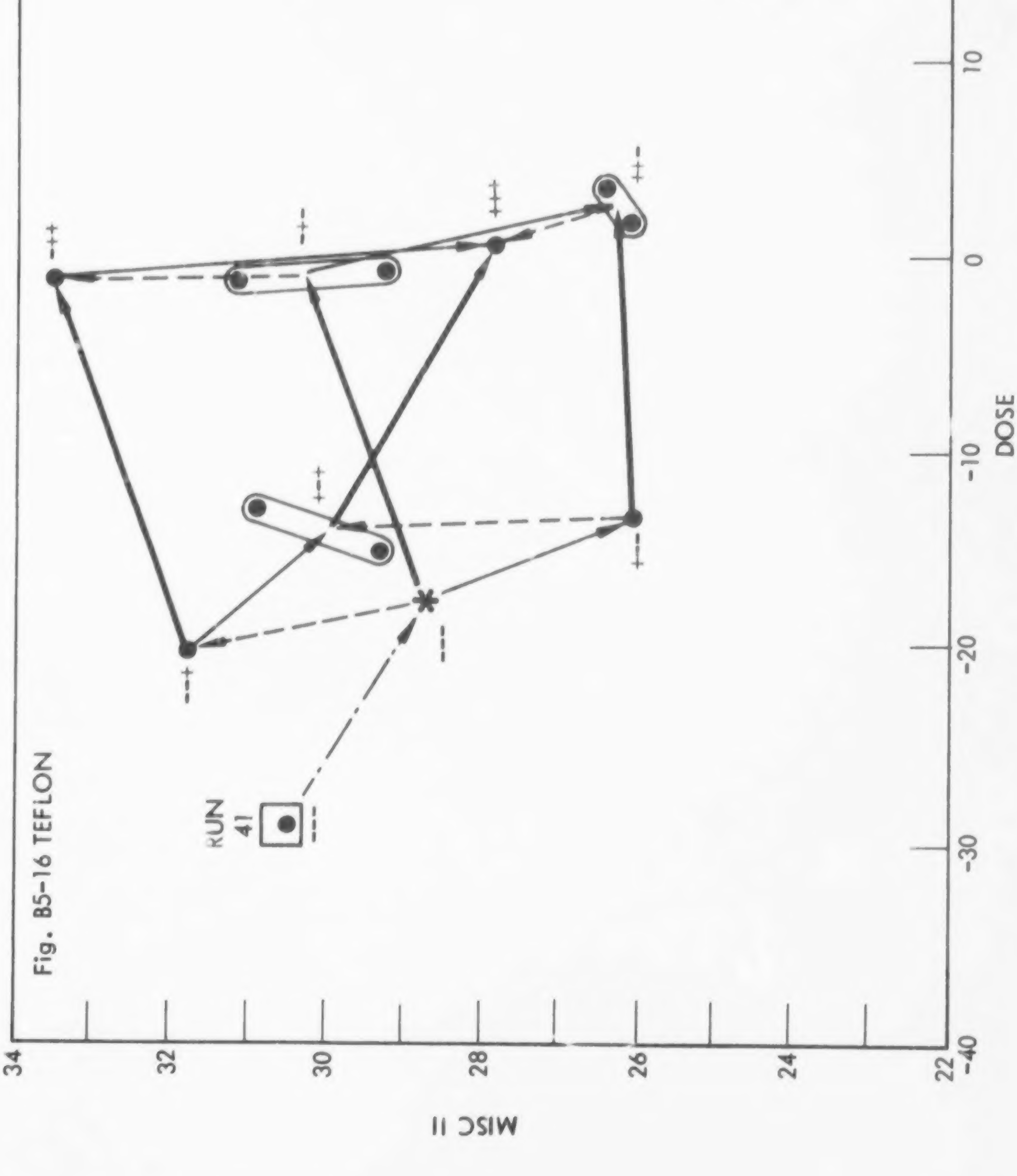

Fig. B5-16 TEFLON

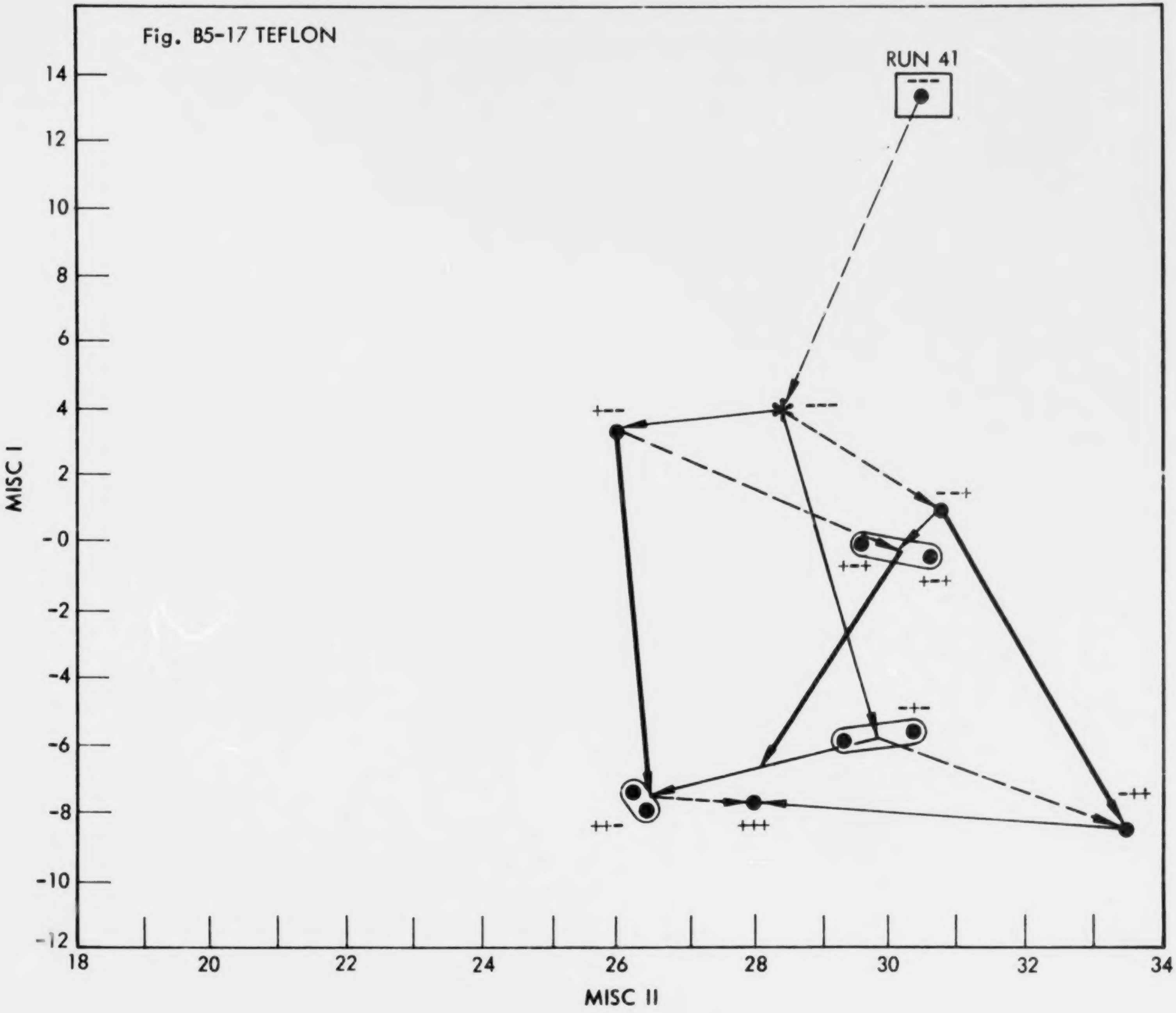

Fig. B5-17 TEFLON

What we have done is visually adjust the data for run 41 so as to bring that diagram into consistent form as shown. The "adjusted" values of the parameters are shown on the Figures.

Using the adjusted value, an "orthogonalized" analysis of variance was calculated and is presented in the same table. Again we note the absence of interaction in this table.

5.3.3 Pyrex

Figures B5-18 thru B5-23 present plots in the same manner as provided for Teflon and stainless steel. Here the pattern is again substantially less regular than it was for stainless steel and resembles Teflon in that one point (Run 25) stands out as different.

As with the Teflon data we are led to speculate about the validity of this run. It is the slowest run of the entire program, and appears discrepant in three out of the four parameters. Note that Run 31 also is out-of-line but to a lesser extent. (Run 31 is a record holder with respect to initial conditions.) As was done for Teflon the data have been visually adjusted to bring the diagrams into consistent form.

Using the visually adjusted value for Run 25 (but with no adjustment for Run 31), an orthogonalized analysis was calculated and is shown in the table. As might be expected, there is, even after adjustment, a sizeable BC interaction term for both time and dose.

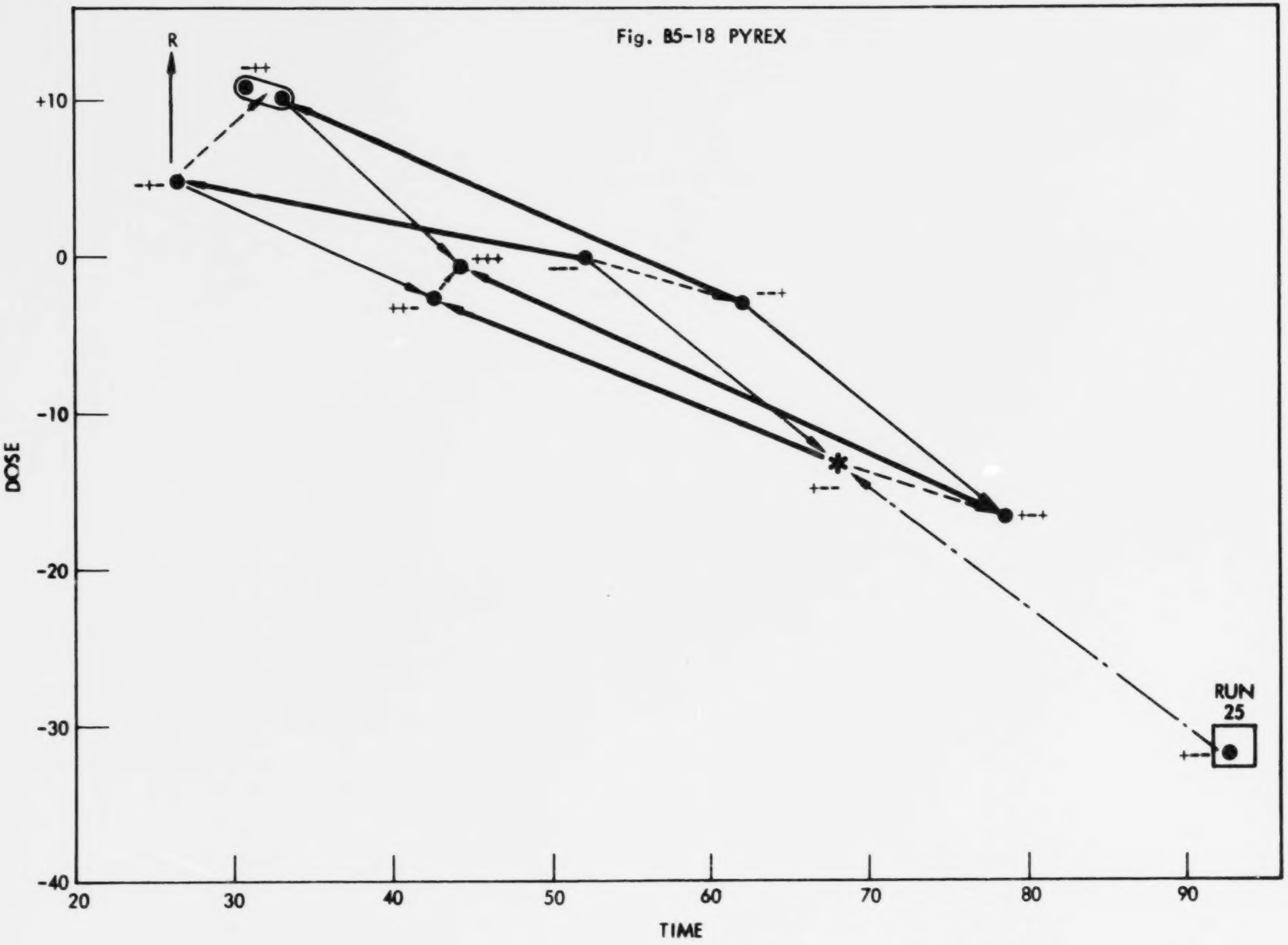

Fig. B5-18 PYREX

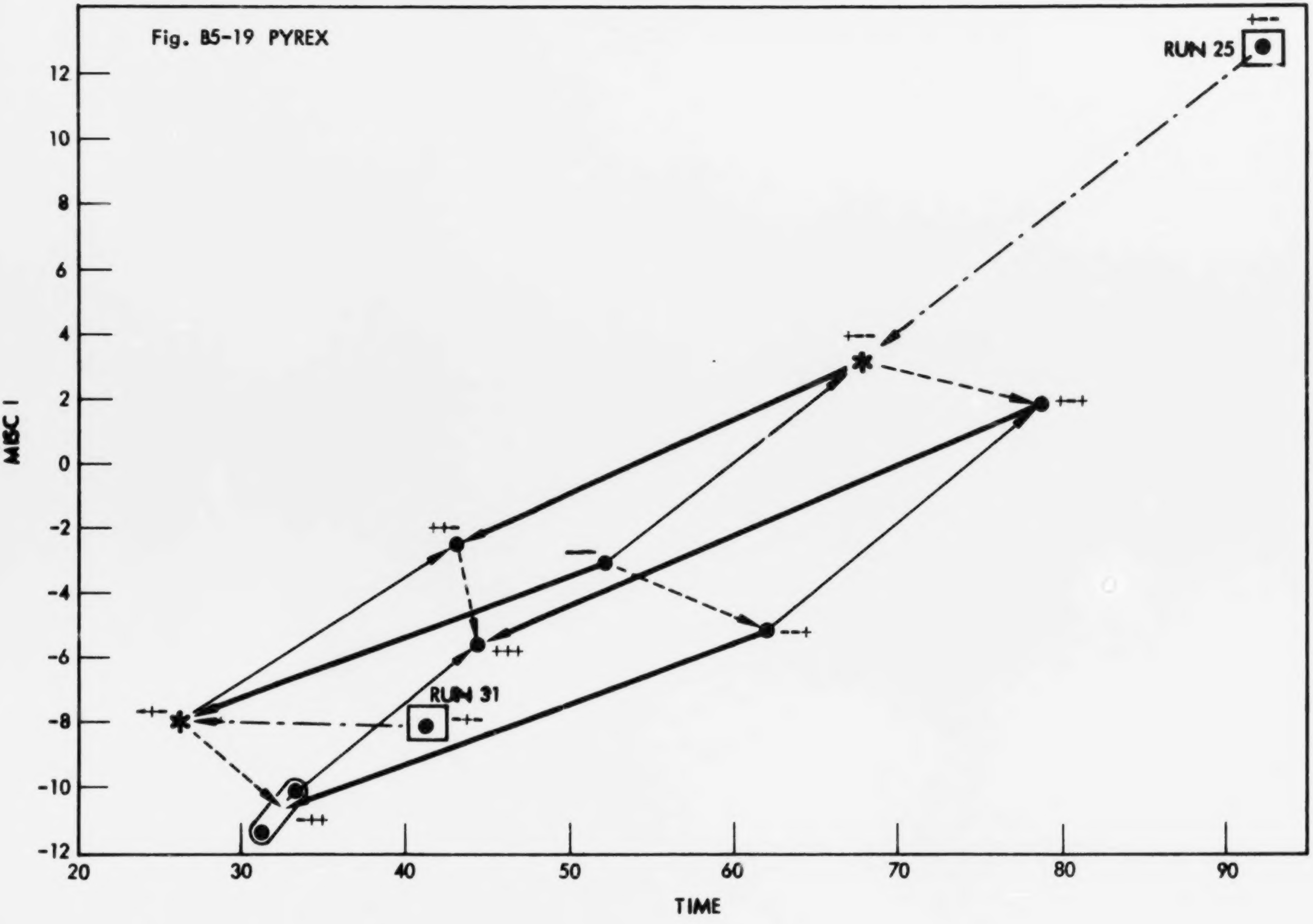
Fig. B5-19 PYREX

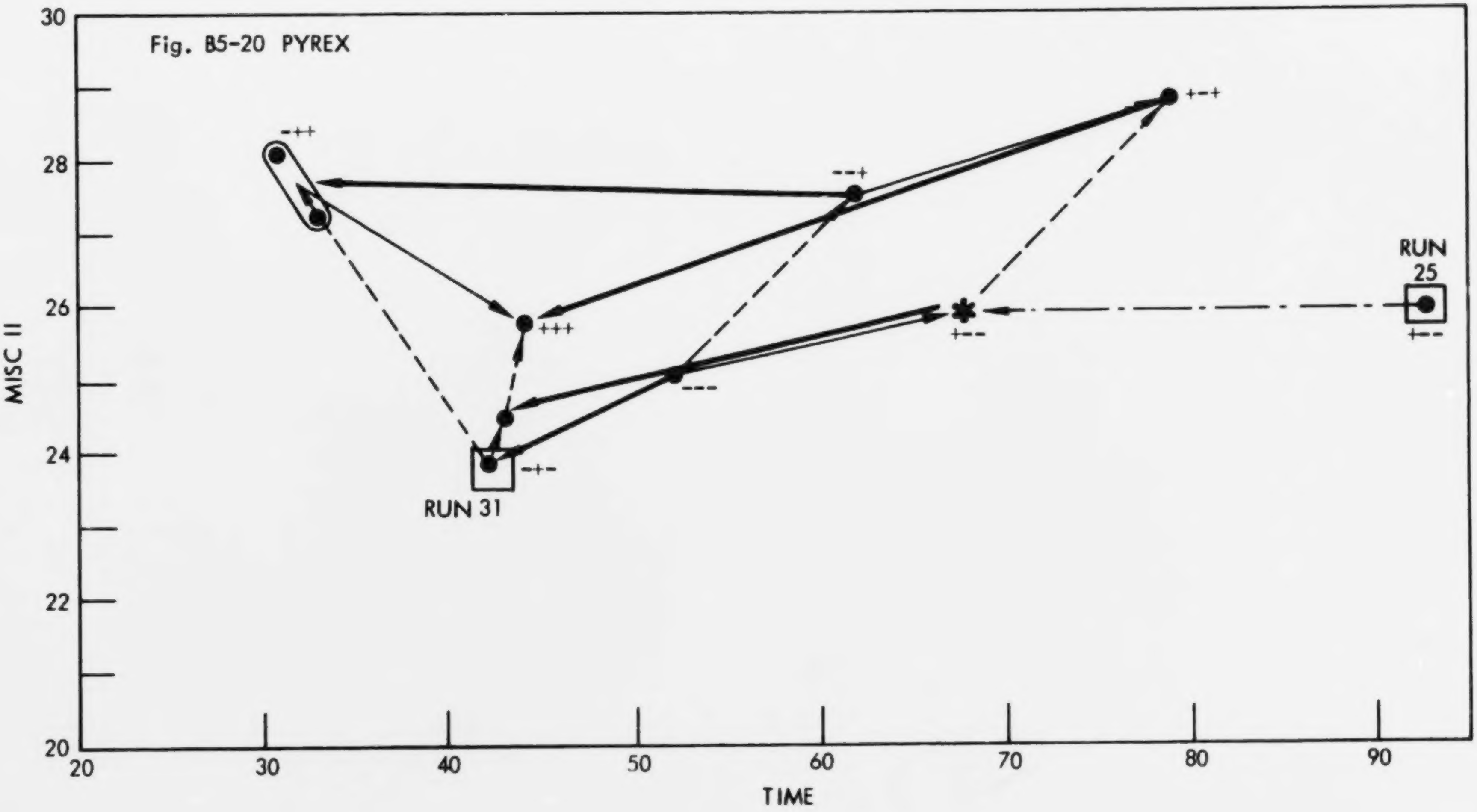

Fig. B5-20 PYREX

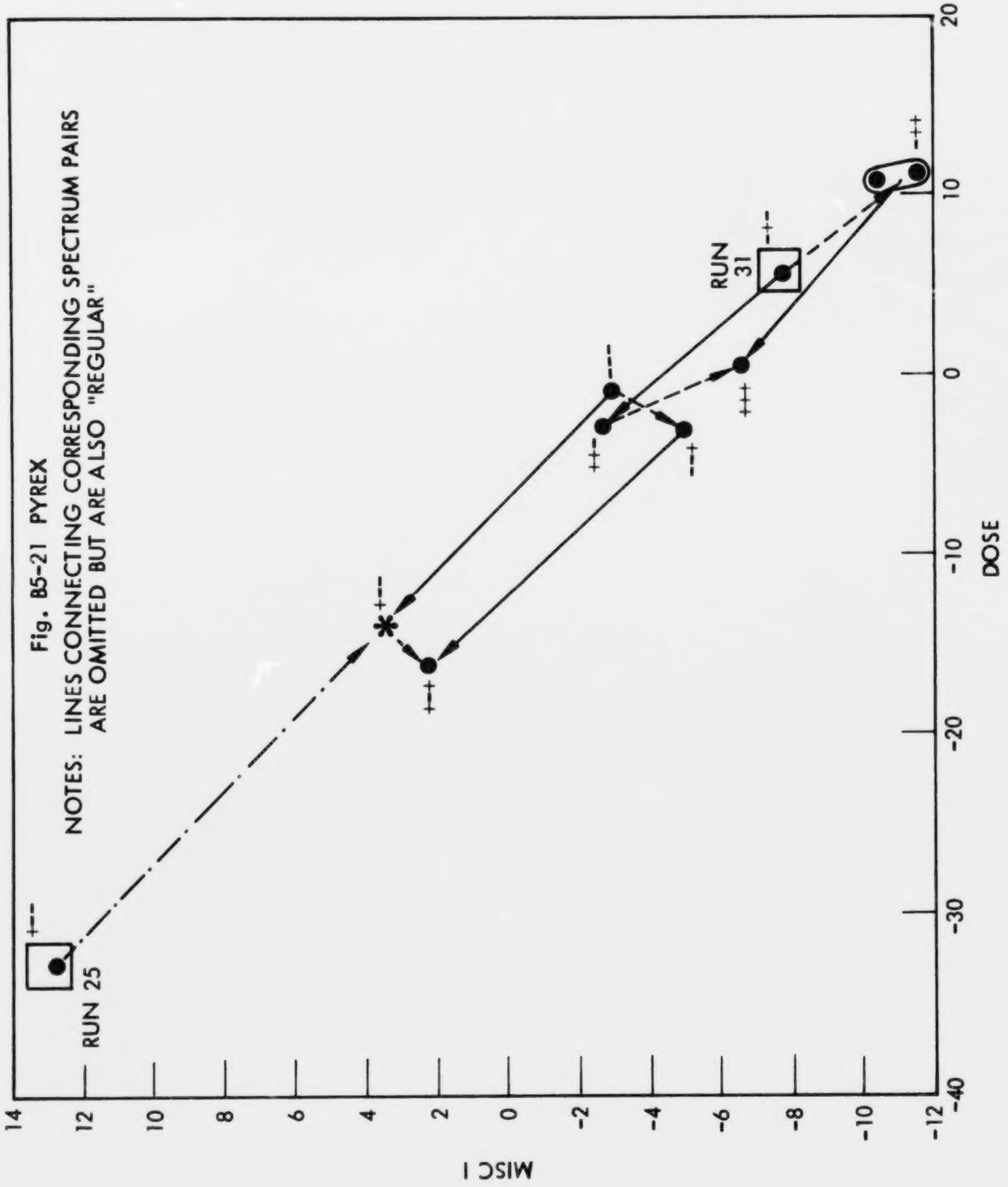

Fig. B5-21 PYREX

NOTES: LINES CONNECTING CORRESPONDING SPECTRUM PAIRS ARE OMITTED BUT ARE ALSO "REGULAR"

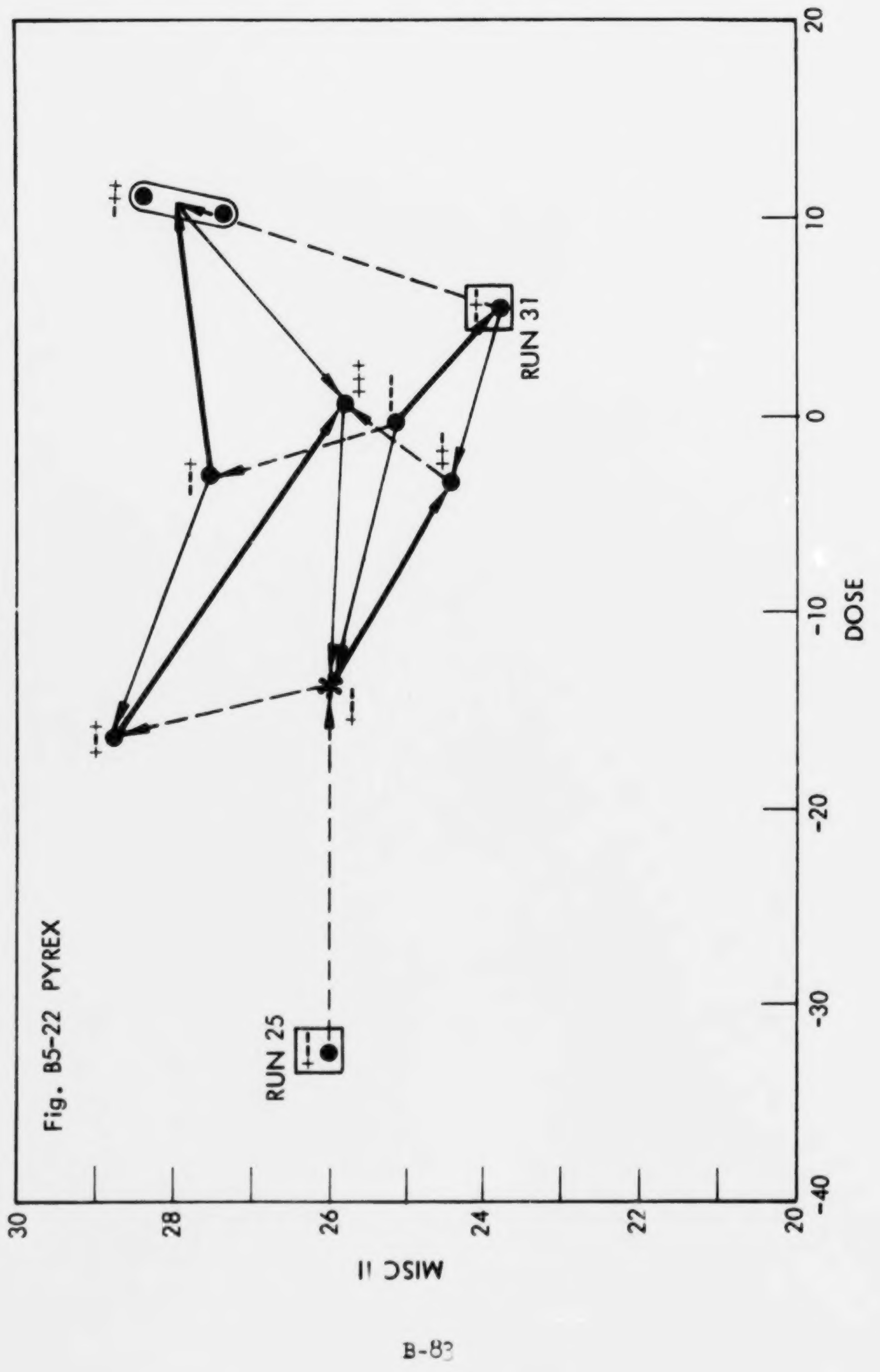

Fig. B5-22 PYREX

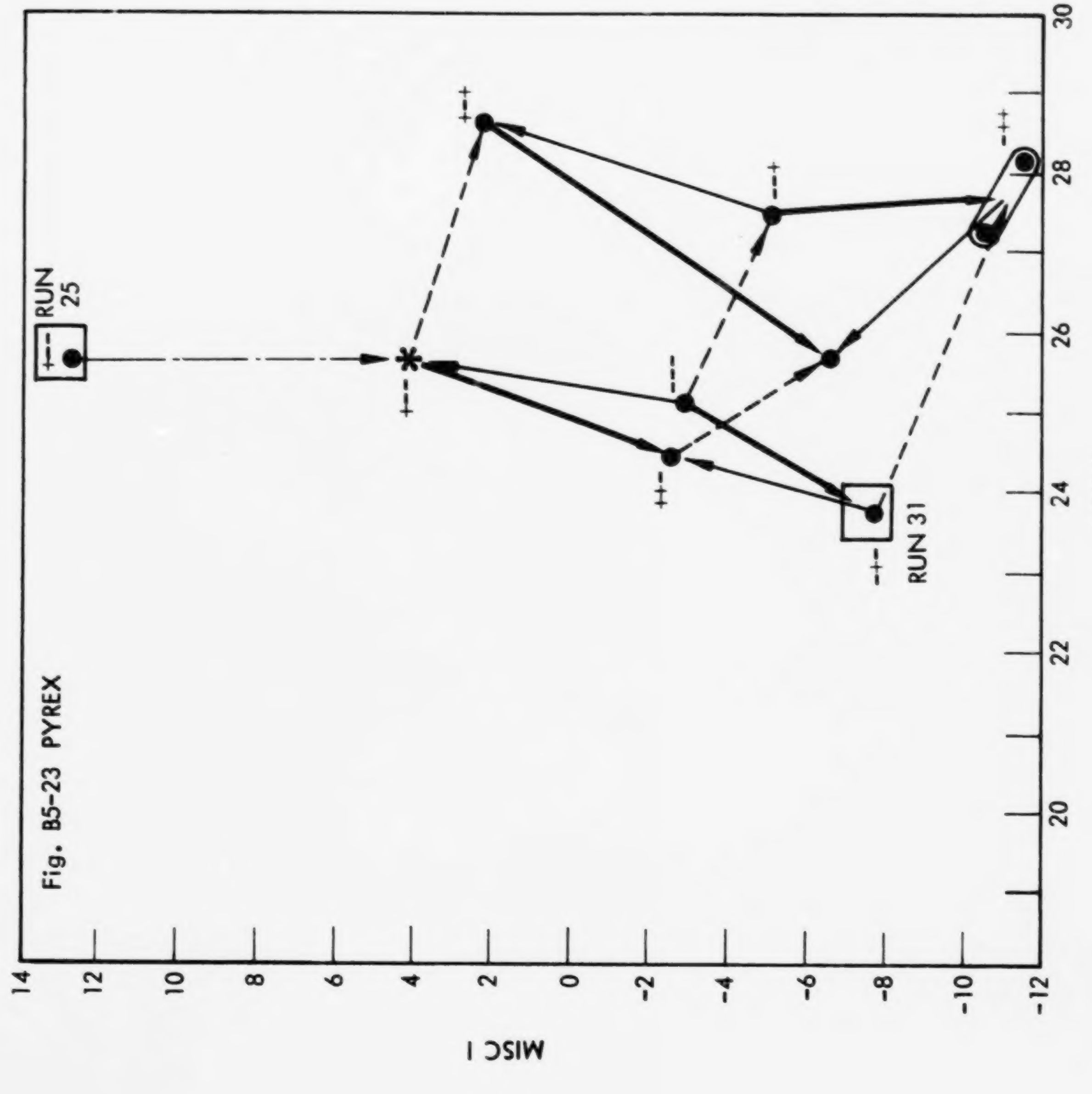
Fig. B5-23 PYREX

5.3.4 Aluminum Reruns

Figures B5-24 thru B5-29 present plots in the same manner as the previous materials. Here the pattern would be fairly regular were it not for the substantial variation among the replicate triple - runs 70, 82 and 84 (+--).

It is difficult to justify dropping any one of these 3 runs, since this variation may in fact be a reflection of experimental error. However, run 70 does stand out among the three and in forming the diagrams it has been suppressed.

Omitting Run 70, an "Orthogonalized" analysis was calculated and is shown in the table. Note in the table the general absence of any big interaction terms.

These conclusions are made:

- After judicious pruning of the data, we find nearly additive effects in all materials (exluding the early aluminum). These are summarized in Table B5-7.
- The data is effectively summarized in terms of 4 parameters. Of these - time and dose are highly correlated. The parameters identified as MISC I and MISC II tend to be associated with maximum values. See Fig. B5-30.
- In all materials spectrum has a marked effect - cut spectrum runs are slower, have reduced dose and lower values of maximums (MISC I).
- Teflon and stainless steel are the most different with somewhat in the middle and aluminum irregularly between and stainless.
- Pyrex is most effected by S/V. High S/V results in increase time, decreased dose and increased max (MISC I).
- There are only moderate cleaning effects in all materials.

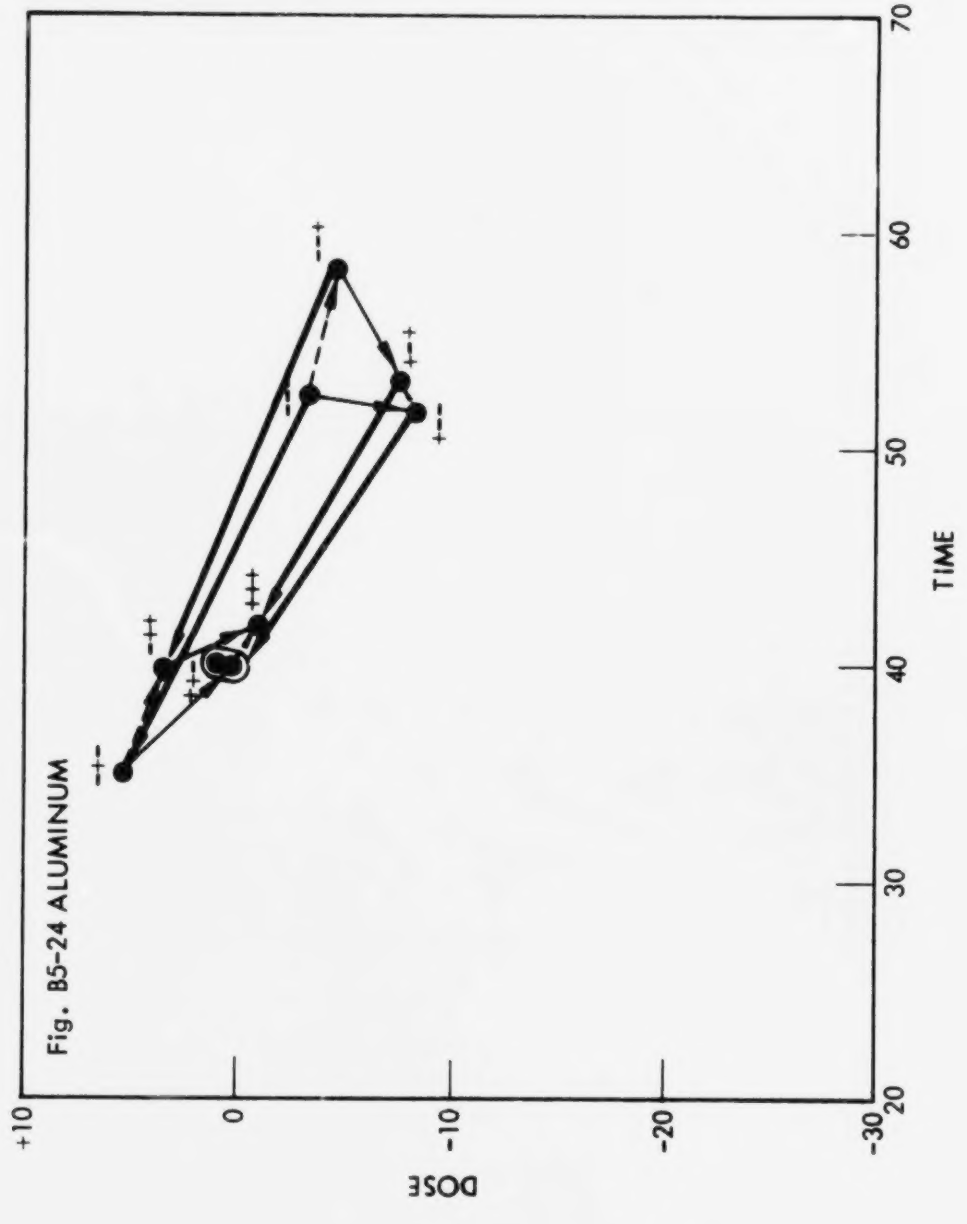

Fig. B5-24 ALUMINUM

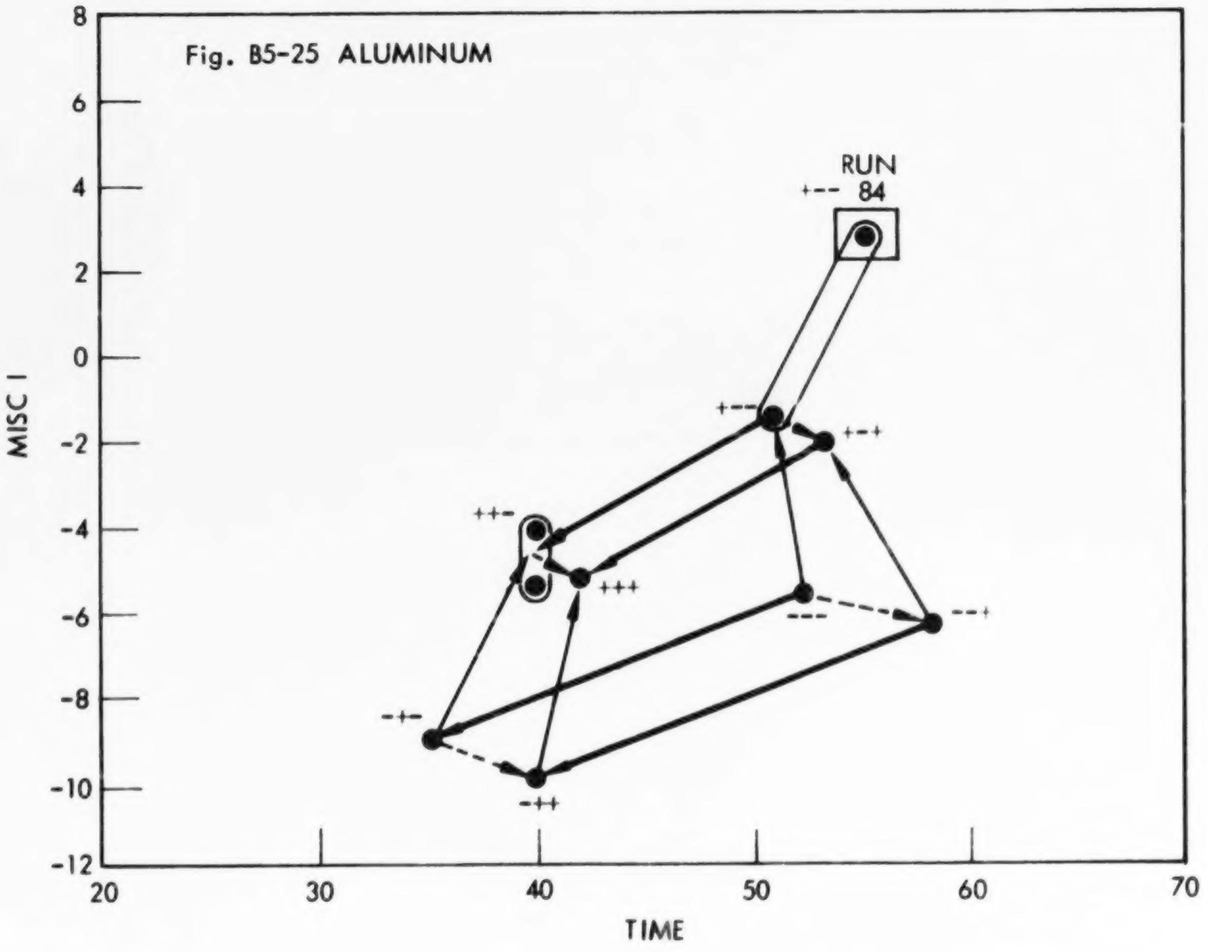

Fig. B5-25 ALUMINUM

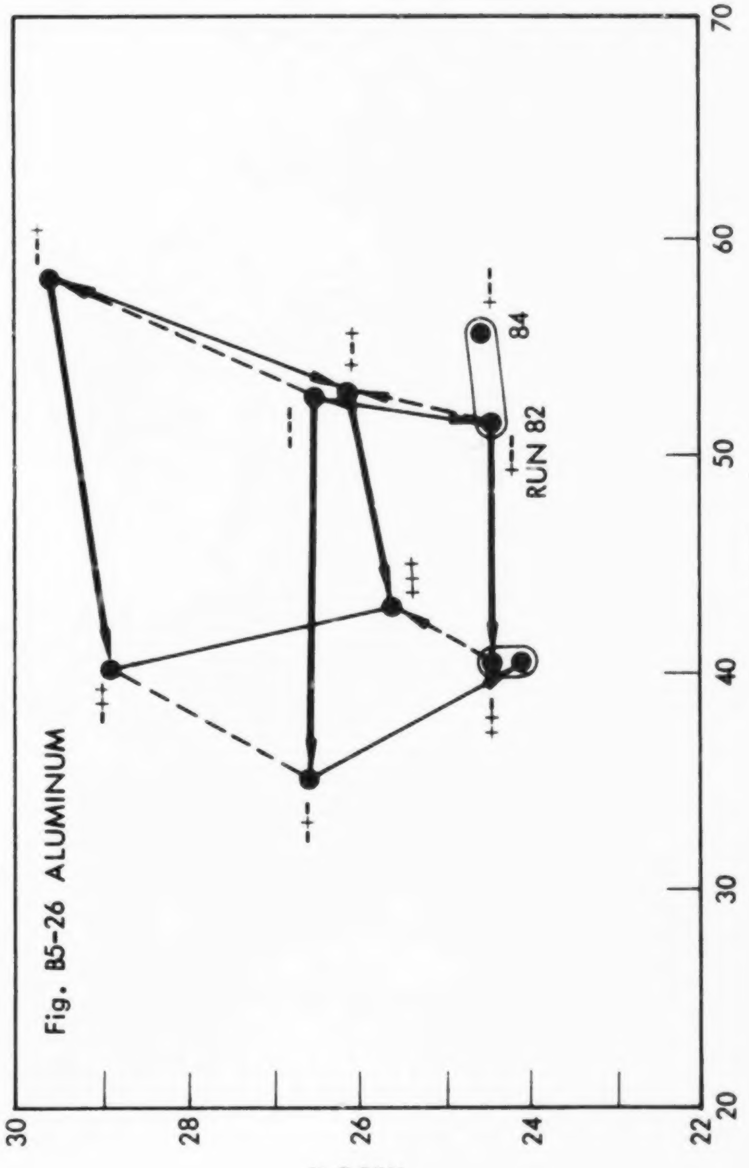

Fig. B5-26 ALUMINUM

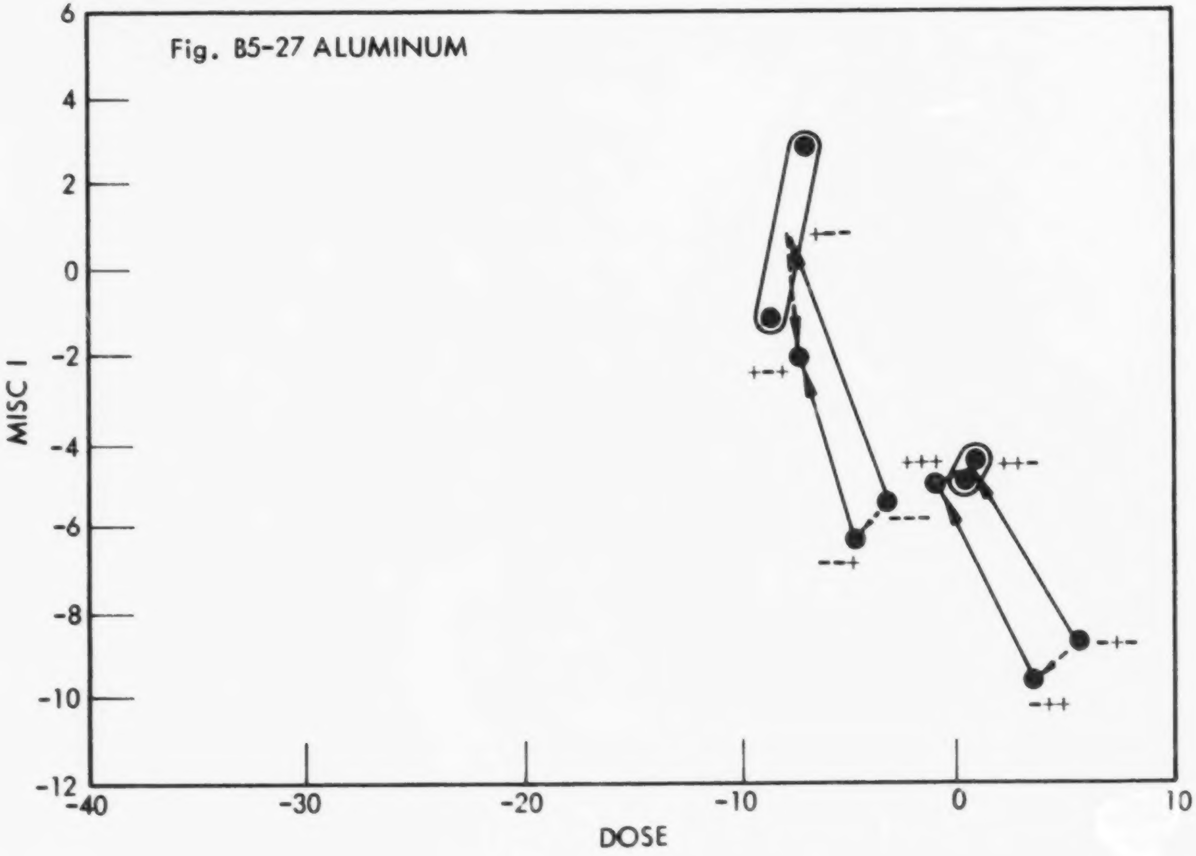

Fig. B5-27 ALUMINUM

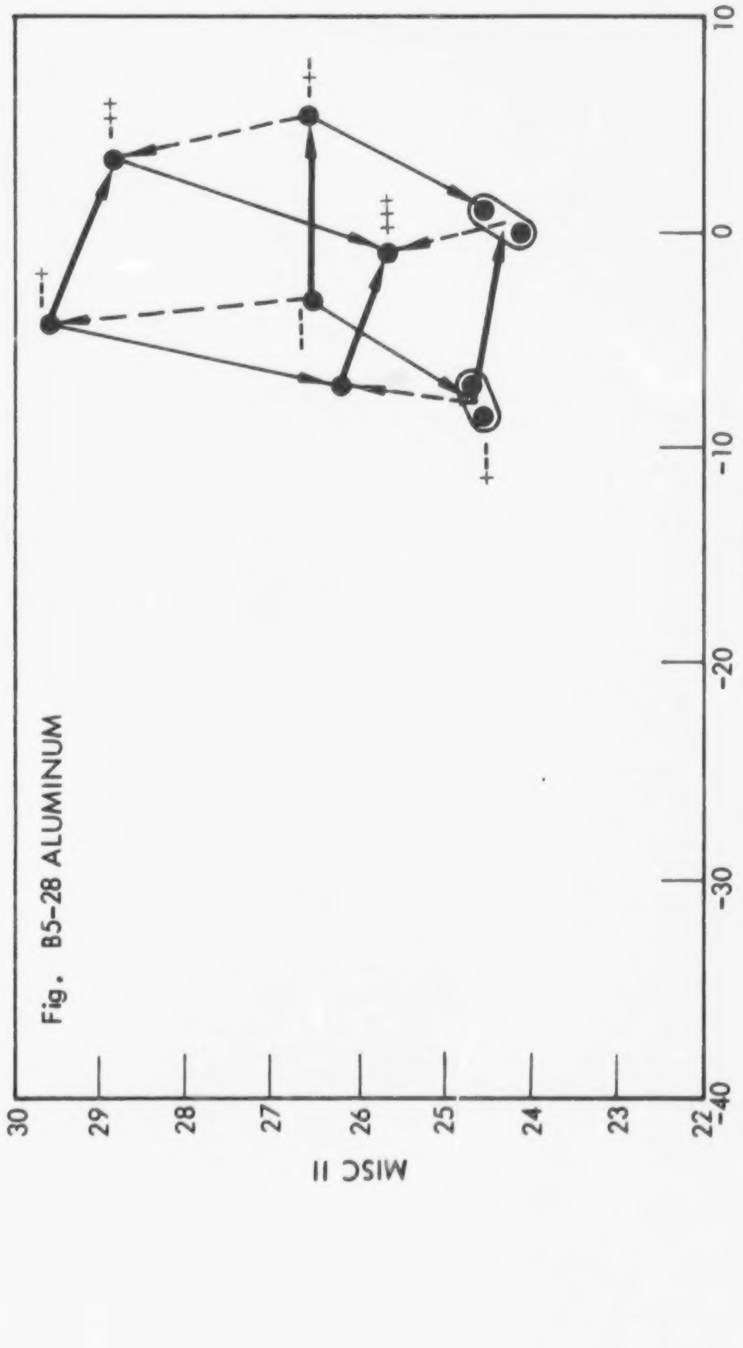

Fig. B5-28 ALUMINUM

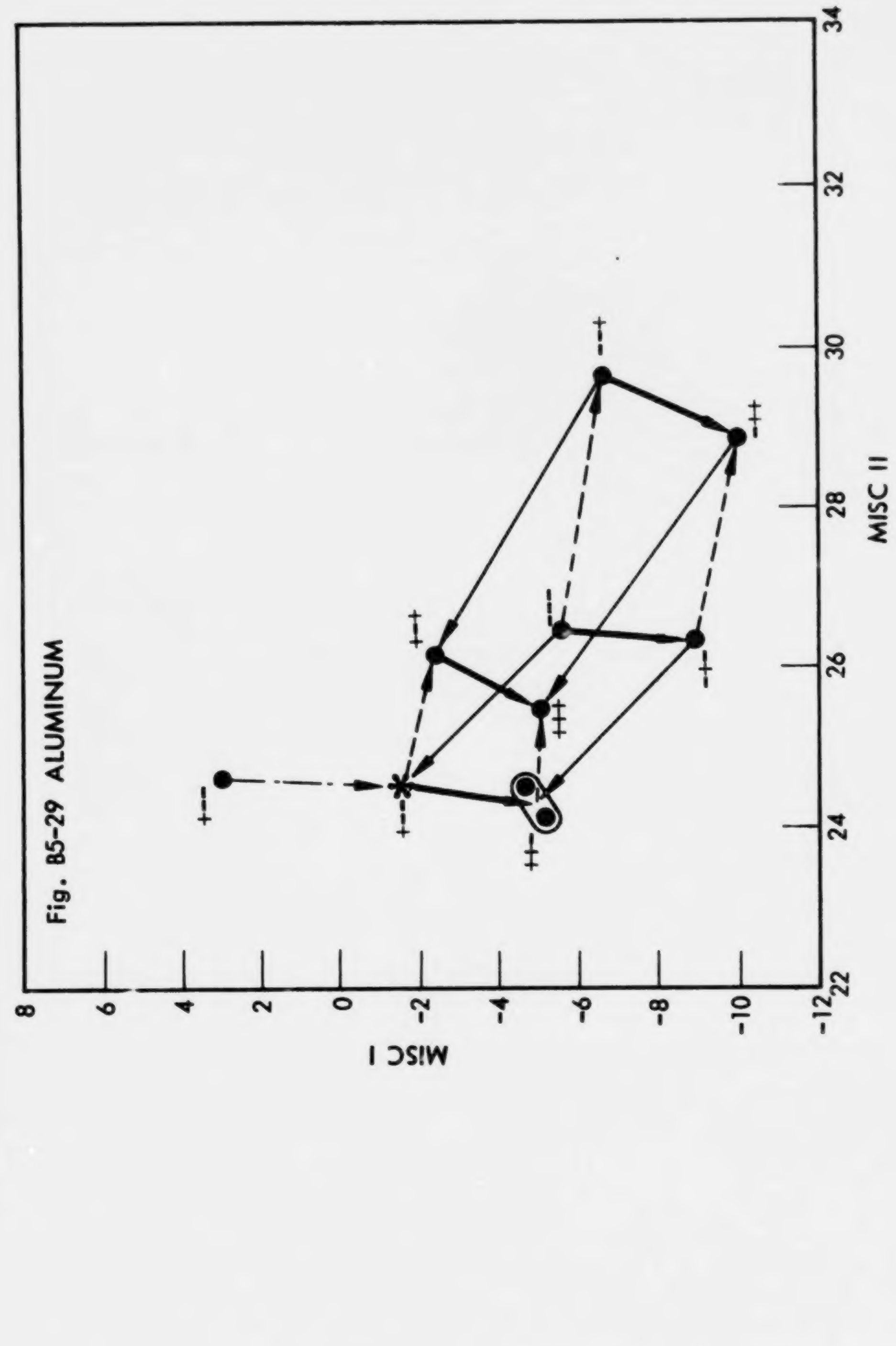

Fig. B5-29 ALUMINUM

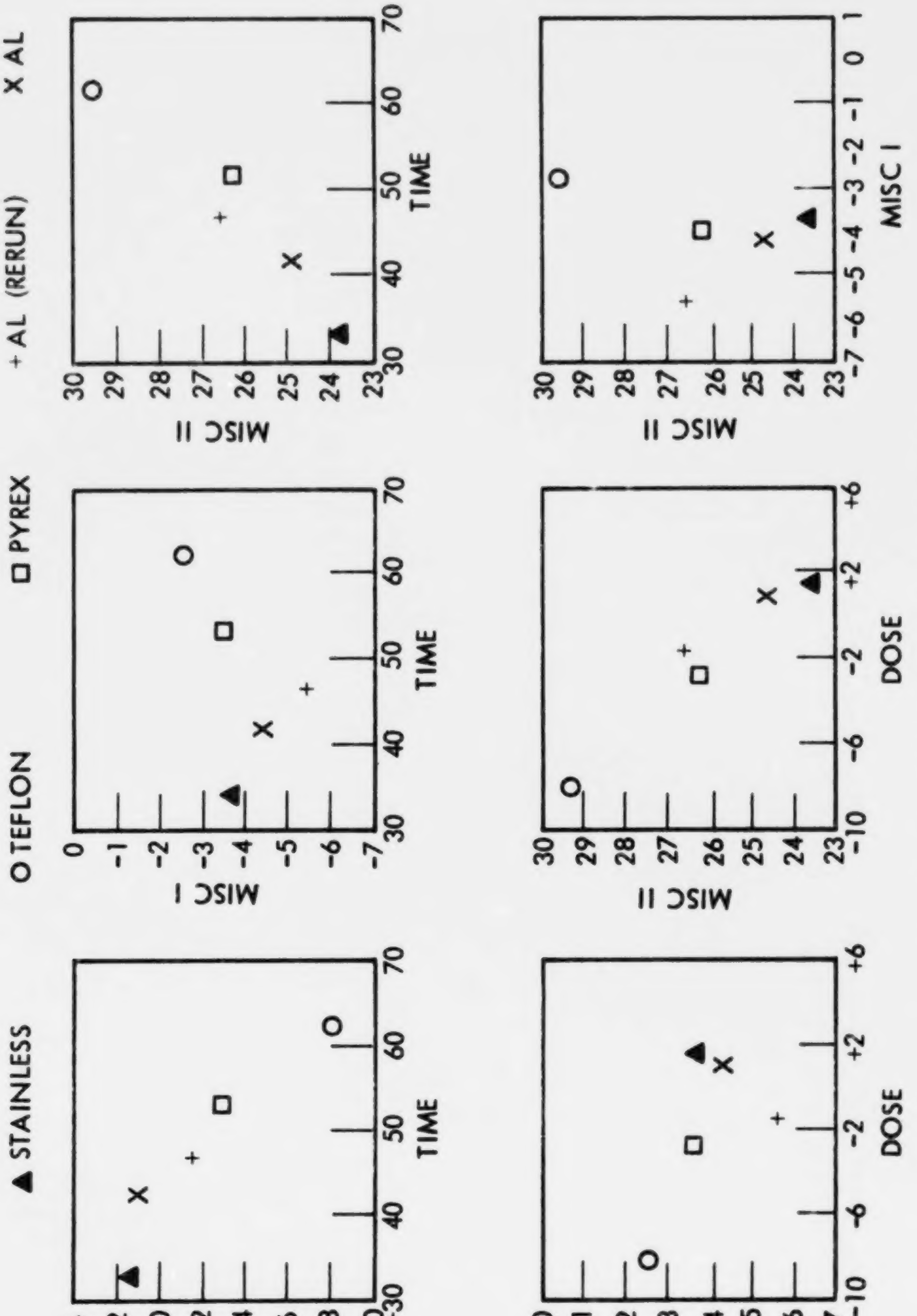

Fig. B5-30 MEAN VALUES BY MATERIALS

5.4 Univariate Analysis

Several of the analyses reported in the preceeding sections were rather informal in character. The following sections provide a more formal analysis.

The four new variables were analyzed univariately using the same basic model given in Section 4. Prior to the analysis of the model, the covariates were investigated to determine if any were useful (it should be recalled that the data had been adjusted for HCinit and %NO_2), and it was found that NO_X or HC/NO_X were beneficial to the study of dose, but that if NO_X is included, HN/NO_X is not necessary. No other dependent variable required any covariate after the HCinit and %NO_2 adjustments.

The model proper was then investigated in the same three ways discussed in Section 4.1, except that dose parameter was first adjusted for NO_X. The results of each analysis are given in Table B5-8. Included in the table are significant effects for each method of testing. Table B5-9 gives tests of reduced models in an attempt to obtain a preferred model. The final optimum model for each dependent variable is given in Table B5-10 with associated prediction coefficients in Table B5-11. Table B5-12 indicates the significance of the single degrees of freedom of the significant model terms.

As in Section 4.1, the results of the univariate analyses are somewhat camouflaged by the material interactions. Consequently, a "by materials" study was again performed, with interesting results. All the variables except MISC II showed a significant spectrum effect, regardless of the material used. S/V was significant the majority of the time, though a consistent pattern was not noted. Of most concern was the covariates: NO_X was

TABLE B5-8

Univariate Tests of Effects

	Time In order of model	Time Weighted squares	Time After Mean	Dose In order, after NO_x	Dose Weighted squares, after NO_x	Dose After mean, NO_x	MISC I In order of model	MISC I Weighted squares	MISC I After mean	MISC II In order of model	MISC II Weighted squares	MISC II After mean
Materials	X	X	X	X	X	X	X	X	X	X	X	X
S/V				X	X	X	X	X	X	X	X	X
Spectrum	X	X	X	X	X	X	X	X	X			
Mat x S/V	X	X	X	X	X	X	X	X	X	X	X	X
Mat x Spec	X	X	X	X	X	X	X	X	X	X	X	X
S/V x Spec			X							X	X	X
Mat x S/V x Spec	X	X	X	X	X	X		X				
Clean	X		X				X	X	X	X	X	X
Mat x Clean		X	X	X	X	X	X	X	X	X	X	
S/V x Clean												
Spec x Clean							X	X	X			

TABLE B5-9

Univariate Tests of Reduced Models

DEP	DF	S.S.E.	R^2	MSE	SS RED	MS RED	F RED	PREFERRED MODEL
TIME FULL	30	459.63	97.029	15.321	-	-	-	
TIME RED	34	489.34	96.837	14.392	29.71	7.43	L1	
TIME W/O MXC	38	640.44	95.860	16.854	180.81	22.60	1.48	
TIME W/O C	35	534.06	96.548	15.259	74.43	14.89	L1	
TIME W/O MXC,C	39	707.22	95.428	18.134	247.59	27.51	1.80	*
DOSE FULL	29	173.30	96.1096	5.9759	-	-	-	*
DOSE RED	33	189.14	95.753	5.7316	15.84	3.96	L1	*
MISC I FULL	30	90.819	94.051	3.0273	-	-	-	
MISC I RED	32	91.430	94.011	2.8572	.611	.305	1	*
MISC I W/O	36	139.10	90.889	3.8638	48.28	8.05	2.66*	
MISC II FULL	30	47.882	91.645	1.5961	-	-	-	
MISC II RED	37	59.934	89.543	1.6198	12.052	1.722	1.08	*
MISC II W/O MXC	41	84.231	85.303	2.0644	36.349	3.304	2.07	

TABLE B5-10

Optimum Univariate Models on Principal Components

TIME = μ + MAT + SPEC + MAT x S/V + MAT x SPEC + MAT x S/V + SPEC + ϵ

DOSE = μ + (NOX) + MAT + S/V SPEC + MAT x S/V + MAT x SPEC + MAT x S/V x SPEC + MAT x CL + ϵ

MISC I = μ + MAT + S/V + SPEC + MAT x S/V + MAT x SPEC + MAT x S/V x S/V x SPEC + CL + MAT x CL + SPEC x CL + ϵ

MISC II = μ + MAT + S/V + MAT x S/V + MAT x SPEC + S/V x SPEC + CL + MAT x CL + ϵ

TABLE B5-11

Coefficients for Univariate Models After Prin Components

	TIME	DOSE	MISC I	MISC II
CONSTANT	48.916	-2.580	-3.4336	26.317
(NOX-1.487)	-	-15.601	-	-
MATERIAL 1	-4.0573	1.0637	-.055081	-.58796
2	1.5738	-1.8314	-.46526	.84906
3	4.3197	-2.4776	.50078	1.7328
4	6.9811	-3.1876	1.3192	1.0305
S/V	-	-1.6585	1.8183	-1.4895
SPECTRUM	-10.885	6.3551	-3.9054	-
MAT x S/V 1	-.83580	.021104	.19419	-.40300
2	1.4312	-.85480	.68750	.082604
3	-6.0230	5.3457	-.26374	-.91306
4	1.8307	-.38398	-.23285	.14814
MAR x SP 1	1.1226	-.33427	.020128	.34839
2	-.067122	.45021	.48477	-.62572
3	.18841	.53569	-.87956	.26770
4	-3.9066	2.7403	-1.2903	-.37077
S/V x SPEC	-	-	-	-.39243
MAT x S/V x SP 1	.17448	-.12435	.12279	-
2	.0083518	.51410	-.062527	-
3	3.2095	-3.0629	1.5109	-
4	-1.3128	.63217	.077586	-
CLEANING	-	-	-1.1976	.72846
MAT x CL 1	-	-.43487	.13723	-.04753
2	-	-.069927	-.30636	.68668
3	-	-1.1050	.16873	-.071662
4	-	1.0557	-.95245	.56177
S/V x CL	-	-	-	-
SPEC x CL	-	-	.51965	-

TABLE B5-12

Material Contrasts in Optimum Models

	TIME	DOSE	MISC I	MISC II
MAT 1	X	X		X
MAT 2	X	X		
MAT 3	X	X		X
MAT 4	X	X	X	X
MAT x S/V 1	X		X	X
MAT x S/V 2			X	
MAT x S/V 3	X	X	X	X
MAT x S/V 4	X			
MAT x SP 1	X			X
MAT x SP 2				X
MAT x SP 3				
MAT x SP 4	X	X	X	X
MAT x S/V x SP 1				-
MAT x S/V x SP 2				-
MAT x S/V x SP 3	X	X	X	-
MAT x S/V x SP 4				-
MAT x CL 1	-	X		
MAT x CL 2	-			X
MAT x CL 3	-			
MAT x CL 4	-	X	X	X

X Signifies Significance

Contrast	Comparison
1	S.S. vs Rest
2	Orig Alum vs Redone Alum
3	Pyrex vs Teflon
4	Orig & Redone Alum vs Pyrex & Teflon

significant for the time data of stainless steel, and HC/NOX was significant for the dose data of the redone aluminum. Neither of these covariate results are consistent with what was expected from previous covariate results. Table B5-13 summarizes the "by materials" significant terms, Table B5-14 tests the reduced model for the optimum model, and Table B5-15 presents the "by material" prediction coefficients for the optimum models.

5.5 Results of Multivariate Analysis

Repeating the univariate analysis in a multivariate fashion, the covariates were again tested for significance. As has been prevalent in the previous multivariate analyses, NO_X, was a significant covariate in the multivariate analysis. The model given in Section 4 was then analyzed, with NO_X included in the model, according to the three approaches presented and Section 4.1. As a result of this analysis, the S/V by spectrum and S/V by cleaning interactions were found to be neglible and were consequently dropped from the model. Table B5-16 gives the results of the significance tests of the effects, with the optimum model, and Table B5-17 gives the prediction coefficients associated with the optimum model.

5.6 Recommended Model

On the basis of the heretofore reported models, the following models are recommended as best describing the original 23 dependent variables:

Original Alum: $Y = \mu + \beta_1 HC_{init} + \beta_2 \%NO_2 + S/V$
$+ \text{spectrum} + \text{spectrum x cleaning} + \epsilon$

Pyrex: $Y = \mu + \beta_1 HC_{init} + \beta_2 \%NO_2 + \beta_3 NO_X$
$S/V + \text{spectrum} + \epsilon$

TABLE B5-13

BY MATERIALS

DEP VAR	ORIG ALUM	PYREX	TEFLON	S.S.	REDONE ALUM	TOTAL
TIME						
S	X	-	-	X	-	2
A	X	X	X	X	X	5
SA	-	-	-	-	-	0
C	-	-	-	X	0	1
SC	-	-	-	-	-	0
AC	-	-	-	X	-	1
COV	-	-	-	NOX	-	1
DOSE						
S	-	X	X	X	X	4
A	X	X		X	X	5
SA	-	-	X	X	-	2
C	-	-	-	X	-	1
SC	-	-	-	-	-	0
AC	-	-	-	X	-	1
COV	-	-	-	-	HC/NOX	1
MISC I						
S	-	X	-	X	X	3
A	X	X	X	X	X	5
SA	-	-	X	X	-	2
C	-	-	X	X	-	2
SC	-	-	-	-	-	0
AC	-	-	X	-	-	1
COV	-	-	-	-	-	0
MISC II						
S	X	-	X	X	X	4
A	-	-	-	X	-	1
SA	-	-	-	-	-	0
C	-	X	X	-	-	2
SC	-	-	-	-	-	0
AC	-	-	-	-	-	0
COV	-	-	-	-	-	0

S = S/V A = SPEC C = CLEAN

TABLE B5-14

Tests of Reduced "By Materials" Model

PARAMETER	MODEL	ERROR DF	SSE	MSE	SS RED	MS RED	F RED	OPTIMUM MODEL	R^2
TIME	Full	5	22.566	4.5113	-	-	-	-	97.50
TIME	Red	9	60.167	6.6852	37.601	9.40	2.1	*	93.33
DOSE	Full	5	35.312	7.0624	-	-	-		80.89
DOSE	Red	10	75.362	7.5362	40.050	8.010	2	*	59.21
MISC I	Full	5	18.886	3.7772	-	-	-		88.16
MISC I	Red	10	35.943	3.5943	17.057	3.4114	1	*	77.48
MISC 2	Full	5	19.303	3.8607	-	-	-		70.76
MISC 2	Red	10	44.658	4.4658	25.355	5.071	2	*	32.34
TIME	Full	2	163.89	81.947	-	-	-		95.38
TIME	Red	7	163.2	166.89	962.3	192.26	2.35	*	68.25
DOSE	Full	2	53.775	26.887	-	-	-	*	96.47
DOSE	Red	6	240.76	40.127	186.98	46.745	2	*	84.18
MISC I	Full	2	8.592	4.296	-	-	-		98.05
MISC I	Red	5	47.177	9.435	38.585	12.862	3.0	*	89.30
MISC II	Full	2	1.586	.793	-	-	-		93.21
MISC II	Red	7	7.060	1.009	5.474	1.095	2	*	69.74
TIME	Full	4	45.454	11.364	-	-	-		98.35
TIME	Red	9	228.88	25.431	183.426	36.685	3.2	*	91.69
DOSE	Full	4	13.367	3.342	-	-	-		98.85
DOSE	Red	7	50.513	7.216	37.146	12.382	3.7	*	95.67
MISC I	Full	4	10.051	2.513	-	-	-		97.70
MISC I	Red	6	36.834	6.139	26.783	13.392	5.36	*	91.57
MISC II	Full	4	6.232	1.558	-	-	-		90.06
MISC II	Red	8	8.446	1.056	2.215	.5537	1	*	86.53
TIME	Full	6	5.489	.9149	-	-	-		99.41
TIME	Red	8	11.653	1.4566	6.164	3.0546	3.3	*	98.76
DOSE	Full	7	5.571	.7958	-	-	-		98.58
DOSE	Red	8	6.765	.8456	1.194	1.1942	2	*	98.27
MISC I	Full	7	2.638	.3769	-	-	-		99.07
MISC I	Red	9	3.442	.3825	.804	.4020	2	*	98.79
MISC II	Full	7	9.330	1.3328	-	-	-		94.51
MISC II	Red	11	15.447	1.4043	6.117	1.5293	2	*	90.90
TIME	Full	4	60.777	15.194	-	-	-		92.29
TIME	Red	9	109.04	12.116	48.263	9.6526	1	*	86.17
DOSE	Full	3	.669	.2231	-	-	-		99.75
DOSE	Red	7	2.118	.3025	1.448	.3621	2	*	99.20
MAX I	Full	4	12.598	3.1495	-	-	-		92.31
MAX I	Red	8	21.448	2.6810	8.858	2.2145	1	*	86.90
MAX 2	Full	4	6.166	1.5414	-	-	-		81.67
MAX 2	Red	9	17.101	1.9001	10.935	2.1871	2	*	49.15

TABLE B5-15

"By Material" Prediction Coefficients for Univariate Principal Components Data

		Orig Alum	Pyrex	Teflon	S.S.	Rerun Alum
TIME	Const	44.557	55.235	63.766	33.937	47.606
	S/V	-1.8053	-	-	-2.8295	-
	Spec	-8.2458	-16.502	-15.218	-6.9444	-7.8917
	S/V x Spec	-	-	-	-	-
	Clean	-	-	-	4.0072	-
	S/V x CL	-	-	-	-	-
	Spec x CL	-	-	-	-2.0461	-
	(NOX - 1.482)	-	-	-	17.003	-
DOSE	Const	1.7026	-4.8816	-9.444	1.8344	-1.985
	S/V	-	-7.9752	3.3249	-1.4769	-1.5782
	Spec	3.0618	8.2119	9.9576	5.3734	4.5361
	S/V x Spec	-	-	-1.9924	-.56349	-
	Clean	-	-	-	-1.2735	-
	S/V x CL	-	-	-	-	-
	Spec x CL	-	-	-	.69670	-
	(HC/NOX-2.05)	-	-	-	-	18.618
MISC I	Const	-4.4090	-2.3872	-1.4645	-3.6053	-4.9768
	S/V	-	3.8556	-	2.6143	2.7306
	Spec	-3.2552	-4.1634	-5.9243	-3.9788	-2.2917
	S/V x Spec	-	-	1.1883	.46127	-
	Clean	-	-2.2830	-2.2897	-.56056	-
	S/V x CL	-	-	-	-	-
	Spec x CL	-	-	1.4864	-	-
MISC II	Const	25.206	26.146	29.678	23.733	26.601
	S/V	-	-	-1.8616	-3.1543	-1.2740
	Spec	-1.3525	-	-	1.6028	-
	S/V x Spec	-	-	-	-	-
	Clean	-	1.3525	1.4267	-	-
	S/V x CL	-	-	-	-	-
	Spec x CL	-	-	-	-	-

TABLE B5-16

Multivariate Test of Effects

	In order after NO_x	Weighted squares after NO_x	After , NO_x	Questioned
Material	X	X	X	
S/V	X	X	X	
Spectrum	X	X	X	
Mat x	X	X	X	
Mat x Spec	X	X	X	
S/V x Spec			X	X
Mat x S/V x Spec	X	X	X	
Cleaning	X	X	X	
Mat x Clean	X	X	X	
S/V x Clean				
Spec x Clean	X	X	X	

NO_x: F = 5.431 with 4, 26 D.F.

Error Det W/O W/V x Cleaning = 3.3009D + 07 (30 D.F.)
Error Det W/O S/V x Cleaning or S/V x Spec = 3.8925D + 07 (31 D.F.)
U = .848
Optimum Model: $Y = \mu + NO_x + MAT + S/V + SPEC + MAT \times S/V$
$+ MAT \times SPEC + MAT \times S/V \times SPEC + CLEAN$
$MAT \times CL + SPEC \times CL + \epsilon$

TABLE B5-17

Coefficients for Multivariate Model After Principal Components

Model Term	Time	Dose	Max I	Max 2
CONSTANT	49.218	-2.514	-3.437	26.310
(NO_x -1.487)	3.8289	-18.589	2.5979	-3.6848
MAT 1	-3.8695	1.0743	-.0504	-.6104
MAT 2	1.5168	-1.8243	-.4564	.8848
MAT 3	4.2159	-2.4491	.5229	1.7100
MAT 4	6.9024	-3.1933	1.2806	1.0934
S/V	.3619	-1.6058	1.7952	-1.4738
SPECTRUM	-10.917	6.4115	-3.9416	.3075
MAT 1 x S/V	-8.534	-.0015	.2054	-.4316
MAT 2 x S/V	1.5761	-.7846	.6714	.1449
MAT 3 x S/V	-5.9708	5.2283	-2.5770	-1.0087
MAT 4 x S/V	1.7102	-.3885	-.2518	.1651
MAT 1 x SPEC	1.0667	-.3556	.0353	.3107
MAT 2 x SPEC	-.0308	.4053	.6208	-.7602
MAT 3 x SPEC	.3168	.5818	-.8339	.1426
MAT 4 x SPEC	3.7014	2.7594	-1.2875	-.3104
MAT 1 x S/V x SPEC	.1485	-.1322	.1214	-.0071
MAT 2 x S/V x SPEC	-.1155	.5000	-.0923	.2866
MAT 3 x S/V x SPEC	3.4650	-3.1403	1.5754	-.1101
MAT 4 x S/V x SPEC	-1.3544	.6550	.0638	.0339
CLEANING	.9283	.5660	-1.2382	.8006
MAT 1 x CLEAN	.6633	-.4801	.1543	-.0803
MAT 2 x CLEAN	.0201	-.0303	-.2994	.6460
MAT 3 x CLEAN	1.5937	-1.1534	.1750	-.0244
MAT 4 x CLEAN	-.5485	1.1069	-.9697	.6234
SPEC x CLEAN	-.4320	.0411	.5143	-.0015

Teflon:

$$Y = \mu + \beta_1 HC_{init} + \beta_2 \% NO_2 + S/V + \text{spectrum} + S/V \times \text{spectrum} + \epsilon$$

Stainless Steel:

$$Y = \mu + \beta_1 HC_{init} + \beta_2 \% NO_2 + S/V + \text{spectrum} + \text{cleaning} + \epsilon$$

Redone Alum:

$$Y = \mu + \beta_1 HC_{init} + \beta_2 \% NO_2 + \beta_3 HC/NO_X + S/V + \text{spectrum} + \epsilon$$

This recommendation is made after consideration of the univariate and multivariate analyses, both before and after the principal components have been used. It is felt that these models are the most implicated models as being descriptive of the data.

The manner in which this analysis proceeded was as follows:

- Covariance corrections were calculated for the 23 parameters separately.
- A multivariate analysis of covariance was used to check that the covariates selected were appropriate.
- Using the covariate corrected data, principal components for TIME, DOSE, MISC I and MISC II were developed.
- These new parameters were reanalyzed using both univariate and multivariate analysis of covariance.
- Somewhat less formal techniques revealed that certain especially #25 and #41 were possible outliers. Suppression of these points led to a substantially simplier model.

The outliers had an opportunity to influence, perhaps strongly influence, the covariance corrections. Thus to be completely consistent they should be suppressed and the entire analysis redone. This has not been done both for reasons of time and budget and also because it is felt that further effort should be devoted towards deriving better descriptors of the original data. It is clear that for this data the parameters were excessively redundant. It is possible that some features of the original graphs have been overlooked and this merits investigation.